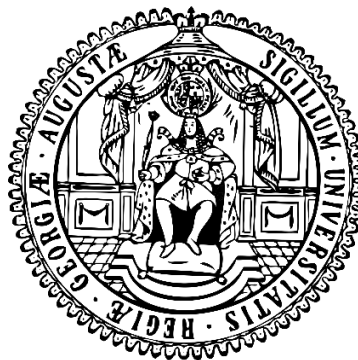


Identification of factors involved in cell wall
homeostasis and tolerance towards quaternary
ammonium compounds in
Listeria monocytogenes by genomic adaptation

Dissertation

for the award of the degree

“Doctor rerum naturalium”



Division of Mathematics and Natural Sciences
of the Georg-August-Universität Göttingen
within the doctoral program “Microbiology & Biochemistry”
of the Georg-August University School of Science (GAUSS)

submitted by

Lisa Maria Schulz

from Coesfeld

Göttingen 2023

Examination board

Thesis advisory committee

Dr. Jeanine Rismondo (Supervision and 1st Reviewer)

Institute of Microbiology and Genetics, Department for General Microbiology, University of Göttingen

Prof. Dr. Rolf Daniel (2nd Reviewer)

Institute of Microbiology and Genetics, Department for Genomic and Applied Microbiology, University of Göttingen

Prof. Dr. Carsten Lüder

University Medical Center Göttingen, Department of Medical Microbiology, University of Göttingen

Further members of the Examination Board

Prof. Dr. Gerhard Braus

Institute of Microbiology and Genetics, Department of Molecular Microbiology and Genetics, University of Göttingen

PD Dr. Michael Hoppert

Institute of Microbiology and Genetics, Department for General Microbiology, University of Göttingen

Prof. Dr. Pöhlmann

German Primate Center, Department of Infection Biology, Göttingen

Date of oral examination: 11.05.2023

Statement of Authorship

I hereby declare that the doctoral thesis entitled “Identification of factors involved in cell wall homeostasis and tolerance towards quaternary ammonium compounds in *Listeria monocytogenes* by genomic adaptation” has been written independently and with no other sources and aids than quoted.

Lisa Maria Schulz

Danksagung

Liebe Jeanine, ich danke dir für die großartige Betreuung und das Vertrauen, das du mir von Beginn an entgegengebracht hast. Für all die fachbezogenen und privaten Diskussionen sowohl für deine Ehrlichkeit und für deine ansteckende Begeisterung für die Forschung mit Listerien. Ich bin froh, dass unsere vehementen Versuche eine Zellwand-unabhängige Arbeit zu schreiben doch sehr erfolgreich gescheitert sind und du mir viel von deiner Expertise zeigen und diese an mich weitergeben konntest. Des Weiteren möchte ich mich auch bei Jörg bedanken, nicht nur für die Zeit des Doktors, sondern auch für die Zeit während iGEM und des Masters und mich für alle fachlichen Hinweise und kritischen Fragen bedanken.

Mein besonderer Dank geht an Carsten Lüder und Rolf Daniel dafür, dass Ihr Teil meines Thesis Committee wart, euch die Zeit für mich genommen habt und meine Arbeit mit interessanten Fragen und Anmerkungen weiter vorangetrieben habt. Danke auch an die Mitglieder meines Prüfungskomitees: Gerhard Braus, Stefan Pöhlmann und Michael Hoppert. Vor allem Michael möchte ich nochmals für die Expertise und Hilfe mit dem TEM danken.

Meine Zeit in der AGC, AGS und AGJ wurde natürlich (abseits von einem kurzen Zwischenstopp im HIF Labor) von allen Leuten des S2 geprägt. Zuallererst danke an Johannes für die Bekanntmachung mit Listerien im damaligen Masterpraktikum und dass du und Fabian mich herzlich in die Welt der Listerien aufgenommen und eingeführt habt. Ohne dich und das Praktikum wäre mein Weg vermutlich anders verlaufen. Vielen Dank an Neil und vor allem Rica für die musikalische Aufwertung im S2, für die stets gelassene und gute Laune und für all eure Geschichten (auch trotz 40°C Lab-coat summer hours). Danke Neil, dass du immer meine Expertise über den Grad der Orangefärbung des Mediums geschätzt hast. Ein großer Dank geht natürlich auch an Julia für die gute Zusammenarbeit und jeglichen Klatsch und Tratsch.

Mein Dank gilt auch allen ehemaligen und derzeitigen Mitgliedern der AGC, AGS und AGJ. Besonders möchte ich mich aber bei Tiago für alle lunch-sessions und dein ehrliches Feedback bedanken und auch an Björn für alle guten Ratschläge, dein Interesse an meiner Arbeit und deiner generellen Hilfsbereitschaft, vor allem in der Zeit, als wir uns noch ein Büro geteilt haben. Ein großes Danke geht auch an Martin, für dein Vertrauen deine Arbeit weiterzuführen und für jedes Bier in Prag. Ich hoffe, ich werde bei meiner Feier genauso viel Spaß haben, wie du bei deiner.

Natürlich möchte ich mich auch bei meinen zahlreichen Studenten bedanken. Danke Tayfun, Tayfun, Ostap, Lisa, Fabienne, Lorenz, Alicia und Lea für die Hilfe an meiner Arbeit. Ich hoffe ihr habt die Zusammenarbeit gleichermaßen genossen und ich konnte meine Begeisterung vor allem für S2 Organismen weitergeben.

Mein Dank geht natürlich auch an Christina, Sabine und Silvia für all die Unterstützung und für das Teilen eurer Expertise, die Ihr über die Jahre angesammelt habt. Ihr seid wirklich der Stützpfiler der Abteilung.

Nicht zu vergessen sind natürlich die Ehrenmitglieder des iGEMs Teams, allen voran natürlich unser Team-Captain Rica (as mentioned above), als auch Jonas, Marie, Dennis, Janek und Robert. Der Weg zu dieser fertigen Arbeit ist mir mit euch als Mitstreiter deutlich leichter gefallen. Dabei darf man natürlich Linda und Tim nicht vergessen. Danke für alle Grill-, Glühwein-, Feuerzangenbowle- und Pizza-Sessions die wir zusammen verbringen konnten. Vor allem an Marie, die meine Motivation auch in der doch recht chaotischen Zeit der Corona-Tests aufrechterhalten hat und mir immer mit Rat und Tat zur Seite stand.

Außerdem möchte ich mich bei allen Verwandten (würde ich alle namentlich erwähnen, würde meine Arbeit zu teuer werden) und Freunden bedanken, die mich moralisch unterstützt haben. Ein besonderer Dank geht dabei an Linette und Kerrin, dir mir in unserer gemeinsamen Zeit den Stress genommen haben. Vor allem du, Kerrin hast mir verdeutlicht, dass alles ganz einfach ist „wenn man einfach alles weiß“. An meine Leidensgenossin Alisa: Danke für jeden einzelnen Kaffeeklatsch.

Ich wäre bestimmt nicht da gelandet wo ich jetzt bin ohne die Unterstützung der Mitglieder der Bereitschaft und der Superhelden. Danke, dass ihr mich zu der gemacht habt, die ich heute bin und dass ihr mir gezeigt habt, dass alles „kpfLMS“ ist.

Diese Arbeit wird vor allem auch Küso gewidmet, der zu einem großen Teil für den Erfolg dieser Arbeit mit verantwortlich ist. Danke für deine moralische Unterstützung und den Ansporn. Ich bin froh einen so tollen Cheerleader in meinem Leben zu haben.

Last but not least: Danke an Mama, Papa, Jens, Jasmin, Arne und Juli für die mentale, emotionale und natürlich auch finanzielle Unterstützung. Danke, ohne euch wäre das alles hier nicht möglich gewesen!

List of publications

Benda, M*., **Schulz, L.M***., Stülke, J., and Rismondo, J. (2021) Influence of the ABC Transporter YtrBCDEF of *Bacillus subtilis* on competence, biofilm formation and cell wall thickness. *Frontiers in Microbiology*.

*shared co-authorship

Rismondo, J., and **Schulz, L.M.** (2021) Not just transporters: Alternative functions of ABC transporters in *Bacillus subtilis* and *Listeria monocytogenes*. *Microorganisms*.

Rismondo, J., **Schulz, L.M.**, Yacoub, M., Wadhawan, A., Hoppert, M., Dionne, M.S., and Gründling, A. (2021) EslB Is required for cell wall biosynthesis and modification in *Listeria monocytogenes*. *Journal of Bacteriology*.

Schulz, L.M., Rothe, P., Halbedel, S., Gründling, A., and Rismondo, J. (2022) Imbalance of peptidoglycan biosynthesis alters the cell surface charge of *Listeria monocytogenes*. *The Cell Surface*.

Schulz, L.M., Dreier, F., Sousa Miranda, L.M. de, and Rismondo, J. (2023) Adaptation mechanisms of *Listeria monocytogenes* to quaternary ammonium compounds. *bioRxiv*.

Additional publications

Schulz, L. M.; Konrath, A.; Rismondo, J. (2023) Physiological studies on pH and salt tolerance and the utilization of diverse carbon sources by *Listeria monocytogenes*. *bioRxiv*.



Table of contents

Chapter 1 Abstract/ Zusammenfassung	1
Chapter 2 Introduction	3
2.1 The foodborne pathogen <i>Listeria monocytogenes</i>	3
2.2 Classification of antibiotics.....	4
2.3 Cell wall biosynthesis.....	6
2.4 Peptidoglycan modification and lysozyme resistance.....	15
2.5 Cell wall hydrolases	17
2.6 Wall teichoic acid biosynthesis.....	21
2.7 Cell elongation and division	23
2.8 Tolerance to quaternary ammonium compounds	28
2.9 Aims.....	33
Chapter 3 Role of EslB in cell wall biosynthesis and lysozyme resistance	35
Chapter 4 YtrBCDEF determines cell wall thickness and competence	65
Chapter 5 Involvement of EslB in cell wall homeostasis	95
Chapter 6 QAC tolerance in <i>Listeria monocytogenes</i>	131
Chapter 7 Discussion	161
7.1 The importance of EslB in cell wall homeostasis.....	161
7.2 The putative ABC transporter EslABC.....	162
7.3 Potential role of EslB in cell wall biosynthesis.....	169
7.4 Detrimental activity of the cell wall hydrolase CwLO in the ΔesB strain	175
7.5 Suppression by restoring general cell wall homeostasis.....	177
7.6 Involvement of EslB in wall teichoic acid synthesis and modification	178
7.7 Absence of EslB leads to altered localization of cell division proteins.....	180
7.8 Conclusion and future remarks	183
7.9 Tolerance towards quaternary ammonium compounds	185
7.10 Overexpression of efflux system is the dominant mode of tolerance	185

7.11 Efflux-independent QAC tolerance	189
Chapter 8 References	191
Chapter 9 Supplementary material.....	223
9.1 Mutation F976fs in <i>mfd</i> suppresses <i>eslB</i> phenotypes.....	223
9.2 GlcNAc utilization of the $\Delta eslB$ strain.....	224
9.3 Aberrant localization of mNeonGreen-DivIVA in $\Delta eslB$	225
9.4 Interaction of OatA with the Min system.....	226
9.5 <i>E. coli</i> strains used in this study.....	227
9.6 <i>E. coli</i> strains constructed in this study	228
9.7 <i>L. monocytogenes</i> strains used in this study	233
9.8 <i>L. monocytogenes</i> strains constructed in this study	235
9.9 <i>B. subtilis</i> strains used in this study	238
9.10 <i>B. subtilis</i> strains constructed in this study	239
Curriculum vitae.....	241

Chapter 1 | Abstract/ Zusammenfassung

Listeria monocytogenes is one of the most successful food-borne pathogens worldwide. Despite available treatment with cell wall targeting antibiotics an infection with concomitant development of listeriosis results in death in approximately 13% of the cases. Hence, the cell wall has been subject to extensive studies due to its potential as a target for novel drugs. Nevertheless, various involved factors are still uncharacterized, and how the associated pathways are interconnected and communicate with each other remains elusive. *L. monocytogenes* outbreaks are often associated with strains that are tolerant towards quaternary ammonium compounds (QAC), the active agent in disinfectants, which is commonly applied to prevent contamination. The underlying genomics of QAC adaptation are poorly understood and studies often solely focus on tolerance towards benzalkonium chloride (BAC). In our study we employed an intensive in-depth suppressor screen to A) investigate the potential role of the putative ABC transporter EslABC in cell wall biosynthesis, lysozyme resistance and cell division and B) identify mechanisms that confer tolerance towards the two QACs BAC and cetyltrimethylammonium bromide (CTAB). The identification of mutations in a strain lacking the transmembrane protein EslB revealed an involvement of the transporter in several processes associated with cell wall homeostasis. Phenotypic defects of the $\Delta es/B$ strain, such as sensitivity towards lysozyme or a cell division defect, could be rescued via different mechanisms, including increased production of peptidoglycan (PG) biosynthesis as well as reduced PG hydrolysis. We hypothesised that the phenotypes are a consequence of a combination of several disrupted processes associated with cell wall homeostasis that potentially result from altered levels or availability of UDP-GlcNAc. This is demonstrated by reduced PG levels established in a thinner cell wall, as well as an overall more negative surface charge that enables increased binding and activity of cationic compounds such as lysozyme and hydrolases. Altogether EslB is a prime example which demonstrates that the loss of a single factor can have implementations on various crucial processes, highlighting the intricate nature of communication and harmonization of cell wall associated pathways. The second part of the thesis revealed that the EGD-e wildtype strain readily adapts to BAC and CTAB stress predominantly via mutations that result in overexpression of the efflux systems FepA and SugE1/2, respectively. FepA seems to have a higher affinity for BAC, while SugE1/2 is the main system for CTAB tolerance. Interestingly, *fepA* associated mutations additionally conferred resistance towards gentamycin and ciprofloxacin, raising the question if it is more beneficial to use CTAB as the active agent in disinfectants to avoid cross-adaptation. Altogether, this study revealed the underlying mechanisms responsible for CTAB and BAC adaptation in *L. monocytogenes*.

Die manifeste Listeriose, die durch das Human Pathogen *Listeria monocytogenes* ausgelöst wird, führt trotz Behandlung mit Zellwandantibiotika in ca. 13% der Fälle zum Tod. Bei der Entwicklung neuartiger Medikamente steht die bakterielle Zellwand als potenzieller Angriffspunkt im Fokus. Trotz zahlreicher Studien gibt es jedoch immer noch etliche unbestimmte Faktoren und viele offene Fragen in Bezug auf das Zusammenspiel und die Abhängigkeit der verschiedenen Prozesse, die zum Aufbau der Zellwand beitragen. Zur Bekämpfung von Kontamination wird häufig auf die Verwendung von Desinfektionsmittel, die quaternäre Ammoniumverbindungen (QACs) als antimikrobiellen Wirkstoff beinhalten, zurückgegriffen. Daher stehen Ausbrüche häufig in Verbindung mit Stämmen, die eine erhöhte transiente Toleranz gegenüber QACs aufweisen. Die genomischen Variationen, die für die QAC-Adaption verantwortlich sind, werden allerdings oft nur am Rande behandelt. Mit dieser Arbeit wird das Ziel verfolgt, zum einen die Rolle des putativen ABC Transporters EslABC im Kontext der Zellwandbiosynthese, der Zellteilung und der Sensitivität gegenüber Lysozym zu beleuchten und zum anderen die zugrundeliegenden genomischen Mechanismen zu identifizieren, die für die Toleranz gegenüber den beiden QACs BAC und Cetyltrimethylammoniumbromid (CTAB) verantwortlich sind. Suppressor Mutationen, die in einem Stamm identifiziert wurden, der das Transmembranprotein EslB des Transporters nicht mehr aufweist, legen die Beteiligung des Transporters in der Zellwandhomöostase nahe. Die phänotypischen Defekte der $\Delta es/B$ Mutante, wie zum Beispiel eine erhöhte Sensitivität zu Lysozym oder ein Zellteilungsdefekt, konnten unter anderem durch reduzierte Aktivität von Zellwand Hydrolasen, oder durch erhöhte Peptidoglycan (PG) Biosynthese aufgehoben werden. Wir vermuten, dass die Phänotypen ein Resultat aus der Kombination von verschiedenen gestörten Prozessen sind, die an der Erhaltung der Zellwandhomöostase beteiligt sind. Veränderte UDP-GlcNAc Mengen, oder Verfügbarkeit, die sich durch reduzierte PG Mengen, einer damit verbundenen dünneren Zellwand, so wie eine erhöhte negative Zellladung, widerspiegelt, spielen dabei vermutlich eine ausschlaggebende Rolle. Am Beispiel von EslB wird hervorgehoben, dass der Verlust eines einzelnen Faktors Auswirkungen auf diverse grundlegende Prozesse haben kann. Diese verdeutlichen die Komplexität der Abhängigkeit, Kommunikation und Balance zwischen verschiedenen Prozessen, die einer reibungslosen Zellwandarchitektur zu Grunde liegen. In dem zweiten Teil der Arbeit konnte gezeigt werden, dass die Überproduktion von den Effluxpumpen FepA und SugE1/2, die durch Mutationen hervorgerufen wurden zur Toleranz gegenüber BAC und CTAB führen. Dabei legen die Daten nahe, dass FepA eine größere Rolle für die BAC-Toleranz spielt, während SugE1/2 wichtiger für CTAB-Anpassung sind. Da Mutationen im *fepA* Gen zusätzliche zur Resistenz gegenüber Ciprofloxacin und Gentamycin führten, ist es vermutlich ratsamer in Desinfektionsmitteln eher auf CTAB als Wirkstoff zurückzugreifen.

Chapter 2 | Introduction

Humans are surrounded by a diverse array of microorganisms, which proliferate not only in natural environments such as soil, river, or plants, but are also present for instance in kitchen sinks, on our phones or in our body. Bacteria display the largest group of microorganisms and are often associated with disease. Contrary to popular believe many bacteria are beneficial for human health, as they comprise a significant portion of the human body and aid in preventing infections by competing with pathogenic bacteria or by creating acidic environments. In addition, they are beneficial due to the production of essential vitamins such as vitamin B12 in our gut (Magnúsdóttir et al. 2015). Generally, microorganisms have adapted to proliferate in various environmental niches. Especially skilled microbes are the ones that can survive and thrive in the environment and additionally infect animals and humans. Those pathogens are often equipped with numerous virulence factors that allow survival under extreme conditions and inside the human host. Counteracting infection and preventing spread of pathogens is hence a crucial task. Understanding intricate pathways such as the composition and organization of the cell wall which is conserved in most bacteria, or resistance mechanisms that can be acquired to withstand common counter measurements is of utmost importance.

2.1 The foodborne pathogen *Listeria monocytogenes*

Listeria monocytogenes is a saprophytic, non-sporeforming, facultative anaerobe gram-positive bacterium. The pathogen is well known for its biphasic lifestyle, which allows its growth as a ubiquitous saprophyte in extracellular environments, feeding on decaying plant material, or as an intracellular pathogen in the cytosol of mammalian cells. Infection of *L. monocytogenes* is commonly caused by ingestion of contaminated foods, such as cheese (Carlin et al. 2022), processed meat (Thomas et al. 2020) or ice-cream (Rietberg et al. 2016). While an infection generally leads to a self-limiting gastroenteritis in healthy individuals, in immunocompromised individuals, such as pregnant women or the elderly, an infection can become systemic, also known as invasive listeriosis, which was reported to have a ~95% hospitalization and a ~13% fatality rate in 2021 in the EU (Allerberger and Wagner 2010; EFSA 2022). In case of severe infections, the pathogen initially gains access to internal organs by crossing the intestinal epithelium, which subsequently enables the crossing of further barriers, such as the blood-brain-barrier or the fetoplacental-barrier, potentially resulting in meningitis or infection of the foetus and in consequence to miscarriage. The spread of *L. monocytogenes* to different parts of the body is facilitated by macrophage migration, enabling evasion of the immune system (Lecuit 2007;

Bakardjiev et al. 2004; Smith et al. 2008; Drevets and Bronze 2008; Hamon et al. 2006). While invasion of macrophages is a passive process, receptor mediated endocytosis or phagocytosis of the pathogen into non-professional phagocytes requires binding of the bacterial surface proteins internalin A (InIA) and internalin B (InIB) to host cell receptors (Schubert et al. 2002). More specifically, InIA and InIB bind to the host cell epithelial-cell protein E-cadherin (Mengaud et al. 1996) and the Met receptor tyrosine kinase of the host cell, respectively (Shen et al. 2000). After internalization, the membrane bound phagosome is lysed with the help of the pore-forming toxin listeriolysin O (LLO) and the cells escape into the cytoplasm, where they surround themselves with actin filaments and divide (Cheng et al. 2017). After division, actin filaments assemble to a so-called actin tail, which allows cell to cell spread without exposure to the host immune system (Tilney and Portnoy 1989; Hamon et al. 2006). The intracellular lifestyle of *Listeria* does not only allow evasion of the immune system, but also complicates adequate antibiotic treatment. Up to date, β -lactam antibiotics, such as penicillin, ampicillin or amoxicillin, are typically used in combination with gentamycin to treat listeriosis. Even though a combined treatment is effective, ~13% of all hospitalized patients still die from infection. In addition, proper prevention of spread can help avoid infection, which is especially important in food processing environments (Temple and Nahata 2000).

2.2 Classification of antibiotics

Antibiotics are typically classified based on their mechanism of action. The biggest group of antibiotics are substances that target bacterial cell wall synthesis. This includes β -lactams, such as ampicillin or penicillin, as well as antibiotics vancomycin or bacitracin, which target different steps in cell wall biosynthesis (Watanakunakorn 1984; Stone and Strominger 1971). Moreover, antibiotics such as polymyxins target the cell membrane. In addition, some antibiotics interfere with protein biosynthesis by inhibiting the 30S or 50S subunit of the ribosome such as tetracycline and aminoglycosides like gentamycin, or clindamycin and chloramphenicol, respectively. Likewise, DNA gyrases, RNA polymerases or folate synthesis can also be the target of antibiotics (Kapoor et al. 2017). Antibiotics that were analysed during the course of this study are represented in Table 2.1 and further discussed in Chapter 2.2. Since cell wall targeting antibiotics are the treatment of choice for invasive listeriosis, the identification of novel factors involved in cell wall biosynthesis is of foremost importance.

Table 2.1 | Cell wall-targeting antibiotics and their mechanism of action.

Antibiotic	Mechanism of action	Reference
Fosfomycin	Inhibits the activity of MurA by binding to the Cys-115 residue	(Marquardt et al. 1994; Eschenburg et al. 2004)
<i>trans</i>-Cinnamaldehyde (t-Cin)	Suggested to interfere with substrate availability of the GlmSMUR pathway leading to inhibition of UDP-GlcNAc synthesis	(Sun et al. 2021b)
Ampicillin	Inhibits the transpeptidase activity of PBPs	(Kaushik et al. 2014)
Penicillin	Inhibits the transpeptidase activity of PBPs	(Yocum et al. 1980)
Moenomycin	Inhibits the glycosyltransferase activity of class A PBPs	(Huber and Neseemann 1968)
Nisin	Blocks the activity of PBPs by binding and encapsulating lipid II, which additionally promotes pore formation in the membrane	(Hsu et al. 2004; Breukink et al. 1999)
Bacitracin	Inhibits dephosphorylation of the Und-P precursor UPP, blocking Und-P synthesis and recycling	(Stone and Strominger 1971)
D-Cycloserine	Analogue of D-alanine. Sequesters the D-Ala pool by targeting Alr and Ddl	(Lambert and Neuhaus 1972; Neuhaus and Lynch 1964)
Tunicamycin	Targets WTA biosynthesis by inhibiting the activity of TarO at low concentrations. Blocks the activity of MraY, thereby inhibiting the formation of lipid I at higher concentrations	(Hakulinen et al. 2017; Pooley and Karamata 2000)
Vancomycin	Binds to the D-alanyl-D-alanine residue at the carboxylic and of the peptidoglycan precursor, thereby sterically hindering activity of PBPs	(Watanakunakorn 1984)

2.3 Cell wall biosynthesis

The cell wall is a crucial component of bacterial cells that provides support and protection against the hostile extracellular environment. The biosynthesis and assembly of the cell wall is a multifaceted process that depends on the coordinated activity of numerous enzymes and metabolic pathways. Understanding the associated underlying molecular mechanisms that are required for proper synthesis of the cell wall and for maintaining its sophisticated architecture is crucial for the development of novel strategies to combat bacterial infections, as well as for exploring the fundamental principles that are required for bacterial proliferation and survival. Hence, the cell wall has been object to research for many decades, and the interest in understanding the structure and biosynthesis has dramatically increased with the identification of penicillin as an antimicrobial agent by Alexander Fleming in 1929 (Fleming 1929). However, even though extensive research has been conducted, numerous open questions remain and novel factors that are involved are identified every day. The bacterial cell wall is a complex structure that is essential for withstanding turgor pressure for maintenance of the cell shape, and that provides protection against harmful extracellular compounds. This is partly achieved due to the incorporation of polyanionic polymers, called lipoteichoic acid (LTA) and wall teichoic acids (WTA) that contribute to the negative surface charge of the cell. The biosynthesis of its main component, peptidoglycan (murein) is a multifaceted process, which is essential for growth and division and involves a diverse range of proteins necessary for synthesis of nucleotide precursors, synthesis of lipid-linked intermediates, polymerization, transport, or hydrolysis, to only name a few (Figure 2.1). Antibiotics that inhibit peptidoglycan (PG) biosynthesis or participate in its degradation, such as the natural antimicrobial lysozyme, typically result in lysis and subsequent cell death. Thus, the identification of factors involved in cell wall biosynthesis are a great tool for the development of novel drugs (Kotnik et al. 2007; Barreteau et al. 2008). Core proteins involved in cell wall biosynthesis and maturation are listed in Table 2.1

Generally, the cell wall is composed of an intricate, multi-layered mesh of cross-linked PG, which is comprised of alternating *N*-acetylglucosamine (GlcNAc) and *N*-acetylmuramic acid (MurNAc) polymers linked by 1,4- β -glycosidic bonds. The first committed step of PG biosynthesis is often designated as the formation of UDP-MurNAc from UDP-GlcNAc, which takes place in the cytoplasm. The synthesis of UDP-GlcNAc from D-fructose-6-phosphate is generally achieved by four consecutive enzymatic reactions catalysed by GlmS, GlmM, and the bifunctional enzyme GlmU (Figure 2.1) (Kotnik et al. 2007; Barreteau et al. 2008). GlmS is a glucosamine-6-phosphate synthase, which catalyses the conversion of D-fructose-6-phosphate into D-glucosamine-6-phosphate (Badet et al. 1988; Golinelli-Pimpaneau et al. 1989). In a second step, the

phosphoglucosamine mutase GlmM converts glucosamine-6-phosphate to glucosamine-1-phosphate (Mengin-Lecreulx and van Heijenoort 1996; Jolly et al. 1999). The final two reactions are catalysed by the bifunctional enzyme GlmU and proposed to be the rate limiting steps of the GlmSMU pathway (Sun et al. 2021b; Pensinger et al. 2023). GlmU is responsible for the transfer of acetyl resulting in the formation of GlcNAc-1-P from glucosamine-1-P and the subsequent transfer of uridyl, yielding UDP-GlcNAc (Gehring et al. 1996; Mengin-Lecreulx and van Heijenoort 1994). Moreover, GlmR (Yvck) has been shown to play an essential role in the production of UDP-GlcNAc in several organisms, including *L. monocytogenes* and *Bacillus subtilis* (Patel et al. 2018; Pensinger et al. 2023). Recently its accessory uridyltransferase activity has been described in *L. monocytogenes*, where GlmR in addition to GlmU catalyses the reaction from GlcNAc-1P and UTP to UDP-GlcNAc (Pensinger et al. 2023). The data also suggest that the uridyltransferase activity of GlmR is not specific for *L. monocytogenes* but conserved in other species such as *Staphylococcus aureus* and *Mycobacterium tuberculosis*. Moreover, GlmR of *B. subtilis* was shown to bind to GlmS in bacterial two-hybrid assays and was suggested to act as an activator in absence or low levels of GlcNAc. An additional study suggested binding of UDP-GlcNAc to GlmR in dependency of an increased UDP-GlcNAc pool, thereby controlling further UDP-GlcNAc synthesis (Patel et al. 2018; Patel et al. 2023). However, the allosteric regulation of GlmS by GlmR that was proposed in *B. subtilis* could not be reproduced for GlmR of *L. monocytogenes*, indicating that the regulatory mechanism is not a conserved (Foulquier et al. 2020; Pensinger et al. 2023). The natural antimicrobial *trans*-cinnamaldehyde (*t*-Cin) was suggested to interfere with substrate availability of the GlmSMUR pathway, thereby inhibiting UDP-GlcNAc synthesis (Sun et al. 2021b).

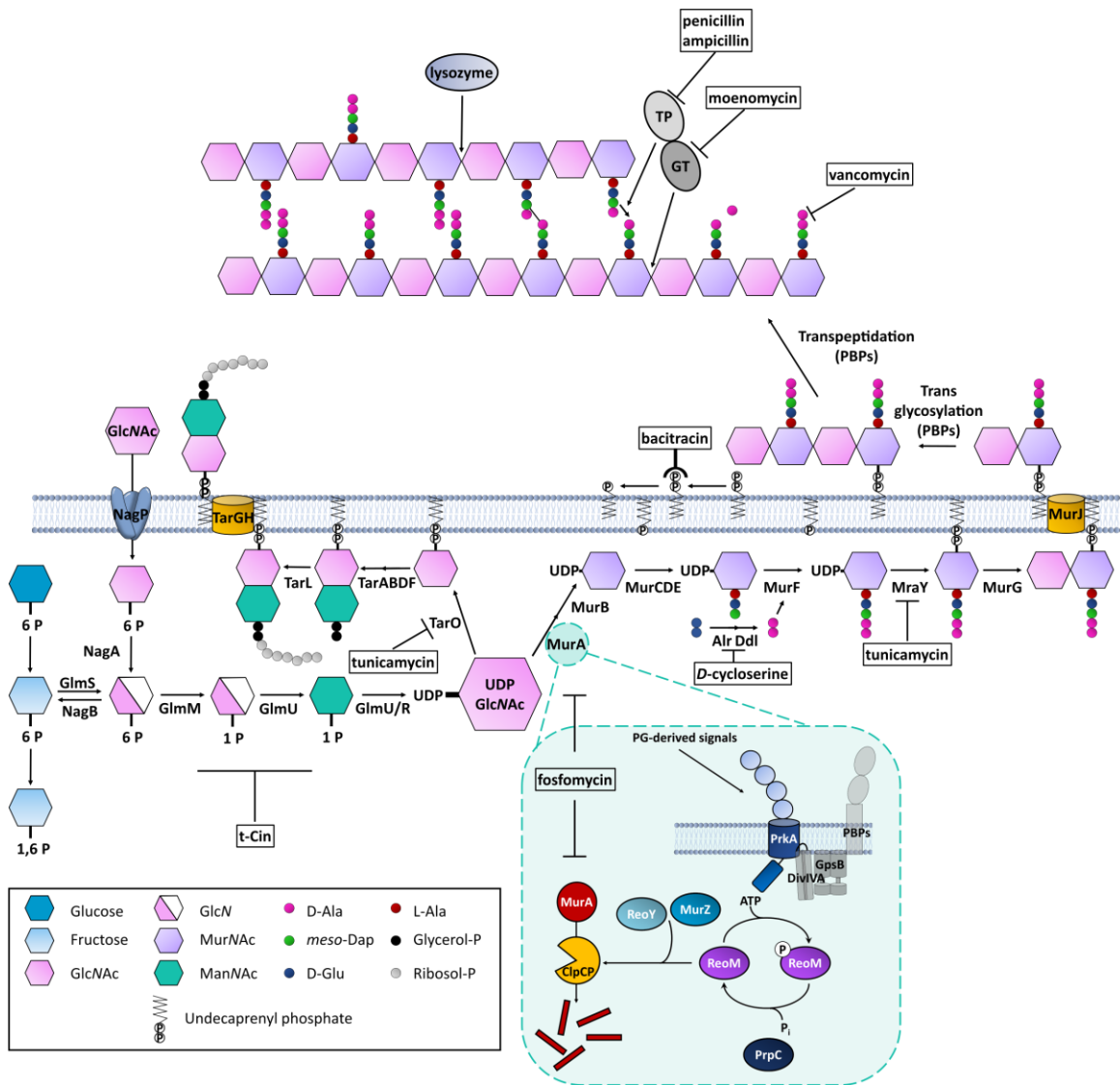


Figure 2.1 | Simplified representation of the biosynthesis of UDP-GlcNAc, peptidoglycan and wall teichoic acids. UDP-GlcNAc is a crucial precursor essential for the biosynthesis of peptidoglycan (PG) and wall teichoic acids (WTA). Synthesis is achieved in consecutive steps catalysed by GlmS, GlmM, GlmU and GlmR, using fructose-6-phosphate as a substrate. The first committed step of PG biosynthesis is catalysed by MurA and MurB, which convert UDP-GlcNAc to UDP-MurNAc. Degradation of MurA by the ClpCP protease is sophisticatedly regulated (turquoise window). ClpCP activity is stimulated by ReoY, MurZ (unknown mechanism) and dephosphorylated ReoM. The serine/threonine protein phosphatase PrpC indirectly stimulates ClpCP activity by dephosphorylating ReoM, while the serine/threonine protein kinase PrkA acts as an antagonist, by phosphorylating ReoM (Wamp et al. 2022). PrkA was proposed to respond to PG-derived signals and interact with divisome-associated proteins including DivIVA and GpsB in *B. subtilis* (Pensinger et al. 2016). UDP-MurNAc is subsequently converted into lipid II, through the action of MurCDEFG, Alr, Ddl and MraY. It is then flipped across the membrane by MurJ and incorporated and cross-linked into the growing glycan strand catalysed by glycosyltransferases (GTases) and transpeptidases (TPases), respectively (Pazos and Peters 2019). Apart from MurA, UDP-GlcNAc can also be used by TarO, the initial enzyme of the WTA biosynthesis pathway. Several enzymes are involved in the generation of the WTA polymer, which is subsequently flipped across the membrane by TarGH (Brown et al. 2013). Antibiotics are depicted in boxes (adapted from (Schulz et al. 2022)).

In the next step of PG biosynthesis, MurA (MurAA) and MurB convert UDP-GlcNAc to UDP-N-acetylmuramic acid (UDP-MurNAc) via a rather unique transfer of an *enol*pyruvyl from phosphoenolpyruvate to the 3'-hydroxyl group of UDP-GlcNAc. This reaction is, besides MurA, only carried out by one other enzyme called AroA, which is involved in the shikimic acid pathway (Barreteau et al. 2008; Walsh et al. 1996; Byczynski et al. 2003). The Cys-115 residue in the active site of MurA plays an essential role in substrate release. The antibiotic fosfomycin was shown to specifically bind to the Cys-115 residue, consequently inhibiting MurA activity and PG biosynthesis (Marquardt et al. 1994; Eschenburg et al. 2005; Eschenburg et al. 2004).

Tight regulation of the UDP-GlcNAc pool is crucial, since it is an essential precursor shared between the synthesis of lipid II and synthesis of WTA (Harrington and Baddiley 1985). By consuming UDP-GlcNAc for production of lipid II, MurA also sequesters the UDP-GlcNAc pool for WTA biosynthesis. Indeed, its regulation is a multifaceted process, including a variety of different enzymes, whose complex relationships have only recently been discovered. The ClpCP protease plays a central role in MurA degradation in *L. monocytogenes* and *B. subtilis* (Figure 2.1) (Kock et al. 2004; Birk et al. 2021). More generally, it was shown to recognize and degrade phosphoarginylated proteins in *B. subtilis*, *S. aureus* and *Mycobacterium smegmatis* (Trentini et al. 2016; Schmidt et al. 2014; Junker et al. 2018; Ogbonna et al. 2022). ClpCP in turn is regulated by several enzymes in *L. monocytogenes*, including ReoY, MurZ (MurA in *B. subtilis*) and ReoM (Wamp et al. 2020; Wamp et al. 2022). While the clear involvement of ReoY and MurZ in ClpCP-dependent proteolysis of MurA is still not fully understood, a clearer picture was recently drawn for ReoM. Dephosphorylated ReoM was shown to indirectly (proposedly via ReoY) activate ClpCP, thereby decreasing the amount of MurA in the cytoplasm (Wamp et al. 2022). Similar to ClpCP, activity of ReoM is sophisticatedly controlled by phosphorylation of the Thr-7 residue catalysed by the PASTA (penicillin-binding protein and serine/threonine-associated) kinase PrkA (deactivation) on the one hand and dephosphorylation by the phosphatase PrpC (activation) on the other hand (Wamp et al. 2020; Kelliher et al. 2021). Consequently, the MurA pool is decreased by PrpC but increased by PrkA. Several studies of PrkA homologs revealed the dependency of PG synthesis and ClpCP-dependent MurA proteolysis, as cell wall components such as muropeptides or lipid II have been shown to activate PrkA homologs in several organisms, including *M. tuberculosis*, *B. subtilis* and *S. aureus* (Mir et al. 2011; Shah et al. 2008; Hardt et al. 2017). In addition, PrkA was also shown to phosphorylate GlmR in *L. monocytogenes* and its *B. subtilis* homologue PrkC was shown to interact with divisome associated proteins such as GpsB and DivIVA (Pensinger et al. 2016). All of these regulatory steps substantiate the importance of proper control of MurA levels and activity.

In the next cytoplasmic step, a growing pentapeptide chain is added to UDP-MurNAc by members of the Mur ligase family (MurC-MurF) (Kotnik et al. 2007; Blumberg and Strominger 1974; van Heijenoort 2001; Scheffers and Pinho 2005). The pentapeptide usually consists of L-alanine and D-glutamic acid, a L-lysine at the third position that is often object to modifications, as well as the dipeptide D-Ala-D-Ala (Ghuysen 1968; Scheffers and Pinho 2005). *L. monocytogenes* has a mesodiaminopimelic acid (*meso*-DAP) at the third position, which is more characteristic, but not unique, for gram-negative bacteria. In contrast, gram-positive bacteria, typically instead contain L-Lys at the third position (Navarre and Schneewind 1999). The conversion from L-Glu and L-Ala to D-Glu and D-Ala is carried out by the two racemases RacE (MurI) and Alr, respectively. The D-alanine ligase (Ddl) then connects two D-alanine via ATP-dependent peptide bond formation, resulting in the D-Ala-D-Ala dipeptide, which is incorporated into the UDP-MurNAc-pentapeptide (Duncan et al. 1990; Barreteau et al. 2008; Kotnik et al. 2007). The antibiotic D-cycloserine is a cyclic analogue of D-alanine and hence targets both Alr and Ddl, consequently sequestering the D-Ala pool and inhibiting cell wall biosynthesis (Neuhaus and Lynch 1964; Prosser and Carvalho 2013; Lambert and Neuhaus 1972). The UDP-MurNAc-pentapeptide is finally fused to the membrane bound lipid carrier undecaprenyl phosphate (Und-P) by MraY to yield lipid I (Lovering et al. 2012). Und-P is one of the compounds shared between PG and WTA biosynthesis as it not only used by MraY for lipid I synthesis but also serves as a substrate for TarO (TagO), the first enzyme of WTA synthesis (Zhao et al. 2016; Brown et al. 2013). This again, is an example for the dependency of the two tightly connected synthesis pathways. Only about 40% of Und-P is synthesized *de novo* in gram-positive bacteria. In *B. subtilis* undecaprenyl pyrophosphate (UPP) is synthesised by UppS and subsequently dephosphorylated yielding Und-P, which then carries out its lipid carrier function. After the final glycan transfer, about 60% of the released UPP is recycled via dephosphorylation and can re-enter the cycle of PG or WTA synthesis (Figure 2.1) (Kotnik et al. 2007; El Ghachi et al. 2005; Zhao et al. 2016). Dephosphorylation of the Und-P precursor UPP can be inhibited by the polypeptide antibiotic bacitracin, thereby blocking both *de novo* synthesis and recycling (Stone and Strominger 1971). Finally, in the last step, UDP-GlcNAc is fused to lipid I at the membrane by MurG, yielding lipid II, which is then translocated across the membrane by flippases (Bouhss et al. 2008; van Heijenoort 2007).

There are several proteins that were proposed to translocate lipid II across the membrane, namely MurJ, FtsW, and Amj. MurJ was shown to be essential for translocation of lipid II *in vivo* in *Escherichia coli* (Sham et al. 2014) and was therefore suggested to be the sole flippase in the gram-negative organisms (Ruiz 2008). However, a contradicting study showed that overexpression of the cell division protein FtsW in membrane vesicles also exhibited increased lipid II translocation,

while depletion resulted in decreased, but not abolished translocation *in vitro* (Mohammadi et al. 2011; Mohammadi et al. 2014). It was suggested but not reported that FtsW is important for translocation of lipid II during cell division, while its paralog RodA carries out the same function during elongation. These findings could, however, not be supported *in vivo*. In contrast to *E. coli*, *B. subtilis* possesses, in addition to MurJ, the flippase Amj, which is overexpressed in the absence of MurJ and both flippases were shown to be synthetically lethal (Meeske et al. 2015). While MurJ and AmJ seem to be exclusively flippases, FtsW and RodA have essential functions in division and elongation, respectively, apart from the putative flippase function, further supporting the idea of MurJ being the main flippase (Sham et al. 2014; Rubino et al. 2018; Ruiz 2016; Taguchi et al. 2019). The two *murJ* homologs *Imo1624* and *Imo1624* are similarly synthetically lethal in *L. monocytogenes* (Rismondo et al., unpublished data). While the growing body of evidence suggest that MurJ is the main flippase, and due to concerns with the experimental setup of the *in vitro* experiments, so far, the flippase activity of FtsW could not be refuted. After lipid II is flipped across the membrane it is polymerized and integrated into the growing glycan strand. Integration is facilitated by the activity of glycosyltransferases and transpeptidases that are responsible for polymerization, and cross-linking of the associated pentapeptides, respectively.

These processes are carried out by penicillin-binding proteins (PBPs), which can be subdivided into high molecular weight (HMW) and low molecular weight (LMW) PBPs. HMW PBPs can be further subdivided into class A PBPs and class B PBPs. Both classes have a transpeptidase domain at the C-terminal end, facilitating the cross-linking reaction. While class B PBPs solely fulfil transpeptidase activity, class A PBPs have an additional N-terminal glycosyltransferase domain and are consequently bifunctional (Höltje 1998; Sauvage et al. 2008; Goffin and Ghuysen 1998). The N-terminal domain of class B PBPs is often involved in binding to cell division proteins like FtsN or FtsW and were thus believed to be especially important in cell division. Though, they have been shown to play a role in both division and elongation. Similar to class B PBPs, monofunctional glycosyltransferases (MGTs) have been identified in several species (Park et al. 1985; Karinou et al. 2019; Wang et al. 2001). Members of the SEDS (shape, elongation, division and sporulation) family of proteins RodA and FtsW act in a similar manner and are important for elongation and division, respectively (Meeske et al. 2016). While PBPs are generally important players in the majority of bacteria, they are often represented in variable numbers, and the function of specific PBPs can overlap but can also be rather distinctive to single organisms. (Zapun et al. 2008; Blaauwen et al. 2008; Sauvage et al. 2008). Generally, PBPs carry out their peptidase activity by targeting the D-Ala-D-Ala bond at the end of the stem peptide which subsequently causes the release of the C-terminal D-ala (Sauvage et al. 2008). The antibiotic vancomycin can likewise bind

to the D-alanyl-D-alanine at the carboxylic end of the peptidoglycan precursor, thereby sterically hindering the activity of PBPs, resulting in precursor accumulation and cell death (Figure 2.1). Apart from its primary mechanism, it has been reported that vancomycin additionally alters membrane permeability (Watanakunakorn 1984). The activity of PBPs can be additionally inhibited by the antibiotics moenomycin, penicillin or ampicillin. While moenomycin inhibits the glycosyltransferase activity of class A PBPs, penicillin and ampicillin inhibit the transpeptidase activity, thereby preventing cross-linking (Figure 2.1) (Huber and Neesemann 1968; Yocum et al. 1980). Moreover, the antibiotic nisin blocks the activity of PBPs by binding and encapsulating lipid II, which subsequently promotes pore formation in the membrane (Hsu et al. 2004; Breukink et al. 1999). When taking a closer look at cell wall biosynthesis it becomes clear that the process is a highly regulated, multifaceted procedure and consequently extremely energy consuming. Hence, reducing the biosynthesis process, by recycling old peptidoglycan that is shed of by hydrolysis reduces the energy cost of the cell considerably. Indeed, PG turnover was detected in several organisms, including *Bacillus*, *Lactobacillus*, *Listeria*, *Staphylococcus*, and *Escherichia* strains (Johnson et al. 2013; Borisova et al. 2016) and communication between hydrolysis of old peptidoglycan from the outer layer and incorporation of newly synthesised PG needs to be tightly controlled to avoid cell wall attenuation and lysis (Sugai et al. 1997; Rohde 2019).

Table 2.2 | Proteins involved in cell wall biosynthesis and maturation.

Protein	Annotation	Function	Reference
Cell wall biosynthesis and maturation – peptidoglycan biosynthesis			
GlmS	Glucosamine-6-phosphate mutase	Important for the biosynthesis of UDP-GlcNAc Catalyses the conversion of D-fructose-6-P to D-glucosamine-6-P	(Badet et al. 1988; Golinelli-Pimpaneau et al. 1989)
GlmM	Phosphoglucosamine mutase	Important for the biosynthesis of UDP-GlcNAc. Converts glucosamine-6-P to glucosamine-1-P	(Mengin-Lecreux and van Heijenoort 1996; Jolly et al. 1999)
GlmU	1-phosphate uridyltransferase	Important for the biosynthesis of UDP-GlcNAc. Converts glucosamine-1-P to GlcNAc-1-P and subsequently to UDP-GlcNAc via an uridyl transfer	(Sun et al. 2021b; Pensinger et al. 2021)
GlmR	Putative uridyltransferase	Catalyses the reaction from GlcNAc-1-P to UDP-GlcNAc via an uridyl transfer in <i>L. monocytogenes</i>	(Pensinger et al. 2021; Patel et al. 2023; Patel et al. 2018)

		GlmR of <i>B. subtilis</i> was shown to bind and activate GlmS in absence of UDP-GlcNAc	
MurA	UDP- <i>N</i> -acetylglucosamine 1-carboxyvinyltransferase	Catalyses together with MurB the conversion from UDP-GlcNAc to UDP-MurNAc	(Barreteau et al. 2008)
MurB	UDP- <i>N</i> -acetylenolpyruvoylglucosamine reductase	Catalysis together with MurA the conversion from UDP-GlcNAc to UDP-MurNAc	(Barreteau et al. 2008)
MurC	UDP- <i>N</i> -acetylmuramoyl- <i>L</i> -alanine synthase	Catalysis together with MurDEF the addition of the pentapeptide chain to UDP-MurNAc	(Liger et al. 1995)
MurD	UDP- <i>N</i> -acetylmuramoyl- <i>L</i> -alanyl- <i>D</i> -glutamate synthetase	Catalysis together with MurCEF the addition of the pentapeptide chain to UDP-MurNAc	(Auger et al. 1998)
MurE	UDP- <i>N</i> -acetylmuramoyl- <i>L</i> -alanyl- <i>D</i> -glutamyl-meso-2,6-diaminopimelate synthetase	Catalysis together with MurCDF the addition of the pentapeptide chain to UDP-MurNAc	(Ito and Strominger 1973)
MurF	UDP- <i>N</i> -acetylmuramoyl- <i>L</i> -alanyl- <i>D</i> -glutamyl-meso-2,6-diaminopimeloyl- <i>D</i> -alanyl- <i>D</i> -alanine synthetase	Catalysis together with MurCDE the addition of the pentapeptide chain to UDP-MurNAc	(Duncan et al. 1990)
MurG	UDP- <i>N</i> -acetylglucosamine- <i>N</i> -acetylmuramyl-(pentapeptide) pyrophosphoryl-undecaprenol <i>N</i> -acetylglucosamine transferase	Catalyses the addition of UDP-GlcNAc to lipid I, producing lipid II	(van Heijenoort 2007)
MraY	Phosphor- <i>N</i> -acetylmuramoyl-pentapeptide-transferase	Catalyses the fusion of membrane bound undecaprenyl phosphate to UDP-MurNAc-pentapeptide	(Bouhss et al. 2004)
Alr	Alanine racemase	Catalyses the conversion of <i>L</i> -alanine to <i>D</i> -alanine	(Walsh 1989)

Ddl	<i>D</i> -alanine- <i>D</i> -alanine ligase	Connects the two <i>D</i> -alanine to form the <i>D</i> -ala- <i>D</i> -ala dipeptide which is incorporated into the UDP-MurNAc-pentapeptide	(Pederick et al. 2020)
PBPA1	Bi-functional penicillin binding protein A1	Catalyses the polymerization of the glycan chain as well as peptide cross-linking via its transglucosylase and transpeptidase domain, respectively	(Guinane et al. 2006)
ClpCP	ATP-dependent Clp protease	Recognizes and degrades phosphoarginylated proteins including MurA (shown in <i>B. subtilis</i>)	(Kock et al. 2004)
ReoY	Effector protein of MurA	Involved in ClpCP-dependent proteolysis of MurA.	(Wamp et al. 2022)
MurZ	Not annotated	Involved in ClpCP-dependent proteolysis of MurA	(Wamp et al. 2022)
ReoM	Effector protein of MurA	Dephosphorylated ReoM indirectly activates ClpCP-dependent degradation of MurA	(Wamp et al. 2022)
PrpC	phosphatase	Dephosphorylates ReoM, resulting in ClpCP-dependent proteolysis of MurA	(Wamp et al. 2020; Kelliher et al. 2021)
PrkA PrkC in <i>B. subtilis</i>	PASTA kinase	Involved in phosphorylation of ReoM in <i>L. monocytogenes</i> as well as phosphorylation of WalR, RodZ and GlmR in <i>B. subtilis</i>	(Wamp et al. 2022; Libby et al. 2015)
Amj	Potential lipid II flippase	Translocation of lipid II across the membrane.	(Meeske et al. 2015)
MurJ	Potential lipid II flippase	Translocation of lipid II across the membrane. Localizes to the division site	(Meeske et al. 2015; Sham et al. 2014)
Cell wall biosynthesis and remodelling – lysozyme sensitivity			
PgdA	<i>N</i> -deacetylase	Prevents binding of lysozyme by removing the acetyl group at the C2 position of GlcNAc	(Boneca et al. 2007)
OatA	<i>O</i> -acetyltransferase	Prevents binding (Aubry <i>et al.</i> 2011) of lysozyme by adding an acetyl group to the C6-hydroxyl residue of ManNAc Potential role of OatA homologues in cell division	(Bernard <i>et al.</i> 2012; Aubry <i>et al.</i> 2011)
Cell wall biosynthesis and remodelling – cell wall hydrolysis			
FtsE-FtsX	ATP-binding cassette transporter.	Required for CwlO hydrolase activity in <i>B. subtilis</i> . Involved in divisome assembly in <i>E. coli</i> .	(Arends <i>et al.</i> 2009; Du <i>et al.</i> 2016; Meisner <i>et al.</i> 2013)

CwIO	<i>D,L</i> - endopeptidase	Cleave between D-glutamate and <i>meso</i> -DAP of the peptidoglycan pentapeptide in <i>B. subtilis</i>	(Yamaguchi et al. 2004)
Cell wall biosynthesis and remodelling – wall teichoic acid biosynthesis			
TarO	Undecaprenyl- phosphate- GlcNAc-1- phosphate transferase	Catalyses the transfer of <i>N</i> -acetylglucosamine-1-P from UDP-GlcNAc to undecaprenyl-P to initiate formation of the linker units of WTA	(Soldo et al. 2002)
TarL	Teichoic acid ribitol-phosphate polymerase	Catalyses ribitol phosphate polymerization of the WTA backbone.	(Meredith et al. 2008)

2.4 Peptidoglycan modification and lysozyme resistance

L. monocytogenes, like many other pathogens, modifies its PG as a maturation process, to protect themselves from hydrolases such as the natural antimicrobial lysozyme or self-hydrolysis (Alexander Fleming 1922). Lysozyme is part of the humane innate immune system and universally found in the body. It targets the 1,4- β -glycosidic bond between MurNAc and GlcNAc, hence disrupting the cell wall of gram-positive bacteria causing lysis of the cell (Callewaert and Michiels 2010). In addition, its cationic attribute allows insertion and pore formation into negatively charged bacterial membranes (Figure 2.2 A). There are two proteins that are mainly responsible for cell wall modifications in *L. monocytogenes*, namely PgdA and OatA (Figure 2.2 B) (Popowska et al. 2009). The *N*-deacetylase PgdA prevents binding of lysozyme by removing the acetyl group at the C2 position of around 50% of all GlcNAc (Boneca et al. 2007). The *O*-acetyltransferase A OatA adds an acetyl group to the C6-hydroxyl MurNAc residue, thereby sterically hindering lysozyme binding (Aubry et al. 2011; Ragland and Criss 2017; Rae et al. 2011). *O*-acetylation occurs at roughly 23% of all MurNAc (Aubry et al. 2011).

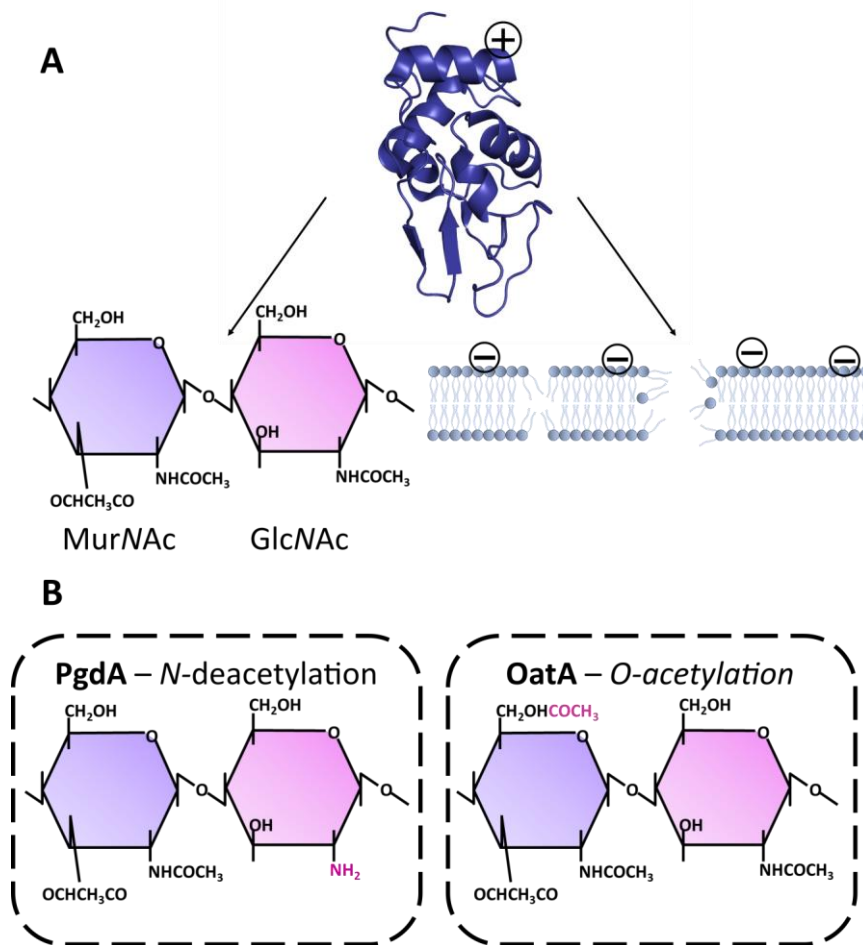


Figure 2.2 | Dual function of lysozyme and associated resistance mechanisms of *L. monocytogenes*. **A** Lysozyme cleaves the 1,4-β-glycosidic bond between MurNAc and GlcNAc (PDB ID 1GXV). As a cation it can additionally alter the permeability of the negatively charged bacterial membrane leading to formation of pores and subsequent cell lysis. **B** *L. monocytogenes* is intrinsically resistant towards lysozyme due to PG modification. Pg dA deacetylates GlcNAc at the C-2 position, while OatA is responsible for O-acetylation at the C-6 position of MurNAc (pink modification), hindering lysozyme binding (adapted from (Gálvez-Irqui et al. 2020)).

Incorporation of newly synthesised PG and subsequent maturation needs to be tightly regulated. Indeed, O-acetylation has been shown to be in close temporal relationship with the cross-linking process (Snowden et al. 1989) and likewise, a decrease in acetylation after application of penicillin has been reported for several organisms, indicating a close relationship between activity of PBPs and the O-acetylation process (Dougherty 1983; Dougherty 1985; Sychantha et al. 2018; Sidow et al. 1990; Martin and Gmeiner 1979; Bonnet et al. 2017). Similarly, bacterial two hybrid assays revealed an interaction between Pg dA and PBP A1 in *L. monocytogenes* (Rismondo et al. 2018) and PBP A1 was proposed to recruit Pg dA following polymerization and insertion of lipid II. Accordingly, a strain lacking both *pgdA* and *pbpA1*, or *oatA* and *pbpA1* were synthetically lethal (Rismondo et al. 2018). Independent from its O-acetylation function, homologs of OatA have been brought in association with cell division in several organisms. For instance, the Pat

O-acetyltransferases of *Bacillus anthracis* are necessary for daughter cell separation (Laaberki et al. 2011). OatA from *Lactobacillus plantarum* localizes at mid-cell right before membrane invaginations and an *oatA* mutant shows a defect in cell elongation. The authors hypothesised participation of OatA in the activity or positioning of the divisome (Bernard et al. 2012). Similarly, the *O*-acetyltransferase Adr from *Streptococcus pneumoniae* localizes to the division site before PG synthesis occurs. Furthermore, *adr* mutants exhibited septation defects, as well as atypical localization of the cell division protein FtsZ (Bonnet et al. 2017). All of these studies indicate a dual role of OatA in *O*-acetylation on the one site and cell division on the other site. Up to date a potential secondary role of OatA in cell division has not been investigated in *L. monocytogenes*. Apart from OatA and PgdA, several additional factors have been linked to lysozyme resistance in *L. monocytogenes* including the carboxypeptidase PbpX, the orphan response regulator DegU and the non-coding RNA Rli31 (Burke et al. 2014). A recent study revealed that a *meso*-diaminopimelic deficient strain also experiences increased susceptibility towards lysozyme, linking AsnB, the amidase that catalyses amidation of *meso*Dap to lysozyme resistance (Sun et al. 2021a). In addition, the putative ABC transporter encoded in the *Imo2769-6 operon* was previously linked to lysozyme sensitivity in a transposon screen (Burke et al. 2014; Durack et al. 2015; Toledo-Arana et al. 2009). Characterization of factors involved in lysozyme resistance, peptidoglycan biosynthesis or PG integration into the growing cell wall might shed light onto the missing link between these three highly complex processes.

2.5 Cell wall hydrolases

Cellular growth due to incorporation of newly synthesised PG and specifically elongation can only move forward by the activity of hydrolases, which cleave the already existing PG so that newly synthesized lipid II can be incorporated into the growing cell wall. In addition, opening of the cell wall also allows the incorporation and assembly of macromolecular structures such as flagella, as well as shedding of cell wall components that serve as signal molecules or pathogen associated molecular patterns to the immune system (Scheurwater et al. 2008). Different kinds of hydrolases exist that are involved in the various steps of cell wall biosynthesis, including amidases, which hydrolyse the amide bond between L-alanine and MurNAc, glycosidases, which cleave the glycosidic bond within the glycan strand or peptidases, which hydrolyse the amide bonds between the amino acids (Lee and Huang 2013; Vollmer et al. 2008; Karamanos 1997; Höltje 1996; Vermassen et al. 2019). Cell wall peptidases can be subdivided into endopeptidases, which exclusively cleave within the PG pentapeptide and carboxypeptidases that are specific to the C-terminal amino acids. (Höltje 1996; Vermassen et al. 2019). *B. subtilis* contains the two

D,L-endopeptidases CwIO and LytE. As the name implies, they specifically cleave between the L- and D-amino acids of the PG pentapeptide and have been shown to be essential for elongation (Smith et al. 2000). Similarly, *L. monocytogenes* contains the D,L-endopeptidases CwIO, as well as the uncharacterized LytM-domain containing protein Lmo2504, which might be the counterpart to LytE of *B. subtilis*. Both endopeptidases are still uncharacterised in *Listeria*. CwIO in *B. subtilis* has been shown to specifically cleave the bond between γ -D-glutamate and meso-DAP (Yamaguchi et al. 2004). Deletion of both hydrolases leads to a halt in cell elongation and subsequent cell death (Hashimoto et al. 2012). Indeed, studies have shown colocalization of LytE and the MreB isoform MreBH implying a direct connection between elongation and hydrolysis. This is supported by the fact that both *lytE* and *mreBH* mutants experience similar phenotypes (Carballido-López et al. 2006). However, a more recent study showed that LytE and CwIO do not impact movement of the elongation machinery (Meisner et al. 2013). The process of cell elongation is discussed in more detail in Chapter 2.6. While there is not a lot known about the regulation of LytE, recent studies showed transcriptional regulation of CwIO and LytE by the two component signalling system WalRK and functional regulation of CwIO by the ABC transporter FtsEX (Figure 1.3) (Meisner et al. 2013; Dobihal et al. 2022). Here, FtsEX does not seem to have a function in translocation of substrates across the membrane but is solely important for activity and localization of CwIO and both the transmembrane protein FtsX, as well as the ATP hydrolysis activity of FtsE are essential for CwIO activity. Similar to a *lytE cwIO* double mutant, the *lytE ftsEX* double mutant is synthetically lethal (Meisner et al. 2013), indicating the essentiality of FtsEX for CwIO activity. Deletion of either *cwIO* or *ftsEX* leads to a distinct phenotype, where the cells are shorter, wider and partially curved and twisted (Meisner et al. 2013; Domínguez-Cuevas et al. 2013). In *B. subtilis*, proper FtsEX-dependent regulation of CwIO is only given in the presence of the co-factors SweC and SweD (Figure 1.3 B) (Brunet et al. 2019). There are several indications that the SweCD-FtsEX-CwIO complex is associated with the cell wall elongation machinery, proposedly via interaction with the actin-like protein Mbl and the bacterial actin homologue MreB (Kawai et al. 2011; Domínguez-Cuevas et al. 2013). However, the nature of the precise relationship remains elusive. Interestingly, FtsEX of *E. coli* has been shown to interact with FtsZ and FtsA, as well as activate the cell wall hydrolase EnvC and hence is important for divisome assembly and cleavage of the septal cell wall (Du et al. 2016; Schmidt et al. 2004; Brunet et al. 2019; Yang et al. 2011), supporting the idea that FtsEX plays a somewhat similar role in *B. subtilis* or generally in gram-positive bacteria. Posttranscriptional regulation of hydrolases via for instance interaction of FtsEX and CwIO allows a way faster response to aberrant hydrolase activity than pure transcriptional regulation. Interestingly, the broadly conserved WalR-WalK system has a dual-regulatory role including both

transcriptional regulation of *lytE* and *cw/O*, as well as post-transcriptional regulation, allowing an accurate and rapid response (Dobihal et al. 2022; Bisicchia et al. 2007). WalRK reacts to dynamic hydrolase activity proposedly by sensing of cleavage products via the PAS-domain of the sensor histidine kinase Walk, which transphosphorylates WalR, leading to dimerization and allowing DNA binding (Dobihal et al. 2019; Takada et al. 2018). Hence, WalRK increased or decreases transcription of *lytE* and *cw/O* in respect to low and high endopeptidase activity, respectively (Dobihal et al. 2019). WalRK additionally increases the activity of LytE by controlling the expression of its inhibitor IseA (Takada et al. 2018; Yamamoto et al. 2008a), thereby allowing a more rapid response to cell wall associated changes. Interestingly, deacetylation of MurNAc by PdaC, the *B. subtilis* homologue of PgdA, reduced Cw/O- and LytE-dependent cleavage, when PG hydrolase activity is too high (Dobihal et al. 2022; Takada et al. 2018) and expression of *pdaC* is repressed by WalRK (Figure 2.3). Consequently, high hydrolase activity leads to a reduction of WalRK-dependent *pdaC* repression and consequently to increased deacetylation, which subsequently decreases Cw/O and LytE activity. Thereby, lower WalRK levels lead to decreased hydrolase activity directly by reduced expression of *cw/O* and *lytE* and more indirectly by increased expression of *pdaC* (Dobihal et al. 2022). Moreover, repression of *pdaC* was dependent on PrkC-dependent phosphorylation of WalR in *in vitro* and *in vivo* experiments (Libby et al. 2015). PrkC is the homologue of PrkA in *L. monocytogenes*, which has been shown to be involved in ClpCP dependent degradation of MurA and thus regulation of PG biosynthesis (Figure 2.1). PrkA responds to PG-derived signals, like lipid II, which may present an additional level of regulation of the WalR regulon (Dubrac et al. 2008; Wamp et al. 2020) (Chapter 2.3). In addition to sensing of extracellular cleavage products via the PAS-domain of Walk, it was proposed that the intracellular PAS domain of Walk might sense cytoplasmic intermediates of PG biosynthesis, which would allow a regulatory response towards changes that occur during cytoplasmic peptidoglycan synthesis (Dubrac et al. 2008). Apart from the regulation of *cw/O* and *pdaC*, WalR additionally positively regulates the transcription of *mreBH*, drawing a regulatory connection between hydrolase activity, cell wall modification and elongation (Huang et al. 2013). Altogether, activity of cell wall hydrolases needs to be tightly regulated and in coherence with general cell wall biosynthesis to avoid diminishing of the integrity of the cell.

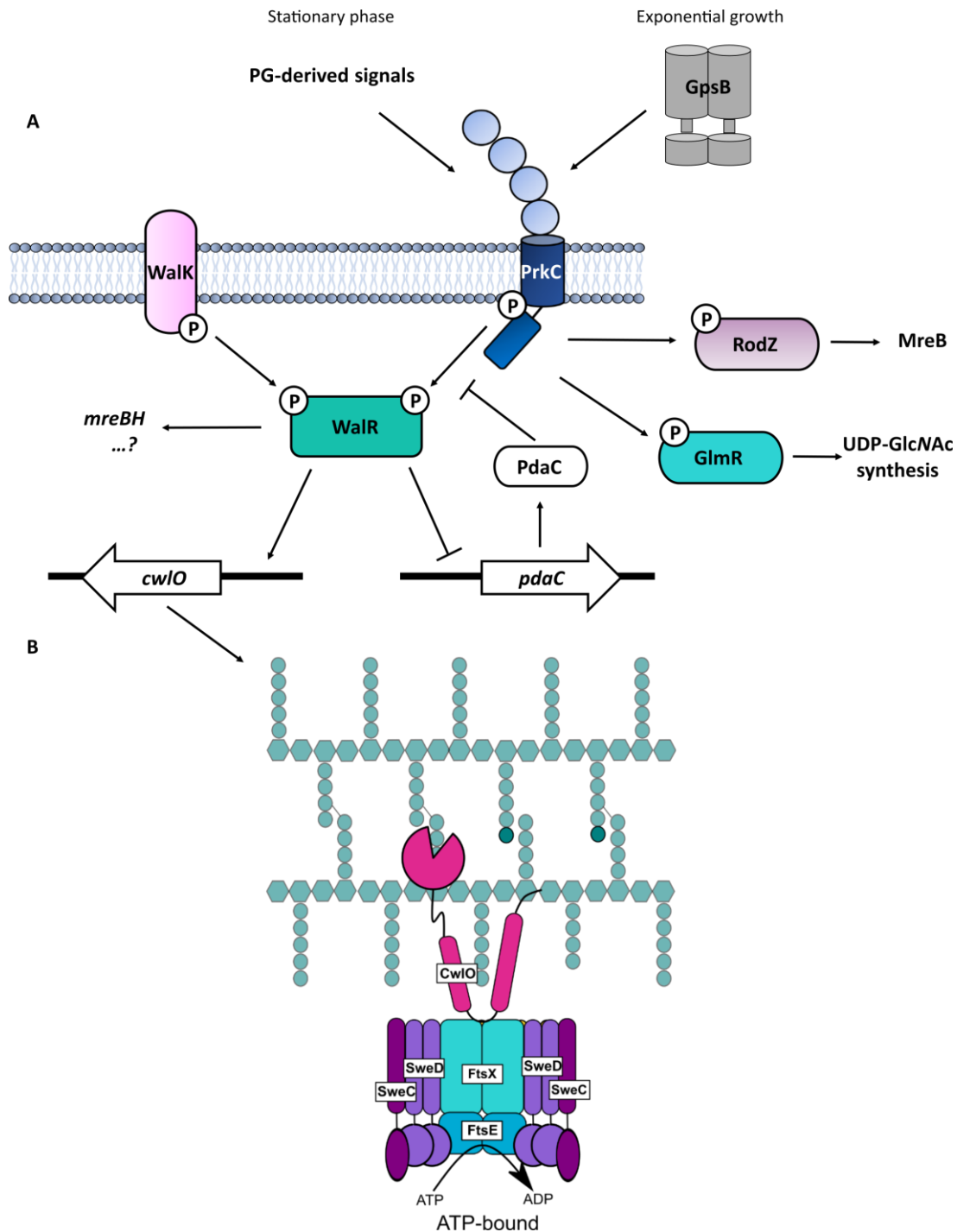


Figure 2.3 | Regulation of the cell wall hydrolase CwIO in *B. subtilis*. **A** The WalRK two-component system stimulates transcription of the cell wall hydrolases *cwIO* and *lytE* and is involved in the regulation of several additional cell wall associated factors, including *mreBH* and *pdaC* (*pgdA* in *L. monocytogenes*). WalR activity can be stimulated by phosphorylation of either Walk or PrkC (PrkA in *L. monocytogenes*). PrkC dependent phosphorylation can in turn be inhibited by PdaC. The extracellular domain of PrkC can interact with PG-derived signals, which stimulate its kinase activity. In contrast, during exponential growth PrkC localizes to the septum in a GpsB-dependent manner. **B** On protein level, the D-L-endopeptidase activity of CwIO is activated by the ABC transporter FtsEX. ATP hydrolysis dependent conformational changes of FtsX facilitates direct interaction with the cell wall hydrolase. The cofactors SweC and SweD are essential for FtsEX dependent regulation (adapted from (Libby et al. 2015; Brunet et al. 2019; Rismondo and Schulz 2021).

2.6 Wall teichoic acid biosynthesis

The peptidoglycan meshwork provides a scaffold for the integration of teichoic acids, including membrane bound lipoteichoic acids (LTAs) and wall teichoic acids (WTAs) that are covalently linked to peptidoglycan. This entails that LTA are generally buried within the peptidoglycan mesh, in contrast, WTA expand well beyond the PG layer (Reichmann and Gründling 2011; Matias and Beveridge 2007; Matias and Beveridge 2006). While the general structure of LTA are rather conserved, the structure of WTA varies even within different *L. monocytogenes* strains due to their diverse decorations (Sumrall et al. 2020; Percy et al. 2016; Shen et al. 2017). Generally, WTA consists of a disaccharide linkage unit and a polymer chain composed of either repeated glycerol-3-phosphate (GroP) units or 1,5-D-ribitol-phosphate (RboP) units (Neuhaus and Baddiley 2003). The 20-40 repeating units are linked to the PG by a linkage unit, which in case of *Listeria* consists of a glycosidic Glucose (Glc)-Glc-GroP-ManNAc-GlcNAc linkage (Figure 2.4) (Uchikawa et al. 1986). GroP units, or in case of *L. monocytogenes* and *S. aureus* repeated RboP units, are linked to the highly conserved ManNAc (β 1-4)GlcNAc 1-phosphate disaccharide linkage at the C4 oxygen of ManNAc (Neuhaus and Baddiley 2003; Kojima et al. 1985; Araki and Ito 1989; Vinogradov et al. 2006). The linker unit is connected to PG via a phosphodiester bond at the C6 hydroxyl group of MurNAc (Ward 1981; Brown et al. 2013). In *L. monocytogenes* the *O*-acetyltransferase OatA *O*-acetylates the C6 position of MurNAc to increase sensitivity towards lysozyme (Chapter 2.4). Hence, OatA and WTAs compete for the same position of the MurNAc residue in the peptidoglycan backbone. The hydroxyl of the RboP can be decorated at position 2 with D-alanine esters, or at position 4 with mono- or oligosaccharides, including glucose and GlcNAc (Neuhaus and Baddiley 2003; Vinogradov et al. 2006). In addition, type II WTAs of different *L. monocytogenes* serotypes can have further decoration attached at the GlcNAc, including glucose, galactose or *O*-acetyl groups (Sumrall et al. 2020; Shen et al. 2017). While attachment of sugar substituents is relatively permanent, D-alanylation can fluctuate in response to environmental factors such as pH, salt or temperature (Neuhaus and Baddiley 2003; Jenni and Berger-Bächi 1998; Collins et al. 2002). The phosphate rich backbone of WTA contributes to a strong negative charge and subsequently to high hydrophilicity of the cell surface (Biswas et al. 2012). Accordingly, incorporation of WTA is especially essential for the adaptation to harsh environments (Brauge et al. 2018). In *L. monocytogenes* synthesis of WTA is poorly investigated, due to the essentiality of the genes involved and due to the fact that the handling is biochemically demanding (Brown et al. 2013). However, the initial steps in biosynthesis are believed to be conserved and similar to the ones studied in *B. subtilis* and *S. aureus* (Brown et al. 2010). Enzymes involved in the WTA biosynthesis process are named according to the glycerol (teichoic acid glycerol) or ribitol (teichoic acid ribitol)

WTA backbone and are accordingly annotated as Tag or Tar enzymes in *B. subtilis* and *S. aureus*, respectively (Boylan et al. 1972). After TagO initially utilizes UDP-GlcNAc, TagABDF elongate the WTA polymer within the cytoplasm using undecaprenyl phosphate, which is like UDP-GlcNAc shuffled between WTA synthesis and PG synthesis. While TagF adds 45-60 glycerol phosphate units to the product of TagABD, TarF only adds a single ribitol-phosphate unit and the additional enzyme TarL adds more than 40 units in the following reaction (Brown et al. 2008; Meredith et al. 2008; Pereira et al. 2008).

In *L. monocytogenes* synthesis is similarly initiated by two TarO-like enzymes that utilize UDP-GlcNAc and only depletion of both inhibits WTA synthesis (Eugster and Loessner 2011). The essentiality of the later enzymes in WTA biosynthesis is proposed to arise from accumulation of toxic intermediates and due to exhaustion of undecaprenol phosphate levels that are as previously mentioned shared with PG synthesis (Brown et al. 2013; D'Elia et al. 2006). WTA synthesis can be inhibited by low concentrations of the natural antibiotic tunicamycin, which inhibits TarO activity (Figure 2.1) (Pooley and Karamata 2000; Campbell et al. 2011; Hancock et al. 1976). Interestingly, it can also block MraY at higher concentrations, the enzyme involved in fusing Und-P and UDP-MurNAc yielding lipid I during PG biosynthesis (Price and Tsvetanova 2007). Finally, the ABC (ATP-binding cassette) transporter TarGH translocates the WTA chain across the membrane (Lazarevic and Karamata 1995). During WTA maturation alanine is added to the second position of ribitol by enzymes encoded by the *dlt* operon (Kovács et al. 2006; May et al. 2005; Perego et al. 1995). The positive charge of the alanine can mask the negative charge of the phosphate backbone (Figure 2.4). Increased D-alanylation can thereby reduce the binding capacity of positively charged compounds including cell wall hydrolases or lysozymes to WTA (Heptinstall et al. 1970; Peschel et al. 2000; Yamamoto et al. 2008b). In contrast, absence of D-alanylation increases the overall negative surface charge of the cell (Vadyvaloo et al. 2004; Peschel et al. 1999). Hence, fluctuation of D-alanylation allows regulation of cell wall hydrolases and consequently impacts cell wall elongation. Indeed, loss of WTA results in a spherical cell shape in *L. monocytogenes* and *B. subtilis* (Eugster and Loessner 2012; Bhavsar et al. 2001) and many enzymes that are involved in WTA biosynthesis and PG biosynthesis interact with each other and co-localize in *B. subtilis*, underlining the tight communication and dependency of the two pathways (Kawai et al. 2011; Formstone et al. 2008). WTA impact the activity and expression of autolytic enzymes on several different levels. They do not only facilitate binding of cationic autolysins due to their negative charge, but also regulate enzyme activity by locally altering the pH (Brown et al. 2013; Biswas et al. 2012; Schlag et al. 2010).

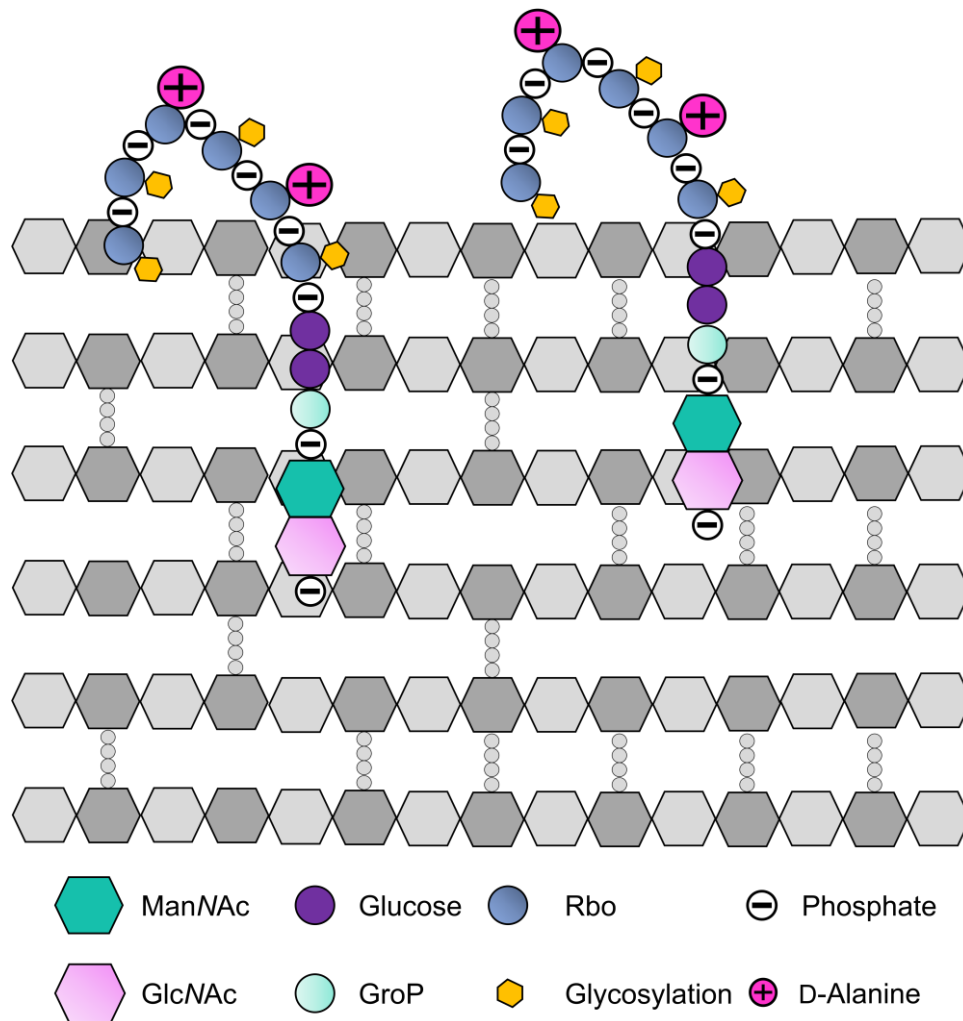


Figure 2.4 | Schematic of type I Wall teichoic acids in *L. monocytogenes*. Wall teichoic acids (WTA) are covalently linked to the C6 hydroxyl group of MurNAc in the peptidoglycan meshwork (grey) via the conserved linker unit consisting of a Glucose-Glucose-glycerol-phosphate-ManNAc-GlcNAc, connecting the 20-40 ribitol-phosphate (RboP) units to the cell wall. The ribitol backbone can be glycosylated at position 2' or 4' and/or D-alanine can be substituted as well, masking the overall negative charge of the phosphate backbone (adapted from (Sumrall et al. 2020; Brown et al. 2013)).

2.7 Cell elongation and division

Peptidoglycan synthesis is important for both elongation of the lateral wall and division of the cell into two separate daughter cells. Both processes are carried out by a multifaceted complex containing a diverse range of proteins, called the elongasome and divisome, respectively (Figure 2.5). The core proteins involved in division and elongation are listed in Table 2.3. For correct cell division, the cell does not only have to properly coordinate and organize all proteins involved in the assembly and function of the divisome but must also facilitate correct communication between the divisome, PG biosynthesis and hydrolysis. Although many proteins involved in the process have been identified, the complex interplay and hierarchies of the different factors and steps remains elusive. This is of course fortified by the fact that even though the general course

of action is somewhat conserved, the division process does not only differ between gram-negatives and gram-positives or spherical and rod-shaped bacteria, but also between different species belonging to the same category. However, the main player essential in almost all bacteria is the filamentous temperature sensitive protein FtsZ (Figure 2.5 A) (Lutkenhaus J. F.; Löwe and Amos 1998; Erickson and Osawa 2010). The tubulin homolog polymerizes into filaments, forming a ring like structure referred to as the Z-ring which marks the site of division (Erickson 1997; Lutkenhaus and Addinall 1997). The two proteins FtsA and SepF serve as anchors for the FtsZ filaments to the cell membrane (Pichoff and Lutkenhaus 2005; Duman et al. 2013). FtsZ is important for the initiation of the division process. SepF was shown to promote the stability and regulation of FtsZ filaments by repressing GTPase activity. This allows for the GTP-dependent curvature of the filaments to result in constriction of the connected membrane which later forms the new poles of the two daughter cells (Bisson-Filho et al. 2017). Treadmilling of FtsZ filaments ensure even distribution of cell wall synthesis along the septum (Caldas et al. 2019). The early cell division protein ZapA stabilizes the filament network and thereby increases the precision of Z-ring assembly (Caldas et al. 2019). Several other Zap proteins additionally stimulate Z-ring formation by connecting the filament network (Rowlett and Margolin 2013; Bisson-Filho et al. 2017).

In gram-positive bacteria, the late cell division protein DivIVA localizes to the division site by sensing membrane invaginations and proposedly forms two rings that sandwich the Z-ring (Eswaramoorthy et al. 2011; Kaval et al. 2014). It is an important recruiter for other late cell division proteins including the Min system in gram-positive bacteria (MinCDE in *E. coli* and MinCDJ in *L. monocytogenes* and *B. subtilis*, which prevents inappropriate divisome re-assembly after division is completed (Rowlett and Margolin 2013). While interactions between MinD and MinJ with DivIVA have been shown in *L. monocytogenes*, recruitment of MinJ seems to be independent of DivIVA indicating that it has a similar but not identical function in *B. subtilis* (Kaval et al. 2014). In addition, DivIVA interacts with PrkC, GpsB and EzrA in bacterial two hybrid assays (Pompeo et al. 2018; Errington and Wu 2017; Hammond et al. 2019). Similar to DivIVA, the recruitment of the late cell division protein GpsB takes place after divisome assembly is achieved (Tavares et al. 2008). It is suggested to be the direct connection between the Z-ring (divisome) and PG biosynthesis. Indeed, preliminary data suggest binding of GpsB to several involved proteins, including ZapA, SepF, EzrA, DivIB, DivIC, PBP A1, PBP A2, PBP B1, PBP B2, PBP B3, as well as MreC and MreBH in *L. monocytogenes* (Rismondo et al. 2016; Cleverley et al. 2019). In fact, it negatively controls the bifunctional protein PBP A1, thereby directly influencing the cross-linking of newly synthesised peptidoglycan building blocks (Rismondo et al. 2016; Cleverley et al. 2019; Hammond et al. 2019; Halbedel and Lewis 2019). Interestingly, GpsB is important for the direct regulation of

FtsZ in *S. aureus*, which seems to be unique to this organism (Eswara et al. 2018). Similarly, EzrA seems to be important for the communication between division and PG synthesis, and has been shown to be essential for proper localization of both FtsZ and PBPs in *B. subtilis* and *S. aureus* (Considine et al. 2011; Claessen et al. 2008; Jorge et al. 2011; Booth and Lewis 2019). Furthermore, proteins DivIB, DivIC and FtsL have been shown to be scaffolding proteins that facilitate a linkage between the Z-ring and PG biosynthesis. In *B. subtilis* MurJ is recruited by FtsL/DivIB/DivIC and is thought to display the signal that guides PG synthesis to the septum, subsequently allowing the integration of novel lipid II into the growing poles (Pinho and Errington 2005). Likewise involved are the biosynthetic proteins FtsW, PBP1 and PBP2B, yet, their exact role remains to be elucidated (Errington et al. 2003; Adams and Errington 2009; Taguchi et al. 2019). *L. monocytogenes* has two FtsW proteins (FtsW1 and FtsW2). While only FtsW1 seems to be essential, artificial overexpression of FtsW2 can compensate for the loss of FtsW1, indicating that they have a redundant function, but that FtsW1 is the main FtsW of *L. monocytogenes*. Deletion of *ftsW1* and *pbp B2* similarly result in the formation of elongated cells and hence seem to be crucial for proper cell elongation. In addition, it was proposed that FtsW2 is positively regulated by the inhibition of PBPs (Rismondo et al. 2019; Rismondo et al. 2015). In *E. coli* FtsW was suggested to control incorporation of newly synthesised lipid II. By binding to lipid II and PBP1B it shields them from the GTase activity of PBP1B and was therefore suggested to serve as a “delivery system” for lipid II after translocation across the membrane. (Leclercq et al. 2017).

The central player for elongation is the actin homologue MreB, and its paralogues MreBH and Mbl (Figure 2.5 B). MreB forms polymers facilitating ATP hydrolysis and the circumferential rotation of those polymers allows integration of newly synthesised peptidoglycan into the growing rod (Domínguez-Escobar et al. 2011; Garner et al. 2011; Errington 2015; Kawai et al. 2009). In *B. subtilis* MreBH has also been shown to be involved in regulation of the cell wall hydrolase LytE, thereby controlling insertion of lipid II into the growing strain (Chapter 2.5) (Carballido-López et al. 2006; Patel et al. 2018). In addition to MreB, MreBH and Mbl, the elongasome of *B. subtilis* also contains MreC, MreD, RodA, RodZ, PBP1, PBP2a and PbpH in *B. subtilis* (Carballido-López et al. 2006; Formstone et al. 2008). The overall motion of the elongasome is driven by the activity of RodA/PBP2 (Turner et al. 2018). MreC is anchored in the membrane and thought to regulate cross-linking by stimulating conformational changes in the non-catalytic domain of the DD-TPase PBP2, thereby positively regulating both the transpeptidase activity of PBP2 and consequentially the glycosyltransferase activity of RodA (Rohs et al. 2018; Egan et al. 2020). RodA is like FtsW a member of the SEDS (shape, elongation, division and sporulation) family of proteins (Henriques et al. 1998) and is the counterpart of FtsW in elongation. Due to its glycosyltransferase activity, it

is important for polymerization of the new peptidoglycan strands. In *B. subtilis* RodA is essential when the strain lacks class A PBPs but still shows weak activity when class B PBPs were deleted (Emami et al. 2017; Meeske et al. 2016). This is in contrast to RodA in *E. coli*, which solely required PBP2 for its glycosyltransferase activity (Rohs et al. 2018). Of the three RodA proteins of *L. monocytogenes* phenotypical changes were only observed when RodA1 was absent or in absence of all three enzymes, suggesting that this is the main enzyme in *L. monocytogenes*. Depleted cells are shorter, similar to the phenotype of cells lacking PBP B1, the elongation specific class B PBP (Rismondo et al. 2015; Rismondo et al. 2019). Recent studies also showed that the serine/threonine kinase PrkC indirectly increases MreB activity by phosphorylating RodZ (Figure 2.3). Binding to peptidoglycan precursors induces the kinase activity of PrkC and hence PrkC can adjust elongation activity based on the PG precursor pool (Ravikumar et al. 2014; Sun et al. 2023). Interestingly, in *B. subtilis* PrkC localizes to the septum during exponential growth, where it regulates GpsB activity independent of lipid II binding (Figure 1.3) (Pompeo et al. 2018; Pompeo et al. 2015; Galinier et al. 2021).

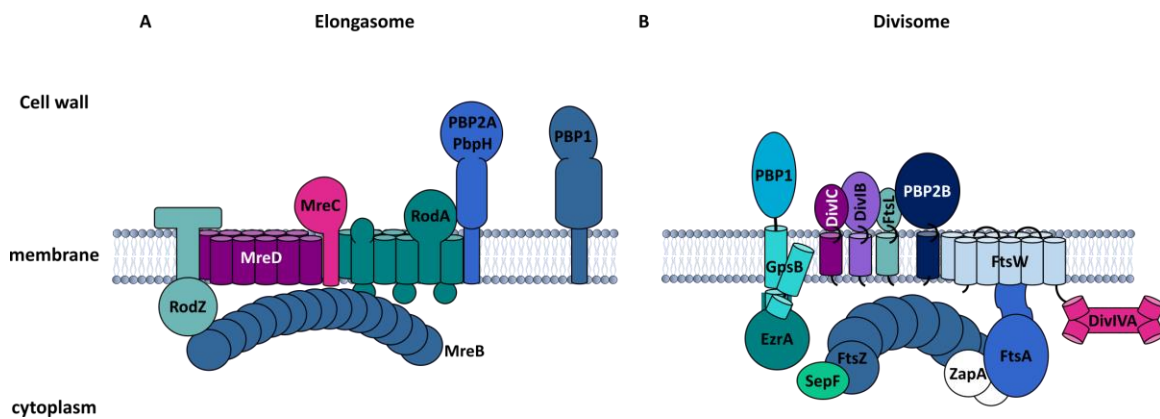


Figure 2.5 | Schematic overview of the *B. subtilis* elongasome and divisome. A Depiction of the elongasome and its involved enzymes (adapted from (Dion et al. 2019)). **B** Depiction of the divisome including associated membrane anchored and cytoplasmic proteins (adapted from (Gamba et al. 2009)).

Table 2.3 | Proteins involved in cell division and elongation. Modified from (Egan et al. 2020).

Protein	Annotation	Function	Reference
Cell division			
FtsZ	Cell division initiation protein	Master regulator of cell division; Tubulin homologue that polymerizes into filaments, forming the ring-like structure called the Z-ring	(Erickson 1997)
FtsA	Cell division protein	Membrane anchor for FtsZ; Involved in divisome initiation after the divisome is fully formed	(Pichoff and Lutkenhaus 2005)
ZapA	Z-ring-associated protein	Stabilizes FtsZ filament network to create a more ordered and persistent Z-ring	(Caldas et al. 2019)
EzrA	FtsZ-interacting protein	Negatively regulates Z-ring assembly; Proposed to connect the division process with PG biosynthesis	(Levin et al. 1999)
SepF	FtsZ-interacting protein	Similar function as FtsA; Recruits FtsZ and negatively regulates its glycosyltransferase activity; Enabling proper Z-ring assembly	(Duman et al. 2013)
GpsB	Cell cycle protein	Adapter protein for multiple cell wall proteins; Regulates the switch between lateral and septal cell wall synthesis via interactions with class A PBPs; Interacts with PrkC in <i>B. subtilis</i>	(Pompeo et al. 2015; Cleverley et al. 2019)
FtsW	(Potential lipid II flippase) Peptidoglycan polymerizing glycosyltransferase.	(Translocation of lipid II across the membrane) Integral membrane protein of the SEDS family; GTase activity when bound by its cognate PBP	(Mohammadi et al. 2014) (Taguchi et al. 2019)
DivIVA	Division site selection protein	Senses membrane invaginations and prevents Z-ring formation by recruiting the Min system; In <i>L. monocytogenes</i> it also involved in recruitment of the two autolysins P60 and NamA that are essential for separation of the daughter cells; Binds to GpsB	(Lenarcic et al. 2009; Kaval et al. 2014; Machata et al. 2005; Halbedel and Lewis 2019)
Cell elongation			
MreB (MreBH)	Actin homologue	Master-player of cell elongation. Utilizes ATP hydrolysis to form polymers; The resulting circumferential rotation allows	(Domínguez-Escobar et al. 2011; Carballido-

		integration of PG into the lateral cell wall	López et al. 2006)
MreD	Elongation protein	Unknown function; Involved in maintaining the rod-shape	(Carballido-López et al. 2006; Domínguez-Escobar et al. 2011; Leaver and Errington 2005)
MreC	Cell shape-determining protein	Membrane anchor; Potentially involved in PG-cross-linking; Binds to PBP2 and induces structural changes; Interacts with MreB and MreD	(Rohs et al. 2018; Leaver and Errington 2005)
RodA	Peptidoglycan polymerizing glycosyltransferase	Integral membrane protein of the SEDS family; Increased glycosyltransferase activity in presence of PBP2	(Emami et al. 2017; Henriques et al. 1998)
RodZ	Morphogenic protein	Scaffolding protein for the elongasome. Regulates MreB polymerization; Required for appropriate positioning of the Z-ring; Phosphorylated by PrkC in <i>B. subtilis</i>	(Alyahya et al. 2009; Sun et al. 2023)

2.8 Tolerance to quaternary ammonium compounds

To counteract infection with *L. monocytogenes*, it is not only important to identify and characterize factors involved in biosynthesis of cell wall components and its subsequent integration into the growing strain to discover new antibiotic targets, but it is equally important to look into the prevention of spread. Infection of *L. monocytogenes* commonly originates from the ingestion of contaminated ready-to-eat foods. The success of the food-borne pathogen is accomplished by its ability to withstand various harsh environmental pressures often found in food-processing plants. This includes its ability to thrive at refrigerator temperatures of 4°C and the survival of the organism at extreme temperatures between -5°C – 45°C, allowing the spread even on frozen goods such as ice-cream. In addition, it can withstand salt concentrations of up to 20%, a high range of different pH values or low water activity (Osek et al. 2022). This adaptation is of course partly due to the composition of the cell wall as discussed in the chapters above, but also due to a variety of additional adaptation mechanisms. One way to prevent the spread of *Listeria monocytogenes* and other pathogens in food-processing plants is the use of disinfectants that contain quaternary ammonium compounds (QACs), such as benzalkonium chloride (BAC) or cetyltrimethylammonium bromide (CTAB) (Gerba 2015; Nicoletti et al. 1993). Generally,

quaternary ammonium compounds consist of an ammonium ion linked to either an alkyl or aryl group. The chain length determines the activity towards bacteria and fungi. Whereas for instance a chain-length of C16 is optimal against gram-negative bacteria, a chain length of C14 is more potent against gram-positives. Hence, disinfectants often contain a mixture of quaternary ammonium compounds with varying chain length (Zinchenko et al. 2004). The charged nitrogen alters the charge distribution of the cell, while the headgroup of BAC binds to the acidic phospholipids of the membrane resulting in decreased fluidity and creation of hydrophilic cavities within the membrane (Figure 2.6) (Daoud et al. 1983; Gilbert and Al-taae 1985). The solubilization of the phospholipids eventually leads to the production of micelles containing BAC, phospholipids and contingently proteins that subsequently result in disruption of the membrane, leakage of intracellular material and cell lysis (Wessels and Ingmer 2013). Moreover, BAC is presumed to additionally bind intracellular targets such as DNA, thereby fortifying cell lysis (Wessels and Ingmer 2013; Zinchenko et al. 2004).

Enhanced tolerance towards BAC and other QACs can arise due to mishandling of disinfectants, improper dilution or storage, which has often been reported in association with pathogenic outbreaks (Weber et al. 2007). In addition, low concentration BAC contaminations have been reported in wastewater and lakes, food samples, and soil samples, creating a platform for bacteria to adapt in presence of subinhibitory concentrations (Martínez-Carballo et al. 2007; Kümmerer et al. 1997; Kreuzinger et al. 2007; Li and Brownawell 2010; EFSA 2013). Most commonly, bacteria become less ceptible by overexpressing efflux systems that allow the export of the toxic substance (Merchel Piovesan Pereira and Tagkopoulos 2019). Additional mechanisms have been described in several different organisms. For instance, *P. aeruginosa* strains were less susceptible due to alterations in phospholipid and fatty acid composition of the membrane (Sakagami et al. 1989). Similarly, *B. cereus* showed changes in fatty acid composition with concomitant altered gene expression for genes involved in fatty acid metabolism (Ceragioli et al. 2010). Prevention of the import of BAC via porins was observed in *Pseudomonas* and *E. coli*, which decreased expression of multiple porin genes (Kovacevic et al. 2016; Kim et al. 2018a; Bore et al. 2007). In addition, biofilm formation was observed to increase tolerance towards BAC to the involved community. Increased tolerance was also observed in association with a decrease in diversity in communities of organisms and resulted in cross-adaptation to penicillin, tetracycline and ciprofloxacin (Tandukar et al. 2013). Interestingly, *Pseudomonas* spp. can not only degrade BAC, but can also further use the resulting compounds as secondary substrates and energy sources (Tandukar et al. 2013; Zhang et al. 2011). Several mechanisms have been identified in isolated *L. monocytogenes* strains or in isolates that were further adapted to BAC or similar QACs (Aase et

al. 2000; Romanova et al. 2002; Soumet et al. 2005; Jiang et al. 2016; Meier et al. 2017). Overexpression of different efflux pump systems seems to be the major mode of tolerance, this includes increased expression of genes coding for QacH, BcrABC, EmrE, MdrL or FepA some of which are located on mobile genetic elements (Meier et al. 2017; Dutta et al. 2013; Müller et al. 2013; Kovacevic et al. 2016). Expression levels of *mdrL* are often used as a chromosomal marker for BAC tolerance in isolates and an allele-substituted mutant of the transporter, constructed in the *L. monocytogenes* isolate LOTM1 showed increased sensitivity towards BAC, as well as cefotaxime and EtBr (Mata et al. 2000). However, deletion of the major facilitator superfamily transporter MdrL in the EGD-e wild type did not alter the MIC towards BAC but only resulted in a growth defect in BAC-containing medium in comparison to the wildtype strain. A role in cefotaxime and EtBr export could also not be verified in this background. This raises the question if the overexpression of *mdrL* has a secondary effect in tolerant isolates (Jiang et al. 2019b). The plasmid based *bcrABC* gene, coding for the TetR transcriptional regulator BcrA and two small multidrug resistance (SMR) pumps BcrB and BcrC has been identified in association with BAC tolerance in isolated strains and was therefore named benzalkonium chloride resistance cassette (BcrABC) (Dutta et al. 2013). A chromosomal homologue of the *bcrABC* operon is encoded by *Imo0852-Imo0853-Imo0854* and was analysed in the EGD-e wild type background due to its compositional similarities. *Imo0852* codes for a TetR family regulator (SugR), while *Imo0853* and *Imo0854* code for the SMR efflux pumps SugE1 and SugE2, respectively (Jiang et al. 2020). Deletion of the two genes encoding SugE1 and SugE2 led to increased susceptibility towards BAC and other QACs, including CTAB, but showed no cross-adaptation to antibiotics or EtBr. Both SugE1 and SugE2 were overexpressed in the presence of BAC and seem to have a redundant function in BAC tolerance. The regulator SugR is a repressor of the *sug* operon in the absence of BAC (Jiang et al. 2020). The gene coding for the efflux pump QacH is located on the transposon Tn6188, which was present in 11% of 91 screened *L. monocytogenes* isolates (Müller et al. 2014; Müller et al. 2013). Deletion and complementation assays showed that QacH is indeed responsible for decreased BAC sensitivity. Moreover, cells harbouring *qacH* were not only more tolerant towards BAC but also towards EtBr and other QACs including CTAB and the gene was upregulated in presence of all of these compounds (Müller et al. 2014). The gene coding for the efflux pump EmrE was identified as part of the genomic island LGI1. In contrast to QacH, the presence of EmrE did not result in cross-adaptation to other antimicrobials or EtBr (Kovacevic et al. 2016). Two independent studies analysed isolates that were serially adapted to BAC or similar biocides and found that the majority of the adapted strains contained mutations in the gene coding for the TetR-like transcriptional regulator FepR (Bolten et al. 2022; Douarre et al. 2022). The *fepR* gene encodes the repressor of

the *fepRA* operon, coding for the regulator itself and the MATE efflux pump FepA. Various mutations have been found in either the putative DNA binding domain or the substrate binding domain of FepR, likely resulting in increased FepA production and subsequently increased BAC export. In addition, the structure of BAC was modelled into the FepR binding site (Guérin et al. 2014). Mutations in *fepR* resulted in cross-adaptation towards norfloxacin, gentamycin, ciprofloxacin, tetracycline, EtBr and other antiseptics (Guérin et al. 2014). Recent studies suggest that mutations in *fepR* are the major mode of tolerance of adapted isolates. Moreover, while various BAC sensitive strains were isolated and analysed, to our knowledge, there is no record of CTAB adapted strains. Increasing the knowledge about distinct tolerance mechanisms could provide guidance for selecting appropriate disinfectants to be used in the food industry.

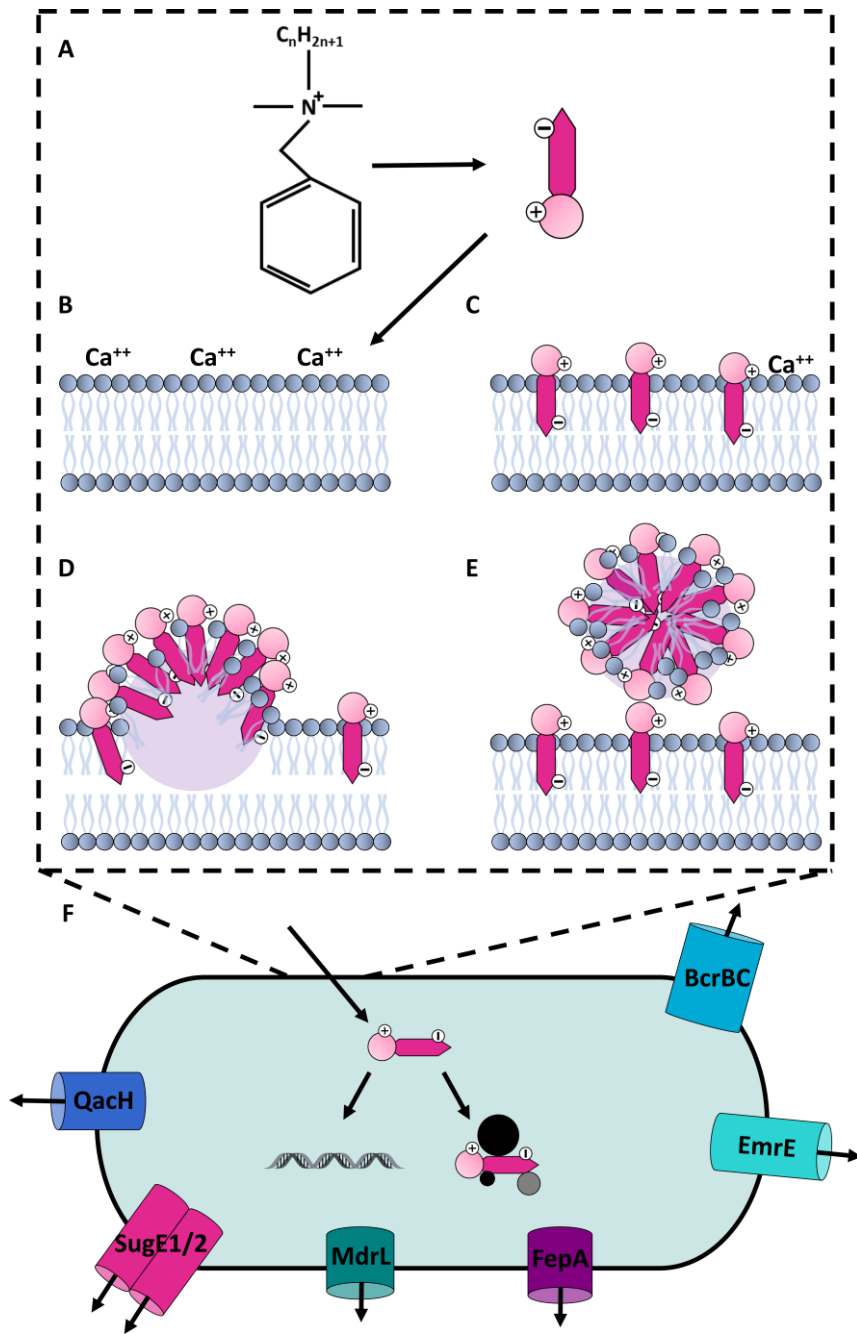


Figure 2.6 | Mode of action of benzalkonium chloride (BAC). **A** Simplified structure of BAC. The chain length (n) can vary and shows different antimicrobial activity against gram-positive and gram-negative bacteria. **B-E** The headgroup of BAC can be immersed to the acidic phospholipids of the bacterial membrane, resulting in alteration of the charge distribution. The fluidity of the bilayer is subsequently decreased, causing the creation of hydrophilic cavities (light purple), which eventually leads to solubilisation and cell lysis (adapted from (Wessels and Ingmer 2013)). **F** Apart from its primary mechanism, BAC might also bind to DNA and proteins intracellularly. Different efflux systems, which have been identified in association with BAC tolerance in *L. monocytogenes* are depicted.

2.9 Aims

L. monocytogenes is one of the most successful food-borne pathogens worldwide. Complex molecular processes and cellular structures, including the cell wall allows the bacterium to survive and thrive in a diverse range of harsh environmental conditions, including food-processing facilities and the survival in the human host. Hence, the cell wall makes up a suitable target for antibiotics. Gaining knowledge about these processes and identifying factors that are involved will aid in the prevention of spread particularly in food processing environments and the fight of infection. In this work we aimed to identify and characterize factors that play a role in cell wall associated processes or in tolerance towards disinfectants that are typically used to prevent the spread of *L. monocytogenes*. The cell wall plays an essential role in protection and survival under various environmental conditions. The biosynthesis of cell wall components, including peptidoglycan, lipoteichoic and wall teichoic acids, the subsequent integration into the growing cell wall and its modification has to be tightly regulated and involves a vast number of enzymes and protein complexes. Even though the different aspects involved in building the cell wall are studied intensively in various organisms, numerous involved factors remain partly uncharacterized and the interrelation between synthesis of peptidoglycan, its integration into the newly growing strain, hydrolysis, decoration, and modification is a complex subject with many open questions. One factor, which was recently identified in a screen for lysozyme sensitive transposon mutants, is the putative ABC transporter EslABC. *L. monocytogenes* is intrinsically resistant towards the natural antimicrobial lysozyme due to cell wall modifications. Preliminary experiments with a strain lacking the transmembrane protein Lmo2768 ($\Delta es/B$) revealed a cell division defect of the transporter mutant. This raised the question about the role of the transporter in lysozyme sensitivity, cell division and possible underlying biosynthetic mechanisms. In this work, we aimed to further characterize the $\Delta es/B$ mutant by assessing additional phenotypic differences in comparison to the *L. monocytogenes* wildtype strain and further elucidating its role in lysozyme sensitivity. One way to get a broader idea about the possible function of the transporter was to characterize $\Delta es/B$ suppressor mutants that readily evolve in presence of different stresses, such as lysozyme. Simultaneously, we aimed to describe the role of its closest homologue YtrABCDE that was recently identified in *B. subtilis* by a former PhD student. Disinfectants containing quaternary ammonium compounds (QACs) are commonly used in food processing plants. In this work, we intended to identify factors that are involved in increased tolerance towards the two QACs benzalkonium chloride (BAC) and CTAB, by evolving the *L. monocytogenes* wild type EGD-e in presence of increasing BAC and CTAB concentrations.



Chapter 3 | Role of EslB in cell wall biosynthesis and lysozyme resistance

The results described in this paper were originally published in *Journal of Bacteriology* (<https://doi.org/10.1128/JB.00553-20>):

EslB is required for cell wall biosynthesis and modification in *Listeria monocytogenes*

Jeanine Rismondo^{a,b}, Lisa M. Schulz^b, Maria Yacoub^a, Ashima Wadhawan^c, Michael Hoppert^b, Marc S. Dionne^c, Angelika Gründling^{a,#}

^a Section of Molecular Microbiology and Medical Research Council Centre for Molecular Bacteriology and Infection, Imperial College London, London SW7 2AZ.

^b Department of General Microbiology, GZMB, Georg-August-University Göttingen, 37077 Göttingen, Germany

^c Department of Life Sciences, Medical Research Council Centre for Molecular Bacteriology and Infection, Imperial College London, London SW7 2AZ.

Author contributions

AG and JR conceived the study. AG, JR, LMS and MSD designed the experiments. JR, LMS, MY and AW carried out the experiments. MH provided excess and guidance for the TEM. JR and MY carried-out MIC and virulence assays. JR constructed the *eslB* mutants and complementation strains. LMS constructed the *eslA* and *eslC* mutant strains, the respective complementation strains and the mNeonGreen-ZapA fusion strains. JR carried out the bacterial-two hybrid experiments, manual growth assays, autolysis assays, and peptidoglycan analysis. LMS carried out the drop dilution assay, *O*-acetylation assay, microscopy of mNeonGreen-ZapA fusion strains, as well as sample preparation, transmission electron microscopy and data analysis. JR analysed the WGS data. Fly survival assays were designed by AW and MSD and conducted by AW. AG and JR wrote the manuscript. All authors approve the manuscript. AG, JR, MSD and LMS acquired funding. JR, AG and MSD provided supervision.

Abstract

Lysozyme is an important component of the innate immune system. It functions by hydrolysing the peptidoglycan (PG) layer of bacteria. The human pathogen *Listeria monocytogenes* is intrinsically lysozyme resistant. The peptidoglycan *N*-deacetylase PgdA and *O*-acetyltransferase OatA are two known factors contributing to its lysozyme resistance. Furthermore, it was shown that the absence of components of an ABC transporter, here referred to as EslABC, leads to reduced lysozyme resistance. How its activity is linked to lysozyme resistance is still unknown. To investigate this further, a strain with a deletion in *eslB*, coding for a membrane component of the ABC transporter, was constructed in *L. monocytogenes* strain 10403S. The *eslB* mutant showed a 40-fold reduction in the minimal inhibitory concentration to lysozyme. Analysis of the PG structure revealed that the *eslB* mutant produced PG with reduced levels of *O*-acetylation. Using growth and autolysis assays, we show that the absence of EslB manifests in a growth defect in media containing high concentrations of sugars and increased endogenous cell lysis. A thinner PG layer produced by the *eslB* mutant under these growth conditions might explain these phenotypes. Furthermore, the *eslB* mutant had a noticeable cell division defect and formed elongated cells. Microscopy analysis revealed that an early cell division protein still localized in the *eslB* mutant indicating that a downstream process is perturbed. Based on our results, we hypothesize that EslB affects the biosynthesis and modification of the cell wall in *L. monocytogenes* and is thus important for the maintenance of cell wall integrity.

Importance

The ABC transporter EslABC is associated with the intrinsic lysozyme resistance of *Listeria monocytogenes*. However, the exact role of the transporter in this process and in the physiology of *L. monocytogenes* is unknown. Using different assays to characterize an *eslB* deletion strain, we found that the absence of EslB not only affects lysozyme resistance, but also endogenous cell lysis, cell wall biosynthesis, cell division and the ability of the bacterium to grow in media containing high concentrations of sugars. Our results indicate that EslB is by a yet unknown mechanism an important determinant for cell wall integrity in *L. monocytogenes*.

Introduction

Gram-positive bacteria are surrounded by a complex cell wall, which is composed of a thick layer of peptidoglycan (PG) and cell wall polymers. The bacterial cell wall is important for the maintenance of cell shape, the ability of bacteria to withstand harsh environmental conditions and to prevent cell lysis (1, 2). Due to its importance, cell wall-targeting antibiotics such as β -lactam, glycopeptide and fosfomycin antibiotics are commonly used to treat bacterial infections (3, 4). These cell-wall targeting antibiotics inhibit enzymes involved in different stages of the PG biosynthesis process or sequester substrates of these enzymes (4). Moenomycin, another cell wall-targeting antibiotic, and β -lactam antibiotics, for instance, block the glycosyltransferase and transpeptidase activity of penicillin binding proteins, respectively, which are required for the polymerization and crosslinking of the glycan strands (5-7). Peptidoglycan is also the target of the cell wall hydrolase lysozyme, which is a component of animal and human secretions such as tears and mucus. Lysozyme cleaves the glycan strands of PG by hydrolysing the 1,4- β -linkage between *N*-acetylmuramic acid (MurNAc) and *N*-acetylglucosamine (GlcNAc). This reaction leads to a loss of cell integrity and results in cell lysis (8). The intracellular human pathogen *Listeria monocytogenes* is intrinsically resistant to lysozyme due to modifications of its PG. The *N*-deacetylase PgdA deacetylates GlcNAc residues, whereas MurNAc residues are acetylated by the *O*-acetyltransferase OatA (9, 10). Consequently, deletion of either of these enzymes results in reduced lysozyme resistance (9, 10). One or both of these enzymes are also present in other bacterial pathogens and important for lysozyme resistance, such as PgdA in *Streptococcus pneumoniae*, OatA in *Staphylococcus aureus* and PgdA and OatA in *Enterococcus faecalis* (11-14). Besides enzymes that directly alter the peptidoglycan structure, a number of other factors have been shown to contribute to lysozyme resistance in diverse bacteria. For instance, the cell wall polymer wall teichoic acid and the two-component system GraRS contribute to lysozyme resistance in *S. aureus* (15, 16). In *E. faecalis*, the extracytoplasmic function sigma factor SigV is required for the upregulation of *pgdA* expression in the presence of lysozyme (11, 17). Recently, some additional factors have been identified, which contribute to the intrinsic lysozyme resistance of *L. monocytogenes* such as the predicted carboxypeptidase PbpX, the transcription factor DegU and the noncoding RNA Rli31 (18). DegU and Rli31 are involved in the regulation of *pgdA* and *pbpX* expression in *L. monocytogenes* (18). Furthermore, components of a predicted ABC transporter encoded by the *Imo2769-6* operon in *L. monocytogenes* and here referred to as *eslABCR* for elongation, sugar- and lysozyme sensitive phenotype (Fig. 1) have been associated with lysozyme resistance (18-20). An *eslB* transposon insertion mutant was also shown to be more sensitive to cefuroxime and cationic antimicrobial peptides (18).

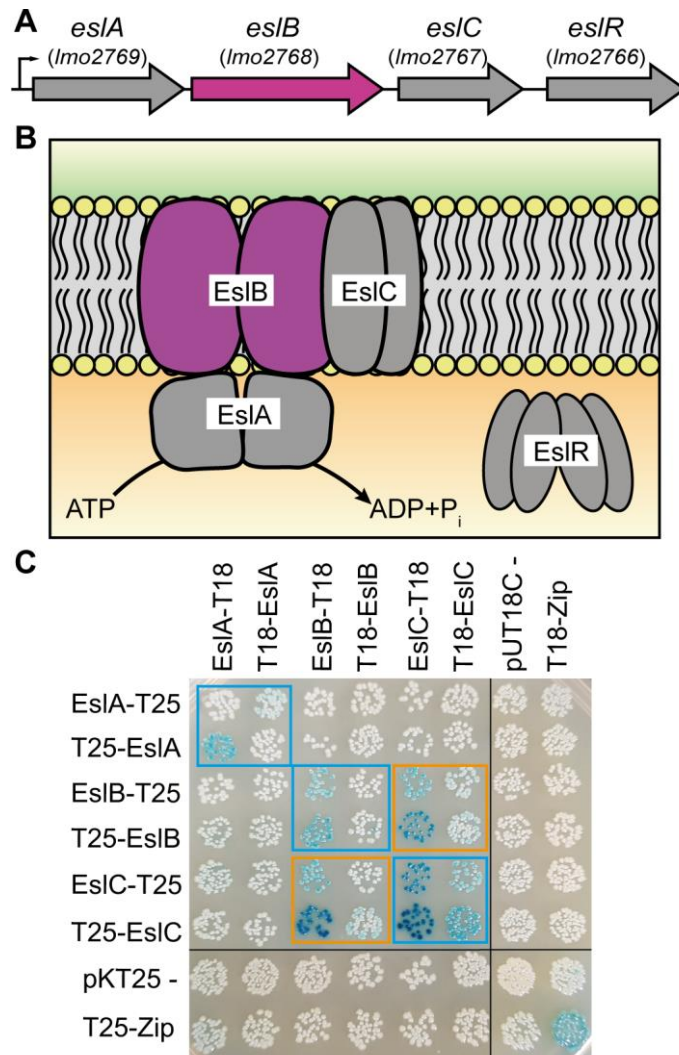


Figure 1 | Schematic representation of the *L. monocytogenes* *esIABCR* operon and interaction of the ABC transporter components EsIABC. (A) Genomic arrangement of the *esIABCR* operon in *L. monocytogenes*. Arrowheads indicate the orientation of the genes. Small black arrow indicates the promoter identified in a previous study (20). (B) Model of the ABC transporter composed of the NBD protein EsIA, which hydrolyses ATP, the TMD proteins EsIB and EsIC, and the cytoplasmic RpiR family transcription regulator EsIR. The *esIB* gene and EsIB protein, which were investigated as part of the study, are highlighted in pink. (C) Interactions between the ABC transporter components. Plasmids encoding fusions of EsIA, EsIB and EsIC and the T18- and T25-fragments of the *Bordetella pertussis* adenylate cyclase were co-transformed into *E. coli* BTH101. Empty vectors pKT25 and pUT18C were used as negative control and pKT25- and pUT18C-Zip as positive control. Black lines indicate where lanes, which were not required, were removed. Self-interactions are marked with blue boxes and protein-protein interactions with orange boxes. A representative image of three repeats is shown.

ABC transporters can either act as importers or exporters. Importers are involved in the uptake of sugars, peptides or other metabolites, which are recognized by substrate binding proteins. On the other hand, toxic compounds such as antibiotics can be exported by ABC exporters (21-23). They are usually composed of homo- or heterodimeric cytoplasmic nucleotide-binding domain (NBD) proteins, also referred to as ATP-binding cassette proteins, and homo- or heterodimeric transmembrane domain (TMD) proteins (24). In addition to NBDs and TMDs, ABC importers have

an extracellular substrate binding protein (SBP) or a membrane-integrated S-component, which are important for the delivery of specific substrate molecules to the transporter or substrate binding, respectively (25-27). The *esI* operon encodes EsIA, the NBD protein, EsIB, the TMD protein forming part of the ABC transporter, EsIC, a membrane protein of unknown function and EsIR, a RpiR-type transcriptional regulator (Fig. 1). So far, it has not been investigated whether EsIC is a component of the ABC transporter encoded in the *esI* operon. EsIB and EsIC could for instance interact with each other and form the transmembrane domain of the ABC transporter, or EsIC could function independent from EsIAB. Furthermore, it is not known whether the predicted ABC transporter EsIABC acts as an importer or exporter and its exact cellular function has not been identified. Here, we show that the absence of EsIB, one of the transmembrane components of the ABC transporter, leads to an increased lysozyme sensitivity due to an altered PG structure. In addition, deletion of *esIB* resulted in the production of a thinner cell wall, and thus to an increased endogenous cell lysis. Furthermore, cell division is perturbed in the absence of EsIB. We hypothesize that EsIB may be required for processes, which are important for the maintenance of the cell wall integrity of *L. monocytogenes* during stress conditions.

Materials and Methods

Bacterial strains and growth conditions. All strains and plasmids used in this study are listed in Table S1. *Escherichia coli* strains were grown in Luria-Bertani (LB) medium and *Listeria monocytogenes* strains in brain heart infusion (BHI) medium at 37°C unless otherwise stated. If necessary, antibiotics and supplements were added to the medium at the following concentrations: for *E. coli* cultures, ampicillin (Amp) at 100 µg/ml, chloramphenicol (Cam) at 20 µg/ml and kanamycin (Kan) at 30 µg/ml, and for *L. monocytogenes* cultures, Cam at 10 µg/ml, erythromycin (Erm) at 5 µg/ml, Kan at 30 µg/ml, nalidixic acid (Nal) at 20 µg/ml, streptomycin (Strep) at 200 µg/ml and IPTG at 1 mM.

Strain and plasmid construction. All primers used in this study are listed in Table S2. For the markerless in-frame deletion of *lmo2768* (*lmg_01927*, *esIB*), approximately 1kb-DNA fragments up- and downstream of the *esIB* gene were amplified by PCR using primer pairs ANG2532/2533 and ANG2534/2535. The resulting PCR products were fused in a second PCR using primers ANG2532/2535, the product cut with BamHI and XbaI and ligated with plasmid pKSV7 that had been cut with the same enzymes. The resulting plasmid pKSV7- Δ *esIB* was recovered in *E. coli* XL1-Blue yielding strain ANG4236. The plasmid was subsequently transformed into *L. monocytogenes*

strain 10403S and *es/B* deleted by allelic exchange using a previously described procedure (28). The deletion of *es/B* was verified by PCR. The deletion procedure was performed with two independent transformants and resulted in the construction of two independent *es/B* mutant strains 10403S Δ *es/B*₍₁₎ (ANG4275) and 10403S Δ *es/B*₍₂₎ (ANG5662). For complementation analysis, pIMK3-*es/B* was constructed, in which the expression of *es/B* can be induced by IPTG. The *es/B* gene was amplified using primer pair ANG2812/ANG2813, the product cut with NcoI and Sall and fused with pIMK3 that had been cut with the same enzymes. The resulting plasmid pIMK3-*es/B* was recovered in *E. coli* XL1-Blue yielding strain ANG4647. Due to difficulties in preparing electrocompetent cells of *L. monocytogenes es/B* mutant strains, plasmid pIMK3-*es/B* was first electroporated into the wildtype *L. monocytogenes* strain 10403S yielding strain 10403S pIMK3-*es/B* (ANG4678). In the second step, *es/B* was deleted from the genome of strain ANG4678 resulting in the construction of the first *es/B* complementation strain 10403S Δ *es/B*₍₁₎ pIMK3-*es/B* (ANG4688, short 10403S Δ *es/B*₍₁₎ compl.). In addition, complementation plasmid pPL3e-P_{esIA}-*es/ABC* was constructed. To this end, the *es/ABC* genes including the upstream promoter region were amplified by PCR using primers ANG3349/ANG3350. The resulting PCR product was cut with Sall and BamHI and fused with plasmid pPL3e that had been cut with the same enzymes. Plasmid pPL3e-P_{esIA}-*es/ABC* was recovered in *E. coli* XL1-Blue yielding strain ANG5660. Next, plasmid pPL3e-P_{esIA}-*es/ABC* was transformed into *E. coli* SM10 yielding strain ANG5661. Lastly, SM10 pPL3e-P_{esIA}-*es/ABC* was used as a donor strain to transfer plasmid pPL3e-P_{esIA}-*es/ABC* by conjugation into *L. monocytogenes* strain 10403S Δ *es/B*₍₂₎ (ANG5662) using a previously described method (29). This resulted in the construction of the second *es/B* complementation strain 10403S Δ *es/B*₍₂₎ pPL3e-P_{esIA}-*es/ABC* (ANG5663, short 10403S Δ *es/B*₍₂₎ compl.). For the markerless in-frame deletion of *lmo2769* (*lmg_01926, es/A*), and *lmo2767* (*lmg_01928, es/C*), approximately 1kb-DNA fragments up- and downstream of the corresponding gene were amplified by PCR using primer pairs LMS160/161 and LMS159/162 (*es/A*), and LMS155/158 and LMS156/157 (*es/C*). The resulting PCR products were fused in a second PCR using primers LMS159/160 (*es/A*) and LMS155/156 (*es/C*). The products were cut with BamHI and EcoRI (*es/A*) and BamHI and KpnI (*es/C*) and ligated with plasmid pKSV7 that had been cut with the same enzymes. The resulting plasmids pKSV7- Δ *es/A* and pKSV7- Δ *es/C* were recovered in *E. coli* XL1-Blue yielding strains EJR54 and EJR43, respectively. The plasmids were subsequently transformed into *L. monocytogenes* strain 10403S and *es/A* and *es/C* deleted by allelic exchange yielding strains 10403S Δ *es/A* (LJR33) and 10403S Δ *es/C* (LJR7). Plasmid pPL3e-P_{esIA}-*es/ABC* was transferred into LJR33 and LJR7 via conjugation using strain SM10 pPL3e-P_{esIA}-*es/ABC* (ANG5661) as a donor strain, yielding strains 10403S Δ *es/A* pPL3e-P_{esIA}-*es/ABC* (LJR34,

short 10403S Δ *esIA* compl.) and 10403S Δ *esIC* pPL3e-*P_{esIA}-esIABC* (LJR21, short 10403S Δ *esIC* compl.).

For the construction of bacterial two hybrid plasmids, *esIA*, *esIB* and *esIC* were amplified by PCR using primer pairs JR44/45, JR46/47 and JR48/49, respectively. The resulting *esIA* and *esIC* fragments were cut with XbaI and KpnI and ligated into pKT25, pKNT25, pUT18 and pUT18C that had been cut with the same enzymes. The *esIB* fragment was cut with XbaI and BamHI and ligated into XbaI/BamHI cut pKT25, pKNT25, pUT18 and pUT18C. The resulting plasmids were recovered in *E. coli* XL1-Blue yielding strains XL1-Blue pKNT25-*esIA* (EJR4), XL1-Blue pKT25-*esIA* (EJR5), XL1-Blue pUT18-*esIA* (EJR6), XL1-Blue pUT18C-*esIA* (EJR7), XL1-Blue pKNT25-*esIB* (EJR8), XL1-Blue pKT25-*esIB* (EJR9), XL1-Blue pUT18-*esIB* (EJR10), XL1-Blue pUT18C-*esIB* (EJR11), XL1-Blue pKNT25-*esIC* (EJR12), XL1-Blue pKT25-*esIC* (EJR13) and XL1-Blue pUT18C-*esIC* (EJR15). Using this approach, we were unable to construct pUT18-*esIC* without acquiring mutations in *esIC*. In a second attempt to generate pUT18-*esIC*, plasmid pKT25-*esIC* (from strain EJR13) was cut with XbaI and KpnI, the *esIC* fragment extracted and ligated into XbaI/KpnI cut pUT18. The resulting plasmid was recovered in *E. coli* CLG190 yielding strain CLG190 pUT18-*esIC* (EJR14).

For the localization of an early cell division protein, the N-terminus of ZapA was fused to mNeonGreen. For this purpose, *mNeonGreen* and *zapA* genes were amplified using primer pairs JR73/JR39 and JR40/JR74, respectively. The resulting PCR products were fused in a second PCR using primers JR73/JR74, the product was cut with NcoI and Sall and ligated with pIMK2 that had been cut with the same enzymes. pIMK2-*mNeonGreen-zapA* was recovered in *E. coli* XL1-Blue and transformed into *E. coli* S17-1 yielding strains EJR39 and EJR60, respectively. S17-1 pIMK2-*mNeonGreen-zapA* was used as a donor strain to transfer the plasmid pIMK2-*mNeonGreen-zapA* by conjugation into *L. monocytogenes* strains 10403S (ANG1263) and 10403S Δ *esIB*₍₂₎ (ANG5662) resulting in the construction of strains 10403S pIMK2-*mNeonGreen-zapA* (LJR28) and 10403S Δ *esIB*₍₂₎ pIMK2-*mNeonGreen-zapA* (LJR29).

Bacterial two-hybrid assays. Interactions between EsIA, EsIB and EsIC were analyzed using bacterial adenylate cyclase two-hybrid (BACTH) assays (30). For this purpose, 15 ng of the indicated pKT25/pKNT25 and pUT18/pUT18C derivatives were co-transformed into *E. coli* strain BTH101. Transformants were spotted on LB agar plates containing 25 μ g/ml kanamycin, 100 μ g/ml ampicillin, 0.5 mM IPTG and 80 μ g/ml X-Gal and the plates incubated at 30°C. Images were taken after an incubation of 48 h.

Whole genome sequencing. Genomic DNA of *L. monocytogenes* was extracted using the FastDNA™ Kit (MP Biomedicals) and libraries for sequencing were prepared using the Illumina Nextera DNA kit. The samples were sequenced at the London Institute of Medical Sciences using an Illumina MiSeq instrument and a 150 paired end Illumina kit. The reads were trimmed, mapped to the *L. monocytogenes* 10403S reference genome (NC_017544) and single nucleotide polymorphisms (SNPs) with a frequency of at least 80% and small deletions (zero coverage) identified using the CLC workbench genomics (Qiagen).

Growth analysis. *L. monocytogenes* strains were grown overnight in 5 ml BHI medium at 37°C with shaking. The next day, these cultures were used to inoculate 15 ml fresh BHI medium or BHI medium containing 0.5 M sucrose, fructose, glucose, maltose, galactose or sodium chloride to an OD₆₀₀ of 0.05. The cultures were incubated at 37°C with shaking at 180 rpm, OD₆₀₀ readings were taken every hour for 8 h.

Determination of minimal inhibitory concentration (MIC). The minimal inhibitory concentration for the cell wall-acting antibiotics penicillin and moenomycin and the cell wall hydrolase lysozyme was determined in 96-well plates using a microbroth dilution assay. Approximately 10⁴ *L. monocytogenes* cells were used to inoculate 200 µl BHI containing two-fold dilutions of the different antimicrobials. The starting antibiotic concentrations were: 0.025 µg/ml for penicillin G, 0.2 µg/ml for moenomycin and 10 mg/ml or 0.25 mg/ml for lysozyme. The 96-well plates were incubated at 37°C with shaking at 500 rpm in a plate incubator (Thermostar, BMG Labtech) and OD₆₀₀ determined after 24 hours of incubation. The MIC value refers to the antibiotic concentration at which bacterial growth was inhibited by >90%.

Plate spotting assay. Overnight cultures of the indicated *L. monocytogenes* strains were adjusted to an OD₆₀₀ of 1 and serially diluted to 10⁻⁶. 5 µl of each dilution were spotted on BHI agar plates or BHI agar plates containing 100 µg/ml lysozyme, both containing 1 mM IPTG. Images of the plates were taken after incubating them for 20-24 h at 37°C.

Peptidoglycan isolation and analysis. Overnight cultures of 10403SΔ*esB*₍₁₎ and 10403SΔ*esB*₍₁₎ compl. were diluted in 1 L BHI broth (supplemented with 1 mM IPTG for strain 10403SΔ*esB*₍₁₎ compl.) to an OD₆₀₀ of 0.06 and incubated at 37°C. At an OD₆₀₀ of 1, bacterial cultures were cooled on ice for 1h and the bacteria subsequently collected by centrifugation. The peptidoglycan was purified, digested with mutanolysin and the muropeptides analyzed by HPLC using an Agilent 1260 infinity system, as previously described (31, 32). Peptidoglycan of the wildtype *L. monocytogenes*

strain 10403S was purified and analyzed in parallel. The chromatogram of the same wild-type control strain was recently published (33) and also used as part of this study, since all strains were analyzed at the same time. The major peaks 1-6 were assigned according to previously published HPLC spectra (18, 34), with peaks 2, 4, 5 and 6 corresponding to *N*-deacetylated GlcNAc residues. Peaks 1-2 correspond to monomeric and peaks 4-6 to dimeric (crosslinked) muropeptide fragments. The Agilent Technology ChemStation software was used to integrate the areas of the main muropeptide. For quantification, the sum of the peak areas was set to 100% and the area of individual peaks was determined. The sum of values for peaks 3-6 corresponds to the % crosslinking, whereas the deacetylation state was calculated by adding up the values for peaks 4, 5 and 6. Averages values and standard deviations were calculated from three independent extractions.

O-acetylation assay. Peptidoglycan of strains 10403S, 10403S Δ es/B₍₁₎ and 10403S Δ es/B₍₁₎ compl., which had not been treated with hydrofluoric acid and alkaline phosphatase to avoid removal of the *O*-acetyl groups, was used for the *O*-acetylation assays. *O*-acetylation was measured colorimetrically according to the Hestrin method described previously (35) with slight modifications. Briefly, 800 μ g of PG (dissolved in 500 μ l H₂O) were incubated with an equal volume of 0.035 M hydroxylamine chloride in 0.75 M NaOH for 10 min at 25°C. Next, 500 μ l of 0.6 M of perchloric acid and 500 μ l of 70 mM ferric perchlorate in 0.5 M perchloric acid were added. The color change resulting from the presence of *O*-acetyl groups was quantified at 500 nm. An assay reaction with 500 μ l H₂O was used as a blank for the absorbance measurement.

Autolysis assays. *L. monocytogenes* strains were diluted in BHI or BHI medium supplemented with 0.5 M sucrose to an OD₆₀₀ of 0.05 and grown for 4 h at 37°C. Cells were collected by centrifugation and resuspended in 50 mM Tris-HCl, pH 8 to an OD₆₀₀ of 0.7-0.9 and incubated at 37°C. For penicillin- and lysozyme-induced lysis, 25 μ g/ml penicillin G or 2.5 μ g/ml lysozyme was added to the cultures. Autolysis was followed by determining OD₆₀₀ readings every 15 min.

Fluorescence and phase contrast microscopy. Overnight cultures of the indicated *L. monocytogenes* strains were diluted 1:100 in BHI medium and grown for 3 h at 37°C. For staining of the bacterial membrane, 100 μ l of these cultures were mixed with 5 μ l of 100 μ g/ml Nile red solution and incubated for 20 min at 37°C. The cells were washed twice with PBS and subsequently suspended in 50 μ l of PBS. 1-1.5 μ l of the different samples were subsequently spotted on microscope slides covered with a thin agarose film (1.5 % agarose in distilled water), air-dried and covered with a cover slip. Phase contrast and fluorescence images were taken at 1000x

magnification using the Zeiss Axio Imager.A1 microscope coupled to an AxioCam MRm and processed using the Zen 2012 software (blue edition). The Nile red fluorescence signal was detected using the Zeiss filter set 00. The length of 300 cells was measured for each experiment and the median cell length was calculated.

For ZapA-localization studies, overnight cultures of the indicated *L. monocytogenes* strains were grown in BHI medium at 37°C to an OD₆₀₀ of 0.3-0.5. The staining of the bacterial membrane with Nile red was performed as described above. After Nile red staining, cells were fixed in 1.2% paraformaldehyde for 20 min at RT. 1-1.5 µl of the different samples were spotted on microscope slides as described above. Phase contrast and fluorescence images were taken at 1000x magnification using the Zeiss Axioskop 40 coupled to an AxioCam MRm and processed using the Axio Vision software (release 4.7). The Nile red and mNeonGreen fluorescence signals were detected using the Zeiss filter set 43 and 37, respectively.

Transmission electron microscopy. Overnight cultures of *L. monocytogenes* strains 10403S, 10403S Δ esB₍₂₎ and 10403S Δ esB₍₂₎ compl. were used to inoculate 25 ml BHI broth or BHI broth supplemented with 0.5 M sucrose to an OD₆₀₀ of 0.05. Bacteria were grown at 37°C and 200 rpm for 3.5 h (BHI broth) or 6 h (BHI broth containing 0.5 M sucrose). 15 ml of the cultures were centrifuged for 10 min at 4000 rpm, the cell pellet washed twice in phosphate-buffered saline (127 mM NaCl, 2.7 mM KCl, 10 mM Na₂HPO₄, 1.8 mM KH₂PO₄, pH 7.4) and fixed overnight in 2.5 % (w/v) glutaraldehyde at 4°C. Cells were then mixed with 1.5 % (w/v, final concentration in PBS) molten Bacto-Agar, kept liquid at 55°C. After solidification, the agar block was cut into pieces with a volume of 1 mm³. A dehydration series was performed (15 % aqueous ethanol solution for 15 min, 30 %, 50 %, 70 % and 95 % for 30 min and 100 % for 2x 30 min) at 0°C, followed by an incubation step in 66 % (v/v, in ethanol) LR-white resin mixture (Plano) for 2 h at RT and embedded in 100 % LR-white solution overnight at 4°C. One agar piece was transferred to a gelatin capsule filled with fresh LR-white resin, which was subsequently polymerized at 55°C for 24 h. A milling tool (TM 60, Reichert & Jung, Vienna, Austria) was used to shape the gelatin capsule into a truncated pyramid. An ultramicrotome (Reichert Ultracut E, Leica Microsystems, Wetzlar, Germany) and a diamond knife (Delaware Diamond Knives, Wilmington, DE, USA) were used to obtain ultrathin sections (80 nm) of the samples. The resulting sections were mounted on mesh specimen grids (Plano) and stained with 4 % (w/v) uranyl acetate solution (pH 7.0) for 10 min. Microscopy was performed using a Jeol JEM 1011 transmission electron microscope (Jeol Germany GmbH, Munich) at 80 kV. Images were taken at a magnification of 30,000 and recorded with an Orius SC1000 CCD camera (Pleasanton, CA, USA). For each replicate, 20 cells were photographed and cell wall thickness was

measured at three different locations using the ImageJ software (36). The average of the three measurements was calculated and the average and standard deviation of 20 cells plotted. The experiment was performed twice.

Cell culture. Bone marrow-derived macrophages (BMMs) were extracted from female C57BL/6 mice as described previously (37). BMMs were a gift from Charlotte S. C. Michaux and Sophie Helaine. 5×10^5 BMMs were seeded per well of a 24-well plate and grown overnight in 500 μ l high glucose Dulbecco's Modified Eagle Medium (DMEM) at 37°C and 5% CO₂. *L. monocytogenes* strains were grown overnight without shaking in 2 ml BHI medium at 30°C. The next morning, bacteria were opsonized with 8% mouse serum (Sigma-Aldrich) at room temperature for 20 min and BMMs were infected for one hour at a multiplicity of infection (MOI) of 2. BMMs were washed with PBS and 1 ml DMEM containing 40 μ g/ml gentamycin was added to kill extracellular bacteria. After 1 h, cells were washed with PBS and covered with 1 ml DMEM containing 10 μ g/ml gentamycin. The number of recovered bacteria was determined 2, 4, 6 and 8 h post infection. To this end, BMMs were lysed using 1 ml PBS containing 0.1% (v/v) triton X-100 and serial dilutions were plated on BHI agar plates. The number of colony forming units (CFUs) was determined after incubating the plates overnight at 37°C. Three technical repeats were performed for each experiment and average values calculated. Average values and standard deviations from three independent experiments were plotted.

***Drosophila melanogaster* infections.** Fly injections were carried out with microinjection needles produced from borosilicate glass capillaries (World Precision Instruments TW100-4) and a needle puller (Model PC-10, Narishige). Injections were performed using a Picospritzer III system (Parker Hannifin), and the injection volume was calibrated by expelling a drop of liquid from the needle into a pot of mineral oil and halocarbon oil (both Sigma). The expelled drop was measured using the microscope graticule to obtain a final injection volume of 50 nanolitres (nl). Flies were then anesthetized with CO₂ and injected with either 50 nl of bacterial suspension in PBS or sterile PBS. 5-7-day old age matched male flies were used for all experiments. Flies were grouped into uninjected control, wounding control (injection with sterile PBS), and flies infected with *L. monocytogenes*. Each group consisted of 58-60 flies. All survival experiments were conducted at 29°C. Dead flies were counted daily. Food vials were placed horizontally to reduce the possibility of fly death from flies getting stuck to the food, and flies were transferred to fresh food every 3-4 days. For the quantification of the bacterial load, 16 flies per condition and per bacterial strain were collected at the indicated time points. The flies were homogenised in 100 μ l of TE-buffer pH

8 containing 1% Triton X-100 and 1% Proteinase K (NEB, P8107S). Homogenates were incubated for 3 h at 55°C followed by a 10 min incubation step at 95°C. Following incubation, qPCR was carried out using the *actA* gene specific primers EGD-E_ActA_L1 and EGD-E_ActA_R1 to determine the number of bacterial colony forming units. PCR was performed with Sensimix SYBR Green no-ROX (Bioline) on a Corbett Rotor-Gene 6000. The cycling conditions were as follows: Hold 95°C for 10 min, then 45 cycles of 95°C for 15 s, 57°C for 30 s, 72°C for 30 s, followed by a melting curve. Gene abundances were calculated as previously described (38).

Results

EsIC interacts with the transmembrane protein EsIB

Previously it has been shown that *L. monocytogenes* strains with mutations in the *esIABCR* operon (Fig. 1A) display decreased resistance towards the cell wall hydrolase lysozyme (18, 19). The *esI* operon encodes the ATP binding protein EsIA and the transmembrane proteins EsIB and EsIC, which are proposed to form an ABC transporter. However, it is currently unknown if EsIC forms part of the ABC transporter as depicted in Figure 1B and if it is required for the function of the transporter. To gain insights into the composition of the ABC transporter, we assessed the interaction between EsIA, EsIB and EsIC using the bacterial adenylate cyclase-based two-hybrid system. In addition to self-interactions of EsIA, EsIB and EsIC, we observed an interaction between EsIB and EsIC (Fig. 1C), indicating that EsIC might be part of the ABC transporter.

Deletion of *esIB* in *L. monocytogenes* leads to lysozyme sensitivity and an altered peptidoglycan structure.

An *esIA* in-frame deletion mutant and an *esIB* transposon insertion mutant were shown to be more sensitive to lysozyme compared to the wildtype strain (18, 19). However, it is still unknown how the function of an ABC transporter is linked to this phenotype. To investigate this further, strains with markerless in-frame deletions in *esIA*, *esIB* and *esIC* were constructed in the *L. monocytogenes* strain background 10403S. First, the lysozyme resistance of these mutants was assessed using a plate spotting assay. The *esIA* and *esIB* mutants showed reduced growth on BHI plates containing 100 µg/ml lysozyme compared to the wildtype and *esIA* and *esIB* complementation strains (Fig. 2A). On the other hand, no phenotype was observed for the *esIC* mutant (Fig. 2A). Since deletion of *esIA* and *esIB* resulted in a decreased lysozyme resistance, and an *esIA* mutant has already been characterized in previous work (19), we focused here on the characterization of the *esIB* deletion strain.

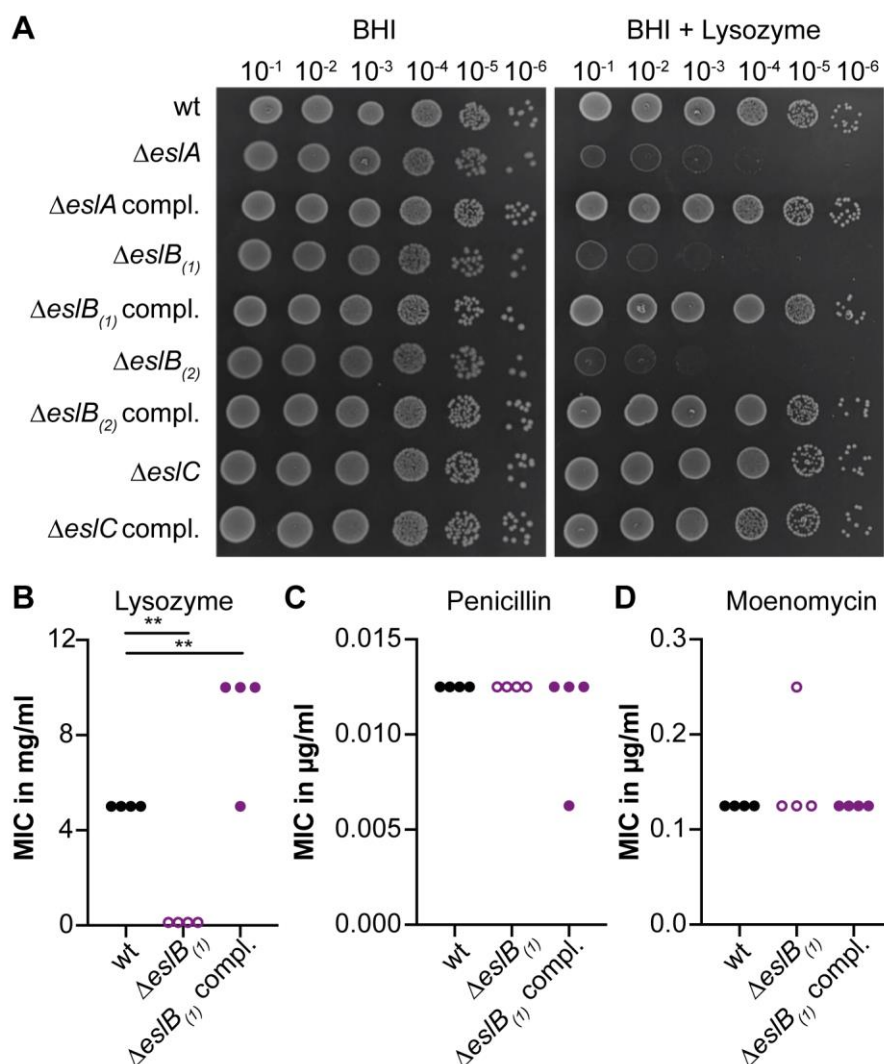


Figure 2 | Impact of *esB* deletion on resistance towards cell wall-targeting antimicrobials. (A) Plate spotting assay. Dilutions of overnight cultures of *L. monocytogenes* strains 10403S (wt), 10403S $\Delta es/A$, 10403S $\Delta es/A$ compl., 10403S $\Delta es/B_{(1)}$, 10403S $\Delta es/B_{(1)}$ compl., 10403S $\Delta es/B_{(2)}$, 10403S $\Delta es/B_{(2)}$ compl., 10403S $\Delta es/C$, and 10403S $\Delta es/C$ compl. were spotted on BHI plates and BHI plates containing 100 μ g/ml lysozyme, both supplemented with 1 mM IPTG. A representative result from three independent experiments is shown. (B-D) Minimal inhibitory concentration (MIC) of *L. monocytogenes* strains 10403S (wt), 10403S $\Delta es/B_{(1)}$ and 10403S $\Delta es/B_{(1)}$ compl. towards (B) lysozyme, (C) penicillin G and (D) moenomycin. Strain 10403S $\Delta es/B_{(1)}$ compl. was grown in the presence of 1 mM IPTG. The results of four independent experiments are shown. For statistical analysis, a one-way ANOVA followed by a Dunnett's multiple comparisons test was used (** $p \leq 0.01$).

In the course of the study, we determined the genome sequence of the originally constructed *esB* mutant (10403S $\Delta es/B_{(1)}$) by whole genome sequencing (WGS) and identified an additional small deletion in gene *lmo2396* coding for an internalin protein with a leucine-rich repeat (LRR) and a mucin-binding domain (Table S3). While to the best of our knowledge, the contribution of *Lmo2396* to the growth and pathogenicity of *L. monocytogenes* has not yet been investigated, other internalins are important and well-established virulence factors (39, 40). Our WGS analysis also revealed a single point mutation in gene *lmo2342*, coding for a pseudouridylylase in

the complementation strain 10403S Δ *esB*₍₁₎ compl. (Table S3). Since we identified an additional mutation in a gene coding for a potential virulence factor in the *esB* mutant, we constructed a second independent *esB* mutant, 10403S Δ *esB*₍₂₎. We also constructed a second complementation strain, strain 10403S Δ *esB*₍₂₎ *P*_{*esIA*}-*esIABC* (or short 10403S Δ *esB*₍₂₎ compl.), in which the *esIABC* genes are expressed from the native *esIA* promoter from a chromosomally integrated plasmid. Our WGS analysis revealed that strain 10403S Δ *esB*₍₂₎ did not contain any secondary mutations (Table S3). A 1-bp deletion in gene *Imo2022* encoding a predicted NifS-like protein required for NAD biosynthesis, was identified in strain 10403S Δ *esB*₍₂₎ compl. (Table S3), which if non-complementable phenotypes are observed needs to be kept in mind. We confirmed that our second *esB* mutant strain 10403S Δ *esB*₍₂₎ showed the same lysozyme sensitivity phenotype and that this phenotype could be complemented in strain 10403S Δ *esB*₍₂₎ compl., in which *esB* is expressed along with *esIA* and *esIC* from its native promoter (Fig. 2A). Since we only identified the genomic alterations in the course of the study, some experiments were performed as stated in the text with the original *esB* mutant and complementation strains 10403S Δ *esB*₍₁₎ and 10403S Δ *esB*₍₁₎ compl., while other experiments were conducted with strains 10403S Δ *esB*₍₂₎ and 10403S Δ *esB*₍₂₎ compl.

Using microbroth dilution assays, we observed a 40-fold lower MIC for lysozyme for *L. monocytogenes* strain 10403S Δ *esB*₍₁₎ as compared to the wildtype strain (Fig. 2B and S1A) (18, 19). This phenotype could be complemented and strain 10403S Δ *esB*₍₁₎ compl., in which *esB* is expressed from an IPTG-inducible promoter, is even slightly more resistant to lysozyme as compared to the wildtype strain (Fig. 2B). Next, we tested whether the resistance towards two cell wall-targeting antibiotics, namely penicillin and moenomycin, is changed upon deletion of *esB*. The MIC values obtained for the wildtype, *esB* deletion and *esB* complementation strains were comparable (Fig. 2C-D), suggesting that the deletion of *esB* does not lead to a general sensitivity to all cell wall-acting antimicrobials but is specific to lysozyme. In *L. monocytogenes*, lysozyme resistance is achieved by the modification of the peptidoglycan (PG) by *N*-deacetylation via PgdA and *O*-acetylation via OatA (9, 10). To assess whether deletion of *esB* affects the *N*-deacetylation and crosslinking of PG, PG was isolated from wildtype 10403S, the *esB* deletion and complementation strains, digested with mutanolysin and the muropeptides analyzed by high performance liquid chromatography (HPLC). This analysis revealed a slight increase in PG crosslinking in the *esB* mutant strain (68 \pm 0.53%) compared to the wildtype (65.47 \pm 0.31%) and the complementation strain grown in the presence of IPTG (64.57 \pm 2.3%) (Fig. 3A-B). The GlcNAc residues of the PG isolated from the *esB* deletion strain were also slightly more deacetylated (71.54 \pm 0.21%) as compared to the wildtype (67.17 \pm 0.31%) and the complementation strain

(67±2.27%) (Fig. 3A-B), which should theoretically result in an increase and not decrease in lysozyme resistance.

While only *N*-deacetylation can be assessed by the PG analysis described above, *O*-acetylation has also been shown to contribute to lysozyme resistance. Indeed, in *Neisseria gonorrhoeae* and *Proteus mirabilis*, a correlation with the degree of *O*-acetylation and lysozyme resistance has been reported (41, 42) When we assessed the degree of *O*-acetylation using a colorimetric assay, the PG isolated from the *esIB* mutant was less *O*-acetylated compared to the wildtype and the complementation strain, suggesting that reduced *O*-acetylation of the PG might contribute to the reduced lysozyme resistance of the *esIB* mutant strain (Fig. 3C). However, while the *esIB* complementation strain displayed even slightly higher lysozyme resistance compared to the wildtype strain (Fig. 2B), the degree of *O*-acetylation was not fully restored to wildtype levels in the complementation strain. This suggests that additional factors besides *O*-acetylation might be altered in the *esIB* mutant.

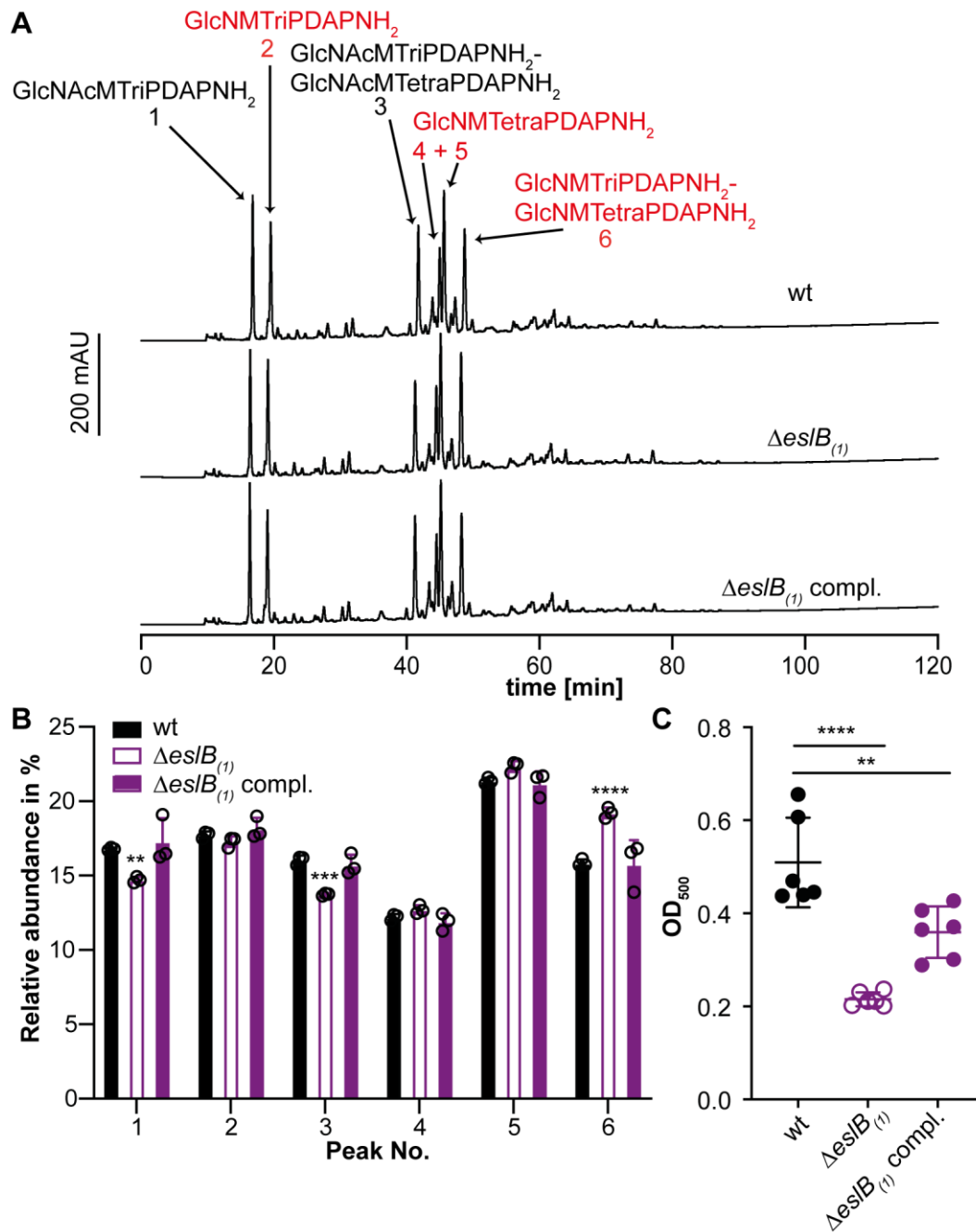


Figure 3 | Deletion of *esIB* leads to changes in the peptidoglycan structure. (A) HPLC analysis of muropeptides derived from mutanolysin digested peptidoglycan isolated from strains 10403S (wt), 10403S $\Delta esIB_{(1)}$ and 10403S $\Delta esIB_{(1)}$ compl.. The muropeptide spectrum of the wildtype strain 10403S has been previously published (33). Major muropeptide peaks are labelled and numbered 1-6 according to previously published HPLC spectra (18, 34), with labels shown in red corresponding to muropeptides with *N*-deacetylated GlcNAc residues and peaks 1-2 corresponding to monomeric and 4-6 to dimeric (crosslinked) muropeptide fragments. Muropeptide abbreviations: GlcNAc – *N*-acetylglucosamine; GlcN – glucosamine; M – *N*-acetylmuramic acid; TriPDAPNH₂ – L-alanyl- γ -D-glutamyl-amidated *meso*-diaminopimelic acid; TetraPDAPNH₂ – L-alanyl- γ -D-glutamyl-amidated *meso*-diaminopimelyl-D-alanine. (B) Quantification of the relative abundance of muropeptide peaks 1-6 for peptidoglycan isolated of strains 10403S (wt), 10403S $\Delta esIB_{(1)}$ and 10403S $\Delta esIB_{(1)}$ compl.. For quantification, the sum of the peak areas was set to 100% and the area of individual peaks was determined. Average values and standard deviations were calculated from three independent peptidoglycan extractions and plotted. For statistical analysis, a two-way ANOVA followed by a Dunnett’s multiple comparisons test was used (** $p \leq 0.01$, *** $p \leq 0.001$, **** $p \leq 0.0001$). (C) The degree of *O*-acetylation of purified peptidoglycan of strains 10403S (wt), 10403S $\Delta esIB_{(1)}$ and

10403S Δ *esB*(₁) compl. was determined by a colorimetric assay as described in the methods section. Average values and standard deviations were calculated from three independent peptidoglycan extractions and two technical repeats and plotted. For statistical analysis, a two-way ANOVA followed by a Dunnett's multiple comparisons test was used (** $p \leq 0.01$, **** $p \leq 0.0001$).

Deletion of *esB* results in a growth defect in high sugar media.

The bacterial cell wall is an important structure to maintain the cell integrity and to prevent lysis due to high internal turgor pressure or when bacteria experience changes in the external osmolality. Alterations of the PG structure or other cell wall defects leading to an impaired cell wall integrity could affect the growth of bacteria in environments with high osmolalities, e.g. in the presence of high salt or sugar concentrations. Next, we compared the growth of the wildtype, the *esB* mutant and complementation strains at 37°C in different media. No growth difference could be observed between the strains tested, when grown in BHI medium (Fig. 4A and S1B). However, the *esB* deletion strain grew slower in BHI medium containing 0.5 M sucrose as compared to the wildtype and the *esB* complementation strain (Fig. 4B and S1C). A similar growth phenotype could be observed when the strains were grown in BHI medium containing either 0.5 M fructose, glucose, maltose or galactose (Fig. S2). In contrast, the presence of 0.5 M NaCl did not affect the growth of the *esB* deletion strain (Fig. 4C). These results suggest that the observed growth defect seen for the *esB* mutant is not solely caused by the increase in external osmolality, but rather seems to be specific to the presence of high concentrations of sugars.

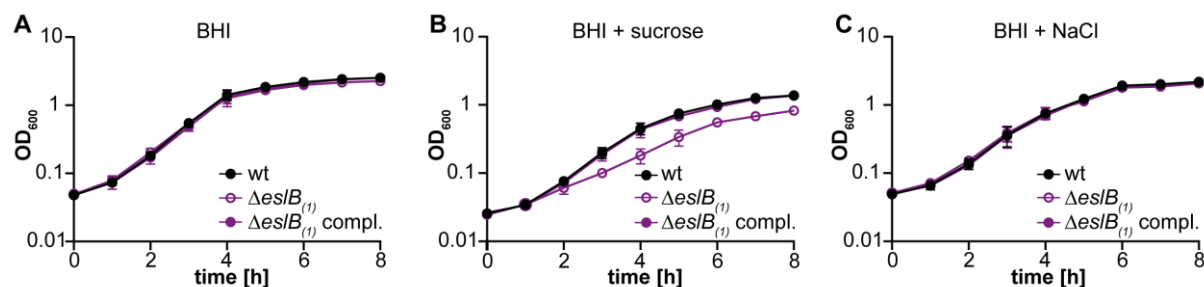


Figure 4 | Addition of sucrose but not NaCl negatively impacts the growth of the *L. monocytogenes* *esB* mutant strain. (A-C). Bacterial growth curves. *L. monocytogenes* strains 10403S (wt), 10403S Δ *esB*(₁) and 10403S Δ *esB*(₁) compl. were grown in (A) BHI broth, (B) BHI broth containing 0.5 M sucrose or (C) BHI broth containing 0.5 M NaCl. Strain 10403S Δ *esB*(₁) compl. was grown in the presence of 1 mM IPTG. OD₆₀₀ readings were determined at hourly intervals and the average values and standard deviations from three independent experiments calculated and plotted.

Deletion of *es/B* results in increased endogenous and lysozyme-induced lysis.

The observed lysozyme sensitivity and the growth defect of the *es/B* deletion strain in media containing high concentrations of sucrose raised the question, whether the absence of EsIB might also cause an impaired cell wall integrity and an increased autolysis due to this impairment. To test this, autolysis assays were performed. To this end, the *L. monocytogenes* wildtype strain 10403S, the *es/B* deletion and complementation strains were grown in BHI medium and subsequently transferred in a Tris-HCl buffer (pH 8). After 2 h incubation at 37°C, the OD₆₀₀ of the suspensions of the wildtype and *es/B* complementation strain had dropped to 89.9±1.6% and 86.5±2.9% of the initial OD₆₀₀, respectively (Fig. 5A). Enhanced endogenous cell lysis was observed for the *es/B* mutant strain and the OD₆₀₀ of the suspensions dropped to 68.8±1.7% within 2 h (Fig. 5A). The addition of penicillin had no impact on the cell lysis of any of the strains tested (Fig. 5B). On the other hand, the addition of 2.5 µg/ml lysozyme increased the rate of cell lysis of all strains, but had a particularly drastic effect on the *es/B* mutant. After 30 min, the OD₆₀₀ reading of a suspension of the *es/B* deletion strain had dropped to 50.3±10.2%. For the wildtype and *es/B* complementation strains, it took 90 min to see a 50% reduction in the OD₆₀₀ readings (Fig. 5C).

Next, we wanted to determine what impact the growth in the presence of high levels of sucrose has on endogenous bacterial autolysis rates. To this end, the wildtype 10403S, *es/B* mutant and complementation strains were grown in BHI medium supplemented with 0.5 M sucrose, cell suspensions prepared in Tris-buffer and used in autolysis assays. While the wildtype and complementation strain showed similar autolysis rates following growth in BHI sucrose medium (Fig. 5D) as after growth in BHI medium (Fig 5A), the *es/B* mutant lysed rapidly following growth in BHI 0.5 M sucrose medium (Fig. 5E). The lysis of the *es/B* mutant strain could be further enhanced by the addition of 25 µg/ml penicillin, a concentration which only acts bacteriostatic on the wildtype *L. monocytogenes* strain 10403S (Fig. 5E).

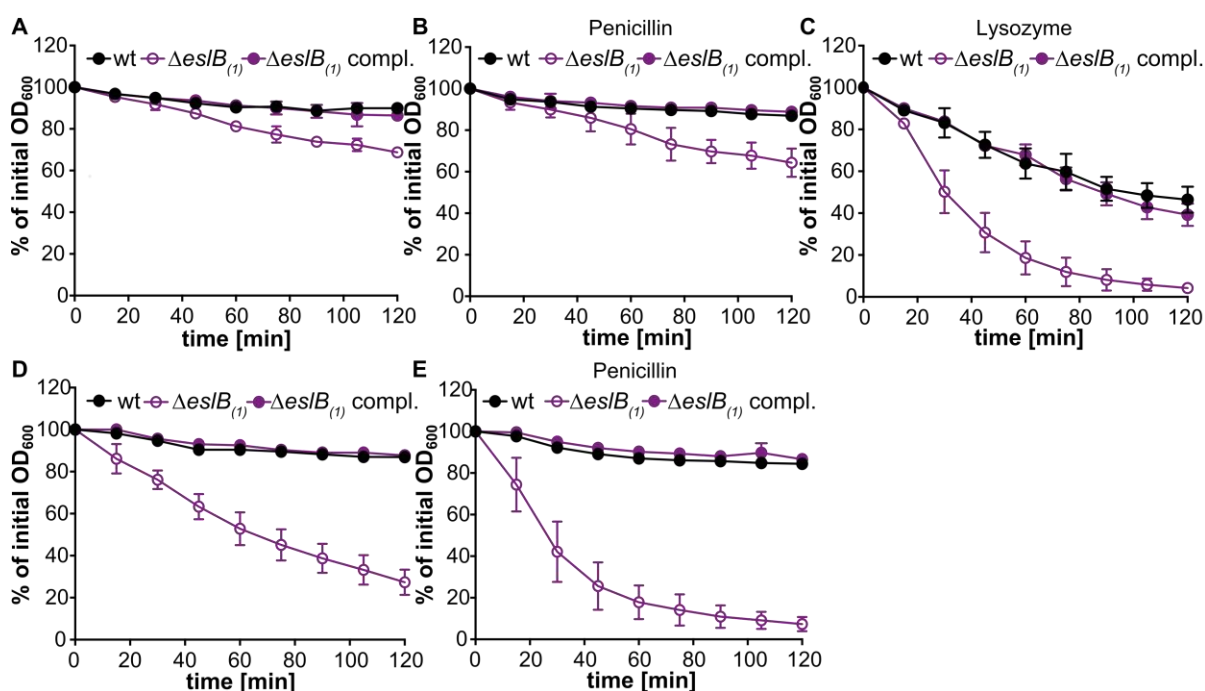


Figure 5 | An *L. monocytogenes* *esIB* deletion strain shows increased endogenous and lysozyme-induced autolysis. Autolysis assays were performed with *L. monocytogenes* strains 10403S (wt), 10403S Δ *esIB*₍₁₎ and 10403S Δ *esIB*₍₁₎ compl.. Bacteria were grown for 4 h in (A-C) BHI medium or (D-E) in BHI medium containing 0.5 M sucrose (containing 1 mM IPTG for 10403S Δ *esIB*₍₁₎ compl.) and subsequently bacterial suspensions prepared in (A, D) 50 mM Tris HCl pH 8, (B, E) 50 mM Tris HCl pH 8 containing 25 μ g/ml penicillin, or (C) 2.5 μ g/ml lysozyme. Cell lysis was followed by taking OD₆₀₀ readings every 15 min. The initial OD₆₀₀ reading for each bacterial suspension was set to 100% and subsequent readings are shown as % of the initial OD₆₀₀ reading. The average % OD₆₀₀ values and standard deviations were calculated from three independent experiments and plotted.

These findings indicate that the *esIB* mutant is sensitive to osmotic downshifts and we thus wondered whether in addition to the changes in the PG modifications and crosslinking, more general differences in the ultrastructure of the cell wall might be observed. To test this, cells of *L. monocytogenes* strains 10403S, 10403S Δ *esIB*₍₂₎ and 10403S Δ *esIB*₍₂₎ compl. were subjected to transmission electron microscopy. The *esIB* deletion strain produces a thinner PG layer of 15.8 ± 1.9 nm, when grown in BHI broth as compared to the wildtype (20 ± 3.4 nm) and the complementation strain (20 ± 4.3 nm, Fig. 6A-B). This phenotype was even more pronounced when the strains were grown in BHI broth containing 0.5 M sucrose. The PG layer of the *esIB* mutant had a thickness of 15 ± 2 nm, while wildtype and the complementation strain produced a PG layer of 21.4 ± 3.1 and 23.3 ± 2.8 nm, respectively (Fig. 6A-B). We hypothesize that the enhanced endogenous lysis as well as the lysozyme sensitivity of the *esIB* mutant is likely caused by a thinner PG layer combined with the observed alterations in PG structure such as reduced *O*-acetylation.

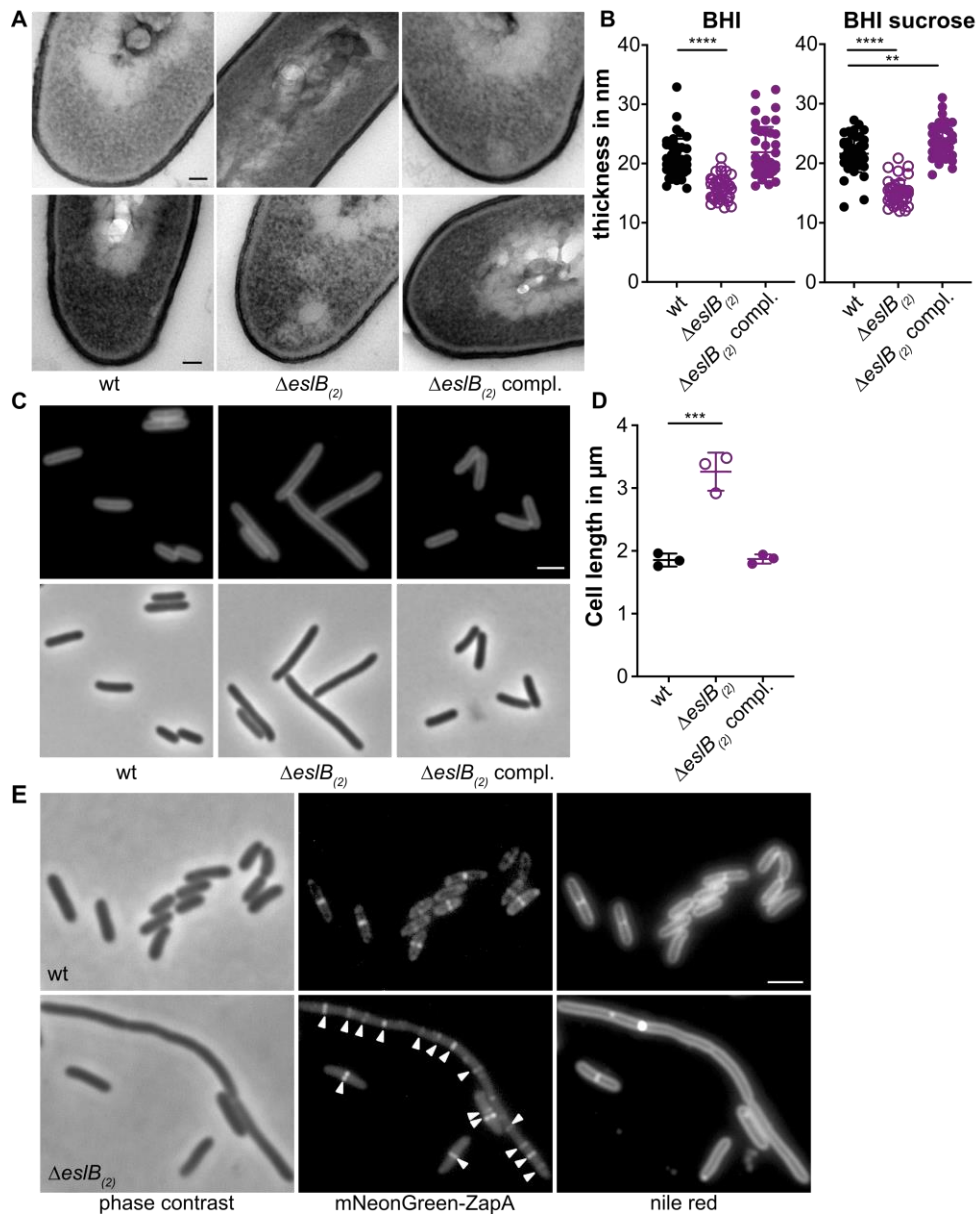


Figure 6 | The *L. monocytogenes* *esIB* mutant produces a thinner cell wall, has a cell division defect and bacteria have an increased cell length. (A) Transmission electron microscopy images. Ultrathin-sectioned cells of *L. monocytogenes* strains 10403S (wt), 10403S $\Delta esIB_{(2)}$ and 10403S $\Delta esIB_{(2)}$ compl. were subjected to transmission electron microscopy after growth in BHI broth (upper panel) or BHI broth containing 0.5 M sucrose (lower panel). Scale bar is 50 nm. Representative images from two independent experiments are shown. (B) Cell wall thickness. Per growth condition, cell wall thickness of 40 cells was measured at three different locations and the average values plotted. For statistical analysis, a two-way ANOVA followed by a Dunnett's multiple comparisons test was used (** $p \leq 0.01$, **** $p \leq 0.0001$). (C) Microscopy images of *L. monocytogenes* strains 10403S (wt), 10403S $\Delta esIB_{(2)}$ and 10403S $\Delta esIB_{(2)}$ compl.. Bacterial membranes were stained with Nile red and cells analyzed by phase contrast and fluorescence microscopy. Scale bar is 2 μm . Representative images from three independent experiments are shown. (D) Cell length of *L. monocytogenes* strains 10403S (wt), 10403S $\Delta esIB_{(2)}$ and 10403S $\Delta esIB_{(2)}$ compl.. The cell length of 300 cells per strain was measured and the median cell length calculated. Three independent experiments were performed, and the average values and standard deviation of the median cell length plotted. For statistical analysis, a one-way ANOVA analysis followed by a Dunnett's multiple comparisons test was used (***) $p \leq 0.001$. (E) Localization of mNeonGreen-ZapA in *L. monocytogenes* strains 10403S (wt) and 10403S $\Delta esIB_{(2)}$. Bacterial membranes were stained with Nile red and cells analyzed by phase contrast (left panel) and fluorescence microscopy to detect mNeonGreen (middle panel) and Nile red fluorescence signals (right panel). White arrows highlight

ZapA foci in cells of the *L. monocytogenes* *eslB* mutant. Scale bar is 2 μm . Representative images from three independent experiments are shown.

The *eslB* deletion strain is impaired in cell division, but not in virulence.

The increased endogenous autolysis together with the observed changes in the PG structure of the *eslB* deletion strain could result in an increased sensitivity to autolysins. The major autolysins of *L. monocytogenes* are p60 and NamA, which hydrolyze PG and are required for daughter cell separation during cell division (43, 44). Absence of either p60 or NamA results in the formation of chains (43, 44). We thus wondered whether deletion of *eslB* causes changes in the cell morphology of *L. monocytogenes*. Microscopic analysis revealed that cells lacking EslB are significantly longer with a median cell length of $3.26 \pm 0.25 \mu\text{m}$ as compared to the *L. monocytogenes* wildtype strain, which produced cells with a length of $1.85 \pm 0.08 \mu\text{m}$ (Fig. 6C-D), highlighting that the absence of EslB results in a cell division defect. To test whether the assembly of the early divisome is affected by the absence of EslB, we compared the localization of the early cell division protein ZapA in the wildtype and the *eslB* mutant background. In *L. monocytogenes* wildtype cells, a signal was observed at midcell for cells, which have initiated the division process (Fig. 6E). While short cells of the *eslB* mutant also only possess a single fluorescent signal, several ZapA fluorescence foci could be observed in elongated cells (Fig. 6E), suggesting that early cell division proteins can still localize in the *eslB* mutant and that a process downstream seems to be perturbed in the absence of EslB.

Next, we wanted to assess whether the impaired cell integrity and the observed cell division defect would also affect the virulence of the *L. monocytogenes* *eslB* mutant. Of note, in a previous study, it was shown that deletion of *eslA*, coding for the ATP-binding protein component of the ABC transporter, has no effect on the cell-to-cell spread of *L. monocytogenes* (19). To determine whether EslB is involved in the virulence of *L. monocytogenes*, primary mouse macrophages were infected with wildtype 10403S, the *eslB* mutant 10403S Δ *eslB*₍₂₎ and complementation strain 10403S Δ *eslB*₍₂₎ compl.. All three strains showed a comparable intracellular growth pattern (Fig. 7A), suggesting that EslB does not impact the ability of *L. monocytogenes* to grow in primary mouse macrophages. Next, we assessed the ability of the *eslB* deletion strains to kill *Drosophila melanogaster* as lysozyme is one important component of its innate immune response (45). All uninfected flies (U/C) and 96.6% of the flies that were injected with PBS survived the duration of the experiment (Fig. 7B). No statistically significant difference could be observed for the survival and bacterial load of flies infected with the different *L. monocytogenes* strains (Fig. 7B-C). These results indicate that, while EslB does not impact the ability of *L. monocytogenes* to infect and kill mammalian macrophages or *Drosophila*

melanogaster, it nonetheless impacts the cell division and cell wall integrity of *L. monocytogenes* and consistent with this we have identified changes in the composition and thickness of the peptidoglycan layer.

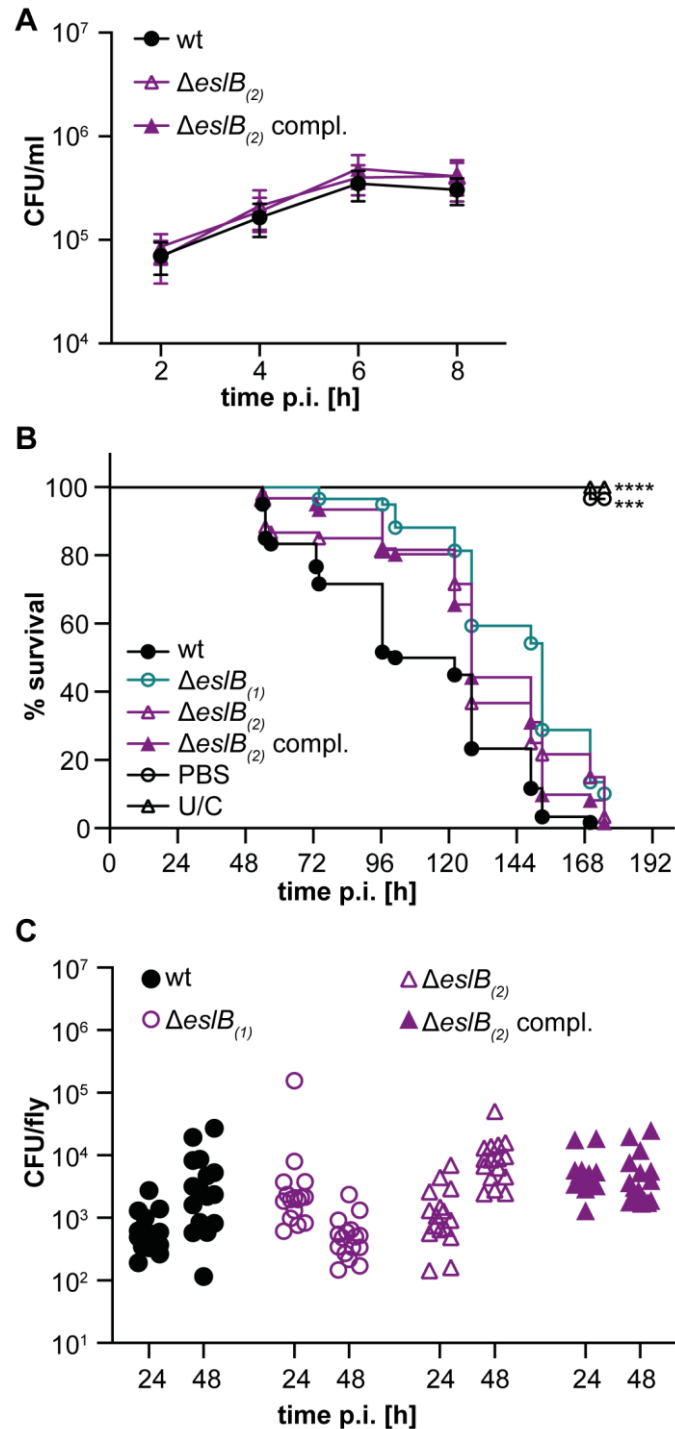


Figure 7 | Impact of the deletion of *esIB* on the virulence of *L. monocytogenes*. (A) Intracellular growth of *L. monocytogenes* strains 10403S (wt), 10403S $\Delta esIB_{(2)}$ and 10403S $\Delta esIB_{(2)}$ compl. in mouse bone marrow-derived macrophages (BMMs). The infection assay was performed as described in the methods section. The average CFU count/ml and standard deviations from three independent experiments were calculated and plotted. (B) Survival curve of flies infected with *L. monocytogenes*. Flies were infected with *L.*

monocytogenes strains 10403S (wt), 10403S Δ *eslB*₍₁₎, 10403S Δ *eslB*₍₂₎ and 10403S Δ *eslB*₍₂₎ compl.. Uninjected control flies (U/C) and flies injected with PBS were used as controls. Fly death was monitored daily. For statistical analysis, a one-way ANOVA followed by a Dunnett's multiple comparisons test was used (** $p \leq 0.001$, *** $p \leq 0.0001$). (C) Bacterial quantification. 16 flies infected with the indicated *L. monocytogenes* strain were collected 24 and 48 h post infection and bacterial load (CFU) determined as described in the methods section. For statistical analysis, a nested one-way ANOVA followed by a Dunnett's multiple comparisons test was used. The observed differences were not statistically significant.

Discussion

Over the past years, several determinants contributing to the intrinsic lysozyme resistance of *L. monocytogenes* have been described (9, 10, 18, 19). One of these is a predicted ABC transporter encoded as part of the *eslABC* operon (18, 19). In this study, we aimed to further investigate the role of the ABC transporter EslABC in lysozyme resistance of *L. monocytogenes*. Using bacterial two hybrid assays, we could show that EslB and EslC interact with each other and hence it is tempting to speculate that the transmembrane component of the ABC transporter consists of a heterodimer of EslB and EslC. However, analysis of different deletion mutants revealed that only EslA and EslB are required for lysozyme resistance of *L. monocytogenes*, suggesting that EslC is not required for the function of the ABC transporter under our assay conditions. Surprisingly, we did not observe an interaction between EslA and EslB using bacterial two hybrid assays, thus, further experiments are required to determine the composition of the ABC transporter and its interaction partners.

Next, we analyzed the PG structure of the *eslB* deletion strain and found that the PG isolated from the *eslB* mutant was slightly more crosslinked and also the fraction of deacetylated GlcNAc residues was slightly increased as compared to the PG isolated from the wildtype strain 10403S. Deacetylation of GlcNAc residues in PG is achieved by the *N*-deacetylase PgdA and has been shown to lead to increased lysozyme resistance (9). Since we saw a slight increase in the deacetylation of GlcNAc residues in the *eslB* mutant strain, our results indicate that the lysozyme sensitivity phenotype of the *eslB* deletion strain is independent of PgdA and that this enzyme functions properly in the mutant strain. A second enzyme required for lysozyme resistance in *L. monocytogenes* is OatA, which transfers *O*-acetyl groups to MurNAc (10, 46, 47). Using a colorimetric *O*-acetylation assay, we were able to show that PG isolated from the *eslB* mutant is less *O*-acetylated. In addition, transmission electron microscopy revealed that the *eslB* mutant produces a thinner PG layer and we assume that this and the reduction in *O*-acetylation contribute to the lysozyme sensitivity of strain 10403S Δ *eslB*.

Growth comparisons in different media revealed that the absence of EslB results in a reduced growth in BHI broth containing high concentrations of mono- or disaccharides. One could speculate that the EslABC transporter might be a sugar transporter with a broad sugar spectrum.

However, we could not identify a potential substrate binding protein encoded in the *esl* operon, which is important for substrate recognition and delivery to ABC importers. EslABC could also be involved in the export of PG components and thus affecting cell wall biosynthesis in *L. monocytogenes*. Indeed, we could show that the *eslB* mutant produces a thinner PG layer as compared to the wildtype strain, suggesting that EslABC affects PG biosynthesis. Future studies will aim to determine how the ABC transporter EslABC influences the biosynthesis and subsequent modification of PG in *L. monocytogenes*.

Absence of EslB leads to the formation of elongated cells, however, it is currently not clear how the function of EslABC is linked to cell division of *L. monocytogenes*. It seems unlikely that the activity or levels of the autolysins p60 and NamA are affected by the absence of EslB. While *iap* and *namA* mutants also form chains of cells, the cell length of individual cells is still similar to wild-type cells, however the bacteria are just unable to separate (43, 44, 48). This is in contrast to the *eslB* mutant, in which the cell length of individual cells is increased suggesting that cell division is blocked at an earlier step. In elongated cells of the *eslB* mutant, we could observe several ZapA foci, suggesting that really early cell division proteins can still be recruited in this strain. Thus, a process downstream of ZapA localization but before the construction of the actual cell septum is perturbed in the absence of EslB. EslABC could potentially affect the activity of cell division proteins or the localization of late cell division-specific proteins. Hence, deletion of *eslB* could lead to a delayed assembly of an active divisome, which could lead to an altered PG biosynthesis at the division site and an impaired cell integrity. Indeed, cells of the *eslB* mutant lysed more rapidly as compared to the *L. monocytogenes* wildtype strain 10403S when shifted from BHI broth to Tris-buffer. The autolysis of cells lacking EslB was strongly induced following growth in BHI supplemented with 0.5 M sucrose prior to the incubation in Tris-buffer. These results indicate that the *eslB* mutant is sensitive to an osmotic downshift and we hypothesize that this is due to the production of a thinner PG layer and a resulting impaired cell integrity.

Reduced lysozyme resistance is often associated with reduced virulence. An *E. faecalis* strain with a deletion in the gene coding for the peptidoglycan deacetylase PgdA, showed a reduced ability to kill *Galleria mellonella* (11). Similarly, a *S. pneumoniae* *pgdA* mutant showed a decreased virulence in a mouse model of infection (13). In our study, we found that inactivation of EslB does not affect the intracellular growth of *L. monocytogenes* in primary mouse macrophages or the ability to kill *Drosophila melanogaster*. These observations are consistent with a previous report that another component of the EslABC transporter, EslA, is dispensable for the ability of *L. monocytogenes* to spread from cell to cell (19). Previously, it was also shown that combined inactivation of PgdA and OatA reduced the ability of *L. monocytogenes* to grow in bone-

marrow derived macrophages, whereas inactivation of PgdA alone had no impact on the virulence of *L. monocytogenes* (46). We therefore reason that the changes in PG structure and associated reduction in lysozyme resistance caused by deletion of *eslB* are not sufficient to affect the ability of *L. monocytogenes* to grow and survive in primary macrophages and flies.

Taken together, we could show that EslB is not only important for the resistance towards lysozyme, its absence also affects the autolysis, cell division and the ability of *L. monocytogenes* to grow in media containing high concentrations of sugars. Our results indicate that the ABC transporter EslABC has a direct or indirect impact on peptidoglycan biosynthesis and maintenance of cell integrity in *L. monocytogenes*.

Data availability

The Illumina reads for the *L. monocytogenes* strains 10403S Δ *eslB*(1), 10403S Δ *eslB*(2), 10403S Δ *eslB*(1) compl. and 10403S Δ *eslB*(2) compl. were deposited in the European Nucleotide Archive under the accession number PRJEB40123.

Acknowledgements

We thank Ivan Andrew and Jaspreet Haywood from the CSC Genomics Laboratory, Hammersmith Hospital, for their help with the whole genome sequencing and Annika Gillis for help with the genome sequence analysis. We would also like to thank Charlotte S. C. Michaux and Sophie Helaine for the bone marrow-derived macrophages and Neil Singh for the support during the transmission electron microscopy experiments. We are grateful to Prof. Jörg Stülke for providing JR and LMS with laboratory space, equipment and consumables. This work was funded by the Wellcome Trust grant 210671/Z/18/Z and MRC grant MR/P011071/1 to AG, the German research foundation (DFG) grants RI 2920/1-1 and RI 2920/2-1 to JR, and the Wellcome Trust grant 207467/Z/17/Z and MRC grant MR/R00997X/1 to MSD. LMS was supported by the Göttingen Graduate School for Neurosciences, Biophysics, and Molecular Biosciences (GGNB, DFG grant GSC226/4).

Supplemental Material

<https://journals.asm.org/doi/10.1128/JB.00553-20>

Figure S1 | Comparison of lysozyme sensitivity and growth of two different *eslB* mutants and complementation strain.

Figure S2 | The *L. monocytogenes* *eslB* mutant has a growth defect in BHI medium containing 0.5 M added sugar.

References

1. Höltje JV. 1998. Growth of the stress-bearing and shape-maintaining murein sacculus of *Escherichia coli*. *Microbiol Mol Biol Rev* 62:181-203.
2. van Heijenoort J. 2001. Formation of the glycan chains in the synthesis of bacterial peptidoglycan. *Glycobiology* 11:25R-36R.
3. Koch AL. 2003. Bacterial wall as target for attack: past, present, and future research. *Clin Microbiol Rev* 16:673-87.
4. Sarkar P, Yarlagadda V, Ghosh C, Haldar J. 2017. A review on cell wall synthesis inhibitors with an emphasis on glycopeptide antibiotics. *Medchemcomm* 8:516-533.
5. Huber G, Neemann G. 1968. Moenomycin, an inhibitor of cell wall synthesis. *Biochem Biophys Res Commun* 30:7-13.
6. Sauvage E, Terrak M. 2016. Glycosyltransferases and Transpeptidases/Penicillin-Binding Proteins: Valuable Targets for New Antibacterials. *Antibiotics (Basel)* 5.
7. Tipper DJ, Strominger JL. 1965. Mechanism of action of penicillins: a proposal based on their structural similarity to acyl-D-alanyl-D-alanine. *Proc Natl Acad Sci U S A* 54:1133-41.
8. Callewaert L, Michiels CW. 2010. Lysozymes in the animal kingdom. *J Biosci* 35:127-60.
9. Boneca IG, Dussurget O, Cabanes D, Nahori MA, Sousa S, Lecuit M, Psylinakis E, Bouriotis V, Hugot JP, Giovannini M, Coyle A, Bertin J, Namane A, Rousselle JC, Cayet N, Prevost MC, Balloy V, Chignard M, Philpott DJ, Cossart P, Girardin SE. 2007. A critical role for peptidoglycan N-deacetylation in *Listeria* evasion from the host innate immune system. *Proc Natl Acad Sci U S A* 104:997-1002.
10. Aubry C, Goulard C, Nahori MA, Cayet N, Decalf J, Sachse M, Boneca IG, Cossart P, Dussurget O. 2011. OatA, a peptidoglycan O-acetyltransferase involved in *Listeria monocytogenes* immune escape, is critical for virulence. *J Infect Dis* 204:731-40.
11. Benachour A, Ladjouzi R, Le Jeune A, Hébert L, Thorpe S, Courtin P, Chapot-Chartier MP, Prajsnar TK, Foster SJ, Mesnage S. 2012. The lysozyme-induced peptidoglycan N-acetylglucosamine deacetylase PgdA (EF1843) is required for *Enterococcus faecalis* virulence. *J Bacteriol* 194:6066-73.
12. Hébert L, Courtin P, Torelli R, Sanguinetti M, Chapot-Chartier MP, Auffray Y, Benachour A. 2007. *Enterococcus faecalis* constitutes an unusual bacterial model in lysozyme resistance. *Infect Immun* 75:5390-8.
13. Vollmer W, Tomasz A. 2000. The *pgdA* gene encodes for a peptidoglycan N-acetylglucosamine deacetylase in *Streptococcus pneumoniae*. *J Biol Chem* 275:20496-501.

14. Bera A, Herbert S, Jakob A, Vollmer W, Götz F. 2005. Why are pathogenic staphylococci so lysozyme resistant? The peptidoglycan O-acetyltransferase OatA is the major determinant for lysozyme resistance of *Staphylococcus aureus*. *Mol Microbiol* 55:778-87.
15. Bera A, Biswas R, Herbert S, Kulauzovic E, Weidenmaier C, Peschel A, Götz F. 2007. Influence of wall teichoic acid on lysozyme resistance in *Staphylococcus aureus*. *J Bacteriol* 189:280-3.
16. Herbert S, Bera A, Nerz C, Kraus D, Peschel A, Goerke C, Meehl M, Cheung A, Gotz F. 2007. Molecular basis of resistance to muramidase and cationic antimicrobial peptide activity of lysozyme in staphylococci. *PLoS Pathog* 3:e102.
17. Le Jeune A, Torelli R, Sanguinetti M, Giard JC, Hartke A, Auffray Y, Benachour A. 2010. The extracytoplasmic function sigma factor SigV plays a key role in the original model of lysozyme resistance and virulence of *Enterococcus faecalis*. *PLoS One* 5:e9658.
18. Burke TP, Loukitcheva A, Zemansky J, Wheeler R, Boneca IG, Portnoy DA. 2014. *Listeria monocytogenes* is resistant to lysozyme through the regulation, not the acquisition, of cell wall-modifying enzymes. *J Bacteriol* 196:3756-67.
19. Durack J, Burke TP, Portnoy DA. 2015. A prl mutation in SecY suppresses secretion and virulence defects of *Listeria monocytogenes* secA2 mutants. *J Bacteriol* 197:932-42.
20. Toledo-Arana A, Dussurget O, Nikitas G, Sesto N, Guet-Revillet H, Balestrino D, Loh E, Gripenland J, Tiensuu T, Vaitkevicius K, Barthelemy M, Vergassola M, Nahori MA, Soubigou G, Regnault B, Coppee JY, Lecuit M, Johansson J, Cossart P. 2009. The *Listeria* transcriptional landscape from saprophytism to virulence. *Nature* 459:950-6.
21. Higgins CF. 1992. ABC transporters: from microorganisms to man. *Annu Rev Cell Biol* 8:67-113.
22. Berntsson RP, Smits SH, Schmitt L, Slotboom DJ, Poolman B. 2010. A structural classification of substrate-binding proteins. *FEBS Lett* 584:2606-17.
23. Tanaka KJ, Song S, Mason K, Pinkett HW. 2018. Selective substrate uptake: The role of ATP-binding cassette (ABC) importers in pathogenesis. *Biochim Biophys Acta Biomembr* 1860:868-877.
24. Locher KP. 2016. Mechanistic diversity in ATP-binding cassette (ABC) transporters. *Nat Struct Mol Biol* 23:487-93.
25. Mächtel R, Narducci A, Griffith DA, Cordes T, Orelle C. 2019. An integrated transport mechanism of the maltose ABC importer. *Res Microbiol* 170:321-337.
26. Slotboom DJ. 2014. Structural and mechanistic insights into prokaryotic energy-coupling factor transporters. *Nat Rev Microbiol* 12:79-87.

27. Davidson AL, Dassa E, Orelle C, Chen J. 2008. Structure, function, and evolution of bacterial ATP-binding cassette systems. *Microbiol Mol Biol Rev* 72:317-64, table of contents.
28. Camilli A, Tilney LG, Portnoy DA. 1993. Dual roles of *plcA* in *Listeria monocytogenes* pathogenesis. *Mol Microbiol* 8:143-57.
29. Lauer P, Chow MY, Loessner MJ, Portnoy DA, Calendar R. 2002. Construction, characterization, and use of two *Listeria monocytogenes* site-specific phage integration vectors. *J Bacteriol* 184:4177-86.
30. Karimova G, Pidoux J, Ullmann A, Ladant D. 1998. A bacterial two-hybrid system based on a reconstituted signal transduction pathway. *Proc Natl Acad Sci U S A* 95:5752-6.
31. de Jonge BL, Chang YS, Gage D, Tomasz A. 1992. Peptidoglycan composition of a highly methicillin-resistant *Staphylococcus aureus* strain. The role of penicillin binding protein 2A. *J Biol Chem* 267:11248-54.
32. Corrigan RM, Abbott JC, Burhenne H, Kaefer V, Gründling A. 2011. c-di-AMP is a new second messenger in *Staphylococcus aureus* with a role in controlling cell size and envelope stress. *PLoS Pathog* 7:e1002217.
33. Rismondo J, Halbedel S, Gründling A. 2019. Cell Shape and Antibiotic Resistance Are Maintained by the Activity of Multiple FtsW and RodA Enzymes in *Listeria monocytogenes*. *MBio* 10.
34. Rismondo J, Möller L, Aldridge C, Gray J, Vollmer W, Halbedel S. 2015. Discrete and overlapping functions of peptidoglycan synthases in growth, cell division and virulence of *Listeria monocytogenes*. *Mol Microbiol* 95:332-51.
35. Gudlavalleti SK, Datta AK, Tzeng YL, Noble C, Carlson RW, Stephens DS. 2004. The *Neisseria meningitidis* serogroup A capsular polysaccharide O-3 and O-4 acetyltransferase. *J Biol Chem* 279:42765-73.
36. Rueden CT, Schindelin J, Hiner MC, DeZonia BE, Walter AE, Arena ET, Eliceiri KW. 2017. ImageJ2: ImageJ for the next generation of scientific image data. *BMC Bioinformatics* 18:529.
37. Stapels DAC, Hill PWS, Westermann AJ, Fisher RA, Thurston TL, Saliba AE, Blommestein I, Vogel J, Helaine S. 2018. *Salmonella* persists undermine host immune defenses during antibiotic treatment. *Science* 362:1156-1160.
38. Sharrock J, Estacio-Gomez A, Jacobson J, Kierdorf K, Southall TD, Dionne MS. 2019. *fs(1)h* controls metabolic and immune function and enhances survival via AKT and FOXO in *Drosophila*. *Dis Model Mech* 12.

39. Gaillard JL, Berche P, Frehel C, Gouin E, Cossart P. 1991. Entry of *L. monocytogenes* into cells is mediated by internalin, a repeat protein reminiscent of surface antigens from gram-positive cocci. *Cell* 65:1127-41.
40. Bierne H, Sabet C, Personnic N, Cossart P. 2007. Internalins: a complex family of leucine-rich repeat-containing proteins in *Listeria monocytogenes*. *Microbes Infect* 9:1156-66.
41. Rosenthal RS, Blundell JK, Perkins HR. 1982. Strain-related differences in lysozyme sensitivity and extent of O-acetylation of gonococcal peptidoglycan. *Infect Immun* 37:826-9.
42. Dupont C, Clarke AJ. 1991. Dependence of lysozyme-catalysed solubilization of *Proteus mirabilis* peptidoglycan on the extent of O-acetylation. *Eur J Biochem* 195:763-9.
43. Pilgrim S, Kolb-Maurer A, Gentschev I, Goebel W, Kuhn M. 2003. Deletion of the gene encoding p60 in *Listeria monocytogenes* leads to abnormal cell division and loss of actin-based motility. *Infect Immun* 71:3473-84.
44. Carroll SA, Hain T, Technow U, Darji A, Pashalidis P, Joseph SW, Chakraborty T. 2003. Identification and characterization of a peptidoglycan hydrolase, MurA, of *Listeria monocytogenes*, a muramidase needed for cell separation. *J Bacteriol* 185:6801-8.
45. Daffre S, Kylsten P, Samakovlis C, Hultmark D. 1994. The lysozyme locus in *Drosophila melanogaster*: an expanded gene family adapted for expression in the digestive tract. *Mol Gen Genet* 242:152-62.
46. Rae CS, Geissler A, Adamson PC, Portnoy DA. 2011. Mutations of the *Listeria monocytogenes* peptidoglycan N-deacetylase and O-acetylase result in enhanced lysozyme sensitivity, bacteriolysis, and hyperinduction of innate immune pathways. *Infect Immun* 79:3596-606.
47. Rismondo J, Wamp S, Aldridge C, Vollmer W, Halbedel S. 2018. Stimulation of PgdA-dependent peptidoglycan N-deacetylation by GpsB-PBP A1 in *Listeria monocytogenes*. *Mol Microbiol* 107:472-487.
48. Halbedel S, Hahn B, Daniel RA, Flieger A. 2012. DivIVA affects secretion of virulence-related autolysins in *Listeria monocytogenes*. *Mol Microbiol* 83:821-39.

Chapter 4 | YtrBCDEF determines cell wall thickness and competence

The results described in this chapter were originally published in *Frontiers Microbiology* (<https://doi.org/10.3389/fmicb.2021.587035>):

Influence of the ABC transporter YtrBCDEF of *Bacillus subtilis* on competence, biofilm formation and cell wall thickness

Martin Benda[†], Lisa Maria Schulz[†], Jörg Stülke* and Jeanine Rismondo*

Department of General Microbiology, Institute of Microbiology and Genetics, Georg-August University Göttingen, Grisebachstr. 8, D-37077 Göttingen, Germany

Author contributions

JR, MB and LMS conceived the study. MB, JR, LMS and JS designed the experiments. MB and LMS carried out the experiments. LMS constructed the *trpC2 ΔytrCD* and *trpC2 ΔytrCD ΔytrA::erm* mutant strains and MB constructed the remaining strains. MB and LMS carried out the qRT-PCR, fluorescence microscopy and competence assays. MB carried out the biofilm assay. MB, JR and JS wrote the manuscript. All authors approve the manuscript. JS and JR acquired funding. JR and JS provided supervision.

Abstract:

Bacillus subtilis develops genetic competence for the uptake of foreign DNA when cells enter stationary phase and a high cell density is reached. These signals are integrated by the competence transcription factor ComK, which is subject to transcriptional, post-transcriptional and post-translational regulation. Many proteins are involved in the development of competence, both to control ComK activity and to mediate DNA uptake. However, for many proteins, the precise function they play in competence development is unknown. In this study, we assessed whether proteins required for genetic transformation play a role in the activation of ComK or rather act downstream of competence gene expression. While these possibilities could be distinguished for most of the tested factors, we assume that two proteins, PNPase and the transcription factor YtrA, are required both for full ComK activity and for the downstream processes of DNA uptake and integration. Further analyses of the role of the transcription factor YtrA for the competence development revealed that the overexpression of the YtrBCDEF ABC transporter in the *ytrA* mutant causes the loss of genetic competence. Moreover, overexpression of this ABC transporter also affects biofilm formation. Since the *ytrGABCDEF* operon is naturally induced by cell wall-targeting antibiotics, we tested the cell wall properties upon overexpression of the ABC transporter and observed an increased thickness of the cell wall. The composition and properties of the cell wall are important for competence development and biofilm formation, suggesting that the observed phenotypes are the result of the increased cell wall thickness as an outcome of YtrBCDEF overexpression.

Introduction

The gram-positive model bacterium *Bacillus subtilis* has evolved many different ways to survive harsh environmental conditions, i. e. it can form highly resistant spores, secrete toxins to kill and cannibalize neighboring cells, form resistant macroscopic biofilms or become competent for transformation (reviewed in (López and Kolter, 2010)).

Development of genetic competence is a strategy, which allows bacterial cells to take up foreign DNA from the environment in order to increase the genetic variability of the population. Competence is developed during the transition from exponential to stationary phase of growth as a response to increased cell density and nutrient limitation. In *B. subtilis*, genetic competence is developed in a bistable manner, meaning that only about 10-20% of the cells of a population change their physiological characteristics and become competent for transformation, leaving the rest of the population non-competent (Haijema et al., 2001; Maamar and Dubnau, 2005). Whether a specific cell becomes competent or not depends on the level of the master regulator ComK (van Sinderen et al., 1995), whose cellular amount is tightly controlled by a complex network of regulators acting on the transcriptional, post-transcriptional as well as on post-translational levels (for a detailed overview see (Maier, 2020)).

Transcription of the *comK* gene is controlled by three repressor proteins, Rok, CodY, and AbrB (Serror and Sonenshein, 1996; Hoa et al., 2002; Hamoen et al., 2003), moreover, *comK* transcription is activated by the transcriptional regulator DegU (Hamoen et al., 2000). Another important player for regulation of *comK* expression is Spo0A-P, which controls the levels of the AbrB repressor and additionally supports activation of *comK* expression by antagonizing Rok (Hahn et al., 1995; Mirouze et al., 2012). The presence of phosphorylated Spo0A directly links competence to other lifestyles, since Spo0A-P is also involved in pathways leading to sporulation or biofilm formation (Aguilar et al., 2010). When ComK levels reach a certain threshold, it binds its own promoter region to further increase its own expression, thereby creating a positive feedback loop, which leads to full activation of competence (Maamar and Dubnau, 2005; Smits et al., 2005).

ComK levels are also controlled post-transcriptionally by the Kre protein, which destabilizes the *comK* mRNA (Gamba et al., 2015). Post-translational regulation is achieved through the adapter protein MecA, which sequesters ComK and directs it towards degradation by the ClpCP protease (Turgay et al., 1998). During competence, this degradation is prevented by a small protein, ComS that is expressed in response to quorum sensing (Nakano et al., 1991).

ComK activates expression of more than 100 genes (Berka et al., 2002; Hamoen et al., 2002; Ogura et al., 2002; Boonstra et al., 2020). Whereas a clear role in competence development has been assigned to many of the ComK regulon members, the roles of some ComK-dependent

genes remain unclear. Similarly, many single deletion mutant strains were identified as competence deficient, for which the reasons for this deficiency are known. However, there are still many single deletion mutants, in which the reason for the loss of competence remains unknown. Typical examples for this are mutants lacking various RNases, namely RNase Y, RNase J or PNPase (Luttinger et al., 1996; Figaro et al., 2013). Recently, a library of *B. subtilis* single gene deletion mutants was screened for various phenotypes, including competence development (Koo et al., 2017). This screen revealed 21 mutants with completely abolished competence. Out of those, 16 are known to be involved in the control of the ComK master regulator, DNA uptake or genetic recombination. However, in case of the other 5 competence-deficient strains the logical link to competence remains elusive.

Here, we have focused on some of these factors to investigate their role in genetic competence in more detail. We took advantage of the fact that artificial overexpression of ComK and ComS significantly increases transformation efficiency independently of traditional ComK and ComS regulation (Rahmer et al., 2015). This enables the identification of genes that are involved in competence development due to a function in *comK* expression or for other specific reasons downstream of ComK activity. We identified the YtrBCDEF ABC transporter, which is encoded in the *ytrGABCDE* operon as an important player for *B. subtilis* differentiation, since its overexpression does not only result in a complete loss of competence by a so far unknown mechanism, it also affects the proper development of other lifestyles of *B. subtilis*. We hypothesize that the production of a thicker cell wall upon overexpression of the proteins encoded by the *ytrGABCDE* operon is likely the cause of the observed competence and biofilm defects.

Materials and Methods

Bacterial strains and growth conditions.

B. subtilis strains used in this study are listed in Table 1. Lysogeny broth (LB) (Sambrook et al., 1989) was used to grow *Escherichia coli* and *B. subtilis*, unless otherwise stated. When required, media were supplemented with antibiotics at the following concentrations: ampicillin 100 $\mu\text{g ml}^{-1}$ (for *E. coli*) and chloramphenicol 5 $\mu\text{g ml}^{-1}$, kanamycin 10 $\mu\text{g ml}^{-1}$, spectinomycin 250 $\mu\text{g ml}^{-1}$, tetracycline 12.5 $\mu\text{g ml}^{-1}$, and erythromycin 2 $\mu\text{g ml}^{-1}$ plus lincomycin 25 $\mu\text{g ml}^{-1}$ (for *B. subtilis*). For agar plates, 15 g l⁻¹ Bacto agar (Difco) was added.

Table 1 | *B. subtilis* strains used in this study.

Strain	Genotype	Source ^a
168	<i>trpC2</i>	Laboratory collection
BKE30420	<i>trpC2 ΔytrE::ermC</i>	(Koo et al., 2017)
BKE30430	<i>trpC2 ΔytrD::ermC</i>	(Koo et al., 2017)
BKE30440	<i>trpC2 ΔytrC::ermC</i>	(Koo et al., 2017)
BKE30450	<i>trpC2 ΔytrB::ermC</i>	(Koo et al., 2017)
PG389	<i>amyE::P_{comG}-lacZ-gfp-cat</i>	(Gamba et al., 2015)
PG10 ^b	<i>yvcA::(P_{mtIA}-comKS)</i>	(Reuß et al., 2017)
DK1042	<i>comI^{Q12L}</i>	(Konkol et al., 2013)
CCB434	<i>ΔrnjA::spc</i>	(Figaro et al., 2013)
CCB441	<i>Δrny::spc</i>	(Figaro et al., 2013)
GP811	<i>trpC2 ΔgudB::cat rocG::Tn10 spc amyE::(gltA-lacZ aphA3) ΔansR::tet</i>	(Flórez et al., 2011)
GP1152	<i>trpC2 ΔansR::tetR</i>	GP811 → 168
GP1748	<i>trpC2 ΔpnpA::aphA3</i>	(Cascante-Esteba et al., 2016)
GP2155	<i>trpC2 ΔnrnA::aphA3</i>	See Materials & Methods
GP2501	<i>trpC2 Δrny::spc</i>	CCB441 → 168
GP2506	<i>trpC2 ΔrnjA::spc</i>	CCB434 → 168
GP2559	<i>comI^{Q12L} ΔymdB::cat</i>	(Kampf et al., 2018)
GP2612	<i>trpC2 ΔgreA::aphA3</i>	See Materials & Methods
GP2618	<i>trpC2 yvcA-P_{mtIA}-comKS-ermC-hisl</i>	See Materials & Methods
GP2620	<i>trpC2 yvcA-P_{mtIA}-comKS-cat-hisl</i>	See Materials & Methods
GP2621	<i>trpC2 yvcA-P_{mtIA}-comKS-ermC-hisl ΔpnpA::aphA3</i>	GP1748 → GP2618
GP2624	<i>trpC2 yvcA-P_{mtIA}-comKS-ermC-hisl Δrny::spc</i>	GP2501 → GP2618

GP2626	<i>trpC2 yvcA-P_{mtlA}-comKS-ermC-hisI ΔrnjA::spc</i>	GP2506 → GP2618
GP2630	<i>trpC amyE::P_{comG}-lacZ-gfp-cat</i>	PG389 → 168
GP2640	<i>trpC2 ΔftsH::aphA3</i>	See Materials & Methods
GP2641	<i>trpC2 ΔytrA::spc</i>	See Materials & Methods
GP2643	<i>trpC2 ΔcomEC::spc</i>	See Materials & Methods
GP2644	<i>trpC2 ΔdegU::aphA3</i>	See Materials & Methods
GP2646	<i>trpC2 ΔytrGABCDEF::ermC</i>	See Materials & Methods
GP2647	<i>trpC2 ΔytrA::ermC</i>	See Materials & Methods
GP2652	<i>trpC2 yvcA-P_{mtlA}-comKS-cat-hisI ΔftsH::aphA3</i>	GP2640 → GP2620
GP2653	<i>trpC2 yvcA-P_{mtlA}-comKS-cat-hisI ΔnrnA::aphA3</i>	GP2155 → GP2620
GP2654	<i>trpC2 yvcA-P_{mtlA}-comKS-cat-hisI ΔgreA::aphA3</i>	GP2612 → GP2620
GP2655	<i>trpC2 yvcA-P_{mtlA}-comKS-cat-hisI ΔytrA::spc</i>	GP2641 → GP2620
GP2659	<i>trpC2 yvcA-P_{mtlA}-comKS-cat-hisI ΔcomEC::spc</i>	GP2643 → GP2620
GP2660	<i>trpC2 yvcA-P_{mtlA}-comKS-cat-hisI ΔdegU::aphA3</i>	GP2644 → GP2620
GP2664	<i>trpC2 amyE::P_{comG}-lacZ-gfp ΔftsH::aphA3</i>	GP2640 → GP2630
GP2665	<i>trpC2 amyE::P_{comG}-lacZ-gfp ΔnrnA::aphA3</i>	GP2155 → GP2630
GP2666	<i>trpC2 amyE::P_{comG}-lacZ-gfp ΔgreA::aphA3</i>	GP2612 → GP2630
GP2667	<i>trpC2 amyE::P_{comG}-lacZ-gfp ΔytrA::spc</i>	GP2641 → GP2630
GP2671	<i>trpC2 amyE::P_{comG}-lacZ-gfp ΔcomEC::spc</i>	GP2643 → GP2630
GP2672	<i>trpC2 amyE::P_{comG}-lacZ-gfp ΔdegU::aphA3</i>	GP2644 → GP2630
GP2700	<i>trpC2 ΔytrF::cat</i>	See Materials & Methods
GP3186	<i>trpC2 ΔytrGABCDE::ermC</i>	See Materials & Methods
GP3187	<i>trpC2 ΔytrF::cat ΔytrA::ermC</i>	GP2647 → GP2700
GP3188	<i>trpC2 ΔytrB</i>	pDR244 → BKE30450
GP3189	<i>trpC2 ΔytrC</i>	pDR244 → BKE30440

GP3190	<i>trpC2 ΔytrD</i>	pDR244 → BKE30430
GP3191	<i>trpC2 ΔytrE</i>	pDR244 → BKE30420
GP3193	<i>trpC2 ΔytrA::ermC ΔytrB</i>	See Materials & Methods
GP3194	<i>trpC2 ΔytrA::ermC ΔytrC</i>	See Materials & Methods
GP3195	<i>trpC2 ΔytrA::ermC ΔytrD</i>	GP2647 → GP3190
GP3196	<i>trpC2 ΔytrA::ermC ΔytrE</i>	See Materials & Methods
GP3197	<i>trpC2 ganA::P_{xyIA}-ytrF-aphA3</i>	pGP2184 → 168
GP3200	<i>trpC2 amyE::P_{comG}-lacZ-gfp-cat ytrGABCDEF::ermC</i>	GP2646 → GP2630
GP3205	<i>trpC2 ΔytrCD::cat</i>	See Materials & Methods
GP3206	<i>trpC2 ΔytrA::ermC ΔytrB ΔytrE</i>	See Materials & Methods
GP3207	<i>comI^{Q12L} ΔytrGABCDEF::ermC</i>	GP2646 → DK1042
GP3212	<i>comI^{Q12L} ΔytrA::spc</i>	GP2641 → DK1042
BLMS2	<i>trpC2 ΔytrCD</i>	See Materials & Methods
BLMS3	<i>trpC2 ΔytrA::erm ΔytrCD</i>	See Materials & Methods

^a Arrows indicate construction by transformation.

^b This genome-reduced strain (see (Reuß et al., 2017) for details) was used to amplify the *P_{mtIA}-comKS* cassette.

DNA manipulation and strain construction

S7 Fusion DNA polymerase (Mobidiag, Espoo, Finland) was used as recommended by the manufacturer. DNA fragments were purified using the QIAquick PCR Purification Kit (Qiagen, Hilden, Germany). DNA sequences were determined by the dideoxy chain termination method (Sambrook et al., 1989). Chromosomal DNA from *B. subtilis* was isolated using the peqGOLD Bacterial DNA Kit (Peqlab, Erlangen, Germany) and plasmids were purified from *E. coli* using the NucleoSpin Plasmid Kit (Macherey-Nagel, Düren, Germany). Oligonucleotides used in this study are listed in Table S1. Deletion of the *degU*, *comEC*, *ftsH*, *greA*, *ytrA*, *nrnA*, and *ytrF* genes as well as *ytrG-ytrE*, and *ytrGABCDEF* regions was achieved by transformation with PCR products containing an antibiotic resistance cassette flanked by up- and downstream fragments of the target genes as described previously (Youngman, 1990; Guérout-Fleury et al., 1995; Wach, 1996).

The identity of the modified genomic regions was verified by DNA sequencing. To construct strains GP2618 and GP2620 harbouring the *P_{mtlA}-comKS* cassette coupled to the antibiotic resistance gene, we first amplified *P_{mtlA}-comKS* from strain PG10 (Reuß et al., 2017) as well as the resistance genes from pDG646 and pGEM-cat, respectively (Youngman, 1990; Guérout-Fleury et al., 1995) and the genes flanking the intended integration site, i. e. *yvcA* and *hisI* from *B. subtilis* 168. Subsequently, those DNA fragments were fused in another PCR reaction and the final product was used to transform *B. subtilis* 168. Correct insertion was verified by PCR amplification and sequencing. Markerless deletions of *ytrB*, *ytrC*, *ytrD* and *ytrE* genes were generated using the plasmid pDR244 as previously described (Koo et al., 2017). In short, strains BKE30450, BKE30440, BKE30430 and BKE30420 were transformed with plasmid pDR244 and transformants were selected on LB agar plates supplemented with spectinomycin at 30°C. Transformants were then streaked on plain LB agar plates and incubated at 42°C to cure the plasmid, which contains a thermo-sensitive origin of replication. Single colonies were screened for spectinomycin and erythromycin/lincomycin sensitivity. The markerless deletion of *ytrCD* was achieved using the cre-lox system. First, Lox71 and Lox66 sites were attached to the kanamycin resistance gene using primers CZ168/169. The resulting PCR product was cut with *EcoRI* and *XbaI* and ligated with plasmid pBluescript II that had been cut with the same enzymes, yielding plasmid pGP2514. The kanamycin resistance cassette flanked by Lox71 and Lox66 sites was subsequently amplified from pGP2514 using primers CZ200/201. Next, 800 bp up- and downstream of *ytrCD* were amplified using primers MB198/LMS262 and MB201/LMS260, respectively. Primers LMS262 and LMS260 contained overhangs complementary to primers CZ200/201. The three fragments were subsequently fused using primers MB198/MB201, the resulting PCR product transformed into the *B. subtilis* wildtype strain 168 and transformants selected on SP medium containing kanamycin. The strain was cured from the kanamycin resistance cassette using plasmid pDR244 as described above, resulting in the construction of strain BLMS2. Markerless deletion was confirmed by PCR with primers flanking the deletion site. The resulting strains GP3188, GP3189, GP3190, GP3191 and BLMS2 were used for subsequent deletion of the *ytrA* gene. For the construction of GP3193, GP3194 and GP3196, the *ytrA* deletion cassette was amplified using primers MB66/69 and genomic DNA of strains GP3188, GP3189 and GP3191, respectively, as template. For the construction of BLMS3, the $\Delta ytrA::erm$ region was amplified using primers MB173/70 and genomic DNA of strain GP2647. The corresponding *ytrA* deletion cassettes were subsequently transformed into GP3188, GP3189, GP3191 and BLMS2. Strain GP3195 was constructed by transformation with genomic DNA of the *ytrA* deletion strain. Deletion of the *ytrA* gene and preservation of selected markerless deletions were confirmed via PCR. To construct GP3206, the

$\Delta ytrA::erm \Delta ytrB$ region of strain GP3193 was amplified using primers MB66 and MB180 and transformed into GP3191.

Transformation of *B. subtilis* strains.

Transformation experiments were conducted based on the two-step protocol as described previously (Kunst and Rapoport, 1995). Briefly, cells were grown at 37°C at 200 rpm in 10 ml MNGE medium containing 2% glucose, 0.2% potassium glutamate, 100 mM potassium phosphate buffer (pH 7), 3.4 mM trisodiumcitrate, 3 mM MgSO₄, 42 μM ferric ammonium citrate, 0.24 mM L-tryptophan and 0.1% casein hydrolysate. During the transition from exponential to stationary phase, the culture was diluted with another 10 ml of MNGE medium (without casein hydrolysate) and incubated for 1 h at 37°C with shaking. For transformation experiments with strain GP3197, 0.5% xylose was added to both media. Afterwards, 250 ng of chromosomal DNA was added to 400 μl of cells and incubated for 30 minutes at 37°C. One hundred microliter of Expression mix (2.5% yeast extract, 2.5% casein hydrolysate, 1.22 mM tryptophan) was added and cells were grown for 1h at 37°C, before spreading onto selective LB plates containing appropriate antibiotics.

Transformation of strains harboring P_{mtlA} -*comKS*, in which the expression of *comK* and *comS* is induced in the presence of mannitol, was performed as previously described (Rahmer et al., 2015). Briefly, an overnight culture was diluted in 5 ml LB to an initial OD₆₀₀ of 0.1 and incubated at 37°C and 200 rpm. After 90 minutes of incubation, 5 ml of fresh LB containing 1% mannitol and 5 mM MgCl₂ were added and the bacterial culture was incubated for an additional 90 minutes. Cells were then pelleted by centrifugation for 10 minutes at 2,000 x g and the pellet was re-suspended in the same amount of fresh LB medium. 1 ml aliquots were distributed into 1.5 ml reaction tubes and 250 ng of chromosomal DNA was added to each of them. The cell suspension was incubated for 1 h at 37°C and transformants were selected on LB plates as described above.

Plasmid construction.

All plasmids used in this study are listed in Table 2. *E. coli* DH5α (Sambrook et al., 1989) was used for plasmid constructions and transformation using standard techniques (Sambrook et al., 1989). To overproduce the YtrF protein, the *ytrF* gene was placed under the control of a xylose inducible promoter. For this purpose, we cloned the *ytrF* gene into the backbone of pGP888 via the XbaI and KpnI sites (Diethmaier et al., 2011).

Table 2 | Plasmids used in this study.

Plasmid	Relevant Characteristics	Primers	Reference
pDR244	<i>cre</i> + Ts origin	-	(Koo et al., 2017)
pGEM-cat	Amplification of the <i>cat</i> cassette	-	(Youngman, 1990)
pDG646	Amplification of the <i>ermC</i> cassette	-	(Guérout-Fleury et al., 1995)
pDG780	Amplification of the <i>aphA3</i> cassette	-	(Guérout-Fleury et al., 1995)
pDG1726	Amplification of the <i>spc</i> cassette	-	(Guérout-Fleury et al., 1995)
pGP888	<i>ganA::P_{xyIA}</i> ; <i>aphA3</i>	-	(Diethmaier et al., 2011)
pGP2184	pGP888- <i>ytrF</i>	MB186/MB187	This study
pGP2514	Amplification of <i>aphA3-lox</i> for the cre-lox system	CZ200/CZ201	This study

Quantitative real-time PCR (qRT-PCR)

For the isolation of RNA, a single colony was used to inoculate 4 ml LB medium containing the appropriate antibiotics. The cells were grown over the day at 37°C with agitation and used to inoculate 10 ml MNGE defined medium and incubated overnight. The next day, 100 ml MNGE medium were inoculated to an OD₆₀₀ of 0.1 and the cells were incubated at 37°C until they reached an OD₆₀₀ of 1.0. 25 ml of each culture were mixed with 15 ml frozen killing buffer (20 mM Tris, pH 7.5, 5 mM MgCl₂, 20 mM NaN₃), followed by a 5-min centrifugation step at 8000 rpm and 4°C. Pellets were snap-frozen in liquid nitrogen and stored at -80°C. Disruption of cells and isolation of RNA was carried out as previously described (Meinken et al., 2003). 5 µg isolated RNA were digested with 5 µl DNase I (1 U/µl, Thermo Scientific) for 40 min at 37°C. The reaction was stopped by adding 2.5 µl 25 mM EDTA and incubating the samples at 65°C for 10 min. To verify that the isolated RNA is free of DNA, a check PCR was performed using primers KG44/KG45. Genomic DNA from *B. subtilis* 168 was used as control.

qRT-PCR was carried out using the One-Step reverse transcription PCR kit, the Bio-Rad iCycler and the Bio-Rad iQ5 software (Bio-Rad, Munich, Germany). Three technical and three biological repeats were performed. Primers KG44/45 and KG42/43 were used to determine transcript amounts of the ribosomal genes *rpsE* and *rpsJ*, respectively, which were used as internal controls. Transcript amounts for *ytrE* and *ytrF* were monitored using primers MB219/220 and

MB224/225, respectively. The average of the cycle threshold (C_T) values of *rpsE* and *rpsJ* were used to normalize the C_T -values obtained for *ytrE* and *ytrF*. For each strain, the fold changes of *ytrE* and *ytrF* expression were calculated using the $\Delta\Delta C_T$ -method.

Biofilm assay

To analyse biofilm formation, selected strains were grown in LB medium to an OD_{600} of about 0.5 to 0.8 and 10 μ l of the culture were spotted onto MSgg agar plates (Branda et al., 2001). Plates were incubated for 3 days at 30°C.

Fluorescence microscopy

For fluorescence microscopy imaging, *B. subtilis* cultures were grown in 10 ml MNGE medium until the transition from exponential to stationary phase and then diluted with another 10 ml of MNGE medium as described for the transformation experiments (see section 2.3). 2 ml of the bacterial culture were harvested and resuspended in 500 μ l PBS. The cell suspension was mixed with 25 μ l of 100 μ g/ml Nile red solution to stain the bacterial membranes. 5 μ l of cells were pipetted on microscope slides coated with a thin layer of 1% agarose and covered with a cover glass. Fluorescence images were obtained with the AxioImager M2 fluorescence microscope, equipped with the digital camera AxioCam MRm and an EC Plan-NEOFLUAR 100X/1.3 objective (Carl Zeiss, Göttingen, Germany). Filter sets 38 (EX BP 470/40, FT 495, EM BP 525/50; Carl Zeiss) and 43 (EX BP 545/25, FT 579, EM BP 605/70; Carl Zeiss) were applied for GFP and Nile red detection, respectively. Images were processed with the AxioVision Rel 4.8 software. Ratio of GFP expressing cells to the total number of cells was determined by manual examination from at least six independent growth experiments. For each experiment, the ratio of GFP expressing wildtype cells was set to 1 and used to calculate the relative GFP fluorescence for each mutant of the same experiment.

Transmission electron microscopy

To examine cell wall thickness of *B. subtilis* strains, cells were prepared for Transmission Electron Microscopy (TEM) as previously described (Rismondo et al., 2021). An overnight culture was inoculated to an OD_{600} of 0.05 in 30 ml MNGE medium and grown to an OD_{600} of 0.6 ± 0.1 at 37°C and 200 rpm. Cells were centrifuged for 10 minutes at 4,000 rpm to obtain a 100 μ l cell pellet, which was then washed twice in phosphate-buffered saline (PBS, 127 mM NaCl, 2.7 mM KCl, 10 mM Na_2HPO_4 , 1.8 mM KH_2PO_4 , pH 7.4) and fixed overnight in 2.5% (w/v) glutaraldehyde at 4°C. Cells were mixed with 1.5% (w/v, final concentration in PBS) molten Bacto-Agar, kept liquid at

55°C. After solidification, the resulting agar block was cut into 1 mm³ pieces. A dehydration series was performed (15% aqueous ethanol solution for 15 minutes, 30%, 50%, 70% and 95% for 30 minutes and 100% for 2 x 30 minutes) at 0°C, followed by an incubation step in 66% LR white resin mixture (v/v, in ethanol) (Plano, Wetzlar, Germany) for 2 hours at room temperature and embedment in 100% LR-White solution overnight at 4°C. One agar piece was transferred to a gelatin capsule filled with fresh LR-white resin, which was subsequently polymerized at 55°C for 24 hours. The gelatin capsule was shaped into a truncated pyramid using a milling tool (TM 60, Fa. Reichert & Jung, Vienna, Austria) An ultramicrotome (Reichert Ultracut E, Leica Microsystems, Wetzlar, Germany) and a diamond knife (Delaware Diamond Knives, Wilmington, DE, USA) were subsequently used to obtain ultrathin sections (80 nm) of the samples. The resulting sections were mounted onto mesh specimen grids (Plano, Wetzlar, Germany) and stained with 4% (w/v) uranyl acetate solution (pH 7.0) for 10 minutes. Microscopy images were taken on a Jeol JEM 1011 transmission electron microscope (Jeol Germany GmbH, Munich, Germany) at 80 kV, with a magnification of 30,000 and recorded with an Orius SC1000 CCD camera (Gatan Inc., Pleasanton, CA, USA). For each replicate, 20 cells were photographed and cell wall thickness was measured at three different locations using the software ImageJ (Rueden et al., 2017).

Results

ComK-dependent and –independent functions of proteins are required for the development of genetic competence

Genetic work with *B. subtilis* is facilitated by the development of genetic competence, a process that depends on a large number of factors. While the specific contribution of many proteins to the development of competence is well understood, this requirement has not been studied for many other factors. In particular, several RNases (RNase Y, RNase J1 and PNPase) are required for competence, and the corresponding mutants have lost the ability to become naturally competent (Luttinger et al., 1996; Figaro et al., 2013). We are interested in the reasons for the loss of competence in these mutant strains, as well as in other single gene deletion mutants, in which the impairment in the development of natural competence is not understood (Koo et al., 2017). Therefore, we first tested the roles of the aforementioned RNases (encoded by the *rny*, *rnjA*, *pnpA*, and *nrnA* genes) as well as of the transcription elongation factor GreA, the metalloprotease FtsH and the transcription factor YtrA (Koo et al., 2017) for the development of genetic competence. For this purpose, we compared the transformation efficiencies of the corresponding mutant strains to that of a wild type strain. The *comEC* and *degU* mutants, which have completely lost their genetic competence for different reasons, were used as controls. The ComEC protein is

responsible for the transport of the DNA molecule across the cytoplasmic membrane. Loss of ComEC blocks competence, but it should not affect the global regulation of competence development and expression of other competence factors (Draskovic and Dubnau, 2005). In contrast, DegU is a transcription factor required for the expression of the key regulator of competence, ComK, and thus indirectly also for the expression of all other competence genes (Hamoen et al., 2000; Shimane and Ogura, 2004). Our analysis confirmed the significant decrease in transformation efficiency for all tested strains (see Table 3). For five out of the seven strains, as well as the two control strains, competence was abolished completely, whereas transformation of strains GP2155 ($\Delta nrrA$) and GP1748 ($\Delta pnpA$) was possible, but severely impaired as compared to the wild type strain. These results confirm the implication of these genes in the development of genetic competence.

Table 3 | Effect of gene deletions on the development of genetic competence in dependence of the competence transcription factor ComK^a.

Mutant	Wild type	<i>P_{mtlA}-comKS</i>
	Colonies per μg of DNA	
Wild type	138,600 \pm 17,006	47,952 \pm 8,854
$\Delta degU$	0 \pm 0	60,853 \pm 13,693
$\Delta comEC$	0 \pm 0	0 \pm 0
$\Delta nrrA$	1,689 \pm 316	34,933 \pm 6,378
$\Delta ftsH$	0 \pm 0	0 \pm 0
$\Delta greA$	0 \pm 0	0 \pm 0
Δrny	0 \pm 0	0 \pm 0
$\Delta rnjA$	0 \pm 0	0 \pm 0
$\Delta pnpA$	17 \pm 6	293 \pm 19
$\Delta ytrA$	0 \pm 0	467 \pm 278

^a Cells were transformed with chromosomal DNA of strain GP1152 harboring a tetracycline resistance marker as described in Material and Methods.

The proteins that are required for genetic competence might play a more general role in the control of expression of the competence regulon (as known for the regulators that govern *comK* expression and ComK stability, e. g. the control protein DegU), or they may have a more specific role in competence development such as the control protein ComEC. To distinguish between these possibilities, we introduced the mutations into a strain that allows for the inducible overexpression of the *comK* and *comS* genes. The overexpression of *comK* and *comS* allows

transformation in rich medium and hence facilitates the transformation of some competence mutants (Rahmer et al., 2015). For this purpose, we first constructed strains that contain mannitol inducible *comK* and *comS* genes fused to resistance cassettes (GP2618 and GP2620, for details see Materials and Methods). Subsequently, we deleted our target genes in this genetic background and assayed transformation efficiency after induction of *comKS* expression (for details see Materials and Methods). In the *B. subtilis* wild type strain 168, deletion of *degU* leads to a complete loss of competence, while the transformation efficiency of a *degU* mutant overexpressing *comKS* is comparable to its isogenic wild type strain. This suggests that DegU affects competence only by its role in *comK* expression and that DegU is no longer required in the strain with inducible *comKS* expression. In contrast, the competence of the *comEC* mutant could not be restored by the overexpression of *comKS*, reflecting the role of the ComEC protein on a process downstream of ComK, namely on DNA uptake (see Table 3). Of the tested strains, only the *rrnA* mutant showed a transformation efficiency similar to that of the isogenic control strain with inducible *comKS* expression. This observation suggests that nanoRNase A might be involved in the control of *comK* expression. In contrast, the *ftsH*, *greA*, *rny* and *rnjA* mutants did not show any transformants even upon *comKS* overexpression, indicating that the corresponding proteins act downstream of ComK. Finally, we have observed a small but reproducible improvement of competence for the *pnpA* and *ytrA* mutants, indicating that PNPase and YtrA might affect *comK* expression. This finding is particularly striking in the case of the *ytrA* mutant, since this strain did not yield a single transformant in the 168 wild type background (see Table 3). However, the low number of transformants obtained with *pnpA* and *ytrA* mutants as compared to the isogenic wild type strain suggests that PNPase and the YtrA transcription factor play also a role downstream of ComK. ComK activates transcription of many competence genes including *comG* (van Sinderen et al., 1995). Therefore, as a complementary approach to verify the results shown above, we decided to assess ComK activity using a fusion of the *comG* promoter to a promoterless GFP reporter gene (Gamba et al., 2015). For this purpose, we deleted the selected genes in strain GP2630 containing the P_{comG} -*gfp* construct. We grew the cells in competence inducing medium using the two-step protocol as we did in the previous transformation experiment. At the time point when DNA would be added to the cells during the transformation procedure, we assessed *comG* promoter activity in the cells using fluorescence microscopy. Since expression of ComK and thus also activation of competence takes place only in a subpopulation of cells (Smits et al., 2005), we determined the ratio of *gfp* expressing cells for each mutant strain compared to the wildtype strain as an indication of ComK activity (see Fig 1). Since RNase mutants tend to form chains, thus making it difficult to study fluorescence in individual cells, we did not include the RNase mutants for this analysis.

In the wild type strain GP2630, about 40% of the cells expressed GFP, similar to previously published results (She et al., 2020), and slightly higher numbers were obtained for the control strain lacking ComEC, which is not impaired in *comK* and subsequent *comG* expression. In contrast, the control strain lacking DegU showed decreased amount of GFP expressing cells as compared to the wild type (Fig 1), which reflects the role of DegU on the activation of *comK* expression. In agreement with our previous finding that nanoRNase A affects *comK* expression or ComK activity, only about 4% of *nrnA* mutant cells showed expression from P_{comG} -*gfp*. Thus, the nanoRNase A encoded by *nrnA* seems to play a role in the regulation of *comK* expression, which has not been described so far. For the strain lacking GreA, we observed similar rates of GFP expressing cells as in the wild-type strain, indicating that ComK activation is not the problem, which causes loss of competence in the *greA* mutant. Surprisingly, we did not find any single cell expressing GFP for the *ftsH* mutant, where ComK expression does not seem to be the cause of competence deficiency as indicated by the previous transformation experiment. Additionally, we observed significantly decreased numbers of GFP producing cells for the *ytrA* deletion mutant, in which the competence deficiency could only be slightly restored by *comKS* overexpression.

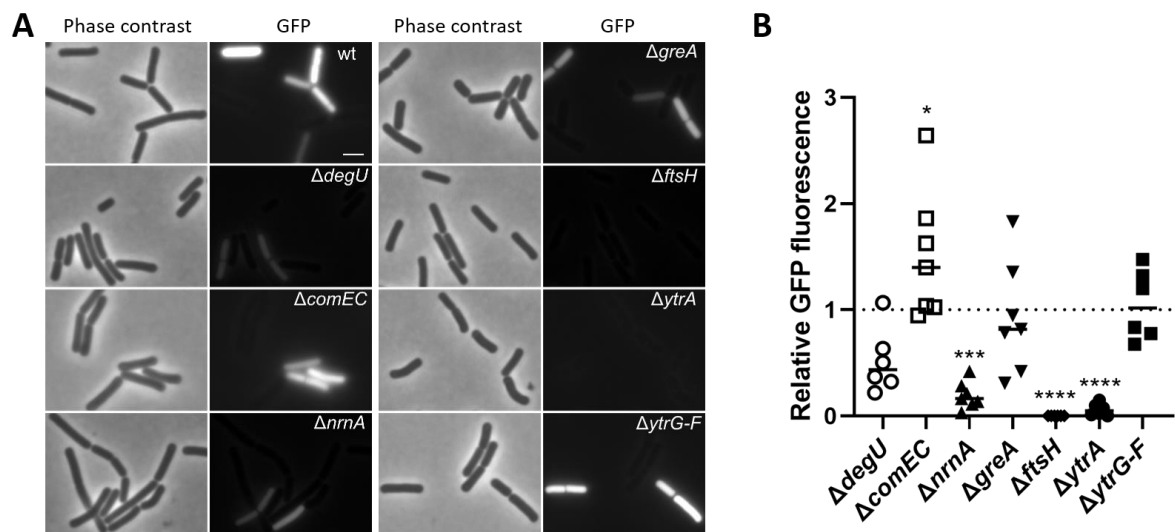


Figure 1 | Effect of gene deletions on the expression of a P_{comG} -*gfp* translational fusion as a readout for the activity of the competence transcription factor ComK (A) Strains harboring the P_{comG} -*gfp* construct were grown in competence inducing medium as described in the methods section. Cells were analyzed by phase contrast and fluorescence microscopy and representative images are shown. Scale bar is 2 μ m. **(B)** The percentage of GFP-expressing cells was determined for each strain. The ratio of GFP-expressing cells of each mutant compared to the wildtype strain was calculated and the result of at least six independent experiments plotted. For statistical analysis, a one-way ANOVA followed by a Dunnett's multiple comparison test was used (* $p \leq 0.05$, *** $p \leq 0.001$, **** $p \leq 0.0001$).

This observation suggests that FtsH and YtrA could potentially play a dual role in the development of genetic competence. On one hand, they both seem to be required for ComK activity but on the other hand, they also seem to have a ComK-independent function. However, it is also possible that the overexpression of *comK* and *comS* using the P_{mtlA} promoter does not lead to the production of sufficient amounts of ComK to fully restore competence of the *ftsH* and *ytrA* mutants. The *ytrA* gene encodes a transcription factor, whose physiological function is poorly understood (Salzberg et al., 2011). Therefore, we focused our further work on understanding the role of YtrA on the development of genetic competence.

3.2. Overexpression of the YtrBCDEF ABC transporter inhibits genetic competence

The *ytrA* gene encodes a negative transcription regulator of the GntR family, which binds to the inverted repeat sequence AGTGTA-13bp-TACACT (Salzberg et al., 2011). In the *B. subtilis* genome, this sequence is present in front of two operons, its own operon *ytrGABCDEF* and *ywoBCD*. The deletion of *ytrA* leads to an overexpression of these two operons (Salzberg et al., 2011). It is tempting to speculate that overexpression of one of these operons is the cause for the loss of competence in the *ytrA* mutant. In case of the *ytrA* mutant used in this study, the expression of the downstream genes, namely *ytrBCDEF*, is controlled by the promoter of the *ermC* gene, which was inserted into the *ytrA* locus. This results in a 335- and 566-fold expression of *ytrE* and *ytrF*, respectively, in the *ytrA* mutant as compared to the *B. subtilis* wildtype strain (Fig S1). To test whether the overexpression of *ytrBCDEF* leads to the competence deficiency of the *ytrA* mutant, we constructed strain GP2646, where the complete *ytrGABCDEF* operon is replaced by the *ermC* gene and assayed its genetic competence. This revealed that although deletion of *ytrA* fully blocks genetic competence, the transformation efficiency of the strain lacking the whole operon is comparable to the wild type strain 168 (Table 4). We conclude that overexpression of the *ytrGABCDEF* operon causes the loss of competence in the *ytrA* mutant strain. In addition, we assessed ComK activity in the mutant lacking the *ytrGABCDEF* operon, using the expression of the P_{comG} -*gfp* fusion as a readout. As observed for the wild type, about 40% of the mutant cells expressed *comG*, indicating that ComK is fully active in the mutant (Fig 1), and that the reduced activity in the *ytrA* mutant results from the overexpression of the operon. Initially we also aimed to delete the *ywoBCD* operon to assess a potential involvement in genetic competence, however several attempts to construct such a strain failed. As we were already able to show that the overexpression of the *ytr* operon causes the loss of competence in the *ytrA* mutant, we decided not to continue with this second YtrA-controlled operon.

The *ytr* operon consists of seven genes (see Fig 2A). Five proteins encoded by this operon (YtrB, YtrC, YtrD, YtrE and YtrF) are components of a putative ABC transporter (see Fig 2B), which was suggested to play a role in acetoin utilization (Quentin et al., 1999; Yoshida et al., 2000). YtrB and YtrE are supposed to be nucleotide binding proteins, YtrC and YtrD membrane spanning proteins and YtrF the substrate binding protein. Finally, *ytrG* is another open reading frame, which is located upstream of *ytrA* and encodes a peptide of 45 amino acids, which is probably not part of the ABC transporter (Salzberg et al., 2011). The expression of the *ytr* operon is usually kept low due to transcriptional repression by YtrA. This repression is naturally relieved in response to several lipid II-binding antibiotics or during cold shock (Beckering et al., 2002; Salzberg et al., 2011; Wenzel et al., 2012). To test the involvement of the individual components of the putative YtrBCDEF ABC transporter in the development of genetic competence, we constructed double mutants of *ytrA* together with each of the other genes of the operon, i.e. *ytrB*, *ytrC*, *ytrD*, *ytrE* and *ytrF*, and assessed their genetic competence. The results revealed that most of the double mutants are deficient in genetic transformation, as observed for the single *ytrA* mutant GP2647 (Table 4). However, strain GP3187 with deletions of *ytrA* and *ytrF* but still overexpressing all the other parts of the transporter had partially restored competence. YtrF could thus be a major player for the loss of competence in the overexpressing strain.

Table 4 | Effect of gene deletions in the *ytrGABCDEF* operon on the development of genetic competence^a.

Mutant	Colonies per μg of DNA
Wild type	138,600 \pm 17,006
$\Delta ytrGABCDEF$	114,733 \pm 14,408
$\Delta ytrA$	0 \pm 0
$\Delta ytrAB$	0 \pm 0
$\Delta ytrAC$	0 \pm 0
$\Delta ytrAD$	24 \pm 2
$\Delta ytrAE$	137 \pm 51
$\Delta ytrAF$	10,180 \pm 549
$P_{xyr}-ytrF$	137,533 \pm 26,595
$\Delta ytrGABCDE$	108,467 \pm 14,836
$\Delta ytrABE$	309 \pm 88
Wild type	142,600 \pm 39,074
$\Delta ytrACD$	1.7 \pm 2.4

^a Cells were transformed with chromosomal DNA of strain GP1152 harboring a tetracycline resistance marker as described in Material and Methods.

To further test the role of YtrF overexpression for the loss of competence, we used two different approaches. First, we constructed a strain with artificial overexpression of *ytrF* from a xylose inducible promoter (GP3197) and second, we created a strain with deletion of all other components (*ytrGABCDE*) of the operon, leaving only overexpressed *ytrF* (GP3186). Overexpression of *ytrF* in strain GP3186 was confirmed by qRT-PCR analysis (Fig 2). In contrast to our expectations, competence was not blocked in any of the two strains, suggesting that increased levels of YtrF alone are not enough to block the competence and that YtrF might need assistance from other components of the putative transporter for its full action and/or proper localization. The *ytr* operon encodes two putative nucleotide binding proteins (YtrB and YtrE) and two putative membrane spanning proteins (YtrC and YtrD), whereas YtrF is the only substrate binding protein that interacts with the transmembrane proteins. Therefore, we hypothesized that YtrF overexpression might only block genetic competence if the protein is properly localized in the membrane via YtrC and YtrD. To check this possibility, we constructed strains GP3206 and BLMS3 lacking YtrA and the nucleotide binding proteins YtrB and YtrE or the membrane proteins YtrC and YtrD, respectively, and tested their transformability. qRT-PCR analysis was again used to confirm that *ytrF* is overexpressed in strains GP3206 and BLMS3 as compared to the wildtype strain 168 (Fig S1). Strain GP3206 showed very few transformants, suggesting that the overexpression of *ytrC*, *ytrD* and *ytrF*, encoding the remaining transporter components, are sufficient to cause the loss of competence. Surprisingly, similar results were obtained for a *B. subtilis* strain lacking YtrA, YtrC and YtrD. We thus conclude that the observed loss of competence as a result of YtrF overexpression does not depend on the nucleotide binding proteins or the transmembrane proteins. Since we did not observe a loss of competence for *B. subtilis* strains, in which only YtrF is overexpressed, we hypothesize that YtrF might require assistance of another, unknown factor.

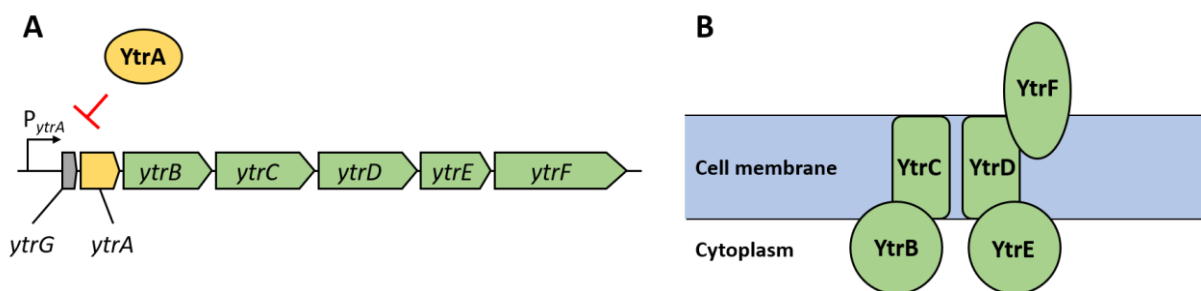


Figure 2 | Genetic organization of the *ytrGABCDE* operon and organization of the putative ABC transporter YtrBCDEF (A) Reading frames are depicted as arrows with respective gene names. Green arrows indicate genes encoding proteins suggested to form the ABC transporter; the yellow arrow indicates the gene coding for the repressor YtrA and the grey arrow indicates the small open reading frame called *ytrG*. The map is based on information provided in Salzberg et al. (2011) **(B)** Organization of the putative ABC transporter YtrBCDEF as suggested by Yoshida et al. (2000). YtrB and YtrE are nucleotide binding proteins, YtrC and YtrD membrane spanning proteins and YtrF is a substrate binding protein. The role and localization of the YtrG peptide remain elusive.

Overexpression of the *ytrGABCDE* operon leads to alterations in colony morphology during biofilm formation

B. subtilis can employ various lifestyles which are tightly interconnected through regulatory proteins (Lopez et al., 2009). Therefore, we anticipated that the overexpression of the YtrBCDEF transporter might also affect other lifestyles of *B. subtilis*. Indeed, it was previously shown that the *ytrA* mutant has a reduced sporulation efficiency (Koo et al., 2017). We thus decided to examine the effect of *ytrA* deletion on biofilm formation. To that end, we deleted the *ytrA* gene or the whole *ytrGABCDE* operon from the biofilm-forming strain DK1042 (Konkol et al., 2013). We then tested the biofilm formation of the resulting strains on biofilm inducing MSgg agar (Branda et al., 2001). As expected, the wild type strain DK1042 formed structured colonies that are indicative of biofilm formation. In contrast, the negative control GP2559, a *ymdB* mutant that is known to be defective in biofilm formation (Kampf et al., 2018), formed completely smooth colonies. The biofilm formed by the *ytrA* mutant GP3212 was less structured, more translucent and with only some tiny wrinkles on its surface, indicating that biofilm formation was slightly inhibited but not fully abolished upon loss of YtrA. In contrast, strain GP3207 lacking the complete *ytrGABCDE* operon formed a biofilm indistinguishable from the one of the parental strain DK1042 (see Fig 3). This observation suggests that overexpression of components of the YtrBCDEF ABC transporter could interfere with biofilm formation in *B. subtilis*.

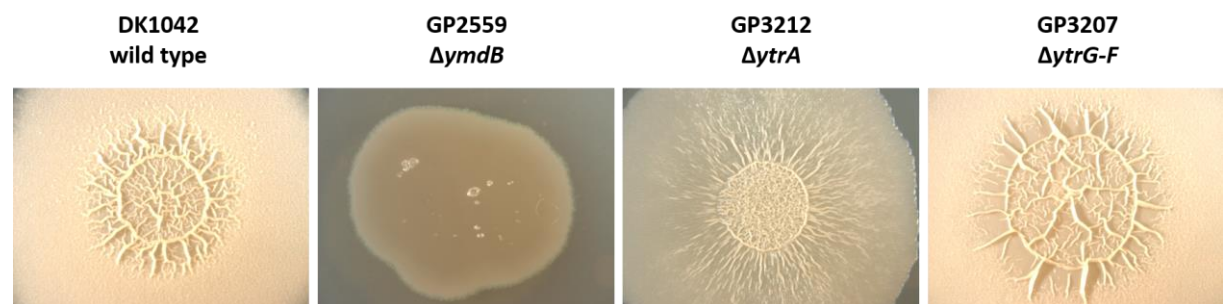


Figure 3 | Biofilm formation is affected by *ytrA* deletion. Biofilm formation was examined in the wild type strain DK1042 and respective deletion mutants of *ymdB* (GP2559), *ytrA* (GP3212) and *ytrGABCDE* (GP3207). The biofilm assay was performed on MSgg agar plates as described in Material and Methods. The plates were incubated for 3 days at 30°C. All images were taken at the same magnification.

Overexpression of the *ytr* operon increases cell wall thickness

In previous experiments, we have shown that the overexpression of the *ytr* operon interferes with the development of genetic competence and, to some extent, with biofilm formation. However, it remains unclear why competence and biofilm formation are affected by the overexpression of the *ytr* operon. The *ytr* operon is repressed under standard laboratory conditions by the YtrA transcription regulator and this repression is naturally relieved upon exposure to very specific stress conditions such as cell wall targeting antibiotics and cold shock (Beckerling et al., 2002; Cao

et al., 2002; Mascher et al., 2003; Salzberg et al., 2011; Nicolas et al., 2012; Wenzel et al., 2012). The possible link between antibiotic resistance, genetic competence, and biofilm formation is not apparent, however, cell wall properties might provide an answer. Indeed, it has been shown that wall teichoic acids, the uppermost layer of the cell wall, are important for biofilm formation and for DNA binding during transformation (Mirouze et al., 2018; Bucher et al., 2015; Zhu et al., 2018).

To test the hypothesis that overexpression of the putative ABC transporter encoded by the *ytrGABCDE* operon affects cell wall properties of *B. subtilis* cells, we compared the cell morphology of the wild type, the non-competent *ytrA*, *ytrAB*, *ytrAE* mutants as well as the competent *ytrGABCDE* mutant lacking the complete operon by transmission electron microscopy. While the wild type strain showed an average cell wall thickness of 21 nm, which is in agreement with previous studies (Beveridge and Murray, 1979), the *ytrA* (GP2647) mutant showed a significant increase in cell wall thickness with an average of 31 nm. *B. subtilis* strains lacking one of the nucleotide binding proteins of the transporter, YtrB or YtrE, in addition to YtrA also produced a thicker cell wall with an average thickness of 30 nm and 31 nm, respectively. In contrast, such an increase was not observed for the whole operon mutant (GP2646) that had an average cell wall thickness of 23 nm (see Fig 4). These observations are in agreement with the hypothesis that the overexpression of the YtrBCDEF ABC transporter affects cell wall properties and could potentially explain the loss of genetic competence and the minor biofilm formation defect of the *ytrA* mutant.

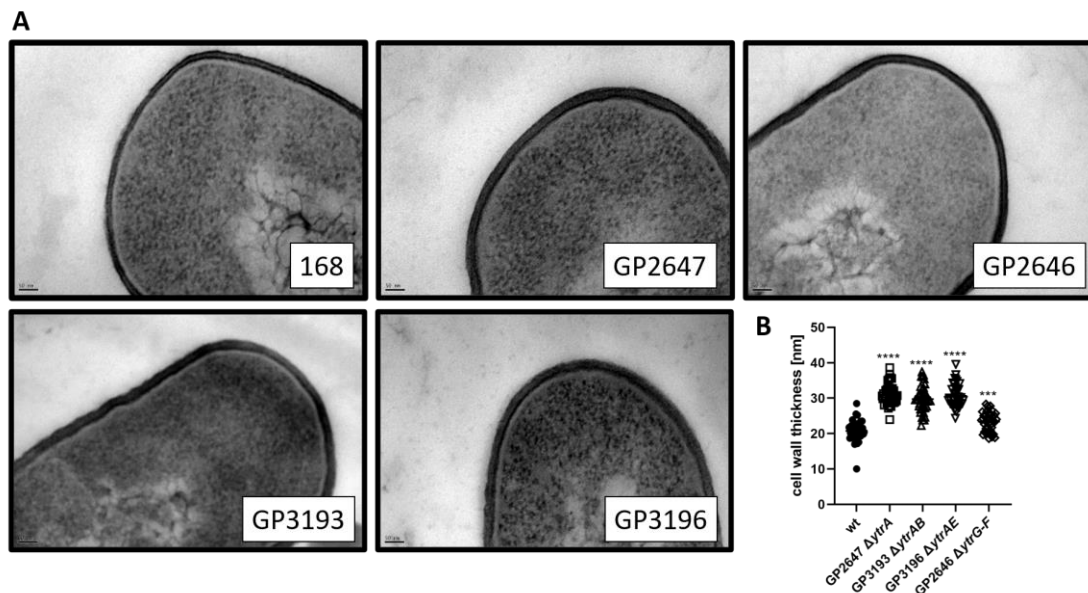


Figure 4 | Cell wall thickness is increased in *ytrA*, *ytrAB* and *ytrAE* mutants. (A) Shown are representative transmission electron microscopy images of the wild type strain 168, the *ytrA* mutant (GP2647), the *ytrAB* (GP3193) and the *ytrAE* (GP3196) double mutants and the *ytrGABCDE* mutant (GP2646). Scale bar is 50 nm. (B) Cell wall thickness of *B. subtilis* wild type and *ytr* mutants. The cell wall thickness of 40 individual cells per strain was measured as described in Material and Methods and plotted. For statistical analysis, a one-way ANOVA followed by a Dunnett's comparison test was used (***) $p \leq 0.001$, ****) $p \leq 0.0001$.

Discussion

Genetic competence is a multifactorial process in the gram-positive organism *B. subtilis*. In a genome-wide study, several single deletion mutants were identified, which are significantly impaired in competence development (Koo et al., 2017). However, it remains to be determined why the deletion of the corresponding genes affect this process. Here, we aimed to investigate the role of the transcription elongation factor GreA, the metalloprotease FtsH, the transcriptional regulator YtrA and the RNases RNase Y, RNase J1, PNPase and nanoRNase A on competence development in *B. subtilis*. In accordance with previous studies, deletion of *greA*, *ftsH*, *ytrA*, *rny* and *rnjA* resulted in a complete loss of competence and the competence of strains lacking the PNPase or nanoRNase A was severely reduced (Figaro et al., 2013; Koo et al., 2017). The overexpression of *comKS*, coding for the master regulator of competence ComK and the small antiadapter protein ComS, could not restore the competence of the *rny*, *rnjA* and *greA* mutants, suggesting that RNase Y, RNase J1 and GreA act downstream of the control of *comK* expression. In contrast, overexpression of *comKS* restored the competence efficiency of the *nrnA* mutant to a level comparable to the isogenic wild type strain and we hypothesize that nanoRNase A directly or indirectly affects *comK* expression. Lack of the metalloprotease FtsH led to a complete loss of genetic competence that could not be restored by the overexpression of *comKS* suggesting that FtsH acts downstream of ComK. However, we could not detect any expression from the *comG* promoter, which contradicts the first result. We hypothesize that FtsH might have a dual role: on one hand, it could influence the expression of *comK* and on the other hand, it could have a ComK-independent role. However, it is also possible that ComK is not properly expressed in the *ftsH* mutant or that FtsH is involved in the turnover of MecA, Rok or AbrB leading to a reduced expression of *comK* or an enhanced degradation of ComK. Further studies are required to understand the precise role of FtsH on competence development in *B. subtilis*. For the *pnpA* and *ytrA* mutants, we observed a slight improvement of competence, suggesting that PNPase and YtrA could play a role in *comK* expression control. However, the genetic competence could not be fully restored by *comKS* overexpression, indicating that ComK might not be the only factor contributing to the competence deficiency of the *pnpA* and *ytrA* mutants. Again, elevated ComK levels might not be sufficient to completely suppress the competence deficiency of these two mutants.

The transcriptional repressor YtrA is encoded in the *ytrGABCDEF* operon, whose expression is induced in the presence of cell wall-acting antibiotics and cold shock (Beckering et al., 2002; Salzberg et al., 2011; Wenzel et al., 2012). The *ytrGABCDEF* operon further codes for a putative ABC transporter, YtrBCDEF, which was suggested to be involved in acetoin utilization in *B. subtilis* (Quentin et al., 1999; Yoshida et al., 2000). Previous work already revealed that lack of

YtrA leads to a competence defect and a decreased sporulation efficiency (Koo et al., 2017). In this work we could show that loss of genetic competence of the *ytrA* mutant is caused by the overexpression of the *ytrGABCDE* operon. Furthermore, this phenotype seems to partially depend on the presence of the substrate binding protein YtrF. Surprisingly, transformations of a *ytrA* mutant also lacking both ATP-binding proteins, YtrB and YtrE, or both transmembrane proteins, YtrC and YtrD, only leads to a small number of colonies, suggesting that the loss of genetic competence of a *ytrA* mutant does not require the activity of the YtrBCDEF transporter.

Based on the partial complementation of genetic competence of the *ytrA* mutant upon *comKS* overexpression, one might expect that the loss of YtrA and the concomitant overexpression of the ABC transporter somehow interfere with a process upstream of ComK activation. However, competence is developed in an all or nothing scenario, and cells in which the ComK levels reach a certain threshold should become competent (Haijema et al., 2001; Maamar and Dubnau, 2005). Our observation that *comKS* overexpression only partially restores competence of the *ytrA* mutant suggests that ComK levels are not the only factor that limit competence of the *ytrA* mutant. If the *ytrA* deletion would only interfere with ComK activation, one would expect wild type-like competence upon overexpression of *comKS*, which was not the case. However, it is also possible that ComK levels in the *ytrA* mutant background are not sufficient to restore genetic competence, even after mannitol-induced overexpression of *comKS*. Another explanation could be that the activity of MecA is enhanced in the absence of YtrA leading to a faster degradation of ComK by the ClpCP complex. In addition to the loss of competence, the *ytrA* mutant produces a thicker cell wall as compared to the *B. subtilis* wild type, which could also have an impact on genetic competence. The DNA uptake apparatus must be adapted to cell wall thickness in order to ensure that the extracellular DNA can reach the ComG/ComE DNA transport complex. Due to the increased cell wall thickness upon overexpression of the YtrBCDEF ABC transporter, the DNA is probably unable to get in contact with the ComG pili. Overexpression of ComK will then result in the increased production of DNA-binding ComG on the cell surface of all cells of the population (compared to about 10% in the wild-type strain transformed with the classical two-step protocol). This would simply increase the probability that foreign DNA reaches the DNA uptake machinery in some cells, which then leads to the appearance of a few transformants as observed in our study. On the other hand, the results obtained by fluorescence microscopy revealed a decreased transcription from the ComK dependent *comG* promoter in the *ytrA* mutant. However, this expression is expected to be wild type-like if the action of the YtrBCDEF ABC transporter would not interfere with ComK activity and only block DNA uptake as a result of the thicker cell wall as suggested above. Again, the thicker cell wall might be responsible, since ComK expression is

induced by the detection of extracellular quorum-sensing signals (both ComXPA and Rap-Phr systems) and this induction depends on the accessibility of the sensor domains for the pheromones (reviewed in (Maier, 2020)), which might be impaired in the strain with altered cell wall thickness.

In addition to the loss of genetic competence, it was previously shown that *ytrA* deletion leads to decreased sporulation efficiency (Koo et al., 2017) and we have shown that it also has a minor effect on biofilm formation. Considering the changed cell wall properties, this is in agreement with previous studies, which showed hampered biofilm formation upon disruption of cell wall biosynthesis (Bucher et al., 2015; Zhu et al., 2018). Taken together, we conclude that the overexpression of the YtrBCDEF ABC transporter upon deletion of *ytrA* leads to pleiotropic effects on alternative lifestyles of *B. subtilis* and to increased cell wall thickness, however, at the current stage it is unknown whether the proteins encoded in the *ytr* operon have a direct impact on competence, sporulation and biofilm formation or whether these pleiotropic effects are indirect consequences of the increased cell wall thickness.

Our results demonstrate that the YtrBCDEF ABC transporter is involved in the control of cell wall homeostasis, but it is not yet clear how this is achieved. An easy explanation would be that the system exports molecules necessary for cell wall synthesis, however, based on the presence of the substrate binding protein YtrF and on the critical role of this protein in preventing genetic competence, it can be assumed that the ABC transporter rather acts as an importer. YtrBCDEF could therefore be involved in the import of components required for the synthesis of peptidoglycan precursors or an unknown signal, which is involved in the regulation of peptidoglycan precursor production. In the latter case, overproduction of the ABC transporter YtrBCDEF would lead to an increased import of this unknown signal molecule and thus, to an enhanced peptidoglycan precursor synthesis leading to the production of a thicker cell wall. It is also possible that YtrBCDEF may not act as a transporter at all and simply modulate the activity of other enzymes that participate in cell wall metabolism. This could potentially explain why the *B. subtilis* strain lacking YtrA as well as the ATP-binding proteins, latter of which are usually essential for the activity of ABC transporters, still produce a thicker cell wall and remain non-competent. Strikingly, the C-terminus of YtrF contains a FtsX-like domain. In *B. subtilis*, the ABC transporter FtsEX activates the cell wall hydrolase CwIO via direct protein-protein interaction thereby affecting cell elongation (Meisner et al., 2013). We speculate that the FtsX-like domain of YtrF could thus be required for the interaction with other proteins.

Based on its expression pattern, the *ytr* operon was described as a reporter for glycopeptide antibiotics, such as vancomycin or ristocetin (Hutter et al., 2004) and antibiotics that

interfere with the lipid II cycle, such as nisin (Wenzel et al., 2012). Whether this induction of *ytrGABCDE*F expression leads to an increased resistance towards those antibiotics is not clear, but recent results indicate that it has indeed an impact on nisin resistance (Senges et al., 2020). Interestingly, the substrate binding lipoprotein YtrF contains a MacB-like periplasmic core domain in its N-terminus. MacB proteins are usually involved in resistance towards antibiotics and peptide toxins (Greene et al., 2018), suggesting that YtrF could potentially bind antibiotics. It is tempting to speculate that cell wall-acting antibiotics serve as an exogenous signal to activate the expression of the ABC transporter YtrBCDEF, which leads to the production of a thicker cell wall and with this, to an increased resistance to these antibiotics. However, how this could still be achieved in the absence of the ATP-binding proteins YtrB and YtrE remains elusive. Future work will need to address the precise mechanism by which the YtrBCDEF ABC transporter affects cell wall synthesis in *B. subtilis*.

Acknowledgements

We wish to thank Julia Busse, Melin Güzel, Christopher Patrick Zschiedrich and Leon Daniau for the help with some experiments. We are grateful to Josef Altenbuchner, Jan Gundlach, Leendert Hamoen, Daniel Kearns, Daniel Reuss, Sarah Wilcken, and the Bacillus Genetic Sock Center for providing *B. subtilis* strains. We thank Dr. Michael Hoppert for providing access to the Transmission Electron Microscope. This research received funding from the Deutsche Forschungsgemeinschaft via SFB860.

Supplemental Material

<https://www.frontiersin.org/articles/10.3389/fmicb.2021.587035/full#supplementary-material>

Figure S1 The *ytrGABCDE*F operon is overexpressed in the *ytrA* mutant

References

- Aguilar, C., Vlamakis, H., Guzman, A., Losick, R., and Kolter, R. (2010). KinD is a checkpoint protein linking spore formation to extracellular-matrix production in *Bacillus subtilis* biofilms. *mBio* 1, e00035–10. doi:10.1128/mBio.00035-10.
- Beckerling, C. L., Steil, L., Weber, M. H. W., Völker, U., and Marahiel, M. A. (2002). Genomewide transcriptional analysis of the cold shock response in *Bacillus subtilis*. *J. Bacteriol.* 184, 6395–6402. doi:10.1128/JB.184.22.6395-6402.2002.
- Berka, R. M., Hahn, J., Albano, M., Draskovic, I., Persuh, M., Cui, X., et al. (2002). Microarray analysis of the *Bacillus subtilis* K-state: Genome-wide expression changes dependent on ComK. *Mol. Microbiol.* 43, 1331–1345. doi:10.1046/j.1365-2958.2002.02833.x.
- Beveridge, T. J., and Murray, R. G. E. (1979). How thick is the *Bacillus subtilis* cell wall? *Curr. Microbiol.* 2, 1–4. doi:10.1007/BF02601723.
- Boonstra, M., Schaffer, M., Sousa, J., Morawska, L., Holsappel, S., Hildebrandt, P., et al. (2020). Analyses of competent and non-competent subpopulations of *Bacillus subtilis* reveal *yhfW*, *yhxC* and ncRNAs as novel players in competence. *Environ. Microbiol.* 22, 2312–2328. doi:10.1111/1462-2920.15005.
- Branda, S. S., González-Pastor, J. E., Ben-Yehuda, S., Losick, R., and Kolter, R. (2001). Fruiting body formation by *Bacillus subtilis*. *Proc. Natl. Acad. Sci. U. S. A.* 98, 11621–11626. doi:10.1073/pnas.191384198.
- Bucher, T., Oppenheimer-Shaan, Y., Savidor, A., Bloom-Ackermann, Z., and Kolodkin-Gal, I. (2015). Disturbance of the bacterial cell wall specifically interferes with biofilm formation. *Environ. Microbiol. Rep.* 7, 990–1004. doi:10.1111/1758-2229.12346.
- Cascante-Estepa, N., Gunka, K., and Stülke, J. (2016). Localization of components of the RNA-degrading machine in *Bacillus subtilis*. *Front. Microbiol.* 7, 1492. doi:10.3389/fmicb.2016.01492.
- Diethmaier, C., Pietack, N., Gunka, K., Wrede, C., Lehnik-Habrink, M., Herzberg, C., et al. (2011). A novel factor controlling bistability in *Bacillus subtilis*: The Ymdb protein affects flagellin expression and biofilm formation. *J. Bacteriol.* 193, 5997–6007. doi:10.1128/JB.05360-11.
- Draskovic, I., and Dubnau, D. (2005). Biogenesis of a putative channel protein, ComEC, required for DNA uptake: Membrane topology, oligomerization and formation of disulphide bonds. *Mol. Microbiol.* 55, 881–896. doi:10.1111/j.1365-2958.2004.04430.x.
- Figaro, S., Durand, S., Gilet, L., Cayet, N., Sachse, M., and Condon, C. (2013). *Bacillus subtilis* mutants with knockouts of the genes encoding ribonucleases RNase Y and RNase J1 are viable, with major defects in cell morphology, sporulation, and competence. *J. Bacteriol.* 195,

2340–2348. doi:10.1128/JB.00164-13.

Flórez, L. A., Gunka, K., Polanía, R., Tholen, S., and Stülke, J. (2011). SPABBATS: A pathway-discovery method based on Boolean satisfiability that facilitates the characterization of suppressor mutants. *BMC Syst. Biol.* 5, 5. doi:10.1186/1752-0509-5-5.

Gamba, P., Jonker, M. J., and Hamoen, L. W. (2015). A novel feedback loop that controls bimodal expression of genetic competence. *PLoS Genet.* 11, e1005047. doi:10.1371/journal.pgen.1005047.

Greene, N. P., Kaplan, E., Crow, A., and Koronakis, V. (2018). Antibiotic resistance mediated by the MacB ABC transporter family: A structural and functional perspective. *Front. Microbiol.* 9, 950. doi:10.3389/fmicb.2018.00950.

Guérout-Fleury, A. M., Shazand, K., Frandsen, N., and Stragier, P. (1995). Antibiotic-resistance cassettes for *Bacillus subtilis*. *Gene* 167, 335–336. doi:10.1016/0378-1119(95)00652-4.

Hahn, J., Roggiani, M., and Dubnau, D. (1995). The major role of Spo0A in genetic competence is to downregulate *abrB*, an essential competence gene. *J. Bacteriol.* 177, 3601–3605. doi:10.1128/JB.177.12.3601-3605.1995.

Haijema, B.-J., Hahn, J., Haynes, J., and Dubnau, D. (2001). A ComGA-dependent checkpoint limits growth during the escape from competence. *Mol. Microbiol.* 40, 52–64. doi:10.1046/j.1365-2958.2001.02363.x.

Hamoen, L. W., Kausche, D., Marahiel, M. A., Sinderen, D., Venema, G., and Serror, P. (2003). The *Bacillus subtilis* transition state regulator AbrB binds to the –35 promoter region of comK. *FEMS Microbiol. Lett.* 218, 299–304. doi:10.1111/j.1574-6968.2003.tb11532.x.

Hamoen, L. W., Smits, W. K., de Jong, A., Holsappel, S., and Kuipers, O. P. (2002). Improving the predictive value of the competence transcription factor (ComK) binding site in *Bacillus subtilis* using a genomic approach. *Nucleic Acids Res.* 30, 5517–5528. doi:10.1093/nar/gkf698.

Hamoen, L. W., Van Werkhoven, A. F., Venema, G., and Dubnau, D. (2000). The pleiotropic response regulator DegU functions as a priming protein in competence development in *Bacillus subtilis*. *Proc. Natl. Acad. Sci. U. S. A.* 97, 9246–9251. doi:10.1073/pnas.160010597.

Hoa, T. T., Tortosa, P., Albano, M., and Dubnau, D. (2002). Rok (YkuW) regulates genetic competence in *Bacillus subtilis* by directly repressing *comK*. *Mol. Microbiol.* 43, 15–26. doi:10.1046/j.1365-2958.2002.02727.x.

Hutter, B., Fischer, C., Jacobi, A., Schaab, C., and Loferer, H. (2004). Panel of *Bacillus subtilis* reporter strains indicative of various modes of action. *Antimicrob. Agents Chemother.* 48, 2588–2594. doi:10.1128/AAC.48.7.2588-2594.2004.

- Kampf, J., Gerwig, J., Kruse, K., Cleverley, R., Dormeyer, M., Grünberger, A., et al. (2018). Selective pressure for biofilm formation in *Bacillus subtilis*: Differential effect of mutations in the master regulator SinR on bistability. *mBio* 9, e01464-18. doi:10.1128/mBio.01464-18.
- Konkol, M. A., Blair, K. M., and Kearns, D. B. (2013). Plasmid-encoded ComI inhibits competence in the ancestral 3610 strain of *Bacillus subtilis*. *J. Bacteriol.* 195, 4085–4093. doi:10.1128/JB.00696-13.
- Koo, B. M., Kritikos, G., Farelli, J. D., Todor, H., Tong, K., Kimsey, H., et al. (2017). Construction and analysis of two genome-scale deletion libraries for *Bacillus subtilis*. *Cell Syst.* 4, 291–305. doi:10.1016/j.cels.2016.12.013.
- Kunst, F., and Rapoport, G. (1995). Salt stress is an environmental signal affecting degradative enzyme synthesis in *Bacillus subtilis*. *J. Bacteriol.* 177, 2403–2407. doi:10.1128/jb.177.9.2403-2407.1995.
- López, D., and Kolter, R. (2010). Extracellular signals that define distinct and coexisting cell fates in *Bacillus subtilis*. *FEMS Microbiol. Rev.* 34, 134–149. doi:10.1111/j.1574-6976.2009.00199.x.
- Lopez, D., Vlamakis, H., and Kolter, R. (2009). Generation of multiple cell types in *Bacillus subtilis*. *FEMS Microbiol. Rev.* 33, 152–163. doi:10.1111/j.1574-6976.2008.00148.x.
- Luttinger, A., Hahn, J., and Dubnau, D. (1996). Polynucleotide phosphorylase is necessary for competence development in *Bacillus subtilis*. *Mol. Microbiol.* 19, 343–356. doi:10.1046/j.1365-2958.1996.380907.x.
- Maamar, H., and Dubnau, D. (2005). Bistability in the *Bacillus subtilis* K-state (competence) system requires a positive feedback loop. *Mol. Microbiol.* 56, 615–624. doi:10.1111/j.1365-2958.2005.04592.x.
- Maier, B. (2020). Competence and transformation in *Bacillus subtilis*. *Curr. Issues Mol. Biol.* 37, 57–76. doi:10.21775/cimb.037.057.
- Meinken, C., Blencke, H.-M., Ludwig, H., and Stülke, J. (2003). Expression of the glycolytic *gapA* operon in *Bacillus subtilis*: differential syntheses of proteins encoded by the operon. *Microbiology* 149, 751–761. doi:10.1099/mic.0.26078-0.
- Meisner, J., Montero Llopis, P., Sham, L. T., Garner, E., Bernhardt, T. G., and Rudner, D. Z. (2013). FtsEX is required for CwIO peptidoglycan hydrolase activity during cell wall elongation in *Bacillus subtilis*. *Mol. Microbiol.* 89, 1069–1083. doi:10.1111/mmi.12330.
- Mirouze, N., Desai, Y., Raj, A., and Dubnau, D. (2012). Spo0A~P imposes a temporal gate for the bimodal expression of competence in *Bacillus subtilis*. *PLoS Genet.* 8, e1002586. doi:10.1371/journal.pgen.1002586.

- Mirouze, N., Ferret, C., Cornilleau, C., and Carballido-López, R. (2018). Antibiotic sensitivity reveals that wall teichoic acids mediate DNA binding during competence in *Bacillus subtilis*. *Nat. Commun.* 9, 5072. doi:10.1038/s41467-018-07553-8.
- Nakano, M. M., Xia, L. A., and Zuber, P. (1991). Transcription initiation region of the *srfA* operon, which is controlled by the *comP-comA* signal transduction system in *Bacillus subtilis*. *J. Bacteriol.* 173, 5487–5493. doi:10.1128/JB.173.17.5487-5493.1991.
- Nicolas, P., Mäder, U., Dervyn, E., Rochat, T., Leduc, A., Pigeonneau, N., et al. (2012). Condition-dependent transcriptome reveals high-level regulatory architecture in *Bacillus subtilis*. *Science* 335, 1103–1106. doi:10.1126/science.1206848.
- Ogura, M., Yamaguchi, H., Kobayashi, K., Ogasawara, N., Fujita, Y., and Tanaka, T. (2002). Whole-genome analysis of genes regulated by the *Bacillus subtilis* competence transcription factor ComK. *J. Bacteriol.* 184, 2344–2351. doi:10.1128/JB.184.9.2344-2351.2002.
- Quentin, Y., Fichant, G., and Denizot, F. (1999). Inventory, assembly and analysis of *Bacillus subtilis* ABC transport systems. *J. Mol. Biol.* 287, 467–484. doi:10.1006/jmbi.1999.2624.
- Rahmer, R., Morabbi Heravi, K., and Altenbuchner, J. (2015). Construction of a super-competent *Bacillus subtilis* 168 using the P_{mtIA} -*comKS* inducible cassette. *Front. Microbiol.* 6, 1431. doi:10.3389/fmicb.2015.01431.
- Reuß, D. R., Altenbuchner, J., Mäder, U., Rath, H., Ischebeck, T., Sappa, P. K., et al. (2017). Large-scale reduction of the *Bacillus subtilis* genome: Consequences for the transcriptional network, resource allocation, and metabolism. *Genome Res.* 27, 289–299. doi:10.1101/gr.215293.116.
- Rismondo, J., Schulz, L. M., Yacoub, M., Wadhawan, A., Hoppert, M., Dionne, M. S., et al. (2021). EslB is required for cell wall biosynthesis and modification in *Listeria monocytogenes*. *J. Bacteriol.* 203, e00553-20. doi:10.1128/JB.00553-20.
- Rueden, C. T., Schindelin, J., Hiner, M. C., DeZonia, B. E., Walter, A. E., Arena, E. T., et al. (2017). ImageJ2: ImageJ for the next generation of scientific image data. *BMC Bioinformatics* 18, 529. doi:10.1186/s12859-017-1934-z.
- Salzberg, L. I., Luo, Y., Hachmann, A.-B., Mascher, T., and Helmann, J. D. (2011). The *Bacillus subtilis* GntR family repressor YtrA responds to cell wall antibiotics. *J. Bacteriol.* 193, 5793–5801. doi:10.1128/JB.05862-11.
- Sambrook, J., Fritsch, E. F., and Maniatis, T. (1989). *In: Molecular cloning: A laboratory manual, Cold Spring Harbor Laboratory, Cold Spring Harbor, New York.* 2nd ed. Cold Spring Harbor Laboratory Press.
- Senges, C. H. R., Stepanek, J. J., Wenzel, M., Raatschen, N., Ay, Ü., Märten, Y., et al. (2021).
-

- Comparison of proteomic responses as global approach to antibiotic mechanism of action elucidation. *Antimicrob. Agents Chemother.* 65, e01373-20. doi:10.1128/AAC.01373-20.
- Serror, P., and Sonenshein, A. L. (1996). CodY is required for nutritional repression of *Bacillus subtilis* genetic competence. *J. Bacteriol.* 178, 5910–5915. doi:10.1128/jb.178.20.5910-5915.1996.
- She, Q., Hunter, E., Qin, Y., Nicolau, S., Zalis, E. A., Wang, H., et al. (2020). Negative interplay between biofilm formation and competence in the environmental strains of *Bacillus subtilis*. *mSystems* 5, e00539-20. doi:10.1128/mSystems.00539-20.
- Shimane, K., and Ogura, M. (2004). Mutational analysis of the helix-turn-helix region of *Bacillus subtilis* response regulator DegU, and identification of cis-acting sequences for DegU in the *aprE* and *comK* promoters. *J. Biochem.* 136, 387–397. doi:10.1093/jb/mvh127.
- Smits, W. K., Eschevins, C. C., Susanna, K. A., Bron, S., Kuipers, O. P., and Hamoen, L. W. (2005). Stripping *Bacillus*: ComK auto-stimulation is responsible for the bistable response in competence development. *Mol. Microbiol.* 56, 604–614. doi:10.1111/j.1365-2958.2005.04488.x.
- Turgay, K., Hahn, J., Burghoorn, J., and Dubnau, D. (1998). Competence in *Bacillus subtilis* is controlled by regulated proteolysis of a transcription factor. *EMBO J.* 17, 6730–6738. doi:10.1093/emboj/17.22.6730.
- van Sinderen, D., Luttinger, A., Kong, L., Dubnau, D., Venema, G., and Hamoen, L. (1995). *comK* encodes the competence transcription factor, the key regulatory protein for competence development in *Bacillus subtilis*. *Mol. Microbiol.* 15, 455–462. doi:10.1111/j.1365-2958.1995.tb02259.x.
- Wach, A. (1996). PCR-synthesis of marker cassettes with long flanking homology regions for gene disruptions in *S. cerevisiae*. *Yeast* 12, 259–265. doi:10.1002/(SICI)1097-0061(19960315)12:3<259::AID-YEA901>3.0.CO;2-C.
- Wenzel, M., Kohl, B., Münch, D., Raatschen, N., Albada, H. B., Hamoen, L., et al. (2012). Proteomic response of *Bacillus subtilis* to lantibiotics reflects differences in interaction with the cytoplasmic membrane. *Antimicrob. Agents Chemother.* 56, 5749–5757. doi:10.1128/AAC.01380-12.
- Yoshida, K.-I., Fujita, Y., and Ehrlich, S. D. (2000). An operon for a putative ATP-binding cassette transport system involved in acetoin utilization of *Bacillus subtilis*. *J. Bacteriol.* 182, 5454–5461. doi:10.1128/JB.182.19.5454-5461.2000.
- Youngman, P. (1990). Use of transposons and integrational vectors for mutagenesis and construction of gene fusions in *Bacillus subtilis*. *Mol. Biol. methods Bacillus*, 221–266.

Zhu, X., Liu, D., Singh, A. K., Drolia, R., Bai, X., Tenguria, S., et al. (2018). Tunicamycin mediated inhibition of wall teichoic acid affects *Staphylococcus aureus* and *Listeria monocytogenes* cell morphology, biofilm formation and virulence. *Front. Microbiol.* 9, 1352. doi:10.3389/fmicb.2018.01352.

Chapter 5 | Involvement of EsIB in cell wall homeostasis

The results described in this paper were originally published in *The Cell Surface*

(<https://doi.org/10.1016/j.tcsw.2022.100085>):

Imbalance of peptidoglycan biosynthesis and hydrolysis alters the cell surface charge of *Listeria monocytogenes*

Lisa Maria Schulz¹, Patricia Rothe³, Sven Halbedel³, Angelika Gründling², Jeanine Rismondo^{1,2*}

¹ Department of General Microbiology, Institute of Microbiology and Genetics, GZMB, Georg-August University Göttingen, Grisebachstr. 8, 37077 Göttingen, Germany

² Section of Molecular Microbiology and Medical Research Council Centre for Molecular Bacteriology and Infection, Imperial College London, London SW7 2AZ, United Kingdom

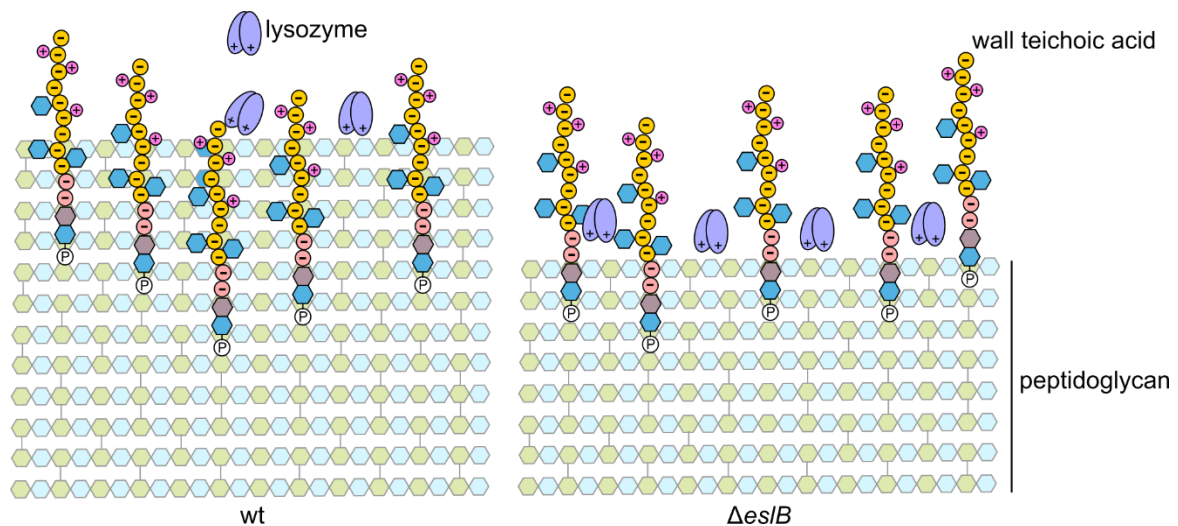
³ FG11, Division of Enteropathogenic bacteria and *Legionella*, Robert Koch Institute, Burgstraße 37, 38855 Wernigerode, Germany

Author contributions

AG, JR and LMS conceived the study. JR and LMS designed the experiments. JR, LMS and PR carried out the experiments. JR isolated the $\Delta esIB$ suppressors in the presence of lysozyme and sucrose penicillin. LMS constructed the *L. monocytogenes* mutants and overexpression strains and characterized the phenotypes. LMS carried out drop dilution assays, microscopy, disc-diffusion assays, cytochrome C assay, as well as the β -gal assay in *B. subtilis*. PR and SH carried to the western blot analysis. JR carried out the moenomycin drop dilution assay. JR and LMS wrote the manuscript. All authors approved the manuscript. AG and JR acquired funding. JR provided supervision.

Abstract

The bacterial cell wall is composed of a thick layer of peptidoglycan and cell wall polymers, which are either embedded in the membrane or linked to the peptidoglycan backbone and referred to as lipoteichoic acid (LTA) and wall teichoic acid (WTA), respectively. Modifications of the peptidoglycan or WTA backbone can alter the susceptibility of the bacterial cell towards cationic antimicrobials and lysozyme. The human pathogen *Listeria monocytogenes* is intrinsically resistant towards lysozyme, mainly due to deacetylation and *O*-acetylation of the peptidoglycan backbone via PgdA and OatA. Recent studies identified additional factors, which contribute to the lysozyme resistance of this pathogen. One of these is the predicted ABC transporter, EsIABC. An *esIB* mutant is hyper-sensitive towards lysozyme, likely due to the production of thinner and less *O*-acetylated peptidoglycan. Using a suppressor screen, we show here that suppression of *esIB* phenotypes could be achieved by enhancing peptidoglycan biosynthesis, reducing peptidoglycan hydrolysis or alterations in WTA biosynthesis and modification. The lack of EsIB also leads to a higher negative surface charge, which likely stimulates the activity of peptidoglycan hydrolases and lysozyme. Based on our results, we hypothesize that the portion of cell surface exposed WTA is increased in the *esIB* mutant due to the thinner peptidoglycan layer and that latter one could be caused by an impairment in UDP-*N*-acetylglucosamine (UDP-GlcNAc) production or distribution.

Graphical Abstract

Introduction

In recent years, antibiotic resistance became a serious threat for public health. One of the main targets of currently available antibiotics is the bacterial cell wall (Fig. 1). In gram-positive bacteria, the cell wall consists of a thick layer of peptidoglycan and cell wall polymers, which are either tethered to the cell membrane or covalently linked to peptidoglycan and referred to as lipoteichoic (LTA) and wall teichoic acid (WTA), respectively. Peptidoglycan biosynthesis starts in the cytoplasm by the conversion of UDP-*N*-acetylglucosamine (UDP-GlcNAc) to UDP-*N*-acetylmuramic acid (UDP-MurNAc) via MurA and MurB. The activity of the UDP-GlcNAc 1-carboxyvinyltransferase MurA can be specifically inhibited by the antibiotic fosfomycin (Fig. 1)(Kahan et al., 1974). In the subsequent steps, which are depicted in Figure 1, the peptidoglycan precursor lipid II is synthesized in the cytoplasm and transported across the membrane by the flippase MurJ (Meeske et al., 2015; Ruiz, 2008; Sham et al., 2014). Lipid II is then incorporated into the growing glycan strand by members of the SEDS (shape, elongation, division, sporulation) protein family, namely RodA and FtsW, which act in concert with class B penicillin binding proteins (PBPs) that have a transpeptidase activity (Cho et al., 2016; Leclercq et al., 2017; Taguchi et al., 2019). Recent findings led to the conclusion that class A PBPs, which possess a glycosyltransferase and a transpeptidase domain, are mainly involved in filling gaps and/or repair defects in the peptidoglycan mesh, rather than being the main enzymes involved in peptidoglycan polymerization and crosslinking (Cho et al., 2016; Dion et al., 2019; Vigouroux et al., 2020). The ability of bacterial cells to elongate and divide depends on the activity of peptidoglycan hydrolases. In the gram-positive model organism *Bacillus subtilis*, which is closely related to *L. monocytogenes*, two DL-endopeptidases, CwIO and LytE, are essential for cell elongation. In addition to its role in cell elongation, LytE is also involved in cell separation (Carballido-López et al., 2006; Ohnishi et al., 1999; Vollmer et al., 2008). Both enzymes cleave the peptide bond between D-glutamic acid and *meso*-diamino pimelic acid of the peptidoglycan peptide, thereby allowing the insertion of new peptidoglycan material (Yamaguchi et al., 2004). Lack of CwIO results in cell shortening, while absence of CwIO and LytE is lethal (Domínguez-Cuevas et al., 2013; Hashimoto et al., 2012). Peptidoglycan biosynthesis and hydrolysis need to be tightly regulated to prevent cell lysis. In *B. subtilis*, this regulation is partly achieved by controlling expression of *cwIO* and *lytE* via the essential two-component system WalRK, whose expression is for instance induced during heat stress (Bisicchia et al., 2007; Dubrac et al., 2008; Takada et al., 2018). On the other hand, activity of CwIO depends on a direct protein-protein interaction with the ABC transporter FtsEX (Meisner et al., 2013). The FtsEX-dependent regulation of *B. subtilis* CwIO further depends

on the presence of two cofactors, SweC and SweD (Brunet et al., 2019; Rismondo and Schulz, 2021).

UDP-GlcNAc is synthesized from fructose-6-phosphate via a four-step reaction catalyzed by GlmS, GlmM, GlmU and GlmR and serves as a substrate of MurA. Recent findings suggest that the UDP-GlcNAc biosynthetic pathway can be inhibited by *trans*-cinnamaldehyde (*t*-Cin) (Fig. 1)(Pensinger et al., 2021; Sun et al., 2021). UDP-GlcNAc is also consumed by TarO/TagO, which catalyzes the first committed step for the synthesis of WTA (Soldo et al., 2002). The activity of TarO/TagO can be blocked by tunicamycin, which also affects the activity of MraY at high concentrations (Campbell et al., 2011; Hakulinen et al., 2017; Price and Tsvetanova, 2007; Watkinson et al., 1971). In *L. monocytogenes* 10403S, WTA is composed of a glucose-glucose(Glc-Glc)-glycerol phosphate-GlcNAc-*N*-acetylmannosamine (ManNAc) linker unit and an anionic ribitol phosphate backbone, which can be modified with rhamnose, GlcNAc and D-alanine residues (Shen et al., 2017). The modification of WTA with positively charged D-alanine residues helps to mask the negative charge of the ribitol phosphate backbone, thereby conferring resistance towards cationic antimicrobial peptides and lysozyme (Brown et al., 2013; Vadyvaloo et al., 2004).

Lysozyme is an enzyme that cleaves the β -1,4-glycosidic bond between MurNAc and GlcNAc of the bacterial peptidoglycan backbone and is found in human body fluids such as tears, saliva and mucus. *L. monocytogenes* is intrinsically resistant towards lysozyme, which is mainly achieved by modifications of the peptidoglycan. PgdA, an *N*-deacetylase, and OatA, an *O*-acetyltransferase, deacetylate and acetylate the GlcNAc and MurNAc residues, respectively (Aubry et al., 2011; Boneca et al., 2007). In addition to peptidoglycan modifying enzymes, lysozyme resistance of *L. monocytogenes* is affected by the activity of the predicted carboxypeptidase PbpX, the non-coding RNA Rli31 and the transcription factor DegU (Burke et al., 2014). Interestingly, it was also been observed that the lack of components of the putative ABC transporter EslABC leads to a strong reduction in lysozyme resistance (Burke et al., 2014; Durack et al., 2015; Rismondo et al., 2021b). Recently, we could show that the absence of EslB, one of the transmembrane proteins of the EslABC transporter, resulted in the production of a thinner peptidoglycan layer and a reduction in *O*-acetylation of the peptidoglycan, which likely contributes to the reduced lysozyme resistance. Additionally, we observed that the *eslB* mutant is unable to grow in media containing high sugar concentrations and that the strain has a cell division defect (Rismondo et al., 2021b; Rismondo and Schulz, 2021).

In the current study, we used a suppressor screen to gain further insights into the role of EslABC on the physiology of *L. monocytogenes*. This screen revealed that phenotypes of the *eslB* mutant can either be suppressed by enhancing peptidoglycan biosynthesis, reducing

peptidoglycan hydrolysis or by altering WTA production or modification. Using a cytochrome C assay, we further demonstrate that the lack of EsIB manifests in a higher negative surface charge, which likely affects the activity of peptidoglycan hydrolases and provides an additional explanation for the increased lysozyme sensitivity of the *esIB* mutant.

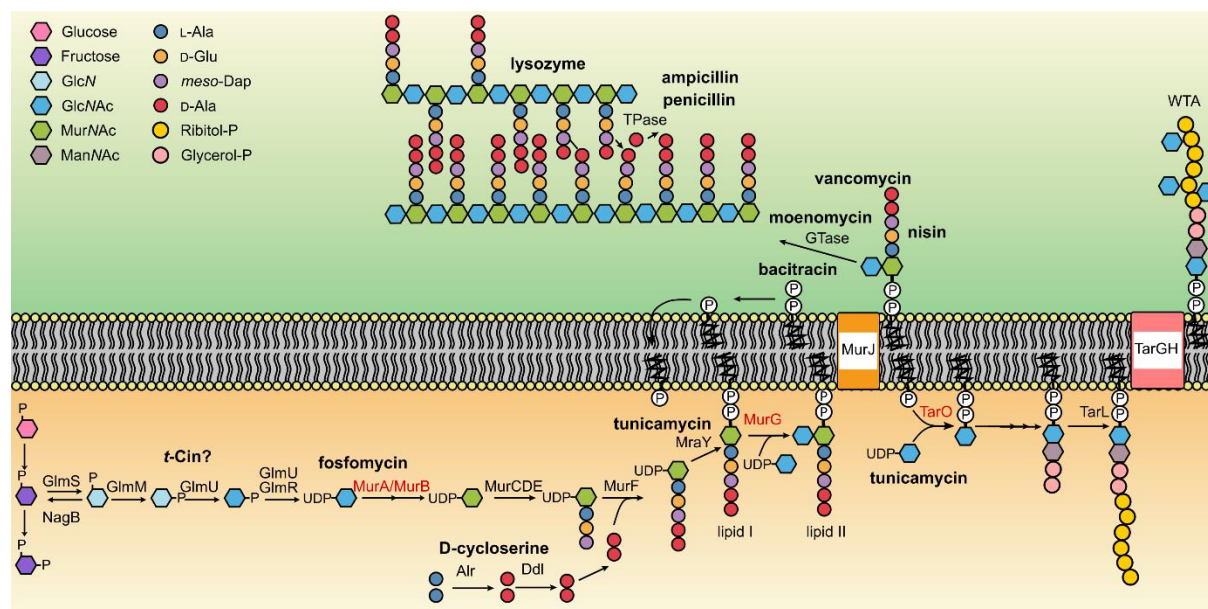


Figure 1 | Schematic of the UDP-GlcNAc, peptidoglycan and wall teichoic acid biosynthesis pathway. UDP-GlcNAc, which is required for peptidoglycan and wall teichoic acid (WTA) biosynthesis, is synthesized from Fructose-6-phosphate in a four-step reaction catalyzed by GlmS, GlmM, GlmU and GlmR. MurA, an UDP-GlcNAc-1-carboxyvinyltransferase catalyzing the first step of peptidoglycan biosynthesis, and MurB convert UDP-GlcNAc to UDP-MurNAc. Lipid II is produced in subsequent steps, which are performed by MurCDEF, Alr, Ddl, MraY and MurG, flipped across the membrane by MurJ and inserted into the growing glycan strand by glycosyltransferases (GTases). Finally, peptidoglycan is crosslinked by the action of transpeptidases (TPases) (Pazos and Peters, 2019). UDP-GlcNAc also serves as a substrate of TarO, the first enzyme of the WTA biosynthesis pathway. After the WTA polymer is synthesized by a subset of enzymes, it is transported across the membrane via TarGH (Brown et al., 2013) and, in case of *L. monocytogenes* 10403S, decorated with GlcNAc residues (Shen et al., 2017). UDP-GlcNAc-consuming enzymes are labelled in red. Antibiotics targeting different steps of the UDP-GlcNAc, peptidoglycan and WTA biosynthesis pathways or degrade peptidoglycan are depicted in bold (Campbell et al., 2011; Pensinger et al., 2021; Sarkar et al., 2017).

Materials and Methods

Bacterial Strains and growth conditions. All strains and plasmids used in this study are listed in Table S1. *Escherichia coli* strains were grown in Luria-Bertani (LB) medium and *Listeria monocytogenes* strains in brain heart infusion (BHI) medium at 37°C unless otherwise stated. Where required, antibiotics and supplements were added to the medium at the following concentrations: for *E. coli* cultures, ampicillin (Amp) at 100 µg ml⁻¹, kanamycin (Kan) at 30 µg ml⁻¹, and for *L. monocytogenes* cultures, chloramphenicol (Cam) at 10 µg ml⁻¹, erythromycin (Erm) at 5 µg ml⁻¹, Kan at 30 µg ml⁻¹, nalidixic acid (Nal) at 30 µg ml⁻¹, streptomycin (Strep) at 200 µg ml⁻¹ and IPTG at 1 mM.

Strain and plasmid construction. All primers used in this study are listed in Table S2. For the construction of pIMK3-*murA*, pIMK3-*glmR*, pIMK3-*glmU* and pIMK3-*glmM*, the *murA*, *glmR*, *glmU* and *glmM* genes were amplified using primer pairs JR90/JR91, JR134/JR135, JR136/JR137 and JR138/JR139, respectively, cut with *NcoI* and *SaI* and ligated into plasmid pIMK3 that had been cut with the same enzymes. The resulting plasmids pIMK3-*murA*, pIMK3-*glmR*, pIMK3-*glmU* and pIMK3-*glmM* were recovered in *E. coli* XL1-Blue yielding strains XL1-Blue pIMK3-*murA* (EJR52), XL1-Blue pIMK3-*glmR* (EJR106), XL1-Blue pIMK3-*glmU* (EJR107) and XL1-Blue pIMK3-*glmM* (EJR108). Next, plasmids pIMK3-*murA*, pIMK3-*glmR*, pIMK3-*glmU* and pIMK3-*glmM* were transformed into *E. coli* S17-1 yielding strains S17-1 pIMK3-*murA* (EJR59), S17-1 pIMK3-*glmR* (EJR132), S17-1 pIMK3-*glmU* (EJR133) and S17-1 pIMK3-*glmM* (EJR134). *E. coli* strain S17-1 pIMK3-*murA* (EJR59) was used as a donor strain to transfer plasmid pIMK3-*murA* by conjugation into *L. monocytogenes* strains 10403S (ANG1263) and 10403S Δ *esB*₍₂₎ (ANG5662) using a previously described method (Lauer et al., 2002). This resulted in the construction of strains 10403S pIMK3-*murA* (LJR26) and 10403S Δ *esB*₍₂₎ pIMK3-*murA* (LJR27), in which the expression of *murA* is under the control of an IPTG-inducible promoter. Strains carrying the empty pIMK3 vector were used as controls. For this purpose, pIMK3 was transformed into *E. coli* S17-1 yielding strain EJR58. S17-1 pIMK3 was subsequently used as a donor strain to transfer plasmid pIMK3 by conjugation into *L. monocytogenes* strains 10403S (ANG1263) and 10403S Δ *esB*₍₂₎ (ANG5662), which resulted in the construction of strains 10403S pIMK3 (LJR24) and 10403S Δ *esB*₍₂₎ pIMK3 (LJR25). For the construction of pIMK3-*glmS*, the *glmS* gene was amplified using primer pair JR140/JR141. The resulting PCR product was cut with *Bam*HI and *Xma*I and ligated into plasmid pIMK3 that had been cut with the same enzymes. Plasmid pIMK3-*glmS* was recovered in *E. coli* XL1-Blue and subsequently transformed into *E. coli* S17-1 yielding strains XL1-Blue pIMK3-*glmS* (EJR112) and S17-1 pIMK3-*glmS* (EJR135), respectively. *E. coli* strains S17-1 pIMK3-*glmR* (EJR132), S17-1 pIMK3-*glmU* (EJR133), S17-1 pIMK3-*glmM* (EJR134) and S17-1 pIMK3-*glmS* (EJR135) were used to transfer plasmids pIMK3-*glmR*, pIMK3-*glmU*, pIMK3-*glmM* and pIMK3-*glmS* by conjugation into *L. monocytogenes* strain 10403S Δ *esB*₍₂₎ (ANG5662) yielding strains 10403S Δ *esB*₍₂₎ pIMK3-*glmR* (LJR63), 10403S Δ *esB*₍₂₎ pIMK3-*glmU* (LJR64), 10403S Δ *esB*₍₂₎ pIMK3-*glmM* (LJR65) and 10403S Δ *esB*₍₂₎ pIMK3-*glmS* (LJR66).

For the construction of a markerless deletion of *cwI*O (*Imrg_01743*), 1-kb DNA fragments up- and downstream of *cwI*O were amplified by PCR with primers LMS106/107 and LMS104/105. The resulting PCR products were fused in a second PCR using primers LMS105/106, the product cut with *Bam*HI and *Kpn*I and ligated into pKSV7 that had been cut with the same enzymes. The resulting plasmid pKSV7- Δ *cwI*O was recovered in *E. coli* XL1-Blue yielding strain XL1-Blue pKSV7-

$\Delta cw/O$ (EJR63). Plasmid pKSV7- $\Delta cw/O$ was subsequently transformed into *L. monocytogenes* 10403S and *cw/O* deleted by allelic exchange according to a previously published method (Camilli et al., 1993) yielding strain 10403S $\Delta cw/O$ (LJR37). Since attempts of producing electrocompetent *cw/O* cells were unsuccessful, plasmid pIMK3-*cw/O* was first conjugated into strain 10403S $\Delta cw/O$ (LJR37), which allows for IPTG-inducible expression of *cw/O*, and resulting in the construction of strain 10403S $\Delta cw/O$ pIMK3-*cw/O* (LJR103). For the construction of pIMK3-*cw/O*, *cw/O* was amplified using the primer pair LMS226 and LMS227. The fragment was cut with *NcoI* and *BamHI*, ligated into pIMK3 that had been cut with the same enzymes and recovered in *E. coli* XL1-blue and S17-1, yielding strains EJR114 and EJR115, respectively. To generate a *cw/O* *esIB* double mutant, plasmid pKSV7- $\Delta esIB$ was first transformed into *L. monocytogenes* strain 10403S $\Delta cw/O$ pIMK3-*cw/O* (LJR103) resulting in strain 10403S $\Delta cw/O$ pIMK3-*cw/O* pKSV7- $\Delta esIB$ (LJR114). The *esIB* gene was then deleted by allelic exchange. This resulted in the construction of strain 10403S $\Delta cw/O$ $\Delta esIB$ pIMK3-*cw/O* (LJR119).

For the construction of promoter-*lacZ* fusions, the plasmid pAC7 was used. The promoter region of the *dlt* operon was amplified from genomic DNA of the *L. monocytogenes* wildtype 10403S and the *esIB* suppressor strain 10403S $\Delta esIB_{(3)}$ P_{dlt}^* (ANG5746) containing a mutation 31 bp upstream of the ATG start codon, using the primer pair LMS93 and LMS94. The PCR products were digested with *BamHI* and *EcoRI* and ligated into pAC7. The resulting plasmids pAC7- P_{dlt} and pAC7- P_{dlt}^* were recovered in XL1-Blue resulting in strains XL1-Blue pAC7- P_{dlt} (EJR50) and XL1-Blue pAC7- P_{dlt}^* (EJR51). Subsequently, both plasmids were integrated into the *amyE* site of the *B. subtilis* wildtype strain 168, resulting in *B. subtilis* strains 168 pAC7- P_{dlt} (BLMS4) and 168 pAC7- P_{dlt}^* (BLMS5), respectively.

Generation of *esIB* suppressors and whole genome sequencing. For the generation of *esIB* suppressors, overnight cultures of three independently generated *L. monocytogenes* *esIB* mutants, strains 10403S $\Delta esIB_{(1)}$ (ANG4275), 10403S $\Delta esIB_{(2)}$ (ANG5662) and 10403S $\Delta esIB_{(3)}$ (ANG5685), were adjusted to an OD₆₀₀ of 1. 100 μ l of 10⁻¹ and 10⁻² dilutions of these cultures were plated on BHI plates containing (A) 0.5 M sucrose and 0.025 μ g ml⁻¹ penicillin, (B) 0.5 M sucrose and 0.05 μ g ml⁻¹ penicillin or (C) 100 μ g ml⁻¹ lysozyme, conditions under which the *esIB* mutant is unable to grow while the *L. monocytogenes* wildtype strain 10403S can grow. The plates were incubated at 37°C overnight and single colonies were re-streaked on BHI plates. This procedure was repeated at least three independent times per condition. The genome sequence of a selection of *esIB* suppressors was determined by whole genome sequencing (WGS) using an Illumina MiSeq machine and a 150 paired end Illumina kit as described previously (Rismondo et al., 2021b). The

reads were trimmed, mapped to the *L. monocytogenes* 10403S reference genome (NC_017544) and single nucleotide polymorphisms (SNPs) with a frequency of at least 90% identified using CLC workbench genomics (Qiagen) and Geneious Prime® v.2021.0.1. The whole genome sequencing data were deposited at the European Nucleotide Archive (ENA) under accession number PRJEB55822.

Determination of resistance towards antimicrobials. For the disk diffusion assays, overnight cultures of the indicated *L. monocytogenes* strains were adjusted to an OD₆₀₀ of 0.1. 100 µl of cultures were spread on BHI agar plates using a cotton swap. Plates contained 1 mM IPTG were indicated. 6 mm filter disks were placed on top of the agar surface, soaked with 20 µl of the appropriate antibiotic stock solution and the plates were incubated at 37°C. The diameter of the inhibition zone was measured the next day. The following stock solutions were used: 50 mg ml⁻¹ fosfomycin, 1 mg ml⁻¹ *t*-Cin, 5 mg ml⁻¹ tunicamycin, 15 mg ml⁻¹ D-cycloserine, 60 mg ml⁻¹ nisin, 30 mg ml⁻¹ vancomycin, 5 mg ml⁻¹ moenomycin, 1 mg ml⁻¹ penicillin, 10 mg ml⁻¹ ampicillin and 250 mg ml⁻¹ bacitracin.

Spot plating assays. Overnight cultures of *L. monocytogenes* strains were adjusted to an OD₆₀₀ of 1 and serially diluted to 10⁻⁶. 5 µl of each dilution were spotted on BHI agar plates, BHI agar plates containing 0.5 M sucrose and 0.025 µg ml⁻¹ penicillin; 100 µg ml⁻¹ lysozyme; 0.025 µg/ml moenomycin, 500 µl DMSO (≥99.5%), 0.05 µg ml⁻¹ or 0.5 µg ml⁻¹ tunicamycin and plates incubated at 37°C unless otherwise stated. Where indicated, plates were supplemented with 1 mM IPTG or 20 mM MgCl₂. Images of plates were taken after 20-24 hours of incubation.

Cell length analysis. Overnight cultures of the indicated *L. monocytogenes* strains were inoculated to an OD₆₀₀ of 0.1 and grown to an OD₆₀₀ of 0.3-0.6 at 37°C with agitation in BHI medium or BHI medium containing 1 mM IPTG and the appropriate antibiotic. To stain the bacterial membranes, 800 µl of the bacterial cultures were mixed with 40 µl of 100 µg ml⁻¹ Nile red and incubated for 20 min at 37°C. The cells were washed twice in PBS buffer and subsequently re-suspended in the same buffer. Cells were then fixed in 1.12% paraformaldehyde for 20 min at room temperature in the dark and 1-1.5 µl of the cell suspension was spotted on microscope slides covered with a thin agarose layer (1.5% in ddH₂O). Phase contrast and fluorescence images were taken using a Zeiss Axioskop 40 microscope equipped with an EC Plan-NEOFLUAR 100X/1.3 objective (Carl Zeiss, Göttingen, Germany) and coupled to an AxioCam MRm camera. Filter set 43 was used for the detection of the Nile red signal. The images were processed using the Axio Vision software (release

4.7). The length of 50 cells per replicate was measured for each strain and the mean calculated. Statistical analysis was performed using the software GraphPad Prism (version 8).

Isolation of cellular proteins and western blotting. Bacteria from a 20 ml culture were harvested by centrifugation and washed with ZAP buffer (10 mM Tris-HCl, pH 7.5, 200 mM NaCl). The cells were subsequently resuspended in 1 ml ZAP buffer containing 1 mM PMSF and disrupted by sonication. Cellular debris was removed by centrifugation, the resulting supernatant collected and separated by SDS polyacrylamide gel electrophoresis (PAGE). Proteins were transferred onto positively charged polyvinylidene fluoride (PVDF) membranes using a semi-dry transfer unit. MurA and DivIVA were detected using a polyclonal rabbit antiserum raised against the *B. subtilis* MurAA protein (Kock et al., 2004), which also cross reacts with the *L. monocytogenes* MurA protein, and DivIVA (Marston et al., 1998) as primary antibody and an anti-rabbit immunoglobulin G conjugated to horseradish peroxidase antibody as the secondary antibody. Blots were developed using ECL chemiluminescence reagents (Thermo Scientific) and imaged using a chemiluminescence imager (Vilber Lourmat).

Cytochrome C binding assay. Cytochrome C binding assays were performed as previously described (Kang et al., 2015). Briefly, overnight cultures of *L. monocytogenes* were used to inoculate fresh cultures to an OD₆₀₀ of 0.05 in 4 ml BHI medium and the cultures were grown to an OD₆₀₀ of 0.6-0.8 at 37°C and 200 rpm. Bacteria from 2 ml of the culture were harvested by centrifugation at 16,200 x g for 1 min. Cells were then washed twice with 20 mM MOPS (3-(N-morpholino) propanesulfonic acid) buffer (pH 7) and adjusted to an OD₆₀₀ of 0.25 in the same buffer. Cytochrome C was added at a final concentration of 50 µg ml⁻¹ and the suspension was incubated in the dark for 10 min at room temperature. The suspension was centrifuged for 5 min at 16,200 x g, the supernatant removed and the absorbance of the supernatant was measured at 410 nm (OD₄₁₀ + cells). A reaction without cells was used as blank (OD₄₁₀ - cells). The percentage of bound cytochrome C was calculated as follows:

$$\% \text{ cytochrome C bound} = 100 - [(OD_{410} + \text{cells}) / (OD_{410} - \text{cells})]$$

β-galactosidase assay. To compare the *dlt* promoter activity of the *L. monocytogenes* wildtype and suppressor strain 10403SΔ*eslB*(3)*P_{dlt}** (ANG5746), β-galactosidase assays were performed. For this purpose, promoter-*lacZ* fusions were integrated into the *amyE* locus of *B. subtilis* 168. The resulting *B. subtilis* strains were grown in CSE-glucose minimal medium at 37°C to an OD₆₀₀ of 0.5-

0.8, bacteria from a culture aliquot harvested and the β -galactosidase activity determined as described previously (Miller, 1972).

Results

$\Delta es/B$ phenotypes are restored in the presence of excess Mg^{2+}

The *es/ABCR* operon encodes the putative ABC transporter EslABC and the RpiR transcriptional regulator EslR. Absence of the transmembrane component EslB leads to a multitude of phenotypes including a cell division defect, decreased lysozyme resistance, the production of a thinner cell wall and a growth defect in media containing high sugar concentrations (Rismondo et al., 2021b). In addition, we observed that the growth of the *es/B* mutant is severely affected when grown on BHI plates at 42°C (Fig. 2A). So far, the cellular function of the transporter EslABC and how it is mechanistically linked to cell division and cell wall biosynthesis in *L. monocytogenes* is unknown. Generally, many cell wall defects can be rescued by the addition of Mg^{2+} , however, the reason for this is still debated. Recently, it was speculated that binding of Mg^{2+} to the cell wall inhibits peptidoglycan hydrolases and thereby stabilizes the bacterial cell wall (Tesson et al., 2022). As the phenotypic defects of the *es/B* mutant suggest that peptidoglycan biosynthesis might be impaired, we speculated that the addition of Mg^{2+} should rescue the growth of this strain. To test this hypothesis, the *L. monocytogenes* wildtype 10403S, the $\Delta es/B$ mutant and the $\Delta es/B$ complementation strain were inoculated on BHI plates containing sucrose and penicillin, lysozyme or were incubated at 42°C in the absence or presence of 20 mM $MgCl_2$. The addition of Mg^{2+} could restore the growth of the $\Delta es/B$ mutant under all conditions tested (Fig. S1), further supporting the hypothesis that peptidoglycan biosynthesis is impaired in *L. monocytogenes* cells lacking EslB.

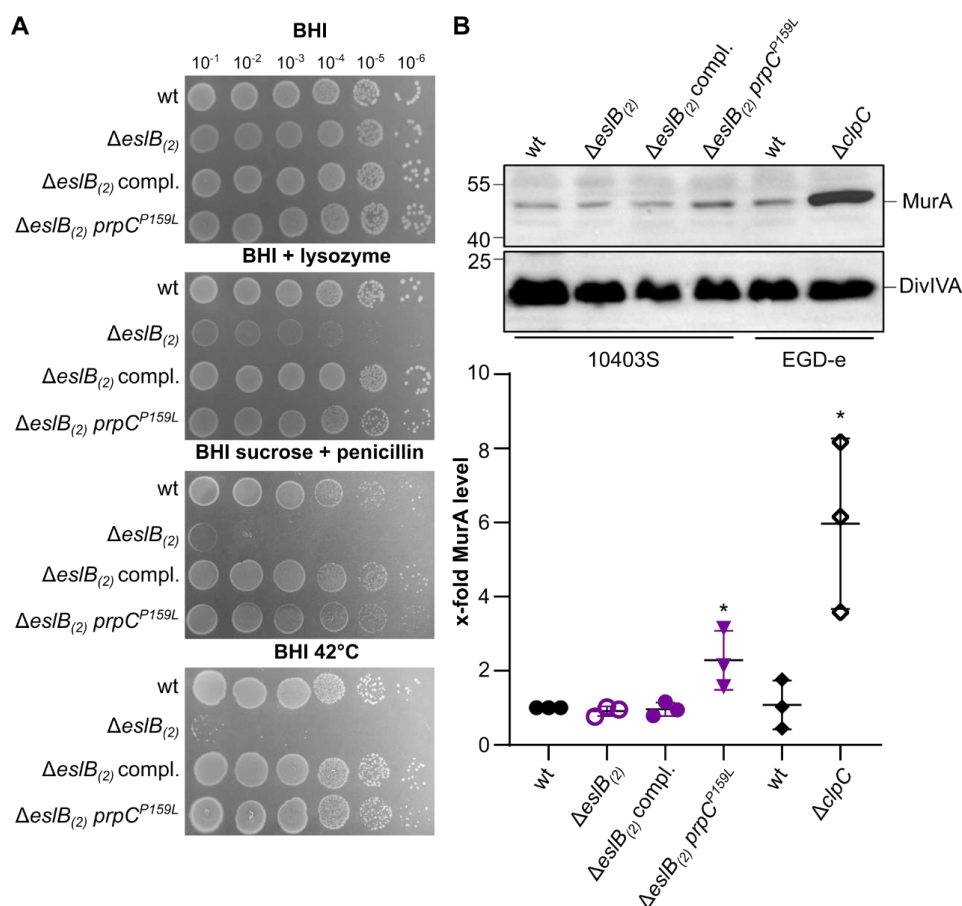


Figure 2 | Mutation P159L in *prpC* suppresses *esIB* phenotypes. (A) Drop dilution assay. Dilutions of *L. monocytogenes* strains 10403S (wt), $\Delta esIB_{(2)}$, $\Delta esIB_{(2)}$ compl., and $\Delta esIB_{(2)}$ *prpC*^{P159L} were spotted on BHI plates, BHI plates containing 100 μ g/ml lysozyme or containing 0.5 M sucrose and 0.025 μ g/ml penicillin G and were incubated at 37°C or on BHI plates and were incubated at 42°C. (B) Western blot. Protein samples of strains 10403S, $\Delta esIB_{(2)}$, $\Delta esIB_{(2)}$ compl. and $\Delta esIB_{(2)}$ *prpC*^{P159L} were separated by SDS PAGE and transferred to a PVDF membrane. MurA was detected using a MurAA-specific antibody as described in the methods section. Protein samples of *L. monocytogenes* wildtype strain EGD-e and a *clpC* mutant were used as controls. A western blot showing DivIVA levels serves as a loading control. MurA level in the protein samples were quantified and plotted. For statistical analysis, an unpaired two-tailed t-test was used (* $p \leq 0.05$).

Resistance profile of the *esIB* mutant towards cell wall-targeting antibiotics

To narrow down which point of the peptidoglycan biosynthesis pathway is impaired in the *esIB* mutant, we performed disk diffusion assays with antibiotics that target different steps of this pathway (Fig. 1). Compared to the wildtype, the *esIB* mutant was more sensitive towards *t*-Cin and fosfomicin (Fig. 3), which target the UDP-GlcNAc biosynthetic pathway and MurA, respectively (Marquardt et al., 1994; Pensinger et al., 2021; Sun et al., 2021). In contrast, the resistance towards D-cycloserine, nisin, vancomycin, moenomycin, penicillin, ampicillin and bacitracin (Fig. 1), which target processes downstream of MurA, was not altered in the *esIB* mutant (Fig. S2). The *esIB* mutant was more resistant towards tunicamycin, whose main target at low concentrations is TarO, the first enzyme functioning in the WTA biosynthesis pathway (Fig. 3). As we have seen above, the inhibition of WTA biosynthesis seems to be beneficial for the *esIB* mutant likely due to

an increased flux of UDP-GlcNAc towards peptidoglycan biosynthesis. This antibiotic screen therefore suggests that one of the limiting factors of the *esIB* mutant might be the synthesis or correct distribution of UDP-GlcNAc, a precursor, which is used for both peptidoglycan biosynthesis and the synthesis and modification of WTA. This hypothesis is supported by the observation that overproduction of GlmM and GlmR, two proteins involved in the production of UDP-GlcNAc, can partially suppress the *esIB* phenotypes (Fig. S3).

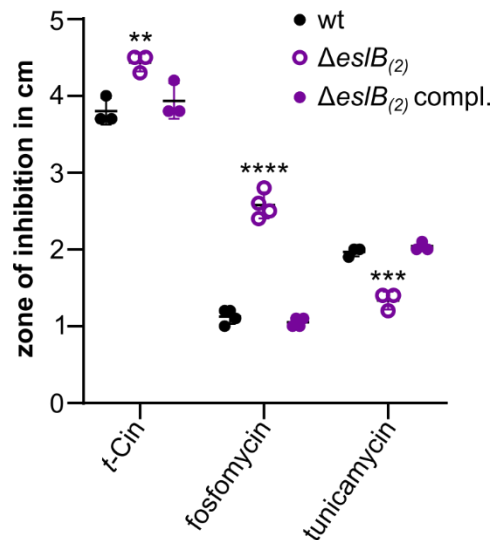


Figure 3 | Alterations in the resistance of the *esIB* mutant towards cell wall-targeting antibiotics. Disk diffusion assay. *L. monocytogenes* strains 10403S (wt), $\Delta esIB_{(2)}$ and $\Delta esIB_{(2)}$ compl. were spotted on BHI plates. Antibiotic-soaked disks placed on top the agar surface and the plates incubated for 24h at 37°C. The inhibition zones for the indicated strains were measured and the average values and standard deviation of at least three independent experiments were plotted. For statistical analysis, a one-way ANOVA coupled with a Dunnett's multiple comparison test was used (** $p \leq 0.01$, *** $p \leq 0.001$, **** $p \leq 0.0001$).

Table 1: Identified sequence alterations in *L. monocytogenes* *esIB* deletion strains and suppressors.

Strain number	Reference position ¹	Type ²	Ref ³	Allele ⁴	Frequency ⁵	Annotations ⁶	AA change ⁷	Condition ⁸
ANG4275 10403SΔ<i>esIB</i>(1)	2425786- 2425875	DEL			100%	<i>Imo2396</i>, internalin	30 aa deletion	
ANG5386	2583855	DEL	T	-	100%	<i>murZ</i> , UDP- <i>N</i> -acetylglucosamine 1-carboxyvinyltransferase	M240fs	P
ANG5479	310043	SNV	G	A	100%	<i>walk</i> , histidine kinase of TCS WalRK	R553H	P
ANG5480	309234	SNV	C	G	100%	<i>walk</i> , histidine kinase of TCS WalRK	N283E	P
ANG5488	2537835	SNV	C	G	100%	<i>ftsX</i> , membrane component of ABC transporter FtsEX	G243R	P
ANG5489	310094	SNV	C	T	100%	<i>walk</i> , histidine kinase of TCS WalRK	A570V	P
ANG5499	1491251	DEL	T	-	100%	<i>reoM</i> , regulator of MurA degradation	L23fs	P
ANG5662 10403SΔ<i>esIB</i>(2)	-							
ANG5698	2582654	DEL	G	-	100%	<i>murZ</i> , UDP- <i>N</i> -acetylglucosamine 1-carboxyvinyltransferase	Q307fs	P
ANG5699	310133	SNV	T	C	97.4%	<i>walk</i> , histidine kinase of TCS WalRK	I583T	P
ANG5708	1852252	SNV	G	A	100%	<i>prpC</i> , serine threonine phosphatase	P159L	P
ANG5710	2537273	SNV	C	T	98%	<i>cwlO</i> , peptidoglycan DL-endopeptidase	R106H	P
ANG5714	2538568	SNV	G	A	98.4%	<i>ftsE</i> , ATP binding protein of ABC transporter FtsEX	Q220-	P
ANG5733	308133	SNV	A	G	100%	<i>walR</i> , response regulator of TCS WalRK	S216G	L
ANG5734	309772	SNV	C	G	100%	<i>walk</i> , histidine kinase of TCS WalRK	H463D	L
ANG5737	309085	SNV	G	T	100%	<i>walk</i> , histidine kinase of TCS WalRK	V234L	L
ANG5741	309824	SNV	G	A	100%	<i>walk</i> , histidine kinase of TCS WalRK	R480H	L
ANG5685 10403SΔ<i>esIB</i>(3)	-							
ANG5717	1921373	SNV	G	A	100%	<i>pbpA1</i> , bifunctional penicillin binding protein	G125D	P
ANG5729	1090622	SNV	C	T	100%	<i>tarL</i> , teichoic acid ribitol-phosphate polymerase	P282L	P
ANG5746	988580	SNV	T	C	100%	Promoter of <i>dlt</i> operon, involved in D-alanylation of wall teichoic and lipoteichoic acids	-	L

¹ Reference position is based on the position in the *L. monocytogenes* 10403S reference genome (NC_01744). ² Type of mutation: SNV = single nucleotide variant; DEL = nucleotide deletion. ³ Ref indicates base in reference genome. ⁴ Allele indicates base at the same position in the sequenced strain. ⁵ Frequency at which the base change was found in the sequenced strain. ⁶ AA change indicates the resulting amino acid change in the protein found in the reference strains as compared to the sequenced strain. ⁷ TCS = Two-component system ⁸ Condition, which was used to raise suppressors. L = BHI plates containing 100 µg/ml lysozyme. P = BHI plates containing 0.5 M sucrose and 0.025 or 0.05 µg/ml penicillin.

Isolation of *esIB* suppressor mutants

To gain insights into the function of EsIABC, we took advantage of the observation that the *esIB* mutant forms suppressors when grown on BHI plates that contain either 100 $\mu\text{g ml}^{-1}$ lysozyme, or 0.5 M sucrose and 0.025 or 0.05 $\mu\text{g ml}^{-1}$ penicillin. Genomic alterations present in independently isolated *esIB* suppressors were determined by whole genome sequencing. A large subset of *esIB* suppressors had mutations in *walR* (*Imo0287*) or *walk* (*Imo0288*), which encode the WalRK two-component system that is involved in cell wall metabolism (Dubrac et al., 2008; Howell et al., 2003). In addition, we identified mutations that mapped to genes associated with peptidoglycan biosynthesis (*murZ* (*Imo2552*), *reoM* (*Imo1503*), *prpC* (*Imo1821*), *pbpA1* (*Imo1892*)), peptidoglycan hydrolysis (*cwlo* (*Imo2505*, *spl*), *ftsX* (*Imo2506*), *ftsE* (*Imo2507*)) and wall teichoic acid (WTA) biosynthesis and modification (*tarL* (*Imo1077*), *dltX* (promoter region, *Imrg_02074*)) (Table 1).

Suppression of *esIB* phenotypes by increased MurA levels

Under sucrose penicillin stress, two *esIB* suppressors with mutations in *murZ* and one *esIB* suppressor with a mutation in *reoM* or *prpC* were isolated. The proteins encoded by all three of these genes affect MurA protein levels (Wamp et al., 2022, 2020). Drop dilution assays were performed to assess whether mutations in *murZ*, *reoM* and *prpC* suppress the growth defect of the *esIB* mutant in the presence of sucrose and penicillin as well as other conditions under which the growth of the *esIB* mutant is severely affected. As expected, the growth of the *L. monocytogenes* strains 10403S Δ *esIB*₍₁₎ *murZ*^{M240fs}, 10403S Δ *esIB*₍₂₎ *murZ*^{Q307fs}, 10403S Δ *esIB*₍₁₎ *reoM*^{K23fs} and 10403S Δ *esIB*₍₂₎ *prpC*^{P159L} on BHI plates containing sucrose and penicillin is comparable to the wildtype strain 10403S. The suppressors with mutations in *murZ*, *reoM* and *prpC* also grew like wild-type on BHI plates containing lysozyme as well as on BHI plates that were incubated at 42°C (Fig. 2A for 10403S Δ *esIB*₍₂₎ *prpC*^{P159L}, data not shown for 10403S Δ *esIB*₍₁₎ *murZ*^{M240fs}, 10403S Δ *esIB*₍₂₎ *murZ*^{Q307fs}, 10403S Δ *esIB*₍₁₎ *reoM*^{K23fs}).

MurZ is a homolog of the UDP-*N*-acetylglucosamine 1-carboxyvinyltransferase MurA, which is required for the first step of peptidoglycan biosynthesis (Fig. 1)(Du et al., 2000; Kock et al., 2004). While MurA is essential for the growth of *L. monocytogenes*, the deletion of *murZ* is possible and results in the stabilization of MurA (Rismondo et al., 2016). MurA is a substrate of the ClpCP protease and a recent study showed that ReoM is required for the ClpCP-dependent proteolytic degradation of MurA in *L. monocytogenes* (Rismondo et al., 2016; Wamp et al., 2020). The activity of ReoM is controlled by the serine/threonine kinase PrkA and the cognate phosphatase PrpC. The phosphorylated form of ReoM stimulates peptidoglycan biosynthesis by

preventing ClpCP-dependent degradation of MurA, while MurA degradation is enhanced in the presence of non-phosphorylated ReoM (Wamp et al., 2022, 2020). The identified mutations in *murZ* and *reoM* in our suppressor strains lead to frameshifts, and thus to the production of inactive MurZ and ReoM proteins. It has been previously shown that MurA protein levels are increased in *murZ* and *reoM* mutants (Rismondo et al., 2016; Wamp et al., 2020) and we thus assume that this is also the case for the *esIB* suppressor strains 10403S Δ *esIB*₍₁₎ *murZ*^{M240fs}, 10403S Δ *esIB*₍₂₎ *murZ*^{Q307fs} and 10403S Δ *esIB*₍₁₎ *reoM*^{K23fs}. The identified mutation in *prpC* in the suppressor strain 10403S Δ *esIB*₍₂₎ *prpC*^{P159L} leads to the production of a variant of PrpC, in which proline at position 159 is replaced by a leucine, however, it is currently not known whether this amino acid exchange leads to decreased or enhanced activity of PrpC. A decreased activity of PrpC would lead to accumulation of MurA (Wamp et al., 2022), while enhanced activity would result in reduced MurA levels. To assess which affect the P159L mutation in *prpC* has on MurA levels, western blots were performed using a MurAA-specific antibody. Protein samples of *L. monocytogenes* strains EGD-e and EGD-e Δ *clpC* were used as controls. In accordance with previous studies, MurA accumulated in the *clpC* mutant (Rismondo et al., 2016). The production of the mutated PrpC variant, PrpC^{P159L}, also led to a slight accumulation of MurA in the *esIB* mutant background (Fig. 2B). Additionally, no change in MurA levels could be observed for the *esIB* mutant compared to the wildtype strain 10403S (Fig 2B). These results suggest that while the decrease in peptidoglycan production seen in the *esIB* mutant is not caused by decreased MurA levels, the growth deficit of the *esIB* mutant can be rescued by preventing MurA degradation. To confirm that the suppression of the *esIB* phenotypes in the strains with mutations in *murZ*, *reoM* or *prpC* is indeed the result of increased MurA protein levels, we integrated a second, IPTG-inducible copy of *murA* into the genome of the *esIB* mutant. First, we determined the resistance towards fosfomycin, which is a known inhibitor of MurA (Fig. 4A-B)(Kahan et al., 1974), for the *L. monocytogenes* wildtype and the *esIB* mutant harboring the empty plasmid pIMK3 or pIMK3-*murA* in the presence of IPTG. Strain 10403S Δ *esIB* pIMK3 is three-fold more sensitive to fosfomycin as compared to the cognate wildtype strain. The induction of *murA* expression increases the resistance of strains 10403S pIMK3-*murA* and 10403S Δ *esIB* pIMK3-*murA* (Fig. 4A-B), suggesting that MurA is indeed overproduced in these strains. Next, we assessed whether the growth phenotypes of the *esIB* mutant can be suppressed by the overexpression of *murA*. In the presence of the inducer IPTG, the growth of strain 10403S Δ *esIB* pIMK3-*murA* was comparable to the corresponding wildtype strain under all conditions tested (Fig. 4C). These results indicate that overproduction of MurA can compensate for the loss of *esIB* and that the suppression of the *esIB* phenotypes in the *murZ*, *reoM* and *prpC* suppressors is likely the result of increased MurA levels. Interestingly, increased MurA production

also leads to the suppression of the cell division defect of the *es/B* mutant. Cells of the *es/B* mutant carrying the empty pIMK3 plasmid have a cell length of $3.19 \pm 0.29 \mu\text{m}$. In contrast, strain 10403S $\Delta es/B$ pIMK3-*murA* produces cells with a length of $2.27 \pm 0.03 \mu\text{m}$, a size that is comparable to the length of *L. monocytogenes* wildtype cells (Fig. 4D-E).

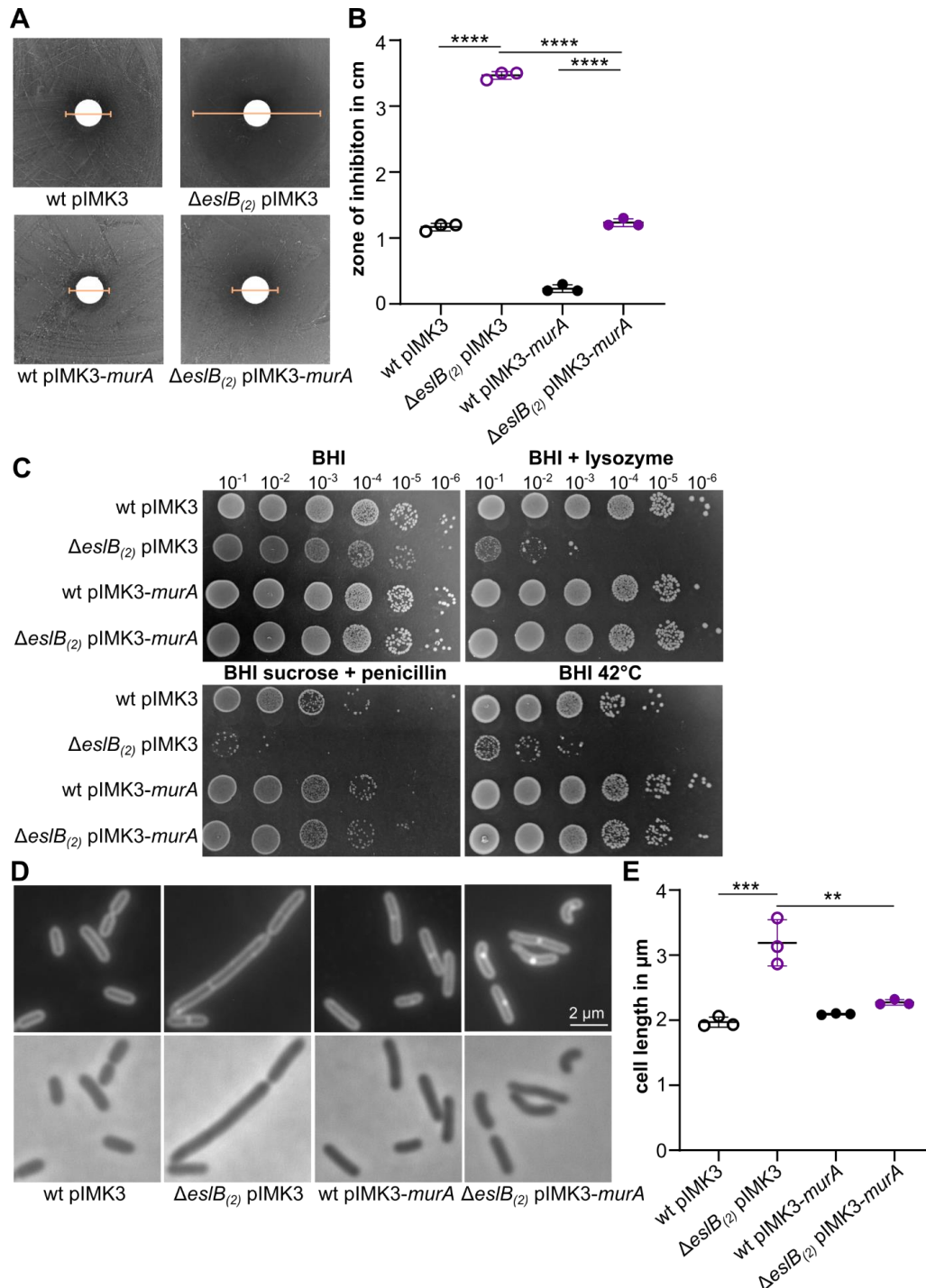


Figure 4 | MurA overexpression leads to suppression of *es/B* phenotypes. (A-B) Fosfomycin disk diffusion assay. (A) *L. monocytogenes* strains wt pIMK3, $\Delta es/B$ pIMK3, wt pIMK3-*murA* and $\Delta es/B$ pIMK3-*murA* were plated on BHI plates containing 1 mM IPTG. Fosfomycin-soaked disks were placed on the agar surface and the plates incubated for 24 h at 37°C. Yellow lines indicate the diameter of the zone of inhibition. (B) The inhibition zones for the indicated strains were measured and the average values and standard deviation of three independent experiments were plotted. (C) Drop dilution assay. Dilutions of *L. monocytogenes* strains

10403S pIMK3 (wt pIMK3), $\Delta esIB$ pIMK3, wt pIMK3-*murA* and $\Delta esIB$ pIMK3-*murA* were spotted on BHI plates, BHI plates containing 100 $\mu\text{g/ml}$ lysozyme or containing 0.5 M sucrose and 0.025 $\mu\text{g/ml}$ penicillin G, which were incubated at 37°C or on BHI plates, which were incubated at 42°C. (D) Microscopy images of *L. monocytogenes* strains. Bacterial membranes were stained with Nile red as described in the methods section. Scale bar is 2 μm . (E) Cell length of *L. monocytogenes* strains shown in panel B. The cell length of 50 cells per strain was determined and the median cell length calculated. The average values and standard deviations of three independent experiments are plotted. For statistical analysis, a one-way ANOVA coupled with Tukey's multiple comparison test was used (** $p \leq 0.01$, *** $p \leq 0.001$, **** $p \leq 0.0001$).

Suppression by reduction of the glycosyltransferase activity of PBP A1

Multiple enzymes are involved in the production of lipid II, the peptidoglycan precursor, within the cytoplasm. After its transport across the membrane via MurJ, lipid II is incorporated into the growing glycan strand by glycosyltransferases, which can either be class A penicillin binding proteins (PBPs), monofunctional glycosyltransferases or members of the SEDS (shape, elongation, division, sporulation) family, such as RodA and FtsW (Cho et al., 2016; Emami et al., 2017; Meeske et al., 2016). *L. monocytogenes* encodes two class A PBPs, PBP A1 and PBP A2, in its genome (Korsak et al., 2010; Rismondo et al., 2015). One of the *esIB* suppressor strains, ANG5717, carries a point mutation in *pbpA1* leading to the substitution of glycine at position 125 by aspartate. Interestingly, this glycine residue is part of the catalytic site of the glycosyltransferase domain, suggesting that the glycosyltransferase activity of the PBP A1 variant PBP A1^{G125D} might be reduced. Drop dilution assays and microscopic analysis revealed that the phenotypes associated with deletion of *esIB* can be rescued by *pbpA1*^{G125D} (Fig. 5A-C). The glycosyltransferase activity of class A PBPs can be inhibited by moenomycin (Huber and Nesemann, 1968). We thus tested whether the presence of moenomycin would enable the growth of the *esIB* mutant under heat stress. As shown in Figure 5D, the *esIB* mutant is unable to grow at 42°C on BHI plates or BHI plates containing DMSO, which was used to dissolve moenomycin. In contrast, nearly wildtype-like growth of the *esIB* mutant was observed on BHI plates that were supplemented with moenomycin. These results suggest that growth deficits of the *esIB* mutant can be rescued by the reduction of the glycosyltransferase activity of class A PBPs.

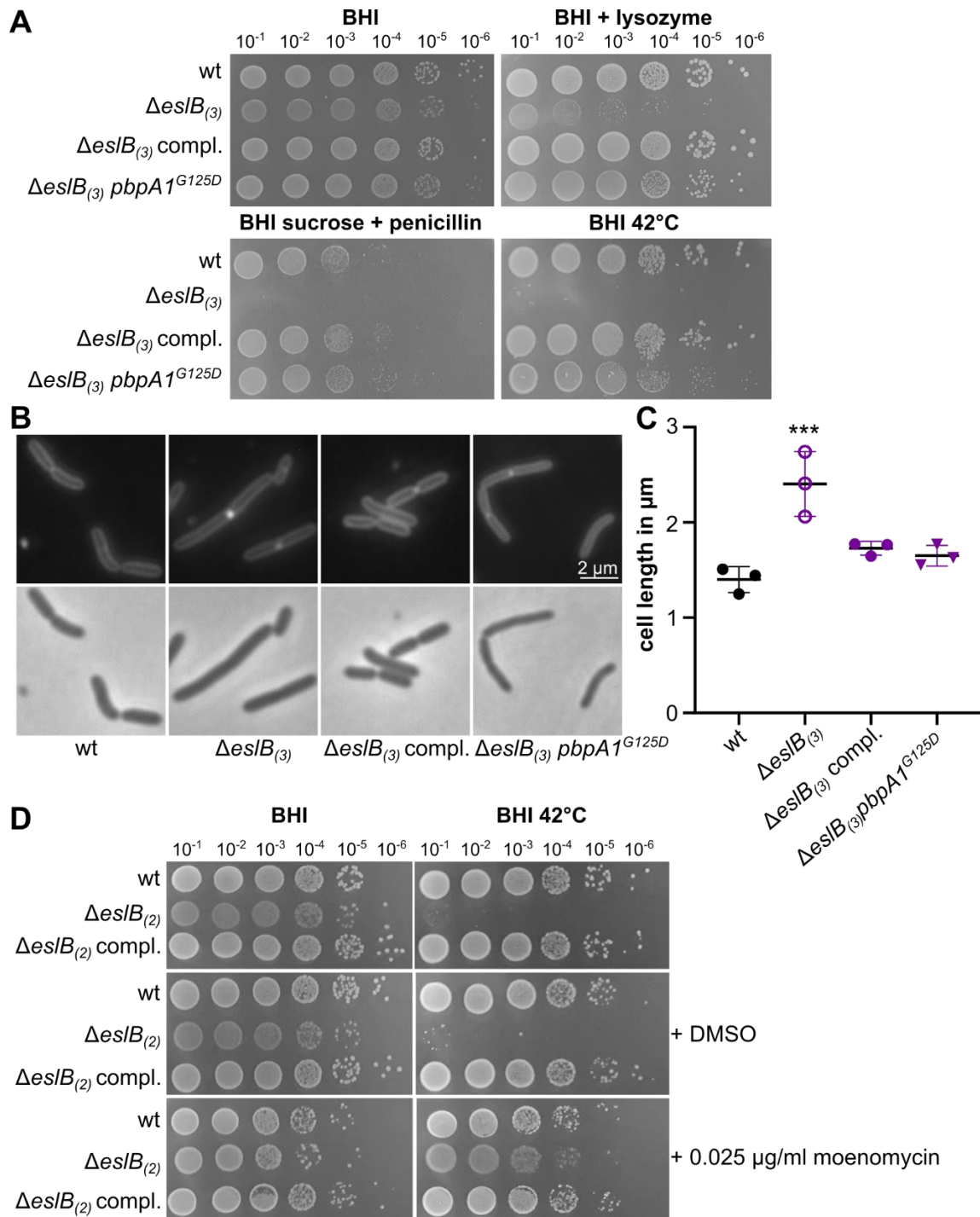


Figure 5: Inactivation of the glycosyltransferase of penicillin binding proteins rescues the *esIB* mutant. (A) Drop dilution assay. Dilutions of *L. monocytogenes* strains 10403S (wt), $\Delta esIB_{(3)}$, $\Delta esIB_{(3)}$ compl. and $\Delta esIB_{(3)}$ *pbpA1*^{G125D} were spotted on BHI plates, BHI plates containing 100 μ g/ml lysozyme or containing 0.5 M sucrose and 0.025 μ g/ml penicillin G, which were incubated at 37°C or on BHI plates, which were incubated at 42°C. (B) Microscopy images of *L. monocytogenes* strains. Bacterial membranes were stained with Nile red as described in the methods section. Scale bar is 2 μ m. (C) Cell length of *L. monocytogenes* strains shown in panel B. The cell length of 50 cells per strain was determined and the median cell length calculated. The average values and standard deviations of three independent experiments are plotted. (D) Drop dilution assay. Dilutions of *L. monocytogenes* strains 10403S (wt), $\Delta esIB_{(2)}$ and $\Delta esIB_{(2)}$ compl. were spotted on BHI plates, BHI plates containing DMSO or containing 0.025 μ g/ml moenomycin and incubated at 37°C or 42°C.

Suppression by reducing *cwIO* expression or CwIO activity

In addition to suppressors associated with MurA and PBP A1, we isolated suppressors carrying mutations in genes that either affect the transcription of *cwIO* or the activity of CwIO. CwIO is a DL-endopeptidase, which opens the existing cell wall to allow for the insertion of new lipid II precursors during cell elongation of *B. subtilis* (Bisicchia et al., 2007; Hashimoto et al., 2012). In *B. subtilis*, transcription of *cwIO* is induced by WalRK in response to low DL-endopeptidase activity (Bisicchia et al., 2007; Dobihal et al., 2019; Dubrac et al., 2008) and CwIO activity is stimulated by a direct interaction with the ABC transporter FtsEX (Meisner et al., 2013). In our suppressor screen, we isolated eight *esIB* suppressor strains that carried mutations in *walk*, which were either isolated under lysozyme or sucrose penicillin stress, and four *esIB* suppressor strains that carried mutations in *walR* from which the majority was isolated in the presence of lysozyme stress. We selected *esIB* suppressors 10403S Δ *esIB*₍₂₎ *walR*^{S216G} and 10403S Δ *esIB*₍₂₎ *walk*^{H463D}, which were isolated under lysozyme stress, and 10403S Δ *esIB*₍₂₎ *walk*^{I583T}, which was isolated under sucrose penicillin stress, for further analysis. In addition, three suppressors with mutations were isolated in *ftsE*, *ftsX* and *cwIO* under sucrose penicillin pressure (Table 1).

Spot plating assays showed that the *esIB* suppressors with mutations in either *walR* or *walk* could overcome the growth defect of the *esIB* mutant under sucrose penicillin, lysozyme and heat stress (Fig. 6). In contrast, *esIB* suppressors harboring mutations in either *ftsE*, *ftsX* or *cwIO*, grow comparable to the wildtype under sucrose penicillin and heat stress, but showed a similar growth defect as the *esIB* mutant on plates containing lysozyme (Fig. 6A). Microscopic analysis of the *esIB* suppressors with mutations in *walR*, *walk*, *ftsE*, *ftsX* and *cwIO* revealed that these cells have a similar cell length to the *L. monocytogenes* wildtype 10403S and thus, the expression of mutated WalR, Walk, FtsE and CwIO variants could restore the cell division defect of the *esIB* mutant (Fig. 6B-C). Additionally, we observed that the cells of suppressor strains 10403S Δ *esIB*₍₂₎ *cwIO*^{R106H} and 10403S Δ *esIB*₍₂₎ *ftsE*^{Q220-} were bent compared to the wildtype strain. This phenotype is characteristic for *B. subtilis* *cwIO* and *ftsE* mutants (Domínguez-Cuevas et al., 2013; Meisner et al., 2013) suggesting that the acquired mutations in *cwIO* and *ftsE* led to inactivation or reduced activity of CwIO and FtsE in *L. monocytogenes*.

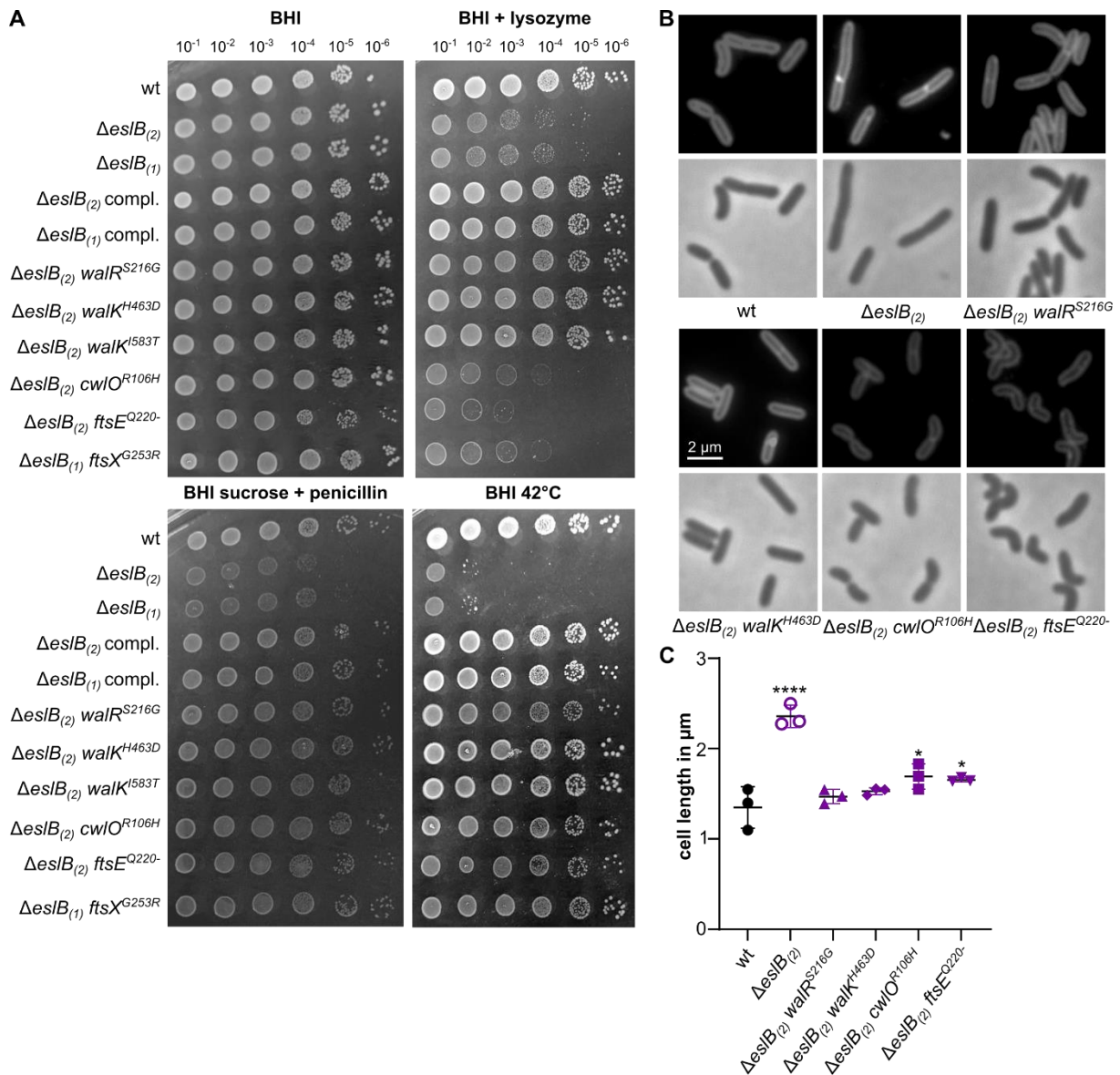


Figure 6 | Mutations in *walR*, *walk*, *cwIO*, *ftsE* and *ftsX* suppress *esIB* phenotypes. (A) Drop dilution assay. Dilutions of *L. monocytogenes* strains 10403S (wt), $\Delta esIB_{(2)}$, $\Delta esIB_{(1)}$, $\Delta esIB_{(2)}$ compl., $\Delta esIB_{(1)}$ compl., $\Delta esIB_{(2)}$ *walR*^{S216G}, $\Delta esIB_{(2)}$ *walk*^{H463D}, $\Delta esIB_{(2)}$ *walk*^{I583T}, $\Delta esIB_{(2)}$ *cwIO*^{R106H}, $\Delta esIB_{(2)}$ *ftsE*^{Q220-} and $\Delta esIB_{(1)}$ *ftsX*^{G253R} were spotted on BHI plates, BHI plates containing 100 µg/ml lysozyme or containing 0.5 M sucrose and 0.025 µg/ml penicillin G and were incubated at 37°C or on BHI plates that were incubated at 42°C. (B) Microscopy images of *L. monocytogenes* strains. Bacterial membranes were stained with Nile red as described in the methods section. Scale bar is 2 µm. (C) Cell length of *L. monocytogenes* strains shown in panel B. The cell length of 50 cells per strain was determined and the median cell length calculated. The average values and standard deviations of three independent experiments are plotted. For statistical analysis, a one-way ANOVA coupled with a Dunnett's multiple comparison test was used (* $p \leq 0.05$, **** $p \leq 0.0001$).

The observation that mutations accumulate in genes associated with CwIO led to the hypothesis that wildtype CwIO activity is toxic, due to the reduced peptidoglycan levels produced by the *esIB* mutant (Rismondo et al., 2021b). To confirm this hypothesis, an *esIB* *cwIO* double mutant was constructed, in which the expression of an ectopic copy of *cwIO* was placed under the control of an IPTG-inducible promoter. As expected, in the absence of the inducer, the *esIB* *cwIO* double

mutant was able to grow on BHI plates supplemented with sucrose and penicillin. In accordance to the results obtained for the suppressors, the growth of a strain lacking both, EslB and CwIO, was still impaired in the presence of lysozyme. Furthermore, individual deletion of either *eslB* or *cwIO* resulted in a severe growth defect at higher temperatures, while the *eslB cwIO* double mutant was able to grow in the absence of IPTG at 42°C. Induction of *cwIO* expression in strain 10403S Δ *cwIO* Δ *eslB* pIMK3-*cwIO* resulted in a growth defect under sucrose penicillin and under heat stress, which is comparable to that of the *eslB* mutant (Fig. 7A). Next, we studied the cell morphology of strains lacking CwIO, EslB or both. In accordance with previous studies investigating the function of CwIO in *B. subtilis* (Domínguez-Cuevas et al., 2013; Meisner et al., 2013), the *L. monocytogenes cwIO* mutant formed slightly smaller, bent cells (Fig. 7B-C). Cells lacking both, EslB and CwIO, were also shorter than cells of the *L. monocytogenes* wildtype 10403S, while induction of *cwIO* expression in strain 10403S Δ *cwIO* Δ *eslB* pIMK3-*cwIO* resulted in the formation of elongated cells (Fig. 7B-C). Altogether, these findings support our hypothesis that the suppression of the *eslB* phenotypes in the *cwIO*, *ftsE* and *ftsX* suppressors is the result of an inactivation of the DL-endopeptidase CwIO.

Suppression by inhibition of WTA biosynthesis

In *B. subtilis*, WalRK does not only stimulate transcription of *cwIO*, but also of the *tagAB* and *tagDEFGH* operons, which encode proteins required for WTA biosynthesis and export (Howell et al., 2003). In *L. monocytogenes* 10403S, WTA is composed of a ribitol phosphate backbone, which is attached to a Glc-Glc-glycerol phosphate-GlcNAc-ManNAc linker unit and modified with GlcNAc, rhamnose and D-alanine residues (Brown et al., 2013; Shen et al., 2017). Thus, UDP-GlcNAc is consumed by several enzymes during WTA biosynthesis and modification. As mentioned above, we isolated suppressors containing mutations in *lmo1077*, encoding a TarL homolog, and the promoter region of the *dlt* operon (Table 1). TarL is a teichoic acid ribitol phosphate polymerase required for the polymerization of the ribitol phosphate backbone of WTA (Fig. 1)(Brown et al., 2013). The *dlt* operon codes for proteins that are essential for the D-alanylation of WTA (Neuhaus and Baddiley, 2003; Perego et al., 1995; Rismondo et al., 2021a).

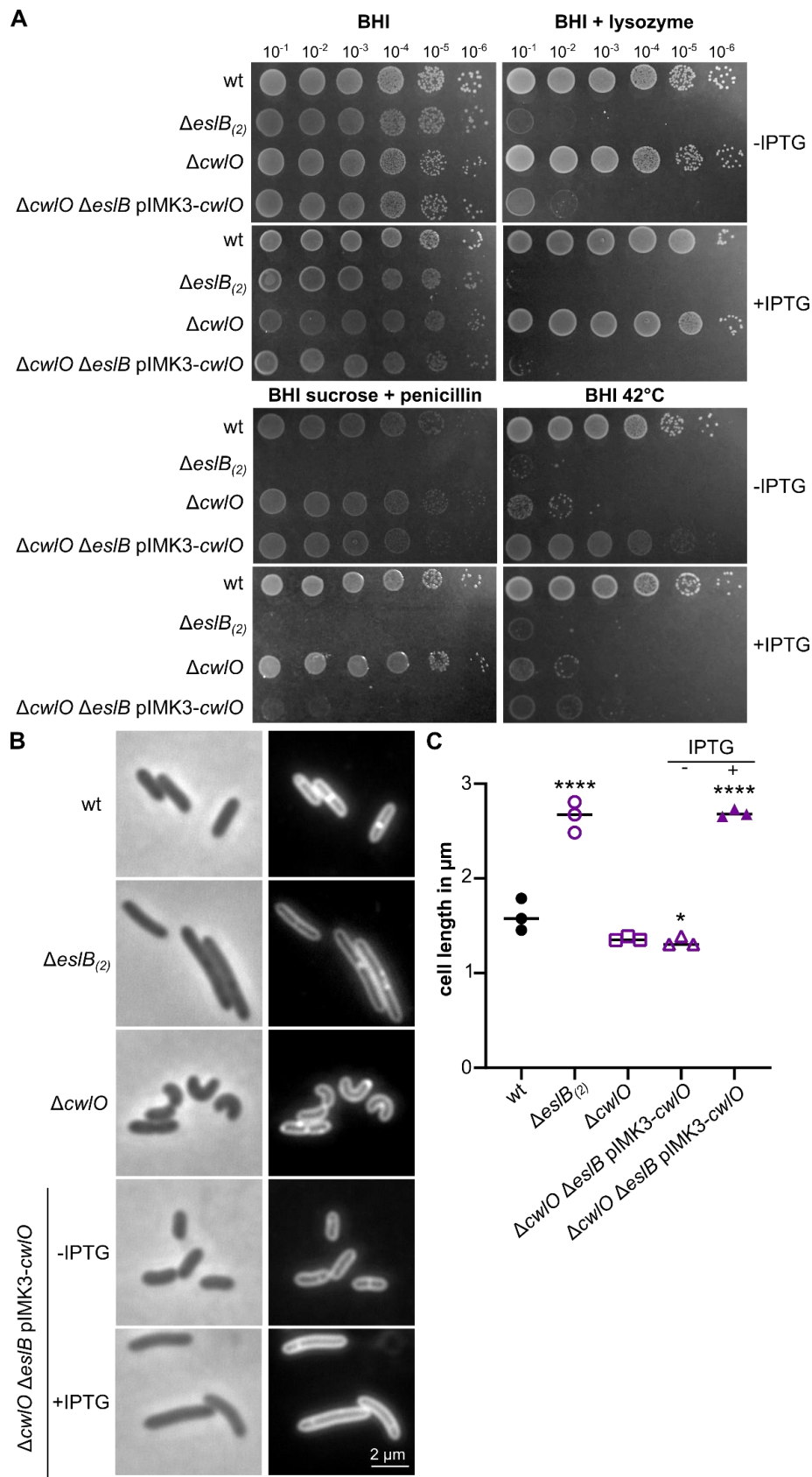


Figure 7 | Absence of Cw/O suppresses most of the *esIB* phenotypes. (A) Drop dilution assay. Dilutions of *L. monocytogenes* strains 10403S (wt), $\Delta esIB_{(2)}$, $\Delta cw/O$ and $\Delta cw/O \Delta esIB \text{ pIMK3-cw/O}$ were spotted on BHI plates, BHI plates containing 100 $\mu\text{g}/\text{ml}$ lysozyme or containing 0.5 M sucrose and 0.025 $\mu\text{g}/\text{ml}$ penicillin G and were incubated at 37°C or on BHI plates that were incubated at 42°C. For induction of *cw/O* expression,

the indicated plates were supplemented with 1 mM IPTG. (B) Microscopy images of *L. monocytogenes* strains. Bacterial membranes were stained with Nile red as described in the methods section. Scale bar is 2 μm . (C) Cell length of *L. monocytogenes* strains shown in panel B. The cell length of 50 cells per strain was determined and the median cell length calculated. The average values and standard deviations of three independent experiments are plotted. For statistical analysis, a one-way ANOVA coupled with a Dunnett's multiple comparison test was used (* $p \leq 0.05$, **** $p \leq 0.0001$).

Figure 8A shows that the *esIB* mutant, which harbors a mutation in *tarL*, could grow again under sucrose penicillin and lysozyme stress, likely due to a reduction in WTA biosynthesis and potentially leading to an increase in the cellular UDP-GlcNAc pool, which can then be used by MurA. However, the *tarL* suppressor is unable to grow at 42°C. A similar phenotype could be observed when the *L. monocytogenes* wildtype strain 10403S is grown at 42°C on a plate containing high concentrations of tunicamycin, which inhibits TarO, the first enzyme required for WTA biosynthesis (data not shown). This indicates that the mutated TarL variant produced by the *esIB* suppressor strain 10403S Δ *esIB*₍₃₎ *tarL*^{P282L} has a reduced activity. To further test if inhibition of WTA biosynthesis is indeed beneficial for the *esIB* mutant, we grew the *esIB* mutant at 42°C on BHI plates containing different concentrations of tunicamycin. We could see partial suppression of the heat sensitivity at a tunicamycin concentration of 0.05 $\mu\text{g/ml}$ and the *esIB* mutant grew comparable to the *L. monocytogenes* wildtype strain 10403S and the complementation strain on plates containing 0.5 $\mu\text{g/ml}$ tunicamycin (Fig. S4). These results demonstrate that reduction of WTA biosynthesis leads to the suppression of the heat phenotype associated of the *esIB* mutant.

Figure 8A further shows that the *esIB* suppressor strain, which harbors a mutation in the *dlt* promoter region, could grow again under all conditions tested. To assess what consequence the point mutation in the promoter region of the *dlt* operon has on gene expression, we place the promoterless *lacZ* gene under the control of the *dlt* promoter or the mutated *dlt* promoter found in suppressor strain 10403S Δ *esIB*₍₃₎ *P*_{*dlt*}^{*}. The *lacZ* promoter gene fusions were introduced into *B. subtilis* and β -galactosidase activities determined. This analysis showed that the mutation in the *dlt* promoter resulted in increased promoter activity and likely increased D-alanylation of teichoic acids in the suppressor strain (Fig. 8B). The D-alanylation state of teichoic acids is an important factor that impacts the bacterial cell surface charge (Vadyvaloo et al., 2004). As we isolated a suppressor that increased the expression of the *dlt* operon, we wondered, whether the surface charge of *esIB* mutant cells is altered. To test this, we determined the binding capability of positively charged cytochrome C to the cell surface of different *L. monocytogenes* strains, which serves as a readout of the bacterial surface charge (Peschel et al., 1999; Wecke et al., 1997). A strain lacking D-alanine residues on LTA and WTA due to a deletion of *dltA* was used as a control. As expected, the cell surface of the *dltA* mutant had a higher negative charge as compared to the *L. monocytogenes* wildtype strain 10403S. A similar result was observed for the *esIB* mutant. The

high negative surface charge of the *esIB* mutant could be partially rescued by the mutation in the *dlt* promoter, which is present in the *esIB* suppressor strain 10403S $\Delta esIB$ P_{dlt}^* (Fig. 8C). This result suggests that either the D-alanylation state of WTAs is altered in the absence of EsIB or that the surface presentation of WTA is changed due to the production of a thinner peptidoglycan layer.

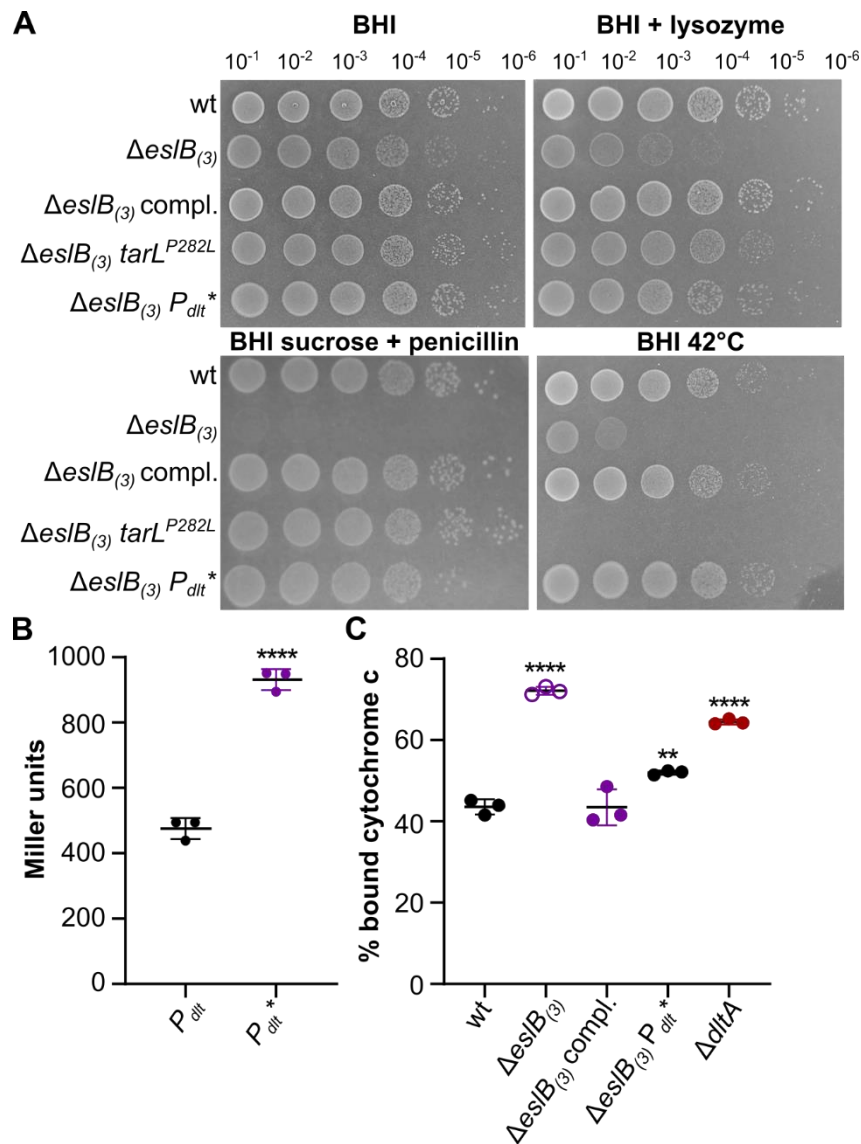


Figure 8 | Suppression of *esIB* phenotypes by alterations in WTA biosynthesis and modification. (A) Drop dilution assay. Dilutions of *L. monocytogenes* strains 10403S (wt), $\Delta esIB_{(3)}$, $\Delta esIB_{(3)}$ compl., $\Delta esIB_{(3)}$ *tarL*^{P282L} and $\Delta esIB_{(3)}$ P_{dlt}^* were spotted on BHI plates, BHI plates containing 100 μ g/ml lysozyme or containing 0.5 M sucrose and 0.025 μ g/ml penicillin G and were incubated at 37°C or on BHI plates that were incubated at 42°C. (B) β -galactosidase assay. The *dlt* promoter of *L. monocytogenes* wildtype 10403S (P_{dlt}) and suppressor strain $\Delta esIB_{(3)}$ P_{dlt}^* (P_{dlt}^*) were fused with *lacZ* and integrated into the *amyE* locus of *Bacillus subtilis*. The promoter activity was determined in Miller units as described in the methods section and the average and standard deviation of three independent experiments were plotted. An unpaired t-test was used for statistical analysis (**** $p \leq 0.0001$). (C) Cytochrome C assay. Cells of *L. monocytogenes* strains 10403S, $\Delta esIB_{(3)}$, $\Delta esIB_{(3)}$ compl. and $\Delta esIB_{(3)}$ P_{dlt}^* were incubated with cytochrome C as described in the methods section. The percentage of cytochrome C, which is bound by the cell surface, was calculated for three independent experiments and plotted. A strain lacking DltA was used as control. For statistical analysis, a one-way ANOVA coupled with a Dunnett's multiple comparison test was used (** $p \leq 0.01$, **** $p \leq 0.0001$).

Discussion

In this study, we aimed to provide further insight into the connection between the predicted ABC transporter EslABC and peptidoglycan biosynthesis. Previous studies have shown that the deletion of *eslB*, coding for one of transmembrane components of the transporter, leads to a growth defect on sucrose containing media, the formation of elongated cells, the production of a thinner peptidoglycan layer, as well as sensitivity towards the natural antibiotic lysozyme and cationic antimicrobial peptides (Burke et al., 2014; Durack et al., 2015; Rismondo et al., 2021b), suggesting its involvement in peptidoglycan biosynthesis and cell division. It was proposed that the addition of Mg^{2+} rescues mutants with a defect in peptidoglycan biosynthesis by reducing the activity of peptidoglycan hydrolases (Tesson et al., 2022). In accordance with this, we observed a suppression of the *eslB* growth deficits under all conditions tested when an excess of Mg^{2+} was added. *L. monocytogenes* encodes several peptidoglycan hydrolases, including the DL-endopeptidase CwIO (Spl), the LytM-domain containing protein Lmo2504 and the two cell wall hydrolases NamA and CwhA (p60), which are required for daughter cell separation (Carroll et al., 2003; Pilgrim et al., 2003). We have isolated several *eslB* suppressors, which carry mutations in *cwIO* or mutations in other genes, e.g. *ftsE* or *ftsX*, which affect CwIO activity. After depletion of CwIO, the *eslB* mutant was able to grow in otherwise non-permissive conditions, suggesting that the activity of CwIO might be deregulated in the *eslB* deletion strain or that the peptidoglycan of the *eslB* mutant is more sensitive to hydrolysis by CwIO. CwIO activity is controlled by a direct protein-protein interaction with the ABC transporter FtsEX (Meisner et al., 2013). It is thus tempting to speculate that the ABC transporter EslABC might also affect CwIO activity or localization of proteins involved in peptidoglycan biosynthesis and/or degradation. Interestingly, a strain lacking both EslB and CwIO is able to grow at elevated temperatures, while both single mutants are not able to grow under this condition.

We could isolate *eslB* suppressor strains with mutations that are associated with stabilization of MurA, the UDP-GlcNAc 1-carboxyvinyltransferase responsible for the first step of peptidoglycan biosynthesis. Elevated levels of MurA, and thus, enhanced peptidoglycan biosynthesis could fully restore the phenotypic defects of the 10403SΔ*eslB* strain. To identify the exact process of peptidoglycan biosynthesis, which is impaired in the *eslB* mutant, we performed a screen with antibiotics targeting different steps of this process. The absence of *eslB* only affected the resistance towards t-Cin and fosfomicin, which reduce the synthesis of UDP-GlcNAc and inhibit MurA, respectively (Marquardt et al., 1994; Pensinger et al., 2021; Sun et al., 2021). Surprisingly, we observed an increased resistance of the *eslB* mutant towards tunicamycin. The primary target of tunicamycin is TarO, the first enzyme of WTA biosynthesis, and, at high

concentrations, also MraY, which is responsible for the production of lipid I during peptidoglycan biosynthesis (Fig. 1)(Campbell et al., 2011; Hakulinen et al., 2017; Price and Tsvetanova, 2007; Watkinson et al., 1971). During WTA biosynthesis, UDP-GlcNAc is used for the synthesis of the linker unit and for the modification of the WTA backbone (Eugster et al., 2015; Rismondo et al., 2018; Shen et al., 2017). Thus, reducing the production of WTA could increase the availability of UDP-GlcNAc for peptidoglycan biosynthesis and therefore support the growth of the *esIB* mutant under non-permissive conditions. In accordance with this, we observed a partial suppression of the *esIB* phenotypes by the overproduction of GlmM and GlmR, two enzymes required for the synthesis of UDP-GlcNAc (Pensinger et al., 2021). These results suggest that either the production or distribution of UDP-GlcNAc as a substrate between different pathways might be disturbed in the *esIB* mutant.

Cell wall stability depends on the balance between peptidoglycan biosynthesis and hydrolysis. An imbalance of one of these processes results in rapid cell lysis (Sassine et al., 2020). Recent studies suggest that new peptidoglycan precursors are inserted into the growing glycan chains by the Rod system, which is composed of several enzymes. In contrast, class A PBPs are thought to fill gaps and/or repair cell wall defects (Cho et al., 2016; Dion et al., 2019; Vigouroux et al., 2020). It was recently shown that enhanced endopeptidase activity leads to the activation of class A PBPs in *E. coli* (Lai et al., 2017). A similar mechanism seems to exist in *B. subtilis*, as either inactivation of PBP1 or inhibition of peptidoglycan hydrolases by the addition of Mg²⁺ suppresses growth and morphological defects of an *mreB* mutant (Tesson et al., 2022). In accordance with this, we also observed suppression of the heat sensitivity of the *esIB* mutant in presence of moenomycin, which specifically inhibits the glycosyltransferase activity of class A PBPs (Ostash and Walker, 2010; Van Heijenoort et al., 1978). In our suppressor screen, we identified a strain carrying a mutation in the *dlt* promoter region, which leads to an overproduction of the Dlt enzymes. These enzymes are required for the modification of teichoic acids (TAs) with D-alanines (Neuhaus and Baddiley, 2003; Percy and Gründling, 2014; Rismondo et al., 2021a). The modification of TAs with D-alanine residues leads to a reduction in the negative surface charge and affects the activity of peptidoglycan hydrolases (Brown et al., 2013; Tesson et al., 2022; Vadyvaloo et al., 2004). Furthermore, lack of D-alanine modifications of TAs was shown to increase lysozyme sensitivity in *Staphylococcus aureus* (Herbert et al., 2007). Interestingly, the cell surface of the *esIB* mutant is more negatively charged, similar to that of a strain lacking D-alanine modifications on TAs. Based on our results, we propose the following model: The absence of EsIB seems to affect the production and/or distribution of UDP-GlcNAc between different pathways, leading to the production of a thinner peptidoglycan layer. The reduced peptidoglycan thickness

could subsequently result in the presentation of a larger portion of WTA on the bacterial cell surface, which would explain the higher negative surface charge (Fig. 9). This higher negative surface charge would enhance the binding capability and/or activity of cationic antimicrobial peptides, lysozyme as well as peptidoglycan hydrolases (Low et al., 2011; Neuhaus and Baddiley, 2003; Ragland and Criss, 2017; Steudle and Pleiss, 2011; Weidenmaier et al., 2003) and furthermore explain the sensitivity of the *esIB* mutant towards CwLO activity, lysozyme and cationic antimicrobial peptides (Burke et al., 2014; Rismondo et al., 2021b).

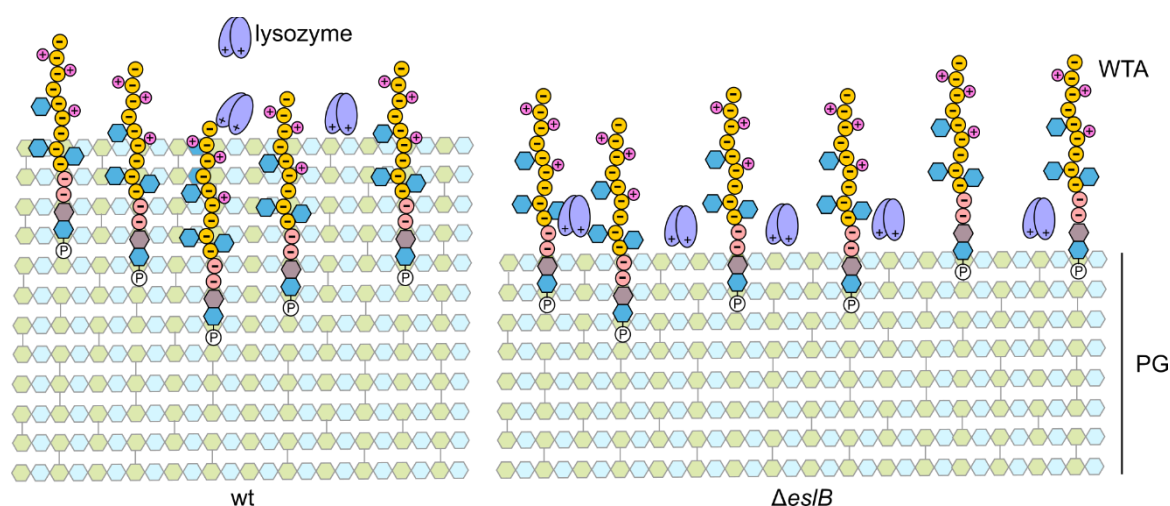


Figure 9 | Model of altered WTA presentation on the cell surface of an *esIB* mutant. The gram-positive cell wall is composed of a thick layer of peptidoglycan (PG) and wall teichoic acids (WTA), which are attached to the MurNAc-moiety of the PG backbone (Brown et al., 2013). WTA of *L. monocytogenes* 10403S are composed of a negatively charged ribitol phosphate backbone (indicated by -), which can be modified with GlcNAc residues (blue hexagons) and positively charged D-alanine residues (indicated by +). The absence of EsIB seems to affect the production and/or distribution of the PG precursor UDP-GlcNAc between different pathways, which results in the production of a thinner PG layer. WTAs are thought to partially stick out of the PG layer and we propose that due to the thinner PG layer produced by the *esIB* mutant, a larger portion of the WTA backbone, which is negatively charged, could be presented on the bacterial cell surface. This would result in a higher negative cell surface charge of the *esIB* mutant, which would affect the binding capability and/or activity of PG hydrolases, lysozyme and cationic antimicrobial peptides (Low et al., 2011; Ragland and Criss, 2017; Steudle and Pleiss, 2011; Weidenmaier et al., 2003).

The essential two-component system WalRK stimulates the transcription of several peptidoglycan hydrolases in gram-positive bacteria (Delaune et al., 2011; Delauné et al., 2012; Dubrac et al., 2008; Dubrac and Msadek, 2004; Howell et al., 2003). In *B. subtilis*, WalRK also regulates the expression of genes involved in WTA biosynthesis and export (Howell et al., 2003). The regulon of the WalRK system has not yet been determined for *L. monocytogenes*, however, it was shown that the system is essential (Fischer et al., 2022). Inactivation of WalRK usually leads to cell death of wildtype cells due to loss of peptidoglycan hydrolase activity, however, cell death could be prevented by the inhibition of peptidoglycan biosynthesis (Salamaga et al., 2021). We have isolated several *esIB* suppressors with mutations in *walR* and *walK*. As it is unlikely that all of these

mutations are gain-of-function mutations, we hypothesize that these mutations result in a reduced activity of the WalRK system. This would lead to a reduced peptidoglycan hydrolase activity as well as a reduction in WTA content, and reduction of the latter would at least partially restore the bacterial cell surface charge of the *esIB* mutant.

Taken together, we could show that the lack of EsIB results in a defect in peptidoglycan biosynthesis, which can be suppressed by modulating the activity of enzymes involved in either peptidoglycan biosynthesis or hydrolysis. Our results suggest that the production or distribution of the peptidoglycan precursor UDP-GlcNAc between different pathways might be disturbed in the *esIB* mutant. Further studies are required to prove this hypothesis and to determine the function of the ABC transporter EsIABC.

Acknowledgements

We thank Ivan Andrew and Jaspreet Haywood from the CSC Genomics Laboratory, Hammersmith Hospital, for their help with the whole genome sequencing and Annika Gillis for help with genome sequence analysis. We also thank Julia Busse for technical assistance and Tayfun Acar for the help with some experiments. We are grateful to Prof. Jörg Stülke for providing JR and LMS with laboratory space, equipment and consumables and to the Göttingen Center for Molecular Biosciences (GZMB) for financial support. This work was funded by the Wellcome Trust grant 210671/Z/18/Z and MRC grant MR/P011071/1 to AG, the German research foundation (DFG) grants RI 2920/1-1, RI 2920/2-1 and RI 2920/3-1 to JR, HA 6830/4 to SH. LMS was supported by the Göttingen Graduate School for Neurosciences, Biophysics, and Molecular Biosciences (GGNB, DFG grant GSC226/4).

Supplemental Material

<https://www.ncbi.nlm.nih.gov/pmc/articles/PMC9593813>

- Figure S1 |** Magnesium rescues growth deficits of the *esIB* mutant.
- Figure S2 |** Resistance of *L. monocytogenes* strains towards cell wall-targeting antibiotics.
- Figure S3 |** Overexpression of *glmM* and *glmR* leads to partial suppression of *esIB* phenotype.
- Figure S4 |** Chemical inactivation of TarO partially rescues heat sensitivity of the *esIB* mutant.

References

- Aubry, C., Goulard, C., Nahori, M.-A., Cayet, N., Decalf, J., Sachse, M., Boneca, I.G., Cossart, P., Dussurget, O., 2011. OatA, a peptidoglycan O-acetyltransferase involved in *Listeria monocytogenes* immune escape, is critical for virulence. *J. Infect. Dis.* 204, 731–740. <https://doi.org/10.1093/infdis/jir396>
- Bisicchia, P., Noone, D., Lioliou, E., Howell, A., Quigley, S., Jensen, T., Jarmer, H., Devine, K.M., 2007. The essential YycFG two-component system controls cell wall metabolism in *Bacillus subtilis*. *Mol. Microbiol.* 65, 180–200. <https://doi.org/10.1111/j.1365-2958.2007.05782.x>
- Boneca, I.G., Dussurget, O., Cabanes, D., Nahori, M.-A., Sousa, S., Lecuit, M., Psylinakis, E., Bouriotis, V., Hugot, J.-P., Giovannini, M., Coyle, A., Bertin, J., Namane, A., Rousselle, J.-C., Cayet, N., Prévost, M.-C., Balloy, V., Chignard, M., Philpott, D.J., Cossart, P., Girardin, S.E., 2007. A critical role for peptidoglycan N-deacetylation in *Listeria* evasion from the host innate immune system. *Proc. Natl. Acad. Sci.* 104, 997–1002. <https://doi.org/10.1073/pnas.0609672104>
- Brown, S., Santa Maria, J.P., Walker, S., 2013. Wall teichoic acids of gram-positive bacteria. *Annu. Rev. Microbiol.* 67, 313–336. <https://doi.org/10.1146/annurev-micro-092412-155620>
- Brunet, Y.R., Wang, X., Rudner, D.Z., 2019. SweC and SweD are essential co-factors of the FtsEX-CwLO cell wall hydrolase complex in *Bacillus subtilis*. *PLOS Genet.* 15, e1008296. <https://doi.org/10.1371/journal.pgen.1008296>
- Burke, T.P., Loukitcheva, A., Zemansky, J., Wheeler, R., Boneca, I.G., Portnoy, D.A., 2014. *Listeria monocytogenes* is resistant to lysozyme through the regulation, not the acquisition, of cell wall-modifying enzymes. *J. Bacteriol.* 196, 3756–3767. <https://doi.org/10.1128/JB.02053-14>
- Camilli, A., Tilney, L.G., Portnoy, D.A., 1993. Dual roles of *plcA* in *Listeria monocytogenes* pathogenesis. *Mol. Microbiol.* 8, 143–157. <https://doi.org/10.1111/j.1365-2958.1993.tb01211.x>
- Campbell, J., Singh, A.K., Santa Maria, J.P., Kim, Y., Brown, S., Swoboda, J.G., Mylonakis, E., Wilkinson, B.J., Walker, S., 2011. Synthetic lethal compound combinations reveal a fundamental connection between wall teichoic acid and peptidoglycan biosyntheses in *Staphylococcus aureus*. *ACS Chem. Biol.* 6, 106–116. <https://doi.org/10.1021/cb100269f>
- Carballido-López, R., Formstone, A., Li, Y., Ehrlich, S.D., Noirot, P., Errington, J., 2006. Actin homolog MreBH governs cell morphogenesis by localization of the cell wall hydrolase LytE. *Dev. Cell* 11, 399–409. <https://doi.org/10.1016/j.devcel.2006.07.017>
- Carroll, S.A., Hain, T., Technow, U., Darji, A., Pashalidis, P., Joseph, S.W., Chakraborty, T., 2003. Identification and characterization of a peptidoglycan hydrolase, MurA, of *Listeria*
-

-
- monocytogenes*, a muramidase needed for cell separation. *J. Bacteriol.* 185, 6801–6808. <https://doi.org/10.1128/JB.185.23.6801-6808.2003>
- Cho, H., Wivagg, C.N., Kapoor, M., Barry, Z., Rohs, P.D.A., Suh, H., Marto, J.A., Garner, E.C., Bernhardt, T.G., 2016. Bacterial cell wall biogenesis is mediated by SEDS and PBP polymerase families functioning semi-autonomously. *Nat. Microbiol.* 1, 16172. <https://doi.org/10.1038/nmicrobiol.2016.172>
- Delauné, A., Dubrac, S., Blanchet, C., Poupel, O., Mäder, U., Hiron, A., Leduc, A., Fitting, C., Nicolas, P., Cavaillon, J.-M., Adib-Conquy, M., Msadek, T., 2012. The WalkR system controls major staphylococcal virulence genes and is involved in triggering the host inflammatory response. *Infect. Immun.* 80, 3438–3453. <https://doi.org/10.1128/IAI.00195-12>
- Delaune, A., Poupel, O., Mallet, A., Coic, Y.-M., Msadek, T., Dubrac, S., 2011. Peptidoglycan crosslinking relaxation plays an important role in *Staphylococcus aureus* WalkR-dependent cell viability. *PLoS One* 6, e17054. <https://doi.org/10.1371/journal.pone.0017054>
- Dion, M.F., Kapoor, M., Sun, Y., Wilson, S., Ryan, J., Vigouroux, A., van Teeffelen, S., Oldenbourg, R., Garner, E.C., 2019. *Bacillus subtilis* cell diameter is determined by the opposing actions of two distinct cell wall synthetic systems. *Nat. Microbiol.* 4, 1294–1305. <https://doi.org/10.1038/s41564-019-0439-0>
- Dobihal, G.S., Brunet, Y.R., Flores-Kim, J., Rudner, D.Z., 2019. Homeostatic control of cell wall hydrolysis by the WalRK two-component signaling pathway in *Bacillus subtilis*. *Elife* 8, e52088. <https://doi.org/10.7554/eLife.52088>
- Domínguez-Cuevas, P., Porcelli, I., Daniel, R.A., Errington, J., 2013. Differentiated roles for MreB-actin isologues and autolytic enzymes in *Bacillus subtilis* morphogenesis. *Mol. Microbiol.* 89, 1084–1098. <https://doi.org/10.1111/mmi.12335>
- Domínguez-Cuevas, P., Porcelli, I., Daniel, R.A., Errington, J., 2013. Differentiated roles for MreB-actin isologues and autolytic enzymes in *Bacillus subtilis* morphogenesis. *Mol. Microbiol.* 89, 1084–1098. <https://doi.org/10.1111/mmi.12335>
- Du, W., Brown, J.R., Sylvester, D.R., Huang, J., Chalker, A.F., So, C.Y., Holmes, D.J., Payne, D.J., Wallis, N.G., 2000. Two active forms of UDP-N-acetylglucosamine enolpyruvyl transferase in gram-positive bacteria. *J. Bacteriol.* 182, 4146–4152. <https://doi.org/10.1128/JB.182.15.4146-4152.2000>
- Dubrac, S., Bisicchia, P., Devine, K.M., Msadek, T., 2008. A matter of life and death: cell wall homeostasis and the WalkR (YycGF) essential signal transduction pathway. *Mol. Microbiol.* 70, 1307–1322. <https://doi.org/10.1111/j.1365-2958.2008.06483.x>
- Dubrac, S., Msadek, T., 2004. Identification of genes controlled by the essential YycG/YycF two-
-

-
- component system of *Staphylococcus aureus*. J. Bacteriol. 186, 1175–1181. <https://doi.org/10.1128/JB.186.4.1175-1181.2004>
- Durack, J., Burke, T.P., Portnoy, D.A., 2015. A *prl* mutation in SecY suppresses secretion and virulence defects of *Listeria monocytogenes secA2* mutants. J. Bacteriol. 197, 932–942. <https://doi.org/10.1128/JB.02284-14>
- Emami, K., Guyet, A., Kawai, Y., Devi, J., Wu, L.J., Allenby, N., Daniel, R.A., Errington, J., 2017. RodA as the missing glycosyltransferase in *Bacillus subtilis* and antibiotic discovery for the peptidoglycan polymerase pathway. Nat. Microbiol. 2, 16253. <https://doi.org/10.1038/nmicrobiol.2016.253>
- Eugster, M.R., Morax, L.S., Hüls, V.J., Huwiler, S.G., Leclercq, A., Lecuit, M., Loessner, M.J., 2015. Bacteriophage predation promotes serovar diversification in *Listeria monocytogenes*. Mol. Microbiol. 97, 33–46. <https://doi.org/10.1111/mmi.13009>
- Fischer, M.A., Engelgeh, T., Rothe, P., Fuchs, S., Thürmer, A., Halbedel, S., 2022. *Listeria monocytogenes* genes supporting growth under standard laboratory cultivation conditions and during macrophage infection. Genome Res. 32, 1711–1726. <https://doi.org/10.1101/gr.276747.122>
- Hakulinen, J.K., Hering, J., Brändén, G., Chen, H., Snijder, A., Ek, M., Johansson, P., 2017. MraY-antibiotic complex reveals details of tunicamycin mode of action. Nat. Chem. Biol. 13, 265–267. <https://doi.org/10.1038/nchembio.2270>
- Hashimoto, M., Ooiwa, S., Sekiguchi, J., 2012. Synthetic lethality of the *lytE cw/O* genotype in *Bacillus subtilis* is caused by lack of D,L-endopeptidase activity at the lateral cell wall. J. Bacteriol. 194, 796–803. <https://doi.org/10.1128/JB.05569-11>
- Herbert, S., Bera, A., Nerz, C., Kraus, D., Peschel, A., Goerke, C., Meehl, M., Cheung, A., Götz, F., 2007. Molecular basis of resistance to muramidase and cationic antimicrobial peptide activity of lysozyme in staphylococci. PLoS Pathog. 3, e102. <https://doi.org/10.1371/journal.ppat.0030102>
- Howell, A., Dubrac, S., Andersen, K.K., Noone, D., Fert, J., Msadek, T., Devine, K., 2003. Genes controlled by the essential YycG/YycF two-component system of *Bacillus subtilis* revealed through a novel hybrid regulator approach. Mol. Microbiol. 49, 1639–1655. <https://doi.org/10.1046/j.1365-2958.2003.03661.x>
- Huber, G., Neesemann, G., 1968. Moenomycin, an inhibitor of cell wall synthesis. Biochem. Biophys. Res. Commun. 30, 7–13. [https://doi.org/10.1016/0006-291x\(68\)90704-3](https://doi.org/10.1016/0006-291x(68)90704-3)
- Kahan, F.M., Kahan, J.S., Cassidy, P.J., Kropp, H., 1974. The mechanism of action of fosfomycin (phosphonomycin). Ann. N. Y. Acad. Sci. 235, 364–386. <https://doi.org/10.1111/j.1749->
-

6632.1974.tb43277.x

- Kang, J., Wiedmann, M., Boor, K.J., Bergholz, T.M., 2015. VirR-Mediated resistance of *Listeria monocytogenes* against food antimicrobials and cross-protection induced by exposure to organic acid salts. *Appl. Environ. Microbiol.* 81, 4553–4562. <https://doi.org/10.1128/AEM.00648-15>
- Kock, H., Gerth, U., Hecker, M., 2004. MurAA, catalysing the first committed step in peptidoglycan biosynthesis, is a target of Clp-dependent proteolysis in *Bacillus subtilis*. *Mol. Microbiol.* 51, 1087–1102. <https://doi.org/10.1046/j.1365-2958.2003.03875.x>
- Korsak, D., Markiewicz, Z., Gutkind, G.O., Ayala, J.A., 2010. Identification of the full set of *Listeria monocytogenes* penicillin-binding proteins and characterization of PBPD2 (Lmo2812). *BMC Microbiol.* 10, 239. <https://doi.org/10.1186/1471-2180-10-239>
- Lai, G.C., Cho, H., Bernhardt, T.G., 2017. The mecillinam resistome reveals a role for peptidoglycan endopeptidases in stimulating cell wall synthesis in *Escherichia coli*. *PLoS Genet.* 13, e1006934. <https://doi.org/10.1371/journal.pgen.1006934>
- Lauer, P., Chow, M.Y.N., Loessner, M.J., Portnoy, D.A., Calendar, R., 2002. Construction, characterization, and use of two *Listeria monocytogenes* site-specific phage integration vectors. *J. Bacteriol.* 184, 4177–4186. <https://doi.org/10.1128/JB.184.15.4177-4186.2002>
- Leclercq, S., Derouaux, A., Olatunji, S., Fraipont, C., Egan, A.J.F., Vollmer, W., Breukink, E., Terrak, M., 2017. Interplay between penicillin-binding proteins and SEDS proteins promotes bacterial cell wall synthesis. *Sci. Rep.* 7, 43306. <https://doi.org/10.1038/srep43306>
- Low, L.Y., Yang, C., Perego, M., Osterman, A., Liddington, R., 2011. Role of net charge on catalytic domain and influence of cell wall binding domain on bactericidal activity, specificity, and host range of phage lysins. *J. Biol. Chem.* 286, 34391–34403. <https://doi.org/10.1074/jbc.M111.244160>
- Marquardt, J.L., Brown, E.D., Lane, W.S., Haley, T.M., Ichikawa, Y., Wong, C.H., Walsh, C.T., 1994. Kinetics, stoichiometry, and identification of the reactive thiolate in the inactivation of UDP-GlcNAc enolpyruvyl transferase by the antibiotic fosfomycin. *Biochemistry* 33, 10646–10651. <https://doi.org/10.1021/bi00201a011>
- Marston, A.L., Thomaidis, H.B., Edwards, D.H., Sharpe, M.E., Errington, J., 1998. Polar localization of the MinD protein of *Bacillus subtilis* and its role in selection of the mid-cell division site. *Genes Dev.* 12, 3419–3430. <https://doi.org/10.1101/gad.12.21.3419>
- Meeske, A.J., Riley, E.P., Robins, W.P., Uehara, T., Mekalanos, J.J., Kahne, D., Walker, S., Kruse, A.C., Bernhardt, T.G., Rudner, D.Z., 2016. SEDS proteins are a widespread family of bacterial cell wall polymerases. *Nature* 537, 634–638. <https://doi.org/10.1038/nature19331>

-
- Meeske, A.J., Sham, L.-T., Kimsey, H., Koo, B.-M., Gross, C.A., Bernhardt, T.G., Rudner, D.Z., 2015. MurJ and a novel lipid II flippase are required for cell wall biogenesis in *Bacillus subtilis*. Proc. Natl. Acad. Sci. 112, 6437–6442. <https://doi.org/10.1073/pnas.1504967112>
- Meisner, J., Montero Llopis, P., Sham, L.-T., Garner, E., Bernhardt, T.G., Rudner, D.Z., 2013. FtsEX is required for CwIO peptidoglycan hydrolase activity during cell wall elongation in *Bacillus subtilis*. Mol. Microbiol. 89, 1069–1083. <https://doi.org/10.1111/mmi.12330>
- Miller, J.H., 1972. Experiments in Molecular Genetics. Cold Spring Harbor Laboratory, NY.
- Neuhaus, F.C., Baddiley, J., 2003. A continuum of anionic charge: structures and functions of D-alanyl-teichoic acids in gram-positive bacteria. Microbiol. Mol. Biol. Rev. 67, 686–723. <https://doi.org/10.1128/MMBR.67.4.686-723.2003>
- Ohnishi, R., Ishikawa, S., Sekiguchi, J., 1999. Peptidoglycan hydrolase LytF plays a role in cell separation with CwIF during vegetative growth of *Bacillus subtilis*. J. Bacteriol. 181, 3178–3184. <https://doi.org/10.1128/JB.181.10.3178-3184.1999>
- Ostash, B., Walker, S., 2010. Moenomycin family antibiotics: chemical synthesis, biosynthesis, and biological activity. Nat. Prod. Rep. 27, 1594–1617. <https://doi.org/10.1039/c001461n>
- Pazos, M., Peters, K., 2019. Peptidoglycan. Subcell. Biochem. 92, 127–168. https://doi.org/10.1007/978-3-030-18768-2_5
- Pensing, D.A., Gutierrez, K. V, Smith, H.B., Vincent, W.J.B., Stevenson, D.S., Black, K.A., Perez-Medina, K.M., Dillard, J.P., Rhee, K.Y., Amador-Noguez, D., Huynh, T.N., Sauer, J.-D., 2021. *Listeria monocytogenes* GlmR is an accessory uridylyltransferase essential for cytosolic survival and virulence. bioRxiv 2021.10.27.466214. <https://doi.org/10.1101/2021.10.27.466214>
- Percy, M.G., Gründling, A., 2014. Lipoteichoic acid synthesis and function in gram-positive bacteria. Annu. Rev. Microbiol. 68, 81–100. <https://doi.org/10.1146/annurev-micro-091213-112949>
- Perego, M., Glaser, P., Minutello, A., Strauch, M.A., Leopold, K., Fischer, W., 1995. Incorporation of D-alanine into lipoteichoic acid and wall teichoic acid in *Bacillus subtilis*. Identification of genes and regulation. J. Biol. Chem. 270, 15598–15606. <https://doi.org/10.1074/jbc.270.26.15598>
- Peschel, A., Otto, M., Jack, R.W., Kalbacher, H., Jung, G., Götz, F., 1999. Inactivation of the *dlt* operon in *Staphylococcus aureus* confers sensitivity to defensins, protegrins, and other antimicrobial peptides. J. Biol. Chem. 274, 8405–8410. <https://doi.org/10.1074/jbc.274.13.8405>
- Pilgrim, S., Kolb-Mäurer, A., Gentschev, I., Goebel, W., Kuhn, M., 2003. Deletion of the gene encoding *p60* in *Listeria monocytogenes* leads to abnormal cell division and loss of actin-
-

- based motility. *Infect. Immun.* 71, 3473–3484. <https://doi.org/10.1128/IAI.71.6.3473-3484.2003>
- Price, N.P.J., Tsvetanova, B., 2007. Biosynthesis of the tunicamycins: a review. *J. Antibiot. (Tokyo)*. 60, 485–491. <https://doi.org/10.1038/ja.2007.62>
- Ragland, S.A., Criss, A.K., 2017. From bacterial killing to immune modulation: Recent insights into the functions of lysozyme. *PLoS Pathog.* 13, e1006512. <https://doi.org/10.1371/journal.ppat.1006512>
- Rismondo, J., Bender, J.K., Halbedel, S., 2016. Suppressor mutations linking *gpsB* with the first committed step of peptidoglycan biosynthesis in *Listeria monocytogenes*. *J. Bacteriol.* 199, e00393-16. <https://doi.org/10.1128/JB.00393-16>
- Rismondo, J., Gillis, A., Gründling, A., 2021a. Modifications of cell wall polymers in gram-positive bacteria by multi-component transmembrane glycosylation systems. *Curr. Opin. Microbiol.* 60, 24–33. <https://doi.org/10.1016/j.mib.2021.01.007>
- Rismondo, J., Möller, L., Aldridge, C., Gray, J., Vollmer, W., Halbedel, S., 2015. Discrete and overlapping functions of peptidoglycan synthases in growth, cell division and virulence of *Listeria monocytogenes*. *Mol. Microbiol.* 95, 332–351. <https://doi.org/10.1111/mmi.12873>
- Rismondo, J., Percy, M.G., Gründling, A., 2018. Discovery of genes required for lipoteichoic acid glycosylation predicts two distinct mechanisms for wall teichoic acid glycosylation. *J. Biol. Chem.* 293, 3293–3306. <https://doi.org/10.1074/jbc.RA117.001614>
- Rismondo, J., Schulz, L.M., 2021. Not just transporters: Alternative functions of ABC transporters in *Bacillus subtilis* and *Listeria monocytogenes*. *Microorganisms* 9, 163. <https://doi.org/10.3390/microorganisms9010163>
- Rismondo, J., Schulz, L.M., Yacoub, M., Wadhawan, A., Hoppert, M., Dionne, M.S., Gründling, A., 2021b. EsIB is required for cell wall biosynthesis and modification in *Listeria monocytogenes*. *J. Bacteriol.* 203, e00553-20. <https://doi.org/10.1128/JB.00553-20>
- Ruiz, N., 2008. Bioinformatics identification of MurJ (MviN) as the peptidoglycan lipid II flippase in *Escherichia coli*. *Proc. Natl. Acad. Sci. U. S. A.* 105, 15553–15557. <https://doi.org/10.1073/pnas.0808352105>
- Salamaga, B., Kong, L., Pasquina-Lemonche, L., Lafage, L., von und zur Muhlen, M., Gibson, J.F., Grybchuk, D., Tooke, A.K., Panchal, V., Culp, E.J., Tatham, E., O’Kane, M.E., Catley, T.E., Renshaw, S.A., Wright, G.D., Plevka, P., Bullough, P.A., Han, A., Hobbs, J.K., Foster, S.J., 2021. Demonstration of the role of cell wall homeostasis in *Staphylococcus aureus* growth and the action of bactericidal antibiotics. *Proc. Natl. Acad. Sci.* 118, e2106022118. <https://doi.org/10.1073/pnas.2106022118>

-
- Sarkar, P., Yarlagadda, V., Ghosh, C., Haldar, J., 2017. A review on cell wall synthesis inhibitors with an emphasis on glycopeptide antibiotics. *Medchemcomm* 8, 516–533. <https://doi.org/10.1039/c6md00585c>
- Sassine, J., Sousa, J., Lalk, M., Daniel, R.A., Vollmer, W., 2020. Cell morphology maintenance in *Bacillus subtilis* through balanced peptidoglycan synthesis and hydrolysis. *Sci. Rep.* 10, 17910. <https://doi.org/10.1038/s41598-020-74609-5>
- Sham, L.-T., Butler, E.K., Lebar, M.D., Kahne, D., Bernhardt, T.G., Ruiz, N., 2014. Bacterial cell wall. MurJ is the flippase of lipid-linked precursors for peptidoglycan biogenesis. *Science* 345, 220–222. <https://doi.org/10.1126/science.1254522>
- Shen, Y., Boulos, S., Sumrall, E., Gerber, B., Julian-Rodero, A., Eugster, M.R., Fieseler, L., Nyström, L., Ebert, M.-O., Loessner, M.J., 2017. Structural and functional diversity in *Listeria* cell wall teichoic acids. *J. Biol. Chem.* 292, 17832–17844. <https://doi.org/10.1074/jbc.M117.813964>
- Soldo, B., Lazarevic, V., Karamata, D., 2002. *tagO* is involved in the synthesis of all anionic cell-wall polymers in *Bacillus subtilis* 168. *Microbiology* 148, 2079–2087. <https://doi.org/10.1099/00221287-148-7-2079>
- Steudle, A., Pleiss, J., 2011. Modelling of lysozyme binding to a cation exchange surface at atomic detail: the role of flexibility. *Biophys. J.* 100, 3016–3024. <https://doi.org/10.1016/j.bpj.2011.05.024>
- Sun, L., Rogiers, G., Michiels, C.W., 2021. The natural antimicrobial *trans*-Cinnamaldehyde interferes with UDP-N-acetylglucosamine biosynthesis and cell wall homeostasis in *Listeria monocytogenes*. *Foods* 10, 1666. <https://doi.org/10.3390/foods10071666>
- Taguchi, A., Welsh, M.A., Marmont, L.S., Lee, W., Sjodt, M., Kruse, A.C., Kahne, D., Bernhardt, T.G., Walker, S., 2019. FtsW is a peptidoglycan polymerase that is functional only in complex with its cognate penicillin-binding protein. *Nat. Microbiol.* 4, 587–594. <https://doi.org/10.1038/s41564-018-0345-x>
- Takada, H., Shiwa, Y., Takino, Y., Osaka, N., Ueda, S., Watanabe, S., Chibazakura, T., Su’etsugu, M., Utsumi, R., Yoshikawa, H., 2018. Essentiality of WalRK for growth in *Bacillus subtilis* and its role during heat stress. *Microbiology* 164, 670–684. <https://doi.org/10.1099/mic.0.000625>
- Tesson, B., Dajkovic, A., Keary, R., Marlière, C., Dupont-Gillain, C.C., Carballido-López, R., 2022. Magnesium rescues the morphology of *Bacillus subtilis mreB* mutants through its inhibitory effect on peptidoglycan hydrolases. *Sci. Rep.* 12, 1137. <https://doi.org/10.1038/s41598-021-04294-5>
- Vadyvaloo, V., Arous, S., Gravesen, A., Héchard, Y., Chauhan-Haubrock, R., Hastings, J.W., Rautenbach, M., 2004. Cell-surface alterations in class IIa bacteriocin-resistant *Listeria*
-

-
- monocytogenes* strains. *Microbiology* 150, 3025–3033. <https://doi.org/10.1099/mic.0.27059-0>
- Van Heijenoort, Y., Derrien, M., Van Heijenoort, J., 1978. Polymerization by transglycosylation in the biosynthesis of the peptidoglycan of *Escherichia coli* K 12 and its inhibition by antibiotics. *FEBS Lett.* 89, 141–144. [https://doi.org/10.1016/0014-5793\(78\)80540-7](https://doi.org/10.1016/0014-5793(78)80540-7)
- Vigouroux, A., Cordier, B., Aristov, A., Alvarez, L., Özbaykal, G., Chaze, T., Oldewurtel, E.R., Matondo, M., Cava, F., Bikard, D., van Teeffelen, S., 2020. Class-A penicillin binding proteins do not contribute to cell shape but repair cell-wall defects. *Elife* 9, e51998. <https://doi.org/10.7554/eLife.51998>
- Vollmer, W., Joris, B., Charlier, P., Foster, S., 2008. Bacterial peptidoglycan (murein) hydrolases. *FEMS Microbiol. Rev.* 32, 259–286. <https://doi.org/10.1111/j.1574-6976.2007.00099.x>
- Wamp, S., Rothe, P., Stern, D., Holland, G., Döhling, J., Halbedel, S., 2022. MurA escape mutations uncouple peptidoglycan biosynthesis from PrkA signaling. *PLoS Pathog.* 18, e1010406. <https://doi.org/10.1371/journal.ppat.1010406>
- Wamp, S., Rutter, Z.J., Rismondo, J., Jennings, C.E., Möller, L., Lewis, R.J., Halbedel, S., 2020. PrkA controls peptidoglycan biosynthesis through the essential phosphorylation of ReoM. *Elife* 9, e56048. <https://doi.org/10.7554/eLife.56048>
- Watkinson, R.J., Hussey, H., Baddiley, J., 1971. Shared lipid phosphate carrier in the biosynthesis of teichoic acid and peptidoglycan. *Nat. New Biol.* 229, 57–59. <https://doi.org/10.1038/newbio229057a0>
- Wecke, J., Madela, K., Fischer, W., 1997. The absence of D-alanine from lipoteichoic acid and wall teichoic acid alters surface charge, enhances autolysis and increases susceptibility to methicillin in *Bacillus subtilis*. *Microbiology* 143, 2953–2960. <https://doi.org/10.1099/00221287-143-9-2953>
- Weidenmaier, C., Kristian, S.A., Peschel, A., 2003. Bacterial resistance to antimicrobial host defenses--an emerging target for novel anti-infective strategies? *Curr. Drug Targets* 4, 643–649. <https://doi.org/10.2174/1389450033490731>
- Yamaguchi, H., Furuhashi, K., Fukushima, T., Yamamoto, H., Sekiguchi, J., 2004. Characterization of a new *Bacillus subtilis* peptidoglycan hydrolase Gene, *yvcE* (named *cw/O*), and the enzymatic properties of its encoded protein. *J. Biosci. Bioeng.* 98, 174–181. <https://doi.org/10.1263/jbb.98.174>
-

Chapter 6 | QAC tolerance in *Listeria monocytogenes*

The results described in this chapter were originally published as a preprint in *bioRxiv*.

Adaptation mechanisms of *Listeria monocytogenes* to quaternary ammonium compounds

Lisa Maria Schulz¹, Fabienne Dreier², Lisa Marie de Sousa Miranda³, Jeanine Rismondo^{4*}

Department of General Microbiology, Institute of Microbiology and Genetics, GZMB, Georg-August University Göttingen, Grisebachstr. 8, 37077 Göttingen, Germany

Author contributions

LMS and JR conceived the study and designed the experiments. JR, LMS and LMdSM evolved suppressors in the EGD-e background. FD, LMS and JR constructed *fepA* and *SugE1/2* deletion strains and the respective complementation. FD constructed the *fepA SugE1/2* double deletion strain and the promoter-*lacZ* fusions. FD evolved suppressors in the $\Delta fepA$, $\Delta SugE1/2$ and $\Delta fepA \Delta SugE1/2$ deletion strains. LMS, JR, LMdSM and FD carried out the drop dilution assays. FD purified the *fepR* proteins. LMS and FD carried out the EMSA assays. LMS, FD and JR carried out the β -galactosidase assay. LMS carried out the EtBr accumulation assay. LMS and JR wrote the manuscript. All authors approve the manuscript. JR acquired funding. JR and LMS provided supervision.

Abstract

Listeria monocytogenes is ubiquitously found in nature and can easily enter food-processing facilities due to contaminations of raw materials. Several countermeasures are used to combat contamination of food products, for instance the use of disinfectants that contain quaternary ammonium compounds, such as benzalkonium chloride (BAC) and cetyltrimethylammonium bromide (CTAB). In this study, we assessed the potential of the commonly used wildtype strain EGD-e to adapt to BAC and CTAB under laboratory growth conditions. All BAC-tolerant suppressors exclusively carried mutations in *fepR* or its promoter region likely resulting in the overproduction of the efflux pump FepA. In contrast, CTAB-tolerance was associated with mutations in *sugR*, which regulates the expression of the efflux pumps SugE1 and SugE2. *L. monocytogenes* strains lacking either FepA or SugE1/2 could still acquire tolerance towards BAC and CTAB. Genomic analysis revealed that the overproduction of the remaining efflux system could compensate for the deleted one. Even in the absence of both efflux systems, tolerant strains could be isolated, which all carried mutations in the diacylglycerol kinase encoding gene *Imo1753* (*dgkB*). DgkB converts diacylglycerol to phosphatidic acid, which is subsequently re-used for the synthesis of phospholipids suggesting that alterations in membrane composition could be the third adaptation mechanism.

Originality-Significance Statement

Survival and proliferation of *Listeria monocytogenes* in the food industry is an ongoing concern, and while there are various countermeasures to combat contamination of food products, the pathogen still successfully manages to withstand the harsh conditions present in food-processing facilities, resulting in reoccurring outbreaks, subsequent infection, and disease. To counteract the spread of *L. monocytogenes* it is crucial to understand and elucidate the underlying mechanism that permit their successful evasion. We here present various adaptation mechanisms of *L. monocytogenes* to withstand two important quaternary ammonium compounds.

Introduction

Listeria monocytogenes is one of the most successful foodborne pathogens worldwide. In high-risk groups such as immunocompromised individuals, the elderly, or pregnant women, an infection can cause invasive listeriosis, resulting in a hospitalization rate of ~95% and a fatality rate of ~13% (Allerberger and Wagner 2010; EFSA and ECDC 13/12/2022). Due to its ability to persist in a wide range of environmental stresses found in the food-processing industry, infection of *L. monocytogenes* is often associated with ingestion of contaminated ready-to-eat foods, such as ice cream (Rietberg et al. 2016), cheese (Carlin et al. 2022), or processed meat (Thomas et al. 2020). The pathogen does not only pose a threat due to its ability to withstand common stresses such as extreme temperatures, pH, or high salt concentrations (up to 20%), but also due to its potential to adapt to biocides that are commonly found in disinfectants or sanitizers used in food-processing plants (Osek et al. 2022). The most frequently used antimicrobial components in disinfectants are a mixture of quaternary ammonium compounds (QACs) that are characterized by its ammonium ion linked to either an alkyl or aryl group. The chain length of QACs determines the antimicrobial potency, hence, a length of C14 or C16 are ideally used against gram-positive and gram-negative bacteria, respectively (Zinchenko et al. 2004). *L. monocytogenes* strains with decreased sensitivity to QACs have been isolated from different locations around the world (Aase et al. 2000; Romanova et al. 2006; Romanova et al. 2002; Soumet et al. 2005; Meier et al. 2017; Lundén et al. 2003; To et al. 2002). This adaptation frequently resulted in cross-adaptation to other disinfectants and antimicrobial agents such as gentamycin, kanamycin or ciprofloxacin (Lundén et al. 2003; Romanova et al. 2006; Guérin et al. 2021; Aase et al. 2000; Guérin et al. 2014; Rakic-Martinez et al. 2011; Bland et al. 2022), emphasising the importance of elucidating the underlying genetic basis. Two of the most extensively used QACs are benzalkonium chloride (BAC) and cetyltrimethylammonium bromide (CTAB) (Jiang et al. 2016; Martínez-Suárez et al. 2016). While a variety of different mechanisms have been linked to increased tolerance towards BAC in isolated *L. monocytogenes* strains, as far as we know, no previous research has investigated the underlying genetics of CTAB tolerance, which is often merely mentioned in association with cross-adaptation towards BAC (Jiang et al. 2020; Müller et al. 2013; Müller et al. 2014).

Several factors have been identified in *L. monocytogenes* strains isolated from food-processing facilities that are associated with the presence or overexpression of efflux systems that aid in extruding the toxic compounds from the intracellular space. Determinants for BAC tolerance are often found on genetic elements, and include genes encoding efflux pumps such as *qacH*, located on the transposon Tn6188 (Müller et al. 2013; Müller et al. 2014), *emrE*, located on the genomic island LGI1

(Kovacevic et al. 2016), or *bcrABC*, which encodes the TetR-family transcriptional regulator BcrA and two small multidrug resistance (SMR) efflux pumps, BcrB and BcrC (Elhanafi et al. 2010; Dutta et al. 2013; Minarovičová et al. 2018). The *sugRE1E2* operon (short: *sug* operon) was analysed as a chromosomal counterpart of *bcrABC* in the laboratory wildtype strain EGD-e and was correspondingly found to be important for tolerance towards QACs such as BAC and CTAB. The genes of the *sug* operon code for the TetR-family regulator SugR and the two SMR efflux pumps SugE1 and SugE2. The self-repressor SugR negatively regulates the operon in the absence of BAC and accordingly, both SugE1 and SugE2 showed increased expression in the presence of the QAC (Jiang et al. 2020). In addition, several studies showed increased expression of the major facilitator superfamily transporter MdrL in isolated, as well as, BAC-adapted *L. monocytogenes* strains, suggesting a direct contribution of this transporter to BAC tolerance (Yu et al. 2018; Romanova et al. 2006). However, a clean deletion of the transporter in EGD-e only resulted in a growth defect in the presence of BAC, but no change in the minimal inhibitory concentration (MIC). Additionally, its role in export of cefotaxime and EtBr that was previously described, could not be confirmed for the laboratory model strain (Mata et al. 2000; Jiang et al. 2019b). It has to be mentioned that the tolerance in isolated or adapted *L. monocytogenes* strains was often transient and lost after passaging the strains in the absence of QAC stress. In contrast, the chromosomally encoded multidrug and toxic compound (MATE) efflux pump FepA was recently identified as the dominant, stable mode of tolerance for BAC in a screen of over 60 serial adapted produce-associated *L. monocytogenes* and other *Listeria* spp. strains (Bolten et al. 2022). An independent study of biocide-adapted strains further supported these findings by showing that 94% of the adapted strains possessed mutations in the gene coding for the TetR-like transcriptional regulator FepR that was previously shown to repress its own expression and the expression of the efflux pump encoding gene *fepA* (Douarre et al. 2022). The identified mutations in *fepR* were thus proposed to increase expression of FepA, resulting in enhanced tolerance towards BAC, as well as norfloxacin and ciprofloxacin (Guérin et al. 2014).

Here we show that the laboratory wildtype strain EGD-e readily acquires stable mutations in the transcriptional regulator *fepR* and that the successional overexpression of the efflux pump FepA is responsible for the increased tolerance towards BAC, CTAB, ciprofloxacin and gentamycin. We further successfully evolved suppressors in presence of CTAB which exclusively carried mutations in the TetR-like transcriptional regulator *sugR* resulting in the overexpression of the SMR efflux pumps SugE1 and SugE2. *L. monocytogenes* strains lacking either *fepA* or *sugE1/2* could still acquire tolerance towards CTAB and BAC by overexpressing the remaining efflux system. In addition, we could further evolve

BAC- and CTAB-tolerant strains in the absence of the two major QAC efflux systems, which acquired mutations in a putative diacylglycerol kinase.

Materials and Methods

Bacterial strains and growth conditions. All strains and plasmids used in this study are listed in Table S1. *Escherichia coli* strains were grown in lysogeny broth (LB) medium and *L. monocytogenes* strains in brain heart infusion (BHI) medium at 37°C unless otherwise stated. If appropriate, antibiotics and supplements were added to the medium at the following concentrations: for *E. coli* cultures ampicillin (Amp) at 100 µg ml⁻¹, kanamycin (Kan) at 50 µg ml⁻¹, and for *L. monocytogenes* strains, chloramphenicol (Cam) at 7.5 µg ml⁻¹, Kan at 50 µg ml⁻¹, erythromycin (Erm) at 5 µg ml⁻¹ and IPTG at 1 mM.

Strain and plasmid construction. All primers used in this study are listed in Table S2. For the markerless in-frame deletion of *fepA* (*Imo2087*) and *sugE1/2* (*Imo0853-Imo0854*), approximately 1-kb DNA fragments up- and downstream of the *fepA* gene were amplified by PCR using the primer pairs LMS484/LMS485 and LMS486/LMS487 (*fepA*) and JR247/JR248 and JR249/JR250 (*sugE1/2*). The resulting PCR products were fused in a second PCR using primers LMS485/LMS487 (*fepA*) and JR247/JR250 (*sugE1/2*). The products were cut with *KpnI* and *Sall* and ligated into pKSV7 that had been cut with the same enzymes. The resulting plasmids pKSV7- Δ *fepA* and pKSV7- Δ *sugE1/2* were recovered in *E. coli* XL1-Blue, yielding strains EJR230 and EJR229, respectively. Plasmids pKSV7- Δ *fepA* and pKSV7- Δ *sugE1/2* were transformed into *L. monocytogenes* EGD-e and the genes deleted by allelic exchange according to a previously published method (Camilli et al. 1993) yielding strains EGD-e Δ *fepA* (LJR261) and EGD-e Δ *sugE1/2* (LJR262), respectively. For the construction of the Δ *fepA* Δ *sugE1/2* double deletion strain, plasmid pKSV7- Δ *sugE1/2* was transformed into EGD-e Δ *fepA* and *sugE1/2* was deleted by allelic exchange, resulting in strain LJR329. For the construction of pIMK3-*fepA* and pIMK3-*sugE1/2*, the *fepA* and *sugE1/2* genes were amplified using the primer pairs LMS478/LMS479 and JR262/JR263, respectively. Fragments were cut with enzymes *NcoI* and *Sall* and ligated into plasmid pIMK3 that had been cut with the same enzymes. The resulting plasmids pIMK3-*fepA* and pIMK3-*sugE1/2* were recovered in *E. coli* XL10-Gold yielding strains EJR227 and EJR259, respectively. Both plasmids were transformed into *L. monocytogenes* strain EGD-e, resulting in the construction of strains LJR231 and LJR301, respectively, in which the expression of *fepA* and *sugE1/2* is under the control of an IPTG-inducible promoter. For the construction of a *fepA* complementation strain, plasmid pIMK3-*fepA* was transformed into EGD-e Δ *fepA* yielding strain LJR265.

For the construction of pWH844-*fepA*, the *fepA* gene was amplified with primer pairs FD1/FD2 using EGD-e wild type DNA or the DNA of suppressor strain LJR218 as template. The PCR fragments were digested with *Bam*HI and *Sal*I and ligated into pWH844 that had been cut with the same enzymes. The resulting plasmids pWH844-*fepR*^{WT} and pWH844-*fepR*^{L24F} were recovered in XL10-Gold, yielding strains EJR242 and EJR248, respectively.

For the construction of promoter *lacZ* fusions, the promoter region of *fepR* was amplified with primers FD5 and FD6 using genomic DNA of the *L. monocytogenes* wildtype strain EGD-e or the BAC-tolerant strains EGD-e *P*_{*fepR*}^{G-27T} (LJR188) or EGD-e *P*_{*fepR*}^{A-33G} (LJR215) as template DNA. The PCR fragments were digested with *Bam*HI and *Sal*I and ligated into plasmid pPL3e-*lacZ*, which contains the promoter-less *lacZ* gene. The resulting plasmids pPL3e-*P*_{*fepR*}-*lacZ*, pPL3e-*P*_{*fepR*}^{G-27T}-*lacZ* and pPL3e-*P*_{*fepR*}^{A-33G}-*lacZ* were recovered in *E. coli* DH5 α yielding strains EJR257, EJR258 and EJR260, respectively. Plasmids pPL3e-*P*_{*fepR*}-*lacZ*, pPL3e-*P*_{*fepR*}^{G-27T}-*lacZ* and pPL3e-*P*_{*fepR*}^{A-33G}-*lacZ* were subsequently transformed into EGD-e yielding strains EGD-e pPL3e-*P*_{*fepR*}-*lacZ* (LJR336), EGD-e pPL3e-*P*_{*fepR*}^{G-27T}-*lacZ* (LJR302) and EGD-e pPL3e-*P*_{*fepR*}^{A-33G}-*lacZ* (LJR303).

Generation of suppressors and whole genome sequencing. For the generation of BAC-adapted suppressors, stationary or exponentially grown EGD-e cultures were selected on BHI plates containing 4 $\mu\text{g ml}^{-1}$ or 6 $\mu\text{g ml}^{-1}$ BAC. For the stationary grown EGD-e cultures, overnight cultures were adjusted to an OD₆₀₀ of 0.1 and 100 μl were plated on BHI plates containing 4 $\mu\text{g ml}^{-1}$ BAC. For exponentially grown cultures, overnight cultures of EGD-e were adjusted to an OD₆₀₀ of 0.1 and grown until they reached an OD₆₀₀ of 0.3-0.5. Cultures were then adjusted to an OD₆₀₀ of 0.1 and 100 μl were plated on BHI plates containing 4 $\mu\text{g ml}^{-1}$ and 6 $\mu\text{g ml}^{-1}$ BAC. The plates were incubated at 37°C overnight and single colonies were re-streaked twice on 4 $\mu\text{g ml}^{-1}$ and 6 $\mu\text{g ml}^{-1}$ BAC, respectively. For adaptation of the wildtype strain to CTAB, as well as EGD-e Δ *fepA*, EGD-e Δ *sugE1/2* and EGD-e Δ *fepA* Δ *sugE1/2* to BAC and CTAB, overnight cultures of the different strains were adjusted to an OD₆₀₀ of 0.1 and grown to an OD₆₀₀ of 0.3-0.5. Cultures were adjusted again to an OD₆₀₀ of 0.1 and 100 μl were plated on BHI plates supplemented with 4 $\mu\text{g ml}^{-1}$, 5 $\mu\text{g ml}^{-1}$ or 6 $\mu\text{g ml}^{-1}$ BAC and 2 $\mu\text{g ml}^{-1}$ or 4 $\mu\text{g ml}^{-1}$ CTAB. Plates were incubated at 37°C overnight or in the case of EGD-e Δ *fepA* and EGD-e Δ *fepA* Δ *sugE1/2* in presence of BAC for 2 days. Again, single colonies were re-streaked twice on BHI plates supplemented with the selective pressure they were originally isolated from. Genomic DNA of a selection of BAC- and CTAB-adapted strains was isolated and either pre-screened for mutations in *fepR* or *sugR*, or send to SeqCoast Genomics (Portsmouth, NH, United States) for whole genome sequencing (WGS). The

genome sequences were determined by short read sequencing (150-bp paired end) using an Illumina MiSeq system (San Diego, CA, United States). The reads were trimmed and mapped to the *L. monocytogenes* EGD-e reference genome (NC_003210) using the Geneious prime[®] v.2021.0.1 (Biomatters Ltd., New Zealand). Single nucleotide polymorphisms (SNPs) with a variant frequency of at least 90% and a coverage of more than 25 reads were considered as mutations. All identified mutations were verified by PCR amplification and Sanger sequencing.

Drop dilution assay. Overnight cultures of the indicated *L. monocytogenes* strains were adjusted to an OD₆₀₀ of 1. IPTG and Kan were supplemented to the overnight cultures of strains carrying pIMK3-plasmids. 5 µl of serial dilutions of each culture were spotted on BHI agar plates, BHI agar plates containing 4 µg ml⁻¹ BAC, 6 µg ml⁻¹ BAC, 2 µg ml⁻¹ CTAB, 4 µg ml⁻¹ CTAB, 1 µg ml⁻¹ ciprofloxacin, 0.5 µg ml⁻¹ gentamycin, or 1 µg ml⁻¹ cefuroxime. Where indicated, plates were supplemented with 1 mM IPTG. Images of plates were taken after 20-24 h of incubation at 37°C. Drop dilution assays were repeated at least three times.

Ethidium bromide assay. The ethidium bromide assay was performed as previously described with minor modifications (Kaval et al. 2015). Briefly, overnight cultures of the indicated *L. monocytogenes* strains were diluted to an OD₆₀₀ of 0.05 in fresh BHI medium and grown until an OD₆₀₀ of 0.4-0.6. Cells of 2 ml were harvested by centrifugation at 1,200 x g for 5 min, washed once in 1 ml PBS buffer (pH 7.4) and finally re-suspended in 1 ml PBS buffer (pH 7.4). Next, the OD₆₀₀ of each sample was adjusted to 0.3 in PBS (pH 7.4) and 180 µl transferred into the wells of a black 96-well plate. 20 µl of 50 µg ml⁻¹ ethidium bromide was added to each well and the absorbance was measured using the Synergy[™] Mx microplate reader (BioTek) at 500 nm excitation and 580 nm emission wavelengths for 50 min.

Expression and purification of His-FepR. For the overexpression of His-FepR and His-FepR^{L24F}, plasmids pWH844-*fepR* and pWH844-*fepR*^{L24F} were transformed into *E. coli* strain BL21 and the resulting strains grown in LB broth supplemented with Amp at 37°C. At an OD₆₀₀ of 0.6-0.8, the expression of *his-fepR* and *his-fepR*^{L24F} was induced by the addition of 1 mM IPTG and the strains were grown for another 2 h at 37°C. Cells were collected by centrifugation at 11,325 x g for 10 min, washed once with 1x ZAP buffer (50 mM Tris-HCl, pH 7.5, 200 mM NaCl) and the cell pellet stored at -20°C until further use. The cell pellets were re-suspended in 1x ZAP buffer and cells passaged three times (18,000 lb/in²) through an HTU DIGI-F press (G. Heinemann, Germany). The cell debris was

subsequently collected by centrifugation at 46,400 x g for 30 min. The supernatant was subjected to a Ni²⁺ nitrilotriacetic acid column (IBA, Göttingen, Germany) and His-FepA and His-FepA^{L24F} were eluted using an imidazole gradient. Elution fractions were analysed by SDS-PAGE and selected fractions subsequently dialysed against 1x ZAP buffer with a spatula pinch of EDTA at 4°C overnight. Protein concentrations were determined by a Bradford protein assay (Bradford 1976) using the Bio-Rad protein assay dye reagent concentrate. Bovine serum albumin was used for a standard curve. The protein samples were stored at 4°C until further use. Two independent purifications were performed for each protein.

Electrophoretic mobility shift assay (EMSA). EMSAs were performed as described elsewhere with minor modifications (Dhiman et al. 2014). Briefly, a 150 bp-DNA fragment containing the *fepR* promoter was amplified using primers FD3 and FD4 from genomic DNA isolated from the wildtype strain EGD-e or EGD-e *P_{fepR}^{G-27T}* (LJR188) and EGD-e *P_{fepR}^{A-33G}* (LJR215). For the comparison of the binding abilities of His-FepR and His-FepR^{L24F} to the *fepR* promoter, 25, 50 and 100 pmol of each protein were mixed with 250 pmol *fepR* promoter DNA. To compare the binding ability of His-FepR to the wildtype and the mutated *fepR* promoters, 25, 50 and 100 pmol of His-FepR were mixed with 250 pmol DNA of either the wildtype or the mutated *fepR* promoters. Apart from DNA and protein, 20 µl binding reactions contained 1 µl of DNA loading dye (50% glycerol, 0.1% bromophenol blue, 1x TAE, H₂O), 50 mM NaCl, 2 µl 10x Tris-acetate buffer (250 mM Tris-base in H₂O, set to pH 5.5 with acetic acid), 0.15 mM bovine serum albumin, 2.5 mM EDTA, 10% glycerol and 20 mM DTT. The samples were incubated for 5 min at 25°C and subsequently separated on 8% native Tris-acetate gels (6% polyacrylic acid, 1x Tris-acetate buffer, 0.15% ammonium persulfate, 0.83% tetramethylethylenediamine) in 0.5x TBE-buffer (0.5 M Tris base, 0.5 M boric acid, 1 mM Na₂EDTA, pH 10). A pre-run of the gels was performed for 90 min at 50 V before the samples were loaded. The run was performed at 50 V for 2.5 h. The gels were stained in 50 ml 0.5x TBE-buffer containing 5 µl HDGreenTM Plus DNA dye (INTAS, Göttingen, Germany) for 5 min and washed for 5 min with 0.5x TBE-buffer, rinsed three times with water and then washed with water for 30 min. The DNA bands were visualized using a Gel DocTM XR+ (Bio Rad, Munich, Germany).

β-galactosidase assays. For the comparison of the activity of the wildtype and mutated *fepR* promoters, overnight cultures (supplemented with Erm) of the indicated *L. monocytogenes* strains were diluted to an OD₆₀₀ of 0.05 in BHI medium and grown for 5 h at 37°C. To determine the response

of the *fepR* promoter to BAC, overnight cultures of EGD-e *P_{fepR}-lacZ* were diluted to an OD₆₀₀ of 0.05 in BHI medium and grown at 37°C to an OD₆₀₀ of 0.5 (± 0.05). The culture was divided into two flasks and incubated for an additional 2 h at 37°C in the presence of 2.5 µg ml⁻¹ BAC or in the absence of BAC. The final OD₆₀₀ was measured for all cultures prior sample collection. For both assays, 1 ml of the corresponding cultures were collected, re-suspended in 100 µl ABT buffer (60 mM K₂HPO₄, 40 mM KH₂PO₄, 100 mM NaCl, 0.1% Triton X-100; pH 7), snap-frozen in liquid nitrogen and stored at -80°C until further use. The sample preparation was performed as described previously (Gründling et al. 2004; Rismondo et al. 2019). Briefly, samples were thawed, and 10-fold dilutions were prepared in ABT buffer. 50 µl of each dilution were mixed with 10 µl of 0.4 mg ml⁻¹ 4-methyl-umbelliferyl-β-D-galactopyranoside (MUG) substrate (Merck, Darmstadt, Germany) that was prepared in dimethyl sulfoxide (DMSO) and incubated for 60 min at room temperature in the dark. A reaction containing ABT buffer and the MUG substrate was used as negative control. After the incubation time, 20 µl of each reaction were transferred into the wells of a black 96-well plate containing 180 µl ABT buffer and fluorescence values were determined using Synergy™ Mx microplate reader (BioTek) at 366 nm excitation and 445 nm emission wavelengths. A standard curve was obtained using 0.015625 µM to 4 µM of the fluorescent 4-methylumbelliferone (MU) standard. β-galactosidase units, or MUG units, were calculated as (pmol of substrate hydrolysed x dilution factor)/(culture volume in ml x OD₆₀₀ x reaction time in minutes). The amount of hydrolysed substrate was determined from the standard curve as (emission reading – y intercept)/slope.

Results

Isolation of BAC-tolerant *L. monocytogenes* strains

The *L. monocytogenes* wildtype strain EGD-e was propagated on BHI agar plates supplemented with BAC to obtain genetically adapted strains. The wildtype strain could still grow in presence of 2 µg ml⁻¹ BAC but was unable to grow on BHI agar plates containing higher BAC concentrations. However, single colonies appeared on plates containing 4 and 6 µg ml⁻¹ BAC after 24 h, which likely acquired mutations to cope with the BAC stress. Since previous studies revealed that BAC-adapted *L. monocytogenes* isolates frequently mutate *fepR*, encoding the transcriptional regulator FepR, we first amplified the *fepR* gene and the *fepR* promoter region and analysed the sequence using Sanger sequencing. Indeed, all adapted strains acquired mutations in *fepR* or its promoter region (Fig. 1). The transcriptional regulator FepR possesses a helix-turn-helix (HTH) domain between residues 23 and 42, which is required for DNA binding. In addition, a putative substrate binding pocket was predicted to

be located in the vicinity of residues 60, 100, 101, 104, 105, 119, 123, 126, 156, 159, 160 and 163 (Douarre et al. 2022). We identified seven BAC-tolerant strains with point mutations, amino acid insertions or deletions in the DNA binding site (S23L, L24F, INS29DIA, Δ 45-46) and two with mutations or amino acid deletions in the putative substrate binding site (V115D, Δ 99). Nine BAC-tolerant strains had mutations leading to a frameshift or the production of a truncated FepR protein (M126fs, W137fs, N170fs, Q140*, Y155*, G157*). We additionally isolated two suppressors that had base exchanges in the promoter region of the *fepRA* operon (G-27T and A-33G). All these mutations likely result in a reduced binding activity of the regulator or a decreased or abolished activity of FepR.

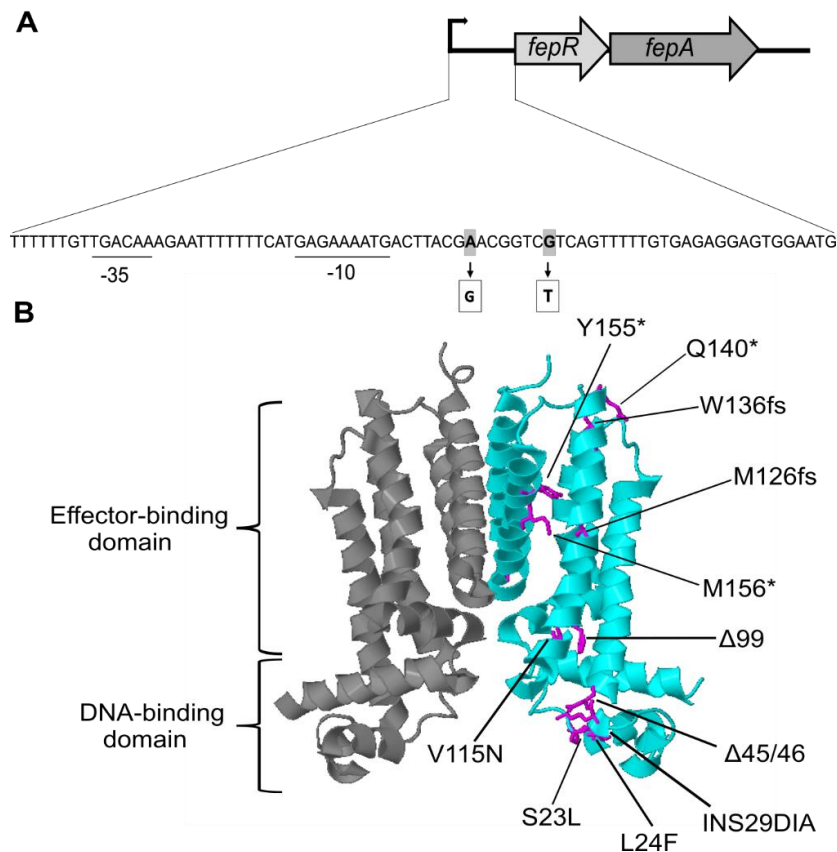


Figure 1 | Mutations in the transcriptional regulator encoding gene *fepR*. **A** Genetic organization of the *fepRA* operon in *L. monocytogenes* EGD-e. The *fepRA* operon is composed of genes coding for the transcriptional regulator FepR and the MATE efflux pump FepA. The predicted promoter region is displayed along with the -10 and -35 regions (underlined). The base exchanges of the two suppressors in the *fepR* promoter are shown in grey. **B** The dimeric protein structure of the transcriptional regulator FepR (PDB: 5ZTC) was modified using Geneious Prime® v.2021.0.1. Single monomers are depicted in dark grey and cyan. Mutated amino acids are shown in magenta. Mutations leading to a stop codon are indicated with an asterisk and frameshift mutations are abbreviated with an fs. Amino acid insertions are indicated by INS and deletion by the Δ symbol.

For further analysis, we focussed on the BAC-tolerant strains EGD-e *fepR*^{Q140*}, EGD-e *fepR*^{V115D} and EGD-e *fepR*^{L24F}. The TetR-family transcriptional regulator FepR represses the expression of the MATE family efflux pump FepA (Guérin et al. 2014). Hence, loss of function of the regulator subsequently leads to enhanced *fepA* expression. To verify that overproduction of FepA results in increased tolerance towards BAC, the IPTG-inducible plasmid pIMK3-*fepA* was constructed and introduced into the wildtype strain (*fepR*⁺). In addition, a *fepA* deletion strain (Δ *fepA*) was constructed to determine its tolerance towards BAC. Indeed, drop dilution assays revealed that while the deletion of *fepA* led to slightly increased susceptibility towards BAC, overexpression of the transporter led to a significant increase in BAC tolerance, similar to that of the three selected *fepR* mutant strains (Fig. 2).

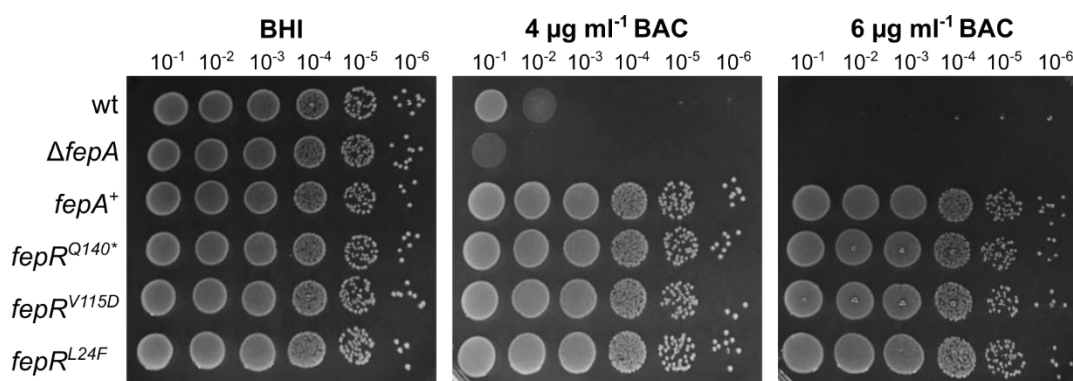


Figure 2 | Increased BAC-tolerance of *fepR* suppressors Drop dilution assays of *L. monocytogenes* strains EGD-e (wt), the *fepA* deletion strain LJR261 (Δ *fepA*), a wt strain containing the IPTG-inducible pIMK3-*fepA* plasmid LJR265 (*fepA*⁺), and the suppressor mutants LJR208 (*fepR*^{Q140*}), LJR211 (*fepR*^{V115D}) and LJR218 (*fepR*^{L24F}). Cells were propagated on BHI plates or BHI plates containing 4 and 6 $\mu\text{g ml}^{-1}$ BAC and plates incubated overnight at 37°C. Plates were supplemented with 1 mM IPTG to induce expression of FepA in the *fepA*⁺ strain. A representative image of at least three biological replicates is shown.

Mutations in FepR alter DNA binding

According to structure predictions, the HTH motif of FepR, which is required for the interaction with DNA, is located between residues 23 and 42. Hence, we assumed that the mutation L24F has a negative effect on DNA binding by FepR. EMSA assays were performed to assess if DNA binding of FepR^{L24F} to the promoter region of the *fepRA* operon is altered. Indeed, in the concentration range used, no DNA-protein complexes could be detected for FepR^{L24F} in comparison to FepR^{wt} (Fig. 3A), indicating that the mutation L24F decreased DNA binding affinity of FepR. Binding of the two proteins to an unspecific DNA sequence from within the operon was not observed (Fig. 3A). We then tested the binding affinity of FepR^{wt} to the mutated promoter regions of the *fepRA* operon of the BAC-tolerant strains EGD-e *P*_{*fepR*}^{G-27T} and EGD-e *P*_{*fepR*}^{A-33G}. The base exchange from G to T 27 bp upstream of the start codon completely abolished binding of FepR^{wt} at the tested protein concentrations (Fig. 3B).

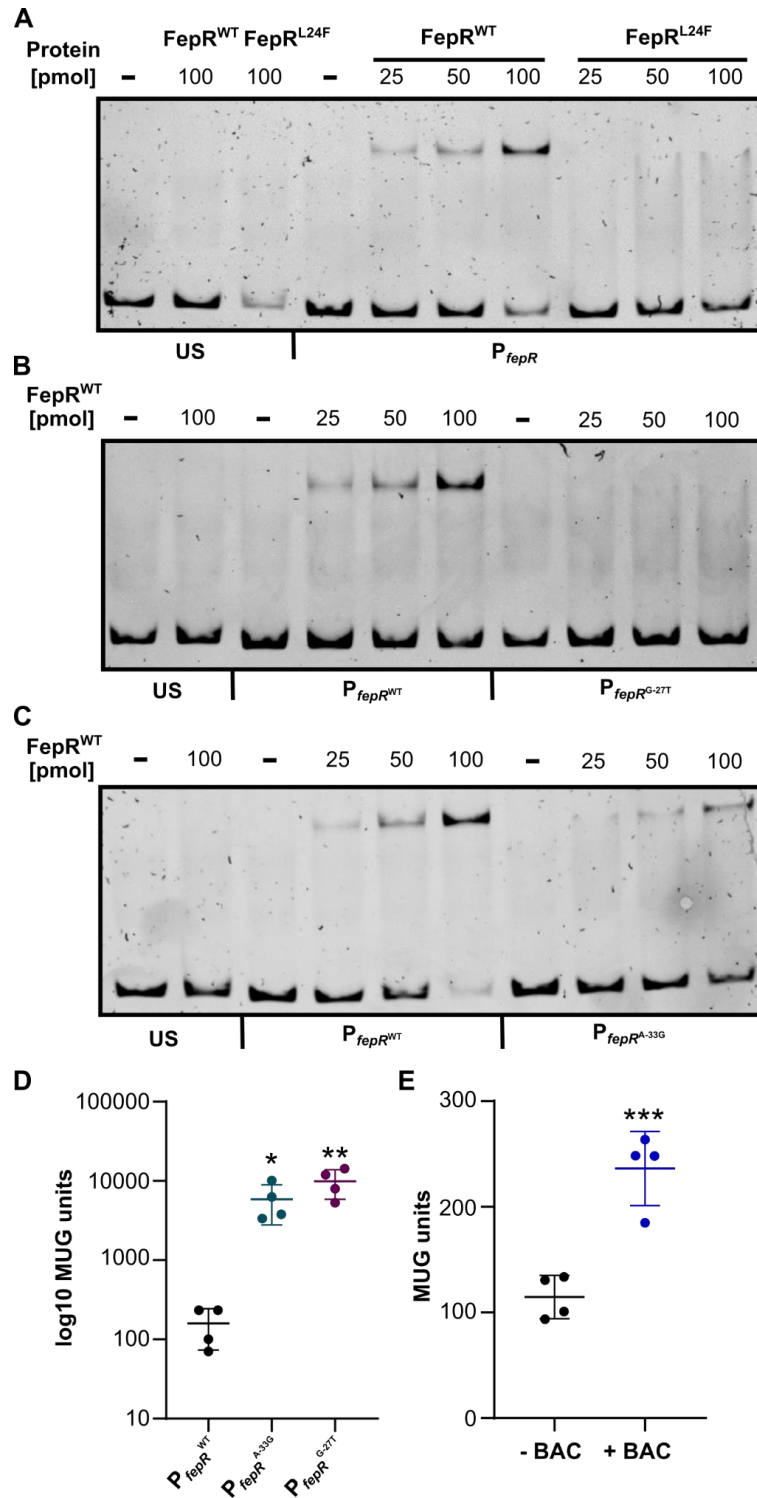


Figure 3 | Interaction of FepR with the *fepRA* promoter and *P_{fepR}* promoter activity **A** Increasing concentrations of recombinant His-FepR^{wt} (lane 5-7) or His-FepR^{L24F} (lane 8-10) were incubated with a 150-bp fragment containing the promoter of the *fepRA* operon. **B** Increasing concentrations of FepR^{wt} were incubated with either the wildtype promoter region (*P_{fepR}^{wt}*) or the promoter region with a base exchange from G to T 27 bp upstream of the ATG (*P_{fepR}^{G-27T}*). **C** Incubation of FepR^{wt} with either *P_{fepR}^{wt}* or the promoter region with a base exchange from A to G 33 bp upstream of the ATG (*P_{fepR}^{A-33G}*). A short DNA sequence amplified from within the operon was

incubated with 100 pmol FepR^{wt} or FepR^{L24F} and was included on each gel to exclude unspecific binding of the two proteins (US). Reactions without protein were used as an additional control (-). **D-E** Promoter activity assays. **D** EGD-e pPL3e-*P_{fepR}^{wt}-lacZ*, EGD-e pPL3e-*P_{fepR}^{A-33G}-lacZ* and EGD-e pPL3e-*P_{fepR}^{G-27T}-lacZ* were grown for 5 h in BHI medium and the promoter activity determined by β -galactosidase activity assays as described in the materials and methods section. Log10 of the MUG units are plotted to visualize the values obtained for EGD-e pPL3e-*P_{fepR}^{wt}-lacZ*. **E** Bacteria from a mid-logarithmic culture of strain EGD-e pPL3e-*P_{fepR}^{wt}-lacZ* were grown for 2 h in the presence or absence of 2.5 $\mu\text{g ml}^{-1}$ BAC. The *P_{fepR}* promoter activity was determined by β -galactosidase activity assays as described in the materials and methods section. For statistical analysis, one-way ANOVA coupled with Dunnett's multiple comparison test was performed (* $p \leq 0.05$; ** $p \leq 0.01$; *** $p \leq 0.001$).

Likewise, decreased binding affinity of FepR^{wt} was observed, when the promoter region contained an A to G substitution 33 bp before the start codon, but to a lesser extent than the G-27T promoter mutation (Fig. 3C). We further compared the promoter activity of the wildtype and mutated *fepR* promoters and determined their response to subinhibitory concentrations of BAC using β -galactosidase activity assays. Both *P_{fepR}^{G-27T}* and *P_{fepR}^{A-33G}* showed significantly increased promoter activity in comparison to the wildtype promoter (Fig. 3D). *P_{fepR}^{G-27T}* hereby showed a higher activity than *P_{fepR}^{A-33G}*, which is in accordance with the difference in FepR binding capability (Fig. 3B-D). Increased β -galactosidase activity could be measured, when EGD-e *P_{fepR}-lacZ* was grown in the presence of BAC (Fig. 3E), indicating that the expression of *fepRA* is slightly induced in response to BAC.

Ethidium bromide is a substrate for the efflux pump FepA

Previous work has shown that the deletion of *fepR* resulted in an increased ethidium bromide (EtBr) resistance (Guérin et al. 2014). To assess, whether this resistance can be explained by the overproduction of FepA, an EtBr accumulation assay was performed with the wildtype, $\Delta fepA$, *fepA*⁺, the EGD-e *fepR*^{Q140*} suppressor mutant and a $\Delta fepA$ complementation strain ($C\Delta fepA$). This assay revealed that a strain lacking the efflux pump FepA accumulated more EtBr as the wildtype strain (Fig. 4). In contrast, the more gradual slope of the EGD-e *fepR*^{Q140*} suppressor indicates slightly reduced accumulation. Similarly, a significantly reduced accumulation of EtBr was observed for the $\Delta fepA$ complementation strain and the *fepA* overexpression strain (*fepA*⁺) (Fig. 4), suggesting that FepA is able to export EtBr.

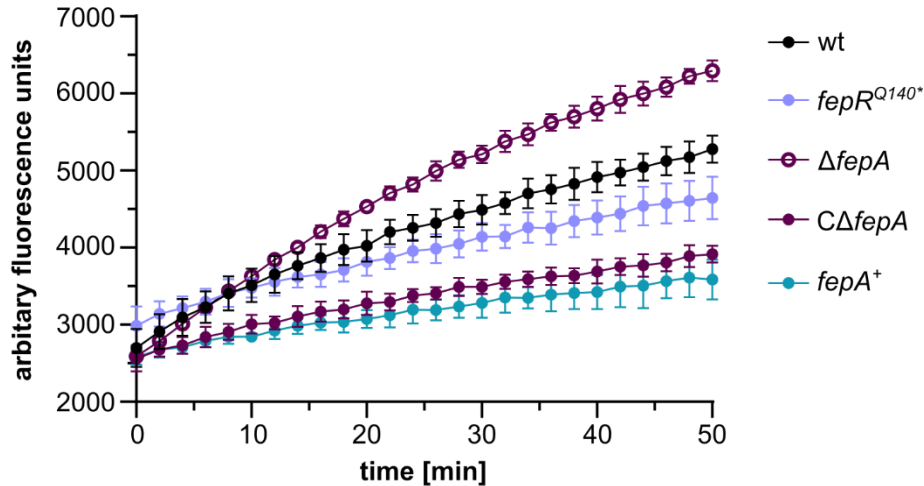


Figure 4 | EtBr accumulation assay Accumulation of ethidium bromide (EtBr) by *L. monocytogenes* EGD-e (wt), the *fepR*^{Q140*} suppressor strain (LJR208), a Δ *fepA* mutant strain (LJR261), a Δ *fepA* complementation strain (C Δ *fepA*) and a *fepA* overexpression strain (*fepA*⁺) was measured at an excitation wavelength of 500 nm and an emission wavelength of 580 nm for 50 min. The average values and standard deviations of three independent experiments are depicted.

FepA contributes to cross-resistance and tolerance towards CTAB

The MATE efflux pump FepA has been previously associated with fluoroquinolone resistance. We thus wondered whether the BAC-tolerant strains are also more tolerant towards other antimicrobials such as the fluoroquinolone antibiotic ciprofloxacin, the aminoglycoside gentamycin, the cephalosporin cefuroxime or the surfactant CTAB. Indeed, growth experiments revealed that the mutations in *fepR*, and hence overexpression of FepA, additionally conferred resistance towards ciprofloxacin, gentamycin and increased tolerance towards CTAB (Fig. 5), but not towards cefuroxime (data not shown). Similar results were obtained for the *fepA*⁺ strain, which artificially overproduces FepA (Fig. 5). Interestingly, we observed suppressor formation in the wildtype strain on plates containing CTAB, which hasn't been described so far.

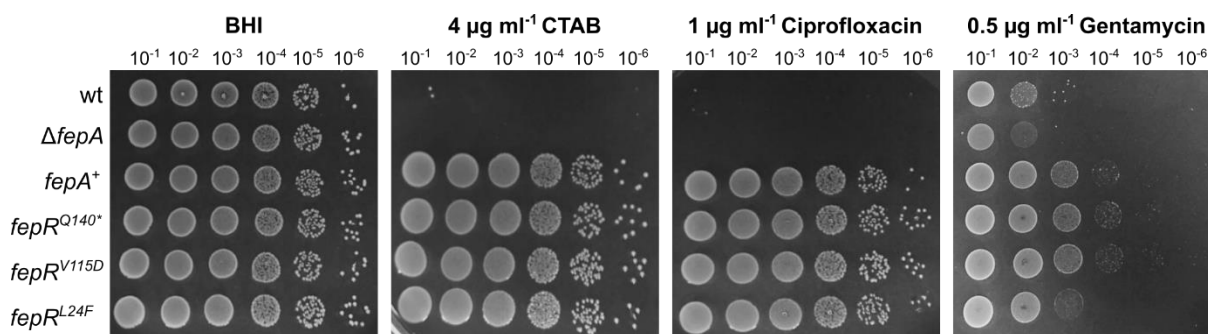


Figure 5 | Cross-resistance of *fepR* mutant strains Drop dilution assays of *L. monocytogenes* strains EGD-e (wt), the *fepA* deletion strain LJR261 ($\Delta fepA$), a wt strain containing the IPTG-inducible pIMK3-*fepA* plasmid LJR265 (*fepA*⁺), and the suppressor mutants LJR208 (*fepR*^{Q140*}), LJR211 (*fepR*^{V115D}), and LJR218 (*fepR*^{L24F}). Cells were propagated on BHI plates or BHI plates containing 4 $\mu\text{g ml}^{-1}$ CTAB, 1 $\mu\text{g ml}^{-1}$ ciprofloxacin or 0.5 $\mu\text{g ml}^{-1}$ gentamycin. All plates were supplemented with 1 mM IPTG to induce expression of *fepA* in the *fepA*⁺ strain. Plates were incubated overnight at 37°C. A representative image of at least three biological replicates is shown.

Mutations in *sugR* confer resistance towards CTAB

For the isolation of CTAB-tolerant *L. monocytogenes* strains, the wildtype strain EGD-e was propagated onto BHI plates containing varying CTAB concentrations. Growth of the wildtype was diminished at concentrations above 1 $\mu\text{g ml}^{-1}$ CTAB and CTAB-tolerant strains were isolated in the presence of 2 and 4 $\mu\text{g ml}^{-1}$ of CTAB. The genome sequence of 2 and 7 of the CTAB-tolerant strains isolated from 2 and 4 $\mu\text{g ml}^{-1}$, respectively, were determined by whole genome sequencing to identify the underlying mutations. All of these strains carried mutations in the coding or promoter region of *sugR*, encoding a TetR-family transcriptional regulator (Fig. 6A-B). 4 of the CTAB-tolerant strains had a 1 bp deletion leading to a frameshift after phenylalanine at position 49, 4 strains carried point mutations leading to a premature stop after 64 or 122 amino acids and one strain carried a point mutation in the *sugR* promoter region. SugR is encoded in an operon together with *sugE1* and *sugE2*, coding for two SMR efflux pumps. Deletion of the regulator *sugR* leads to the overexpression of SugE1 and SugE2 and by this to an increased tolerance towards QACs, including BAC and CTAB (Jiang et al. 2020). However, to our knowledge, this is the first time that strains were isolated that acquired mutations in *sugR* under CTAB treatment. To assess the impact of SugE1 and SugE2 on BAC and CTAB tolerance, drop dilution assays were performed with a strain lacking both efflux pumps, a *sugE1/2* overexpression strain (*sugE1/2*⁺), the two CTAB-tolerant strains EGD-e *sugR*^{D122*} and EGD-e *sugR*^{F49fs}, as well as the wildtype strain. The BAC-tolerant strain EGD-e *fepR*^{Q140*} was included as a control. *sugE1/2*⁺, as well as the two CTAB-tolerant strains showed a growth advantage on BHI plates supplemented with CTAB and BAC in comparison to the wildtype and $\Delta sugE1/2$ deletion strains. However, EGD-e *sugR*^{D122*} and EGD-e *sugR*^{F49fs} were unstable in the presence of BAC as they readily

formed suppressors, while the growth of EGD-e *fepR*^{Q140*} was not affected by BAC (Fig. 6C). Our results therefore indicate that FepA and SugE1/2 are the dominant efflux pumps for BAC and CTAB, respectively. In comparison to the *fepR*-associated suppressors, no cross-resistance towards gentamycin and ciprofloxacin was observed in association with the overproduction of SugE1/2 (Fig. S1).

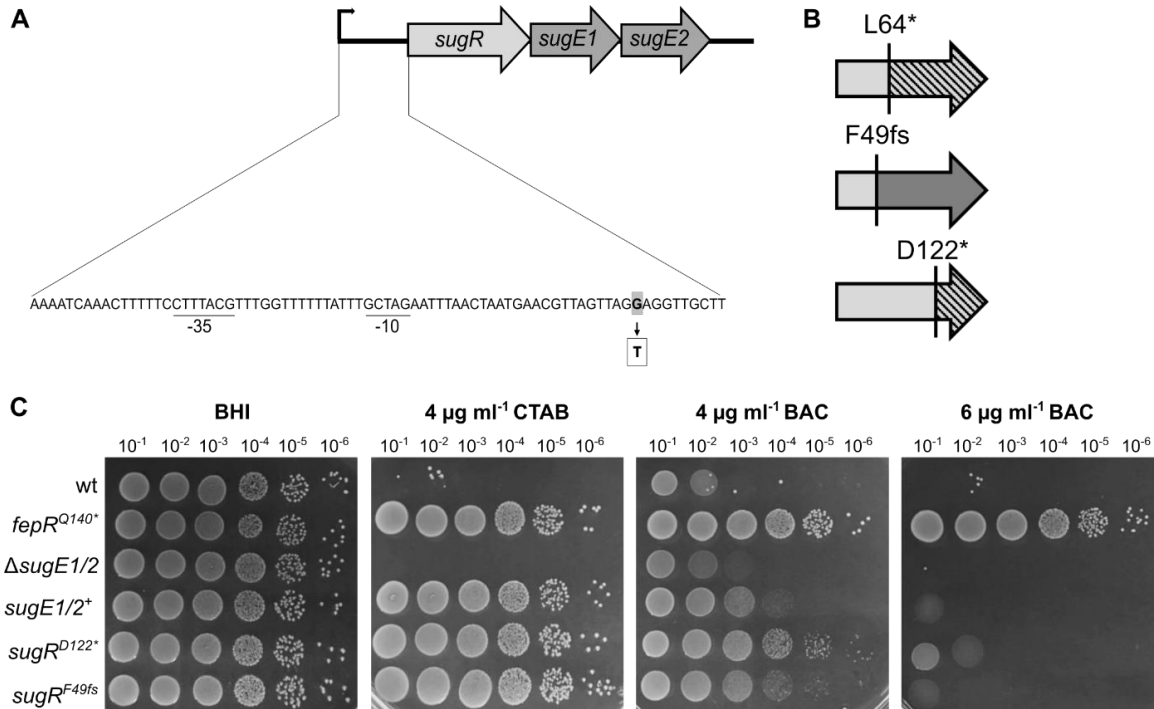


Figure 6 | Acquired CTAB tolerance due to mutations in *sugR* **A** Genetic organization of the *sug* operon in *L. monocytogenes* EGD-e with the predicted promoter region including the -10 and -35 regions (underlined). The *sug* operon contains genes coding for the transcriptional regulator SugR and the two SMR efflux pumps SugE1 and SugE2. Base exchange from one of the suppressors is displayed in grey (adapted from Jiang *et al.*, 2020). **B** Mutations in the *sugR* gene (depicted in light grey) in strains isolated in presence of CTAB. Dark grey colour depicts part of the gene/protein that is affected by the frameshift. The deleted parts of the protein are shown as dashed lines. **C** Drop dilution assays of *L. monocytogenes* strains EGD-e (wt), a *sugE1/2* deletion strain (Δ *sugE1/2*), a wt strain containing the IPTG-inducible pIMK3-*sugE1/2* plasmid LJR301 (*sugE1/2*⁺), and the suppressor mutants *sugR*^{D122*} (LJR248), and *sugR*^{F49fs*} (LJR258). The *fepR*^{Q140*} suppressor mutant (LJR208) was used as a control. Cells were propagated on BHI plates or BHI plates containing 4 μ g ml⁻¹ CTAB, 4 and 6 μ g ml⁻¹ BAC. All plates were supplemented with 1 mM IPTG to induce the expression of *sugE1/2* in the *SugE1/2*⁺ strain. Plates were incubated overnight at 37°C. A representative image of at least three biological replicates is shown.

SugE1/2 and FepA can partially compensate for each other in presence of biocide stress

In an attempt to identify further tolerance mechanisms, the two deletion strains Δ *fepA* and Δ *sugE1/2* were again adapted to BAC and CTAB. Δ *sugE1/2* readily formed suppressors in presence of 6 μ g ml⁻¹ BAC and 4 μ g ml⁻¹ CTAB within a day. The Δ *fepA* strain evolved suppressors in presence of 4 and 6 μ g ml⁻¹ CTAB within a day, while it took two days to isolate BAC-tolerant suppressors (5 μ g ml⁻¹ BAC). To

assess if overproduction of FepA and SugE1/2 can compensate for the lack of SugE1/2 or FepA, respectively, isolated suppressors were screened for mutations in the respective transcriptional regulator. Indeed, all isolated $\Delta sugE1/2$ suppressors carried mutations in the *fepR* gene, regardless of the selective pressure (Fig. 7C). Similarly, all $\Delta fepA$ isolates had mutations in the *sugR* gene, most of which led to either a premature stop or a frameshift. A similar growth behaviour could be observed for the $\Delta fepA$ and $\Delta sugE1/2$ suppressors as compared to the BAC- and CTAB-tolerant wildtype strains (Figs. 2, 5 and 7A-B). $\Delta fepA sugR^{L57*}$ and $\Delta fepA sugR^{F49fs}$ showed enhanced tolerance in presence of 4 $\mu\text{g ml}^{-1}$ CTAB and 4 $\mu\text{g ml}^{-1}$ BAC, while only minor growth was observed in presence of 6 $\mu\text{g ml}^{-1}$ BAC. Interestingly, the wildtype strain harbouring the F49fs mutation in *sugR* seems to be slightly more tolerant towards BAC than the corresponding $\Delta fepA$ strain (Fig. 7A). In addition, no cross-resistance towards ciprofloxacin and gentamycin was observed for $\Delta fepA sugR^{L57*}$ and $\Delta fepA sugR^{F49fs}$ (Fig. S2). In contrast, $\Delta sugE1/2 fepR^{G157*}$ and $\Delta sugE1/2 fepR^{V115fs}$ showed similar growth as the wildtype strain carrying the *fepR*^{Q140*} mutation, where not only increased tolerance towards BAC and CTAB was observed, but also cross-resistance towards ciprofloxacin and gentamycin (Fig. 7B). These results indicate that FepA and SugE1/2 can at least partially compensate for each other.

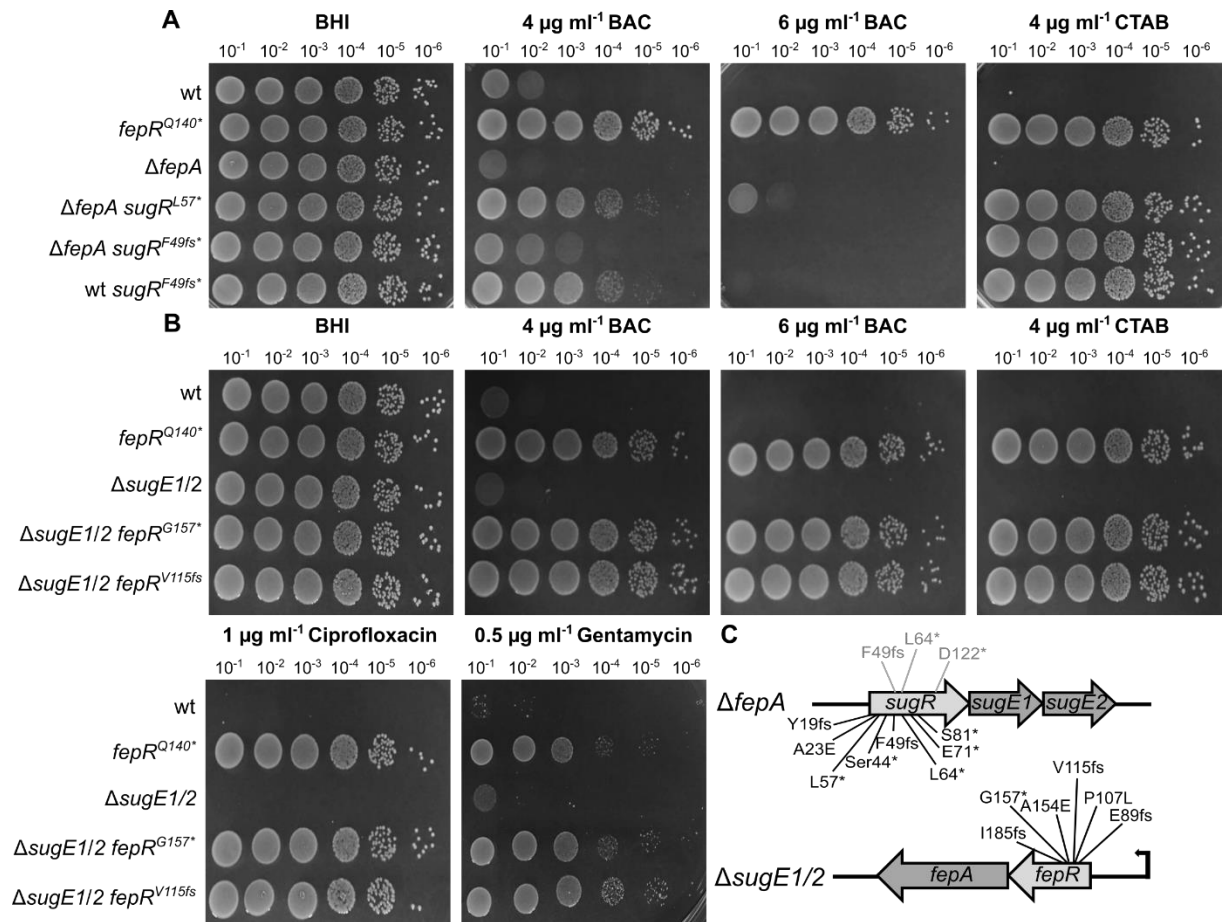


Figure 7 | SugE1/2 and FepA can partially compensate for each other in the presence of biocide stress.

A Drop dilution assays of *L. monocytogenes* strains EGD-e (wt), the *fepA* deletion strain (Δ *fepA*) and the suppressor mutants Δ *fepA sugR*^{L57*} (LJR280), Δ *fepA sugR*^{F49fs} (LJR267) and wt *sugR*^{F49fs} (LJR258). The *fepR*^{Q140*} suppressor mutant (LJR208) was used as a control. Cells were propagated on BHI plates or BHI plates containing 4 and 6 $\mu\text{g ml}^{-1}$ BAC or 4 $\mu\text{g ml}^{-1}$ CTAB and incubated overnight at 37°C. **B** Drop dilution assays of *L. monocytogenes* strains EGD-e (wt), the *sugE1/2* deletion strain (Δ *sugE1/2*), and the suppressor mutants Δ *sugE1/2 fepR*^{G157*} (LJR270), and Δ *sugE1/2 fepR*^{V115fs} (LJR276), isolated on CTAB and BAC, respectively. The *fepR*^{Q140*} suppressor mutant was used as a control. Cells were propagated on BHI plates or BHI plates supplemented with 4 and 6 $\mu\text{g ml}^{-1}$ BAC, 4 $\mu\text{g ml}^{-1}$ CTAB, 1 $\mu\text{g ml}^{-1}$ ciprofloxacin or 0.5 $\mu\text{g ml}^{-1}$ gentamycin and incubated overnight at 37°C. A representative image of at least three biological replicates is shown. **C** Acquired *sugR* and *fepR* mutations in the Δ *fepA* or Δ *sugE1/2* background, respectively. The mutations that were previously identified in the wildtype background are depicted in grey.

Strains lacking the two major QAC efflux systems can still acquire tolerance

To assess whether *L. monocytogenes* possesses a third mechanism to adapt to QACs, the Δ *fepA* Δ *sugE1/2* double deletion strain was constructed and propagated in the presence of BAC and CTAB. Interestingly, no suppressor formation was observed on BHI plates containing 6 $\mu\text{g ml}^{-1}$ BAC or 4 $\mu\text{g ml}^{-1}$ CTAB, which were previously used to isolate BAC- and CTAB-tolerant strains, likely due to the absence of two important efflux systems. However, the Δ *fepA* Δ *sugE1/2* deletion strain could still

adapt to 5 $\mu\text{g ml}^{-1}$ BAC and 2 $\mu\text{g ml}^{-1}$ CTAB. Genomic alterations for two BAC- and two CTAB-tolerant strains were determined by whole genome sequencing. Interestingly, all tolerant isolates acquired mutations in *Imo1753* encoding a putative diacylglycerol kinase and Sanger sequencing of additional mutants likewise identified mutations in *Imo1753*. The phenotype of the suppressors slightly varied in presence of different stresses. The two CTAB-tolerant strains $\Delta\text{fepA}\Delta\text{sugE1/2}$ CTAB1 and $\Delta\text{fepA}\Delta\text{sugE1/2}$ CTAB2 showed only slightly increased tolerance on plates containing 2 $\mu\text{g ml}^{-1}$ CTAB and 4 $\mu\text{g ml}^{-1}$ BAC. In contrast, the BAC-tolerant strain $\Delta\text{fepA}\Delta\text{sugE1/2}$ BAC2 could grow to some extent in the presence of CTAB and showed enhanced growth even in the presence of up to 6 $\mu\text{g ml}^{-1}$ BAC as compared to the wildtype strain and the $\Delta\text{fepA}\Delta\text{sugE1/2}$ deletion strain (Fig. 8). Apart from the mutation in *Imo1753*, this suppressor carried a mutation in the promoter region of *Imo1682*, encoding a putative multidrug efflux pump, whose overexpression is likely responsible for the increased BAC tolerance. The BAC-tolerant strain $\Delta\text{fepA}\Delta\text{sugE1/2}$ BAC1 also showed an enhanced tolerance towards BAC as compared to the $\Delta\text{fepA}\Delta\text{sugE1/2}$ deletion strain, however, no growth advantage could be observed on BHI plates containing CTAB (Fig. 8). Interestingly, $\Delta\text{fepA}\Delta\text{sugE1/2}$ BAC1 was more sensitive towards the antibiotic cefuroxime in comparison to the parental and wildtype strain as well as an increased tolerance to gentamycin similar to EGD-e *fepR*^{Q140*} (Fig. 8). Remarkably, we could neither identify any additional mutations for $\Delta\text{fepA}\Delta\text{sugE1/2}$ BAC1 apart from the mutation in *Imo1753*, which is identical to the mutation in $\Delta\text{fepA}\Delta\text{sugE1/2}$ CTAB1 and CTAB2, nor indications of gene amplification events that could explain the distinct phenotype. No cross-adaption towards ciprofloxacin was observed for any of the $\Delta\text{fepA}\Delta\text{sugE1/2}$ suppressors (Fig. 8).

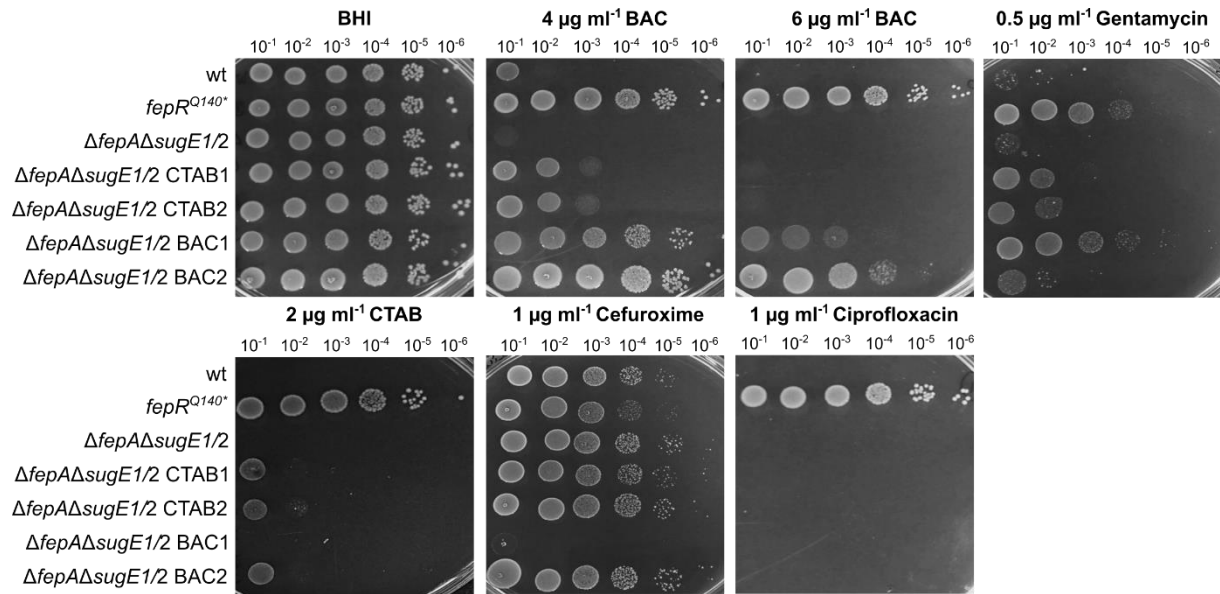


Figure 8 | QAC tolerance of the $\Delta fepA\Delta sugE1/2$ deletion strain

Drop dilution assays of *L. monocytogenes* strains EGD-e (wt), the *fepA sugE1/2* deletion strain ($\Delta fepA\Delta sugE1/2$), the two suppressor mutants that were isolated in presence of CTAB, LJR327 ($\Delta fepA\Delta sugE1/2$ *lmo1753*^{K19fs}, short CTAB1) and LJR328 ($\Delta fepA\Delta sugE1/2$ *lmo1753*^{K19fs}, short CTAB2), and the two suppressor mutants that were isolated in presence of BAC, LJR326 ($\Delta fepA\Delta sugE1/2$ *lmo1753*^{K19fs}, short BAC1) and LJR330 ($\Delta fepA\Delta sugE1/2$ *lmo1753*^{V225fs P_{lmo1682}^{G-37A}, short BAC2). A representative image of at least three biological replicates is shown.}

Discussion

Survival and proliferation of *L. monocytogenes* in the food industry is an ongoing concern, and while there are various countermeasures to combat the contamination of food products, such as osmotic stress, extreme temperatures or the use of disinfectants, the pathogen still successfully manages to withstand the harsh conditions present in food-processing facilities, resulting in reoccurring outbreaks. To counteract the spread of *L. monocytogenes*, it is crucial to understand and elucidate the underlying mechanism that permit their successful evasion. Outbreaks are often associated with strains that tolerate below working concentrations of QACs, such as BAC or CTAB, the most commonly used active agents in disinfectants (Weber et al. 2007). In this study, we assessed the ability of the laboratory wildtype strain EGD-e to adapt to low levels of BAC and CTAB under laboratory growth conditions. Since previous studies have focused on the analyses of *L. monocytogenes* isolates, which exhibit a high frequency of genomic variations, our findings using the laboratory model strain represent a more generalized assessment. While previously isolated strains often merely acquired a transient tolerance towards QACs that was lost after passaging of the strains in absence of the stress, our strains readily formed stable suppressors that allowed growth in presence of BAC and CTAB.

In our study, BAC-tolerant *L. monocytogenes* strains exclusively carried mutations in *fepR*, which encodes a transcriptional regulator. These findings are in accordance with previous studies, which focussed on serial adapted isolated *L. monocytogenes* and *Listeria spp.* strains that were exposed to BAC or ciprofloxacin stress and likewise found that the majority of strains acquired mutations in *fepR* (Bolten et al. 2022; Bland et al. 2022; Douarre et al. 2022). FepR is a TetR-like transcriptional regulator that negatively regulates the *fepRA* operon, which encodes the regulator itself as well as the MATE family efflux pump FepA (Guérin et al. 2014). Strains that carried a mutation in *fepR*, as well as strains that artificially overexpress the efflux pump FepA exhibited increased tolerance not only towards BAC, but also towards CTAB, ciprofloxacin and gentamycin, indicating that extrusion by the transporter is rather unspecific. This observation further supports the previous hypothesis that de-repression of *fepA* is the reason for the observed QAC tolerance (Guérin et al. 2014; Bolten et al. 2022; Bland et al. 2022; Douarre et al. 2022). We further substantiated this hypothesis by showing that a mutation in the DNA binding domain of FepR resulted in decreased binding to the promoter of the *fepRA* operon in comparison to the wildtype FepR protein. Likewise, mutations in the *fepRA* promoter region resulted in reduced binding of the wildtype FepR and thus, to increased promoter activity. This enhanced promoter activity could then result in an enhance production of FepA and subsequent export of BAC. Interestingly, we did not identify any mutations in either of the two chromosomally located efflux pumps MdrL or Lde that were previously described to be involved in QAC adaptation and whose expression is commonly upregulated in tolerant *L. monocytogenes* isolates (Jiang et al. 2012; Godreuil et al. 2003; Mata et al. 2000; Jiang et al. 2019b). This was the case even in the absence of *fepA* and/or *sugE1/2*, suggesting that neither play a significant role in BAC or CTAB tolerance under the tested conditions. Altogether, we can conclude that the acquisition of mutations in *fepR* and the associated elevation of FepA levels and activity is the dominant mode of tolerance towards BAC in the EGD-e wildtype strain. In contrast, suppressors isolated in presence of CTAB stress solely acquired mutations in the *sugR* gene, coding for a different transcriptional regulator. Unexpectedly, none of the isolated suppressors carried mutations in the *fepR* gene. SugR is involved in the repression of the two SMR efflux pumps SugE1 and SugE2 that were previously shown to confer tolerance towards QACs such as BAC, CTAB or didecyldimethylammonium chloride (DDAC) in *L. monocytogenes*. Accordingly, expression of the efflux system was shown to be induced in presence of BAC, suggesting that BAC can inhibit the SugR-dependent repression of *sugE1/2* (Jiang et al. 2020). Similarly to previous findings, the overexpression of SugE1/2 either due to mutations in its repressor or artificially induced did not result in any further cross-adaption in contrast to suppressors with *fepR* mutations

(Jiang et al. 2020; Bland et al. 2022; Guérin et al. 2014). Cross-resistance was also observed for *Pseudomonas aeruginosa* and *E. coli* isolates after BAC adaptation. While *P. aeruginosa* isolates acquired tolerance towards polymyxin B and other, BAC-adapted *E. coli* strains exhibited increased MIC for ampicillin and/or ciprofloxacin (Kim et al. 2018b; Nordholt et al. 2021). This raises the question, if CTAB should be used more frequently in commercial disinfectants than BAC to prevent the emergence of multi-resistant strains. We also found that although both efflux systems could compensate for the loss of the other, overexpression of FepA results in a higher BAC-tolerance than overexpression of SugE1/2, suggesting that the two efflux systems do not have specific substrates, but that the affinity seems to differ for the two QACs, BAC and CTAB. We further evolved a strain that lacks the two major QAC efflux systems FepA and SugE1/2 to identify additional tolerance mechanisms. To our surprise, all isolated suppressors acquired mutations in *Imo1753*, which does not code for an additional efflux system. Instead, *Imo1753* shares 64% sequence identity and 87.2% similarity with the gene coding for the diacylglycerol kinase DgkB from *Bacillus subtilis*, which contributes to the biosynthesis of lipoteichoic acids (LTA) by recycling the toxic intermediate phosphatidic acid (Jerga et al. 2007; Matsuoka et al. 2011). This finding indicates that SugE1/2 and FepA are the key BAC and CTAB efflux systems in the *L. monocytogenes* wildtype strain EGD-e. LTAs make up a great portion of the gram-positive cell wall and have been shown to play crucial roles in cellular growth, morphology and division. They are anchored to the cell membrane and mainly consist of a polyglycerolphosphate backbone that contributes to the overall negative surface charge of the cell (Campeotto et al. 2014). The negatively charged backbone can be masked by decoration with positively charged D-alanylation. This decoration can be rather flexible and can fluctuate according to environmental and cellular cues, allowing adjustment of the cellular surface charge and hence variation in the cation homeostasis of the membrane (Percy and Gründling 2014). A decrease in cellular surface charge was previously associated with the survival of adapted *E. coli* strains in the presence of BAC, as they carried mutations in *lpxM*, encoding an enzyme involved in lipid A biosynthesis (Nordholt et al. 2021). Likewise, an increased negative surface charge was shown to be beneficial in a high-level BAC-tolerant *Pseudomonas fluorescence* strain (Nagai et al. 2003). It is tempting to speculate that mutations in *Imo1753* result in altered LTA synthesis followed by a distorted negative surface charge subsequently hindering binding of the positively charged head groups of BAC and CTAB. While the activity of DgkB has often mainly been discussed in the context of LTA biosynthesis, phosphatidic acid can also be utilized for the production of other glycolipids and phospholipids, including cardiolipin, lysyl-phosphatidylglycerol or phosphatidylethanolamine.

Likewise, diacylglycerol, the substrate of DgkB, is aside from LTA biosynthesis also crucial for the production of triglucoxydiacyl-glycerol (Hashimoto et al. 2013). Hence, aberrant DgkB activity might generally result in an altered lipid profile. Besides efflux systems, changes in fatty acid composition and concomitant altered membrane fluidity have been proposed to contribute to QAC tolerance in several organisms. A study from 2002 described a tolerant *L. monocytogenes* isolate that showed a slight shift in the length of fatty acids (To et al. 2002). General alterations of the fatty acid profile and content was likewise associated with QAC tolerance in *Serratia marcescens* (Chaplin 1952) and *P. aeruginosa* (Guerin-Mechin et al. 2000; Jones et al. 1989). It remains elusive how mutations in *Imo1753* contribute to QAC tolerance, but our findings highlight the ability of *L. monocytogenes* to adapt to QAC via an export-independent mechanism. One of the $\Delta fepA \Delta sugE1/2$ suppressors showed enhanced tolerance towards BAC in comparison to the other isolated mutants with the same genetic background. Interestingly, the strain acquired in addition to the mutation in *Imo1753* a mutation in the promoter region of *Imo1683*, which encodes a putative major facilitator family transporter. To our knowledge, no function was assigned for this transporter so far; however, our study suggests that it might be involved in the export of BAC. Further analysis of the transporter is required to elucidate its role in the efflux of QACs.

It has to be mentioned that all suppressors were isolated on BHI complex medium and in the presence of below working concentrations of BAC and CTAB. Those rather ideal conditions are not commonly found in food-processing facilities. However, similar BAC concentrations are often found in hard to reach places, when disinfectants are not properly applied and concentrations of approximately $0.5 \mu\text{g ml}^{-1}$ were for instance reported in household wastewater, creating an environment that allows adaptation of the pathogen prior to entering food-processing plants (Tezel and Pavlostathis 2015). Altogether, our study supported previous findings that designated the efflux pump FepA as the major BAC extrusion system in *L. monocytogenes*. We further showed that SugE1/2 play a similar role for CTAB-tolerance and that both systems are the two main efflux systems for BAC and CTAB. Our suppressor screen also revealed the ability of *L. monocytogenes* to acquire tolerance independent of the presence and/or overexpression of efflux systems, likely due to alterations in the lipid profile, which will be further analysed in the future.

Acknowledgements

We are grateful to Julia Busse for technical assistance and thank Prof. Jörg Stülke for providing laboratory space, equipment and consumables and to the Göttingen Center for Molecular Biosciences (GZMB) for financial support.

Supplemental Material

<https://www.biorxiv.org/content/10.1101/2023.03.30.534860v1>.

Figure S1 | Cross-resistance of *sugR* mutant strains

Figure S2 | Cross-resistance of Δ *fepA sugR* mutant strains

References

- Aase, B., Sundheim, G., Langsrud, S., and Rørvik, L.M. (2000) Occurrence of and a possible mechanism for resistance to a quaternary ammonium compound in *Listeria monocytogenes*. *International journal of food microbiology*, doi: 10.1016/s0168-1605(00)00357-3.
- Allerberger, F., and Wagner, M. (2010) Listeriosis: a resurgent foodborne infection. *Clinical microbiology and infection: the official publication of the European Society of Clinical Microbiology and Infectious Diseases*, doi: 10.1111/j.1469-0691.2009.03109.x.
- Bland, R., Waite-Cusic, J., Weisberg, A.J., Riutta, E.R., Chang, J.H., and Kovacevic, J. (2022) Adaptation to a commercial quaternary ammonium compound sanitizer leads to cross-resistance to select antibiotics in *Listeria monocytogenes* Isolated from fresh produce environments. *Frontiers in microbiology*, doi: 10.3389/fmicb.2021.782920.
- Bolten, S., Harrand, A.S., Skeens, J., and Wiedmann, M. (2022) Nonsynonymous mutations in *fepR* are associated with adaptation of *Listeria monocytogenes* and other *Listeria* spp. to low concentrations of benzalkonium chloride but do not increase survival of *L. monocytogenes* and other *Listeria* spp. after exposure to benzalkonium chloride concentrations recommended for use in food processing Environments. *Applied and environmental microbiology*, doi: 10.1128/aem.00486-22.
- Bradford, M.M. (1976) A rapid and sensitive method for the quantitation of microgram quantities of protein utilizing the principle of protein-dye binding. *Analytical Biochemistry*, doi: 10.1016/0003-2697(76)90527-3.
- Camilli, A., Tilney, L.G., and Portnoy, D.A. (1993) Dual roles of *plcA* in *Listeria monocytogenes* pathogenesis. *Molecular microbiology*, doi: 10.1111/j.1365-2958.1993.tb01211.x.

- Campeotto, I., Percy, M.G., MacDonald, J.T., Förster, A., Freemont, P.S., and Gründling, A. (2014) Structural and mechanistic insight into the *Listeria monocytogenes* two-enzyme lipoteichoic acid synthesis system. *The Journal of biological chemistry*, doi: 10.1074/jbc.M114.590570.
- Carlin, C.R., Roof, S., and Wiedmann, M. (2022) Assessment of reference method selective broth and plating media with 19 *Listeria* species highlights the importance of including diverse species in *Listeria* method evaluations. *Journal of food protection*, doi: 10.4315/JFP-21-293.
- Chaplin, C.E. (1952) Bacterial resistance to quaternary ammonium disinfectants. *Journal of Bacteriology*, doi: 10.1128/jb.63.4.453-458.1952.
- Dhiman, A., Bhatnagar, S., Kulshreshtha, P., and Bhatnagar, R. (2014) Functional characterization of WalRK: A two-component signal transduction system from *Bacillus anthracis*. *FEBS open bio*, doi: 10.1016/j.fob.2013.12.005.
- Douarre, P.-E., Sévellec, Y., Le Grandois, P., Soumet, C., Bridier, A., and Roussel, S. (2022) FepR as a central genetic target in the adaptation to quaternary ammonium compounds and cross-resistance to ciprofloxacin in *Listeria monocytogenes*. *Frontiers in microbiology*, doi: 10.3389/fmicb.2022.864576.
- Dutta, V., Elhanafi, D., and Kathariou, S. (2013) Conservation and distribution of the benzalkonium chloride resistance cassette *bcrABC* in *Listeria monocytogenes*. *Applied and environmental microbiology*, doi: 10.1128/AEM.01751-13.
- EFSA and ECDC, The European Union One Health 2021 Zoonoses Report. *European Food Safety Authority*, 2022.
- Elhanafi, D., Dutta, V., and Kathariou, S. (2010) Genetic characterization of plasmid-associated benzalkonium chloride resistance determinants in a *Listeria monocytogenes* strain from the 1998-1999 outbreak. *Applied and environmental microbiology*, doi: 10.1128/AEM.02056-10.
- Glaser, P., Frangeul, L., Buchrieser, C., Rusniok, C., Amend, A., Baquero, F., et al. (2001) Comparative genomics of *Listeria* species. *Science (New York, N.Y.)*, doi: 10.1126/science.1063447.
- Godreuil, S., Galimand, M., Gerbaud, G., Jacquet, C., and Courvalin, P. (2003) Efflux pump Lde is associated with fluoroquinolone resistance in *Listeria monocytogenes*. *Antimicrobial agents and chemotherapy*, doi: 10.1128/AAC.47.2.704-708.2003.
- Gründling, A., Burrack, L.S., Bouwer, H.G.A., and Higgins, D.E. (2004) *Listeria monocytogenes* regulates flagellar motility gene expression through MogR, a transcriptional repressor required for virulence. *Proceedings of the National Academy of Sciences of the United States of America*, doi: 10.1073/pnas.0404924101.

- Guérin, A., Bridier, A., Le Grandois, P., Sévellec, Y., Palma, F., Félix, B., *et al.* (2021) Exposure to quaternary ammonium compounds selects resistance to ciprofloxacin in *Listeria monocytogenes*. *Pathogens (Basel, Switzerland)*, doi: 10.3390/pathogens10020220.
- Guérin, F., Galimand, M., Tuambilangana, F., Courvalin, P., and Cattoir, V. (2014) Overexpression of the novel MATE fluoroquinolone efflux pump FepA in *Listeria monocytogenes* is driven by inactivation of its local repressor FepR. *PLoS ONE*, doi: 10.1371/journal.pone.0106340.
- Guerin-Mechin, L., Dubois-Brissonnet, F., Heyd, B., and Leveau, J.Y. (2000) Quaternary ammonium compound stresses induce specific variations in fatty acid composition of *Pseudomonas aeruginosa*. *International journal of food microbiology*, doi: 10.1016/s0168-1605(00)00189-6.
- Hashimoto, M., Seki, T., Matsuoka, S., Hara, H., Asai, K., Sadaie, Y., and Matsumoto, K. (2013) Induction of extracytoplasmic function sigma factors in *Bacillus subtilis* cells with defects in lipoteichoic acid synthesis. *Microbiology (Reading, England)*, doi: 10.1099/mic.0.063420-0.
- Jerga, A., Lu, Y.-J., Schujman, G.E., Mendoza, D. de, and Rock, C.O. (2007) Identification of a soluble diacylglycerol kinase required for lipoteichoic acid production in *Bacillus subtilis*. *The Journal of biological chemistry*, doi: 10.1074/jbc.M703536200.
- Jiang, X., Ren, S., Geng, Y., Yu, T., Li, Y., Liu, L., *et al.* (2020) The *sug* operon involves in resistance to quaternary ammonium compounds in *Listeria monocytogenes* EGD-e. *Applied microbiology and biotechnology*, doi: 10.1007/s00253-020-10741-6.
- Jiang, X., Yu, T., Liang, Y., Ji, S., Guo, X., Ma, J., and Zhou, L. (2016) Efflux pump-mediated benzalkonium chloride resistance in *Listeria monocytogenes* isolated from retail food. *International journal of food microbiology*, doi: 10.1016/j.ijfoodmicro.2015.10.022.
- Jiang, X., Yu, T., Xu, Y., Wang, H., Korkeala, H., and Shi, L. (2019) MdrL, a major facilitator superfamily efflux pump of *Listeria monocytogenes* involved in tolerance to benzalkonium chloride. *Applied microbiology and biotechnology*, doi: 10.1007/s00253-018-9551-y.
- Jiang, X., Zhou, L., Gao, D., Wang, Y., Wang, D., Zhang, Z., *et al.* (2012) Expression of efflux pump gene *lde* in ciprofloxacin-resistant foodborne isolates of *Listeria monocytogenes*. *Microbiology and immunology*, doi: 10.1111/j.1348-0421.2012.00506.x.
- Jones, M.V., Herd, T.M., and Christie, H.J. (1989) Resistance of *Pseudomonas aeruginosa* to amphoteric and quaternary ammonium biocides. *Microbios*, **58**: 49–61.
- Kaval, K.G., Hahn, B., Tusamda, N., Albrecht, D., and Halbedel, S. (2015) The PadR-like transcriptional regulator LftR ensures efficient invasion of *Listeria monocytogenes* into human host cells. *Frontiers in microbiology*, doi: 10.3389/fmicb.2015.00772.

- Kim, M., Weigand, M.R., Oh, S., Hatt, J.K., Krishnan, R., Tezel, U., Pavlostathis, S.G., and Konstantinidis, K.T. (2018) Widely used benzalkonium chloride disinfectants can promote antibiotic resistance. *Applied and environmental microbiology*, doi: 10.1128/AEM.01201-18.
- Kovacevic, J., Ziegler, J., Wałęcka-Zacharska, E., Reimer, A., Kitts, D.D., and Gilmour, M.W. (2015) Tolerance of *Listeria monocytogenes* to quaternary ammonium sanitizers is mediated by a novel efflux pump encoded by *emrE*. *Applied and environmental microbiology*, doi: 10.1128/AEM.03741-15.
- Lundén, J., Autio, T., Markkula, A., Hellström, S., and Korkeala, H. (2003) Adaptive and cross-adaptive responses of persistent and non-persistent *Listeria monocytogenes* strains to disinfectants. *International journal of food microbiology*, doi: 10.1016/s0168-1605(02)00312-4.
- Martínez-Suárez, J.V., Ortiz, S., and López-Alonso, V. (2016) Potential impact of the resistance to quaternary ammonium disinfectants on the persistence of *Listeria monocytogenes* in food processing environments. *Frontiers in microbiology*, doi: 10.3389/fmicb.2016.00638.
- Mata, M.T., Baquero, F., and Pérez-Díaz, J.C. (2000) A multidrug efflux transporter in *Listeria monocytogenes*. *FEMS microbiology letters*, doi: 10.1111/j.1574-6968.2000.tb09158.x.
- Matsuoka, S., Hashimoto, M., Kamiya, Y., Miyazawa, T., Ishikawa, K., Hara, H., and Matsumoto, K. (2011) The *Bacillus subtilis* essential gene *dgkB* is dispensable in mutants with defective lipoteichoic acid synthesis. *Genes & genetic systems*, doi: 10.1266/ggs.86.365.
- Meier, A.B., Guldimann, C., Markkula, A., Pöntinen, A., Korkeala, H., and Tasara, T. (2017) Comparative phenotypic and genotypic analysis of Swiss and Finnish *Listeria monocytogenes* isolates with respect to benzalkonium chloride resistance. *Frontiers in microbiology*, doi: 10.3389/fmicb.2017.00397.
- Minarovičová, J., Véghová, A., Mikulášová, M., Chovanová, R., Šoltýs, K., Drahovská, H., and Kaclíková, E. (2018) Benzalkonium chloride tolerance of *Listeria monocytogenes* strains isolated from a meat processing facility is related to presence of plasmid-borne *bcrABC* cassette. *Antonie van Leeuwenhoek*, doi: 10.1007/s10482-018-1082-0.
- Monk, I.R., Gahan, C.G.M., and Hill, C. (2008) Tools for functional postgenomic analysis of *Listeria monocytogenes*. *Applied and environmental microbiology*, doi: 10.1128/AEM.00314-08.
- Müller, A., Rychli, K., Muhterem-Uyar, M., Zaiser, A., Stessl, B., Guinane, C.M., et al. (2013) Tn6188 - a novel transposon in *Listeria monocytogenes* responsible for tolerance to benzalkonium chloride. *PLoS ONE*, doi: 10.1371/journal.pone.0076835.

- Müller, A., Rychli, K., Zaiser, A., Wieser, C., Wagner, M., and Schmitz-Esser, S. (2014) The *Listeria monocytogenes* transposon Tn6188 provides increased tolerance to various quaternary ammonium compounds and ethidium bromide. *FEMS microbiology letters*, doi: 10.1111/1574-6968.12626.
- Nagai, K., Murata, T., Ohta, S., Zenda, H., Ohnishi, M., and Hayashi, T. (2003) Two different mechanisms are involved in the extremely high-level benzalkonium chloride resistance of a *Pseudomonas fluorescens* strain. *Microbiology and immunology*, doi: 10.1111/j.1348-0421.2003.tb03440.x.
- Nordholt, N., Kanaris, O., Schmidt, S.B.I., and Schreiber, F. (2021) Persistence against benzalkonium chloride promotes rapid evolution of tolerance during periodic disinfection. *Nature Communications*, doi: 10.1038/s41467-021-27019-8.
- Osek, J., Lachtara, B., and Wieczorek, K. (2022) *Listeria monocytogenes* - How this pathogen survives in food-production environments? *Frontiers in microbiology*, doi: 10.3389/fmicb.2022.866462.
- Percy, M.G., and Gründling, A. (2014) Lipoteichoic acid synthesis and function in gram-positive bacteria. *Annual review of microbiology*, doi: 10.1146/annurev-micro-091213-112949.
- Rakic-Martinez, M., Drevets, D.A., Dutta, V., Katic, V., and Kathariou, S. (2011) *Listeria monocytogenes* strains selected on ciprofloxacin or the disinfectant benzalkonium chloride exhibit reduced susceptibility to ciprofloxacin, gentamicin, benzalkonium chloride, and other toxic compounds. *Applied and environmental microbiology*, doi: 10.1128/AEM.05941-11.
- Rietberg, K., Lloyd, J., Melius, B., Wyman, P., Treadwell, R., Olson, G., Kang, M.-G., and Duchin, J.S. (2016) Outbreak of *Listeria monocytogenes* infections linked to a pasteurized ice cream product served to hospitalized patients. *Epidemiology and infection*, doi: 10.1017/S0950268815003039.
- Rismondo, J., Halbedel, S., and Gründling, A. (2019) Cell shape and antibiotic resistance are maintained by the activity of multiple FtsW and RodA enzymes in *Listeria monocytogenes*. *mBio*, doi: 10.1128/mBio.01448-19.
- Romanova, N., Favrin, S., and Griffiths, M.W. (2002) Sensitivity of *Listeria monocytogenes* to sanitizers used in the meat processing industry. *Applied and environmental microbiology*, doi: 10.1128/AEM.68.12.6405-6409.2002.
- Romanova, N.A., Wolffs, P.F.G., Brovko, L.Y., and Griffiths, M.W. (2006) Role of efflux pumps in adaptation and resistance of *Listeria monocytogenes* to benzalkonium chloride. *Applied and environmental microbiology*, doi: 10.1128/AEM.72.5.3498-3503.2006.

- Schirmer, F., Ehrh, S., and Hillen, W. (1997) Expression, inducer spectrum, domain structure, and function of MopR, the regulator of phenol degradation in *Acinetobacter calcoaceticus* NCIB8250. *Journal of Bacteriology*, doi: 10.1128/jb.179.4.1329-1336.1997.
- Smith, K., and Youngman, P. (1992) Use of a new integrational vector to investigate compartment-specific expression of the *Bacillus subtilis* *spoIIIM* gene. *Biochimie*, doi: 10.1016/0300-9084(92)90143-3.
- Soumet, C., Ragimbeau, C., and Maris, P. (2005) Screening of benzalkonium chloride resistance in *Listeria monocytogenes* strains isolated during cold smoked fish production. *Letters in applied microbiology*, doi: 10.1111/j.1472-765X.2005.01763.x.
- Tezel, U., and Pavlostathis, S.G. (2015) Quaternary ammonium disinfectants: microbial adaptation, degradation and ecology. *Current Opinion in Biotechnology*, doi: 10.1016/j.copbio.2015.03.018.
- Thomas, J., Govender, N., McCarthy, K.M., Erasmus, L.K., Doyle, T.J., Allam, M., et al. (2020) Outbreak of listeriosis in South Africa associated with processed meat. *The New England journal of medicine*, doi: 10.1056/NEJMoa1907462.
- To, M.S., Favrin, S., Romanova, N., and Griffiths, M.W. (2002) Postadaptational resistance to benzalkonium chloride and subsequent physicochemical modifications of *Listeria monocytogenes*. *Applied and environmental microbiology*, doi: 10.1128/AEM.68.11.5258-5264.2002.
- Weber, D.J., Rutala, W.A., and Sickbert-Bennett, E.E. (2007) Outbreaks associated with contaminated antiseptics and disinfectants. *Antimicrobial agents and chemotherapy*, doi: 10.1128/AAC.00138-07.
- Yu, T., Jiang, X., Zhang, Y., Ji, S., Gao, W., and Shi, L. (2018) Effect of benzalkonium chloride adaptation on sensitivity to antimicrobial agents and tolerance to environmental stresses in *Listeria monocytogenes*. *Frontiers in microbiology*, doi: 10.3389/fmicb.2018.02906.
- Zinchenko, A.A., Sergeyev, V.G., Yamabe, K., Murata, S., and Yoshikawa, K. (2004) DNA compaction by divalent cations: structural specificity revealed by the potentiality of designed quaternary diammonium salts. *Chembiochem: a European journal of chemical biology*, doi: 10.1002/cbic.200300797.

Chapter 7 | Discussion

Spread of *L. monocytogenes*, and successional infection of animals and humans is an ongoing problem in the medical sector, as well as for livestock. Infections are typically treated with cell wall-targeting antibiotics, while the spread is prevented by treatment with disinfectant that often contain quaternary ammonium compounds (QACs), such as benzalkonium chloride (BAC) or cetyltrimethylammonium bromide (CTAB). Proper cell wall organization requires the interplay of several processes that are involved in maintaining the structure, morphology, and protection of the cell. The identification and characterization of factors involved in either of these processes is crucial for the fight against *L. monocytogenes*. We aimed to investigate both areas, by A – elucidating the role of the putative ABC transporter EslABC in lysozyme sensitivity, cell division and cell wall biosynthesis and B – by identifying factors involved in tolerance towards BAC and CTAB.

7.1 The importance of EslB in cell wall homeostasis

Cellular growth and survival are particularly dependent on the architecture of the bacterial envelope, the building of which includes the involvement of several multifaceted processes that preserve the shape, morphology, and protection of the cell. The overall system is dependent on accurate organization of various essential proteins and metabolites. However, how those pathways are coordinated with each other to ensure proper assembly, as well as continuous expansion and remodelling of the cell wall remains to be unravelled. Recent studies tried to elucidate this interplay and communication and several proteins have been suggested to present a link between the distinct processes. A prime example is the serine/threonine protein kinase PrkC, which has been demonstrated to be essential for the control of MurA levels, thereby regulating the pace of peptidoglycan biosynthesis. At the same time PrkC manages the velocity of elongation and growth rate by mediating the density of MreB filaments (Sun et al. 2023). With that PrkC is a paradigm for a determining factor that is essential for proper cell wall homeostasis. The transcriptional regulator WalR is another example, which seems to be a central regulator for various crucial pathways by regulating the amount of *N*-deacetylation of the GlcNAc residue of peptidoglycan, the wall teichoic acid content, as well as the activity of cell wall hydrolases (Dobihal et al. 2022; Dobihal et al. 2019; Libby et al. 2015). In addition, several factors involved in cell division or elongation have been predicted to interact with and respond to PG synthesis associated proteins and precursors. The

putative ABC transporter EslABC is a key example that demonstrates how the deletion of a single factor impacts cell wall-associated pathways, including PG biosynthesis and modification, cross-linking, cell division, elongation, hydrolase homeostasis, and wall teichoic acid biosynthesis. The following chapters will discuss the consequences of the deletion of the transmembrane protein EslB on different processes that take part in maintaining cell wall homeostasis of the cell.

7.2 The putative ABC transporter EslABC

The putative ABC transporter EslABC (for elongation and sugar-and lyzozyme-sensitive phenotype) is encoded by the *lmo2769-6* operon. Generally, ABC transporters contain a characteristic nucleotide-binding domain (NBD) protein, as well as one or more transmembrane proteins (Locher 2016). Importers often possess an additional substrate binding protein (SBP) that allows binding or demonstration and subsequent translocation of a cognate substrate. ATP hydrolysis of the NBD protein typically stimulates conformational changes in the transmembrane protein which result in subsequent uptake or export of the cognate substrate (Locher 2016; Mächtel et al. 2019; Slotboom 2014; Davidson et al. 2008). Even though ABC transporters are mainly involved in the translocation of substrates across the bacterial membrane, ABC transporters with alternative functions have been described in the literature (Rismondo and Schulz 2021). A model example for this is FtsEX, which does not seem to play a role in transport at all but participates in ATP-dependent regulation of the cell wall hydrolase CwIO. CwIO plays a vital role in cell growth, by cleaving the existing cell wall, allowing the integration of newly synthesized peptidoglycan (Brunet et al. 2019; Meisner et al. 2013). In the *lmo2769-6* operon, *lmo2769* codes for the NBD protein EslA, while *lmo2768* and *lmo2767* code for the transmembrane proteins EslB and EslC, respectively. Interestingly, *lmo2766* codes for an RpiR-type transcriptional regulator, which potentially plays a role in the regulation of the operon. Those regulators are typically involved in phosphate-sugar metabolic pathways and may control the expression of enzymes involved in carbon metabolism. Moreover, they typically contain an N-terminal helix-turn-helix domain and a C-terminal sugar isomerase domain (SIS) (Bateman 1999). A putative EslR-dependent regulation of EslABC portrays a potential link between sugar metabolism and activity of the transporter. However, so far, no experimental evidence could support a regulation of EslABC by EslR, aside from its genomic arrangement. Nevertheless, the presence of the putative RpiR-type regulator, as well as the observation that the deletion of one or several parts of the transporter result in growth defects in presence of high concentrations of certain sugars, such as sucrose and glucose,

raises the question if the transporter is involved in unspecific uptake of sugars (Rismondo et al. 2021). ATP-dependent transport of mono- or disaccharides is usually dependent on binding and delivery of the sugar by a substrate binding protein (Schneider 2001). So far, we could not identify a potential substrate binding protein for EslABC, which does not necessarily exclude its participation in sugar transport but makes it rather unlikely. Moreover, if the transporter is necessary for the uptake of sugar molecules, one would expect that the supplementation of associated mono- or disaccharides is beneficial in the mutant strain and not disadvantageous.

Initial bacterial two-hybrid experiments suggested an interaction between the membrane components EslB and EslC and we therefore we assumed that EslB and EslC form a heterodimer. Unfortunately, further bacterial two-hybrid experiments revealed the sticky and unspecific nature of the transporter proteins in this particular experimental set-up, thus the results need to be interpreted with caution. Curiously, analysis of a $\Delta es/C$ deletion strain revealed that the strain does not share any phenotypic characteristics with $\Delta es/A$ or $\Delta es/B$ deletion strains, raising the question if EslC is involved in the function of the transporter, or if it plays a role in unrelated processes. Subsequent whole genome sequencing of the strain did not reveal any mutations, but it seems that the strain possesses several unspecific gene amplifications, which might explain the lack in phenotypic defects. The role of EslC as part of the EslABC transporter remains to be elucidated. During the course of our study we focused on a $\Delta es/B$ deletion strain.

Both, EslA and EslB were previously associated with lysozyme resistance in *L. monocytogenes* by two independent studies (Burke et al. 2014; Durack et al. 2015). The natural antimicrobial lysozyme is part of the human innate immune system and cleaves the β -1,4-bond between the GlcNAc and MurNAc residue of the glycan strand in the cell wall (Callewaert and Michiels 2010). In *L. monocytogenes*, lysozyme resistance is mainly achieved by *N*-deacetylation of the GlcNAc residue by PgdA and *O*-acetylation of the MurNAc residue of the PG by OatA (Boneca et al. 2007; Aubry et al. 2011). To understand the underlying mechanism responsible for lysozyme sensitivity in the $\Delta es/B$ deletion strain, isolated PG was compared to PG isolated from the 10403S wildtype strain. Interestingly, the PG of the mutant strain was slightly more cross-linked and featured a slight increase in deacetylated GlcNAc, which is normally associated with enhanced lysozyme resistance and reduced autolysis (Rae et al. 2011; Popowska et al. 2009; Rismondo et al. 2021). In contrary, a colorimetric assay revealed that the PG of $\Delta es/B$ is less *O*-acetylated. Hence, it seems that while PgdA localization and function is not altered in the mutant strain, the expression, activity, or localization of OatA might be impaired, resulting in decreased *O*-acetylation and sensitivity towards the natural antimicrobial

lysozyme (Figure 7.1 A). So far, lysozyme sensitivity of OatA was only observed when the gene coding for the *O*-acetyltransferase was deleted in combination with deletion of PgdA. Consequently, the lysozyme sensitivity of the $\Delta es/B$ mutant strain might result from another factor auxiliary to altered OatA activity. Since we observed minor structural changes in the PG as well as a cell division defect, we compared the cell wall thickness of the wildtype, $\Delta es/B$ deletion strain and a complementation strain in BHI medium and BHI medium supplemented with sucrose, where the deletion strain experiences impaired growth. Interestingly, the cell wall is significantly thinner in $\Delta es/B$, potentially leaving it more susceptible towards the activity of lysozyme (and other hydrolases). The decrease in cell wall thickness could also result in increased susceptibility towards osmotic stress in sugar containing media. It has to be mentioned that the sugar-dependent growth defect was only observed for glycolytic sugars such as sucrose and glucose, but not for non-glycolytic carbon sources such as succinate or ribose or in presence of high salt concentrations (data not shown). If the cells are more vulnerable to osmotic stress, one would expect a growth defect in presence of either increased sugar or salt concentrations. However, a transposon-based study in *S. aureus* revealed that distinct osmotic stress does not equal osmotic stress in general and that essentiality and dispensability of genes differ in presence of sucrose and salt stress (Schuster et al. 2020). While for instance the gene coding for the protease ClpCP, which is among others involved in controlling the PG pool, was essential in presence of sucrose stress, it was unessential for cells grown in presence of NaCl. Interestingly, *murAA*, *pbp3* or *dltA* were dispensable in presence of sucrose, while genes from the *dlt* operon *dltABCD*, *tagO*, *murAA* and *mfd* were essential under NaCl stress. The *dlt* operon is important for *D*-alanylation of WTA, while TagO is the first enzyme to initiate WTA biosynthesis. Hence, it seems that WTA plays a rather significant role in NaCl-induced osmotic stress, but not so much under sucrose stress. The phenotypic differences in the $\Delta es/B$ mutant might thus be due to the fact that gene essentiality differs in presence of NaCl and sucrose stress. Another explanation for the phenotype might be justified by the separate metabolic routes, taken by the different sugars inside the cell.

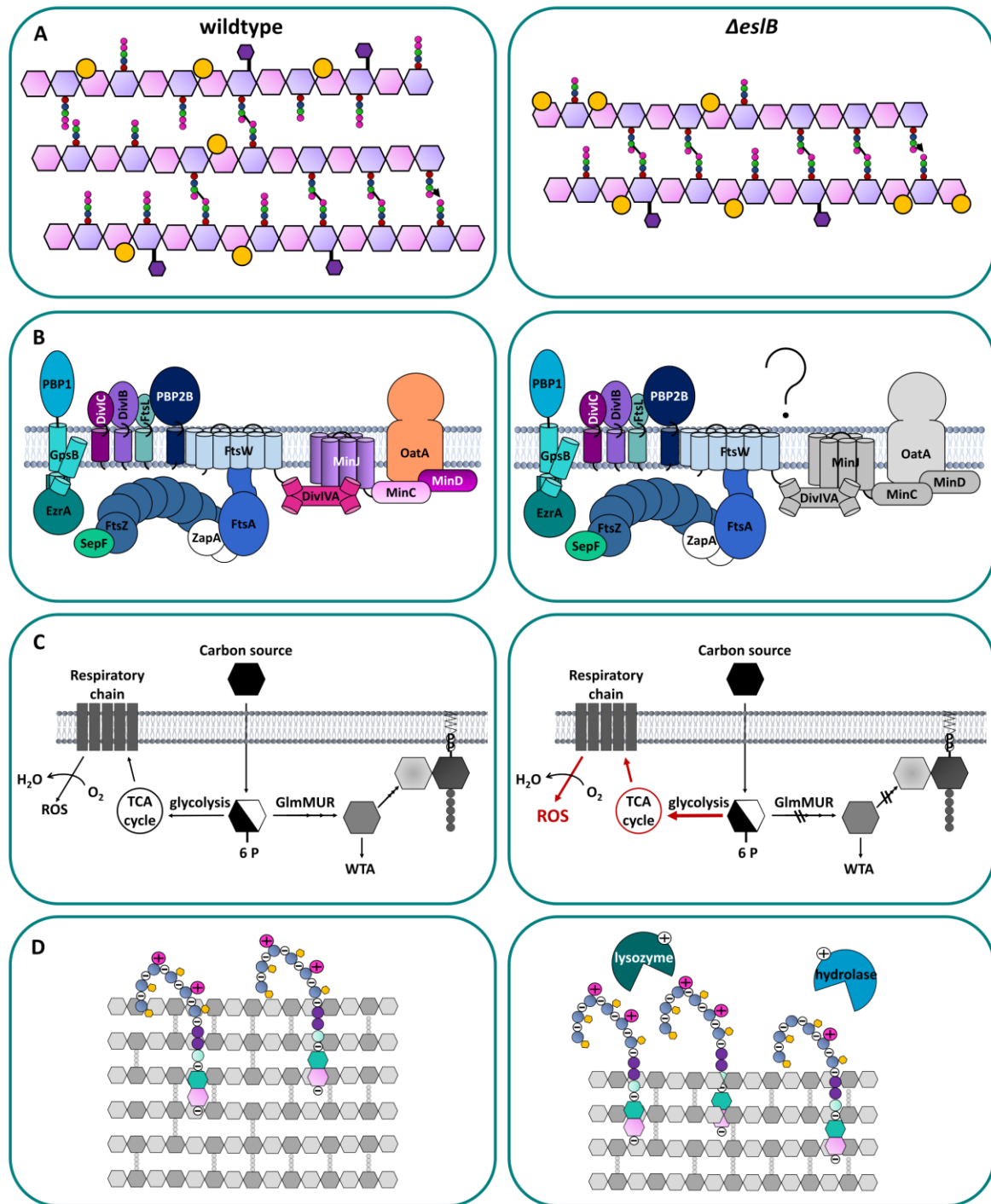


Figure 7.1 | Phenotypic overview of the *es/B* deletion strain. **A** Differences in the PG composition between wildtype and *Δes/B* deletion strain. The peptidoglycan layer of the *Δes/B* mutant is significantly thinner and less *O*-acetylated (purple hexagon). At the same time, it is slightly more cross-linked and *N*-deacetylated (yellow circles) in comparison to the PG of the wildtype. **B** Potential involvement of OatA as part of the divisome complex. In *Δes/B*, the late cell division protein DivIVA does not properly localize, likely due to disrupted activity and/or localization of upstream divisome proteins which results in elongated cells (depicted in grey). Likewise,

disrupted OatA activity could be a result of an interaction with MinCD that possibly also exhibit disrupted activity due to their dependency on DivIVA. **C** Altered carbon flux. A disruption of the PG biosynthesis pathway possibly results in the increased flow of carbon into glycolysis that finally results in the production of reactive oxygen species (ROS). The addition of sugars such as sucrose might enhance this process. **D** Increased surface charge. The wall teichoic acids (WTA) have a characteristic ribitol phosphate backbone that contributes to the overall negative surface charge (indicated as a circle containing a -). The backbone can be decorated with GlcNAc residues (yellow hexagons) and positively charged *D*-alanine (indicated as a pink +), which can mask the overall negative charge. The precursor UDP-GlcNAc is shared between the PG biosynthesis pathway and WTA biosynthesis and hence altered distribution of UDP-GlcNAc, e.g., by directing it into WTA biosynthesis might result in a thinner cell wall and potentially in increased WTA content. A thinner cell wall could additionally increase the portion of the negatively charged WTA backbone that is exposed to the outside of the cell, resulting in a more negatively charged cell surface. This in turn could affect binding and activity of cationic compounds such as lysozyme and cell wall hydrolases.

While glucose and sucrose are directed into glycolysis and subsequently feed into the tricarboxylic acid (TCA) cycle and respiratory chain, the pentose sugar ribose is consumed in the pentose phosphate pathway and succinate is converted to e.g., glucose via gluconeogenesis. Glycolytic sugars are also essential for the biosynthesis of PG. Accordingly, its distribution between glycolysis and PG biosynthesis needs to be tightly regulated. In *B. subtilis*, GlmS is important for directing fructose-6-phosphate towards PG biosynthesis by converting it to glucosamine-6-phosphate, thereby initiating the synthesis of the PG precursor UDP-GlcNAc (Patel et al. 2018; Patel et al. 2023). Activity of GlmS seems to be dependent on interaction with GlmR in *B. subtilis*. However, the GlmR-dependent regulation of GlmS could not be verified in *L. monocytogenes* up to date (Pensinger et al. 2023). Misregulation of the distribution of carbon sources could result in detrimental effects for the cell. An increased sugar flux into glycolysis can in the end lead to accumulation of reactive oxygen species (ROS) in the respiratory chain, as has been reported for bacterial L-forms that lack a cell wall (Kawai et al. 2015; Kawai et al. 2019). This effect can only be seen for glycolytic sugars and is not detrimental when cells are grown in the presence of succinate. Furthermore, a recent study showed that resistance towards the cell wall targeting antibiotic ampicillin could be achieved by regulating glucose uptake, inhibiting glycolysis and the subsequent flux of glucose into the pentose phosphate pathway (Jiang et al. 2023).

In the $\Delta es/B$ strain, a thinner cell wall indicates a disrupted PG biosynthesis, which might result in an increased flux into glycolysis and increased production of reactive oxygen species (Figure 7.1 C). Overexpression of proteins of the GlmSRUM cascade in the $\Delta es/B$ background only resulted in a beneficial effect for GlmM and GlmR and the growth defect in presence of sucrose penicillin could only be partially rescued. If an increased flux of carbon into glycolysis is detrimental, overexpression of GlmSRUM, especially GlmS should have a more beneficial effect. It could be that the activity of

GlmS is downregulated (e.g., by GlmR) and a simple overexpression does not equal enhanced protein activity. In addition, disturbed activity of proteins downstream of the GlmSMUR pathway could still lead to a block of carbon flux and thus the carbon drain might not be altered in an overexpression strain. Interestingly, we isolated a suppressor mutant on BHI agar supplemented with sucrose and penicillin that carried a mutation in *lmo0214*, resulting in a frameshift. The gene codes for the ATP-dependent DNA translocase Mfd, which has been associated with ROS-induced DNA lesion repair and as a factor that regulates transcription in stressed cells in several organisms, including *E. coli* and *B. subtilis* (Martin et al. 2019; Smith et al. 2012; Smith et al. 2007). The *mfd*^{lle976fs} mutation could bypass phenotypic defects in presence of sucrose and penicillin, heat and suppressed the cell division defect, indicating that ROS levels could indeed be altered in the $\Delta es/B$ strain (Figure S1). The *E. coli* Mfd protein consists of 8 domains, from which domain 5 and 6 form an active site, which is surrounded by the N-terminal and C-terminal domain of the protein that form a “clamp”, which masks the active site (Deaconescu et al. 2012; Smith et al. 2007). We hypothesized that the frameshift mutation results in disruption of the C-terminal D7 domain, thereby rendering the active site exposed and the protein in a continuous active state. This would in turn allow for a better stress induced response especially towards ROS generated stress. We additionally isolated a suppressor conferring a frameshift mutation in *lmo2230*, a gene coding for a putative arsenate reductase that is part of the primary stress regulon SigB (Raengpradub et al. 2008; Oliver et al. 2009). Lmo2230 shows 28% sequence identity to the arsenate reductase ArsC from *B. subtilis*, which is involved in heavy metal detoxification and regulated by the disulfide stress regulator SpxA upon oxidative stress (Nakano et al. 2003). So far, the precise function of Lmo2230 remains unclear in *L. monocytogenes* and the characteristic cysteine amino acid residue that is essential for the specific arsenate reductase activity of *B. subtilis* is not present in Lmo2230. The protein was hence suggested to play a broader, more general role in stress response in *L. monocytogenes* (Bennett et al. 2001; Cortes et al. 2019).

Altogether, even though we do not have clear evidence for increased ROS levels in the transporter mutant, it is likely that the growth defect in presence of sucrose is a combinational effect resulting from increased osmotic stress caused by distorted cell integrity and at the same time increased sugar flux into glycolysis and subsequent ROS production due to defects in carbon distribution. Taken this into account, it is likely that the $\Delta es/B$ mutant exhibits altered PG synthesis which results in a thinner cell wall.

A similar cell wall associated phenotype was observed for the closest homologue of EslABC, the YtrBCDEF ABC transporter of *B. subtilis*. YtrB and YtrC/YtrD show 35% and 22% sequence similarity to EslA and EslB, respectively. However, the genomic organization is vastly different. The transporter is located in an operon consisting of *ytrGABCDEF*. *ytrB* and *ytrE* code for two nucleotide binding proteins, and *ytrC* and *ytrD* for two transmembrane domain proteins. *ytrF* codes for a solute binding protein but the overall structure and organization of the transporter complex is still unknown (Yoshida et al. 2000; Quentin et al. 1999). *ytrA* codes for a transcriptional repressor and YtrA-dependent repression of the transporter is prevented during cold shock or in presence of cell wall-targeting antibiotics (Beckering et al. 2002). Interestingly, both EslABC and YtrBCDEF have been annotated as acetoin transporters (Yoshida et al. 2000). Though, the actual role of YtrBCDEF in acetoin import and utilization seems to be rather minor (Yoshida et al. 2000; Rismondo and Schulz 2021). Transformation experiments revealed that especially YtrF is important for competence and overexpression of transporter components led to a thicker cell wall (Koo et al. 2017; Benda et al. 2021). Hence, both EslABC and YtrBCDEF seem to play a role in cell wall metabolism. In contrast to *L. monocytogenes*, *B. subtilis* is naturally competent and thus can take up DNA from its environment, especially in nutrient limiting conditions. Binding and uptake of DNA is mediated by the presence of WTA (Mirouze et al. 2018). It is likely that cell wall thickness affects interaction of DNA *via* WTA and the DNA uptake apparatus ComG/ComE, allowing uptake of foreign DNA (Dubnau 1991). In concordance with its role in cell wall metabolism, the transporter was also associated with resistance towards the cell wall-targeting antibiotics vancomycin and nisin (Hutter et al. 2004; Wenzel et al. 2012). Interestingly, YtrF contains a FtsX like domain. FtsX is part of the FtsEX ABC transporter, which does not have a role in transport of cognate substrates, but is essential for regulation of the activity of the cell wall hydrolase CwLO in *B. subtilis* (Meisner et al. 2013). Consequently, it is tempting to speculate that YtrF might also be directly or indirectly involved in cell wall hydrolysis, and in this manner influences cell wall thickness in response to available extracellular DNA. Further experiments are necessary to clarify the role of YtrBCDEF in cell wall metabolism.

7.3 Potential role of EslB in cell wall biosynthesis

In an attempt to get a better understanding of the function of the EslABC transporter we evolved the $\Delta es/B$ strain under conditions where the strain had a growth defect in comparison to the wild type, including lysozyme stress, heat stress, sucrose (\pm penicillin), and glucose stress. A summary of all suppressors is depicted in Table 7.1. Indeed, various suppressors possessed mutations in genes associated with cell wall biosynthesis, decoration and modification, including *murZ* (*Imo2552*), *prpC* (*Imo1821*), *reoM* (*Imo1503*), *clpCP* (*Imo0231/Imo0232*) and *pbpA1* (*Imo1892*), which are directly involved in peptidoglycan synthesis, *ftsE* (*Imo2507*), *ftsX* (*Imo2506*), and *cwI/O* (*Imo2505*), which are involved in cell wall hydrolysis, as well as *tarL* (*Imo1077*) and the promoter region of *dltX* (*Imrg_02074*), which are involved in WTA biosynthesis and decoration (Figure 7.2). When taking a closer look at the genes associated with peptidoglycan biosynthesis, it becomes clear that they are particularly centred around controlling MurA levels, the enzyme executing the first committed step of PG biosynthesis (Barreteau et al. 2008). Both ReoM and MurZ directly or indirectly stimulate ClpCP-dependent proteolysis of MurA (Wamp et al. 2022; Wamp et al. 2020; Kock et al. 2004; Birk et al. 2021). Knockdown mutations in genes coding for either of the proteins would consequently result in increased MurA levels (Figure 7.2). PrpC is involved in dephosphorylation of ReoM, which in turn stimulates the protease activity of ClpCP (Kelliher et al. 2021; Wamp et al. 2020). Since MurZ, PrpC, and ReoM are all involved in ClpCP-dependent degradation of MurA, we speculated that the suppression mechanism is due to increased MurA activity and hence increased production of PG. MurA, in conjunction with MurB, sequesters UDP-GlcNAc to produce UDP-MurNAc, which is further converted to lipid I and lipid II by MurC-F, MraY and MurG (Vollmer et al. 2008; Egan et al. 2020). Indeed, the artificial overproduction of MurA in the $\Delta es/B$ background similarly suppressed the phenotypic defects of the mutant strain. In line with the idea that PG biosynthesis is disturbed, is the observation that the $\Delta es/B$ mutant strain is more sensitive towards the antibiotics fosfomycin and *t*-Cinnamaldehyde, which directly target the activity of MurA and the steps important for biosynthesis of UDP-GlcNAc, respectively (Sun et al. 2021b; Marquardt et al. 1994). In contrast, no changes in sensitivity were observed for antibiotics that target later steps in the PG biosynthesis pathway, such as vancomycin or nisin (Figure 7.2). These data suggest that either MurA activity is disturbed in the $\Delta es/B$ strain or that the availability of UDP-GlcNAc is reduced, eventually leading to reduced PG levels and a thinner cell wall. As mentioned in Chapter 7.2, overexpression of the enzymes involved in UDP-GlcNAc biosynthesis GlmM and GlmR, could partially rescue the *es/B* phenotypes, further

strengthening the idea that the synthesis or availability of UDP-GlcNAc is disturbed (Pensinger et al. 2023).

Table 7.1 | Overview of sequence alterations in the *L. monocytogenes* Δ eslB background. Assorted colours highlight the associations of the genes in underlying cellular pathways. Light pink: genes associated with MurA degradation. Light purple: genes associated with cell wall homeostasis. Light blue: genes associated with activity of the cell wall hydrolase CwlO. Light turquoise: genes associated with wall teichoic acid synthesis and decoration. Green: genes associated with cell division.

Gene	Mutation ¹	Function ²	Stress ³	Reference
Suppressors in ΔeslB				
<i>murZ</i> (<i>Imo2552</i>)	Met240fs Gln307fs	UDP- <i>N</i> -acetylglucosamine 1-carboxyvinyltransferase Involved in ClpCP-dependent degradation of MurA	BHI 0.5 M Sucrose + Pen G	(Wamp et al. 2020)
<i>cdaA</i> (<i>Imo2120</i>)	Thr146Ile Arg87Cys	Deadenylate cyclase c-di-AMP is mainly involved in cell wall metabolism and osmoregulation	BHI 0.5 M Sucrose + Pen G	(Rosenberg et al. 2015)
<i>walk</i> (<i>Imo0288</i>)	Arg553His Asp283Glu Ala570Val Ile583Thr His463Asp Val234Leu Arg480His His368Tyr Pro600Ser Asp336Gly	Sensor histidine kinase, part of the WalRK two-component system Regulation of autolysins and other cell wall components. Important for cell wall homeostasis	BHI 0.5 M Sucrose + Pen G Lysozyme Sucrose	(Dobihal et al. 2019)
<i>ftsE</i> (<i>Imo2507</i>)	Gln220-	NBD of the FtsEX ABC transporter Essential for the activity of the cell wall hydrolase CwlO	BHI 0.5 M Sucrose + Pen G	(Meisner et al. 2013)
<i>ftsX</i> (<i>Imo2506</i>)	Gly253Arg	TMD of the FtsEX ABC transporter Essential for the activity of the cell wall hydrolase CwlO	BHI 0.5 M Sucrose + Pen G	(Meisner et al. 2013)
<i>cwlO</i> (<i>Imo2505</i>)	Arg106His Arg135Pro	<i>D,L</i> -endopeptidase	BHI 0.5 M Sucrose + Pen G	(Meisner et al. 2013);

		Regulated by WalRK and FtsEX Cleaves the existing PG layer allowing newly synthesised PG to be incorporated		Hashimoto et al. 2012)
<i>mfd</i> (<i>Imo0214</i>)	Ile976fs	Transcription repair coupling factor	BHI 0.5 M Sucrose + Pen G	(Martin et al. 2019)
		Possible regulatory function upon ROS/ general stress response/ protects against ROS in <i>B. subtilis</i>		
<i>reoM</i> (<i>Imo1503</i>)	Lys23fs	Dephosphorylated enhances ClpCP dependent regulation of MurA	BHI 0.5 M Sucrose + Pen G	(Wamp et al. 2020)
<i>corA</i> (<i>Imo1064</i>)	Ala244Thr	Putative Mg ²⁺ and Co ²⁺ transporter	BHI 0.5 M Sucrose + Pen G	(Warren et al. 2004)
<i>prpC</i> (<i>Imo1821</i>)	Pro159Leu	Serine/threonine phosphatase	BHI 0.5 M Sucrose + Pen G	(Wamp et al. 2022)
		Dephosphorylates ReoM → involved in ClpCP dependent degradation of MurA		
<i>tarL</i> (<i>Imo1077</i>)	Pro282Leu	TarL homologue	BHI 0.5 M Sucrose + Pen G	(Brown et al. 2013)
		Adding ribitol-phosphate units to the growing WTA backbone		
<i>walR</i> (<i>Imo0287</i>)	Ser216Gly Ala82Val* Glu12Gly	Transcriptional regulator, part of the WalRK two-component system	Lysozyme	(Dobihal et al. 2019)
	Arg120Cys	Regulation of autolysins and other cell wall components. Important for cell wall homeostasis	Sucrose	
<i>anrA</i> (<i>Imo2114</i>)	Arg180Val Gly148Asp	NBD of the AnrAB ABC transporter	Lysozyme	(Jiang et al. 2019a)
		Involved in antibiotic resistance such as nisin and bacitracin		
<i>lbrA</i> (<i>Imo2241</i>)	Gln23Pro	GntR-family transcriptional regulator	Lysozyme	(Zhu et al. 2011)

		Unknown function		
<i>dltX</i> (<i>Imrg_02074</i>)	<i>p^{T-31C}</i>	Part of the <i>dlt</i> operon Incorporation of D-Ala in teichoic acid backbones	Lysozyme	(Kovács et al. 2006)
<i>clpCP</i> (<i>Imo0231-Imo0232</i>)	deletion of <i>clpP</i> and 1333 bp of <i>clpC</i>	Part of the ClpCP protease Degradation of (among others) MurA	Glucose	(Birk et al. 2021; Wamp et al. 2020)
<i>clpX</i> (<i>Imo1268</i>)	Ala81Asp Gly15Asp	Chaperone, part of the ClpXP protease Regulated by SigB, involved in cell division and degrades FtsZ, DivIVA and MreB degradation	Glucose	(Smith et al. 2014)
<i>P[*]</i>		42°C		
Suppressors in <i>ΔeslB cwI^{O^{R106H}}</i>				
<i>walR</i> (<i>Imo0287</i>)	Arg204Ser	Regulation of autolysins and other cell wall components. Important for cell wall homeostasis	Lysozyme	(Dobihal et al. 2019)
<i>walR</i> (<i>Imo0287</i>)	Asn117Ser	See above	Lysozyme	(Martin et al. 2019)
<i>mutY</i> (<i>Imo1689</i>)	Asp180fs	A/G-specific adenine glycosylase interacts with Mfd which has a possible regulatory function upon ROS/ general stress response/ protects against ROS in <i>B. subtilis</i>		
<i>prpC</i> (<i>Imo1821</i>)	Asp8Asn	Serine/threonine phosphatase Dephosphorylates ReoM → involved in ClpCP dependent degradation of MurA	Lysozyme	(Wamp et al. 2022)

¹ Type of mutation with the amino acid position in the *L. monocytogenes* 10403S reference genome. fs = mutation leading to a frameshift; - = mutation resulting in a premature stop codon.

² functional annotations. NBD = Nucleotide Binding Domain; TMD = Transmembrane Domain; ABC transporter = ATP binding cassette- transporter.

³ conditions used to evolve suppressors: lysozyme 100 µg ml⁻¹; PenG = 0.025 or 0.5 M penicillin G; glucose 0.5 M.

The *cwI^{O^{R106H}}* mutant strain was further evolved in presence of 100 µg ml⁻¹.

Since it is unclear if EslABC is involved in translocation of substrates across the membrane, we took a closer look at possible transport mechanisms that are important for cell wall biosynthesis. One possibility is that EslABC is importing *N*-acetylglucosamine (GlcNAc) into the cell, which is converted to GlcNAc-6-phosphate and utilized by GlmMUR to produce UDP-GlcNAc. Reduced or diminished GlcNAc uptake in the $\Delta es/B$ strain could thus result in a decreased UDP-GlcNAc pool. However, the transporter mutant did not experience a growth disadvantage in LSM defined minimal medium with GlcNAc as the sole carbon source in comparison to LSM medium containing glucose as the sole carbon source (Figure S2). Similarly, the addition of GlcNAc did not have a beneficial effect for the $\Delta es/B$ strain in presence of sucrose and penicillin or heat stress, indicating that EslABC is not involved in GlcNAc transport or merely plays a minor role (Figure S2 B). GlcNAc supplementation should theoretically lead to an increased UDP-GlcNAc pool and therefore to increased PG biosynthesis raising the question why we did not observe a beneficial effect upon its supplementation. One theory is that the GlmMUR pathway is disrupted in the $\Delta es/B$ strain and as a result GlcNAc cannot be utilized to increase the UDP-GlcNAc pool. In *B. subtilis* GlcNAc is translocated across the membrane and phosphorylated by the phosphoenolpyruvate-dependent phosphotransferase system (PTS) transporter NagP to produce GlcNAc 6-phosphate. NagA subsequently converts it to glucosamine 6-phosphate, which can either be directed into PG biosynthesis or glycolysis (Plumbridge 2015). In contrast to *B. subtilis*, *L. monocytogenes* does not possess a NagP homologue and the uptake and intracellular fate of GlcNAc is thus unclear. Consequently, it is difficult to draw a conclusion and further analysis is required to understand the potential impact of EslABC on the GlmMUR pathway.

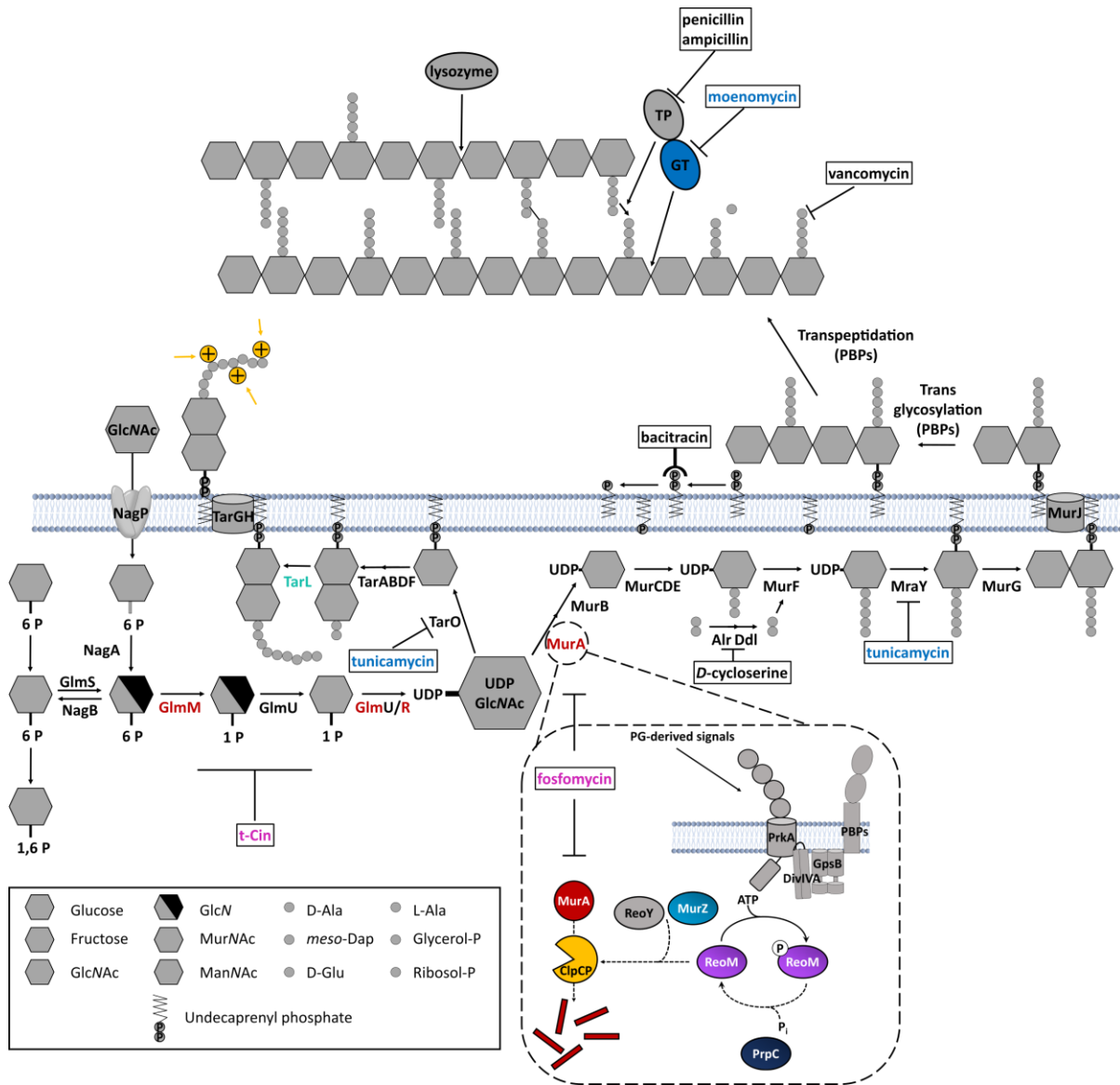


Figure 7.2 Suppression mechanisms associated with cell wall biosynthesis. The general biosynthesis pathway of peptidoglycan and wall teichoic acids is depicted. Proteins with underlying genomic mutations identified in the *ΔesB* suppressors are depicted in colour. MurZ, ReoM, PrpC and ClpCP are involved in MurA degradation and hence knock-down mutations result in enhanced MurA levels and overexpression of MurA can rescue the phenotypes of the transporter mutant. The strain is more sensitive towards the antibiotics *t*-Cinnamaldehyde (*t*-cin) and fosfomicin (shown in pink) which further decrease the production or utilization of UDP-GlcNAc. In contrast the strain is more resistant to tunicamycin (blue) which at low concentrations inhibits WTA biosynthesis and likely increases the availability of UDP-GlcNAc for PG biosynthesis. Mutations in the glycosyltransferase domain in the gene coding for PBP A1 could also rescue phenotypes of the *ΔesB* mutant strain and supplementation with moenomycin, which targets glycosyltransferase activity of PBPs had a similarly beneficial effect. Likewise, increased promoter activity of the *dlt* operon results in increased *D*-alanylation (yellow +) and the overexpression of GlimM, GlimR and MurA (red) also showed a beneficial effect.

Another possibility is that EslABC is involved in the recycling of shed peptidoglycan fragments. Since the multifaceted biosynthesis process is extremely energy consuming, *L. monocytogenes*, like many other gram-positive and gram-negative bacteria, recycles approximately 50% of their PG (Goodell 1985). In *B. subtilis* the *murRQP* operon is important for PG turnover. *murR* codes for a transcriptional regulator of the operon, while *murP* codes for the phosphotransferase system (PTS) transporter MurP, which specifically translocates MurNAc yielding MurNAc-6-phosphate. *murQ* codes for a MurNAc-6-phosphate etherase, which utilizes MurNAc-6-phosphate to produce GlcNAc-6-phosphate that can subsequently be introduced into PG biosynthesis (Borisova et al. 2016). The 10403S *L. monocytogenes* does not possess a homologue of this system, yet a similar system is present in *L. monocytogenes* WSLC1042. We introduced the MurRQP transport system from *B. subtilis*, as well as a system from *L. monocytogenes* WSL1042 into the $\Delta es/B$ deletion strain under the control of an IPTG-inducible promoter (Borisova et al. 2016). We could not observe a beneficial effect when overexpressing any of the two systems, suggesting that PG reshuffling is not disturbed in the $\Delta es/B$ background (data not shown). However, experimental set-up and expression levels of the two systems might not have been ideal in the strain and thus preliminary results have to be taken with caution. Altogether, our data suggests that peptidoglycan levels are reduced in the $\Delta es/B$ deletion strain possibly resulting from an altered UDP-GlcNAc pool.

7.4 Detrimental activity of the cell wall hydrolase Cw/O in the $\Delta es/B$ strain

Apart from suppressors directly related to PG biosynthesis, several suppressors carried mutations in genes associated with activity of the cell wall hydrolase Cw/O. Cw/O is a D,L-endopeptidase, which cleaves the already existing peptidoglycan, so that newly synthesized peptidoglycan precursor can be added into the growing strain by the Rod system (Smith et al. 2000; Cho et al. 2016). Mutations were located either directly in the gene coding for the hydrolase or in genes coding for the subunits of FtsEX, an ABC transporter which is essential for Cw/O activity (Figure 2.3) (Meisner et al. 2013). Under laboratory growth conditions, FtsEX is essential in *L. monocytogenes* and thus mutations presume that this essentiality might be lost in the $\Delta es/B$ background, or that FtsEX activity is only slightly reduced (Fischer et al. 2022). Deletion of *cw/O* in the $\Delta es/B$ mutant strain confirmed that indeed hydrolase activity has a negative effect for the $\Delta es/B$ strain. Nevertheless, it is not clear, if the activity of Cw/O is altered in the $\Delta es/B$ strain or if the cell wall of the $\Delta es/B$ strain is more susceptible towards hydrolysis in general. Interestingly, even though both *es/B* and *cw/O* single mutants experienced reduced growth

at high temperatures, which is characteristic for cell wall mutants, a double deletion could suppress this growth defect. A similar effect was seen for hydrolase defective *S. aureus* strains that were treated with cell wall-targeting antibiotics (Salamaga et al. 2021). Individually, both, deficiency of hydrolase activity and antibiotic-induced inhibition of cell wall biosynthesis, resulted in cell death due to imbalance of cell wall biosynthesis and hydrolysis, however, a combinational defect rescued growth by restoring cell wall homeostasis. A deletion of both *eslB* and *cwIO* might therefore rescue the heat phenotype, by restoring the balance of cell wall biosynthesis and hydrolysis. In contrast, decreased hydrolase activity could not restore resistance towards the natural antimicrobial lysozyme, suggesting that lysozyme sensitivity is not a consequence of disturbed hydrolase activity. In an attempt to elucidate the underlying mechanisms of lysozyme sensitivity, we further evolved the $\Delta eslB cwIO^{R106H}$ strain in presence of lysozyme stress (Table 7.1). Most mutants carried mutations in *walR*, a transcriptional regulator generally involved in cell wall homeostasis, which will be discussed in detail later on. One *walR* mutant carried a tertiary mutation the gene coding for MutY, which interacts with the previously described ATP-dependent DNA translocase Mfd in *B. subtilis* (Martin et al. 2019). Another one had a base exchange in *prpC* leading to a change from aspartic acid to asparagine at position 8, which, as described above, presumably results in increased MurA activity and hence enhanced cell wall biosynthesis (Wamp et al. 2020). Moreover, the supplementation of Mg^{2+} could likewise rescue the phenotypic growth defects of the $\Delta eslB$ strain. Interestingly, the rescue effect of Mg^{2+} for cell wall mutants was proposed to take effect by inhibiting hydrolase activity, probably indirectly *via* binding to the negatively charged surface, thereby competing with the activity of hydrolases (Tesson et al. 2022). Mg^{2+} has been shown to bind both the negatively charged backbone of WTA and the carboxyl groups of PG components (Beveridge and Murray 1980; Kern et al. 2010). The addition of Mg^{2+} might also reduce binding and activity of the cation lysozyme, by masking the negative surface charge. Interestingly, in *E. coli*, increased hydrolase activity has been associated with enhanced activity of class A PBPs, which are involved in polymerization and cross-linking of new glycan strands (Lai et al. 2017). An increased activity of CwIO could potentially influence cross-linking in the PG of the $\Delta eslB$ strain in contrast to the wildtype strain. Moreover, CwIO is predicted to be part of a complex with Mbl and MreB, which are important components of the cell wall elongation machinery (Kawai et al. 2011; Domínguez-Cuevas et al. 2013). The *eslB* mutant strain exhibits a more negative overall surface charge (see Chapter 7.7). This likely increases the binding and activity of the positively charged hydrolase and explains aberrant hydrolase activity in the mutant strain (Figure 7.1 D).

7.5 Suppression by restoring general cell wall homeostasis

Several suppressors carried mutations in either of the genes coding for the two-component system WalRK. The histidine kinase WalK phosphorylates WalR, resulting in dimerization and DNA binding. WalR is additionally regulated by PrkC in *B. subtilis* (PrkA in *L. monocytogenes*), likely in response to PG-associated signals (Libby et al. 2015). PrkA is also involved in the phosphorylation of ReoM and thereby decreases ClpCP-dependent degradation of MurA resulting in increased PG production (Wamp et al. 2020). WalR is known to regulate several crucial processes associated with the cell wall (Figure 2.3). This includes transcription of *cw/O* in response to high or low D,L-endopeptidase activity (Dobihal et al. 2022; Dobihal et al. 2019). Consequently, knock-down mutations could be responsible for reduced Cw/O levels, which have a similarly beneficial effect as the deletion of *cw/O* described above. However, WalR is additionally important for the activation of other cell wall hydrolases, as well as MreBH, which are essential components of the elongasome. In addition, overexpression of WalRK was shown to increase promoter activity of the *ftsAZ* operon in *B. subtilis* that codes for FtsA and FtsZ, two factors essential for cell division (Fukuchi et al. 2000; Huang et al. 2013). Mutations in *walRK* might contribute to proper cell morphology by simultaneously reducing the activity of hydrolases as well as elongasome velocity as a result from reduced MreBH filament density. In contrast, WalR represses transcription of *pdaC* (*pgdA* in *L. monocytogenes*) and is involved in the increase of WTA content (Howell et al. 2003). High hydrolase activity results in increased WalR-dependent de-repression of *pdaC* and consequently to increased *N*-deacetylation (Ravikumar et al. 2014). If enhanced hydrolase activity increases the overall levels of cleavage products in the $\Delta es/B$ strain, WalR activity is likely already reduced, which could result in increased PgdA levels, proposedly explaining the minor increase in *N*-deacetylation of GlcNAc in the PG of $\Delta es/B$. One could speculate that further reduction of WalR activity due to acquired mutations could in turn additionally increase *N*-deacetylation by PgdA ultimately restoring the lysozyme resistance of $\Delta es/B$. It has to be mentioned that while we identified a potential WalR binding domain upstream of *pgdA*, a role of WalR in *pgdA* regulation has not yet been described for *L. monocytogenes*. Additionally, reduced WalRK activity has been brought in association with lysozyme resistance, independent of PgdA (Burke and Portnoy 2016). In contrast to Cw/O-associated suppressor mutants, lysozyme resistance was restored in *walRK* suppressors, further supporting the idea that deactivation of hydrolase activity is not the sole suppression mechanism, and that WalR is involved in the regulation of additional factors that are specifically important for lysozyme resistance. Altogether, WalR plays a crucial regulatory role in

global processes important for the overall cell wall architecture and we hypothesize that the underlying WalRK-dependent suppression mechanism is based on restoring a balanced cell wall homeostasis.

7.6 Involvement of EslB in wall teichoic acid synthesis and modification

As mentioned above, WalRK is also involved in the adjustment of WTA content by regulating the expression of the *tagAB* and *tagDEFG* operon in *B. subtilis* and *S. aureus*, indicating that the suppressor mutations might also impact WTA biosynthesis (Howell et al. 2003; Dubrac et al. 2007). Indeed, several phenotypes and suppressors suggest alterations in the synthesis and presentation of WTA in a strain lacking EslB. A mutation in *Imo1077* could rescue growth defects in presence of sucrose penicillin or lysozyme. *Imo1077* codes for a TarL homologue, which is involved in the polymerization of the WTA backbone by adding over 40 ribitol-phosphate (RboP) units to the linker unit of the growing chain (Brown et al. 2013; Pereira et al. 2008). The synthesized RboP backbone itself can be decorated with D-alanine esters which mask the negative charge of the phosphate backbone, or with monosaccharides, such as GlcNAc, rhamnose or D-glucose (Brown et al. 2013; Shen et al. 2017). The addition of D-alanine is achieved by enzymes encoded in the *dlt* operon and absence of D-alanylation results in an overall increased negative surface charge. Indeed, growth of the ΔesB strain was restored in a suppressor mutant that showed enhanced promoter activity of the *dlt* operon, implying that D-alanylation is beneficial for the ΔesB deletion strain. Interestingly, fluctuation in D-alanine levels have been shown to regulate the activity of cationic cell wall hydrolases subsequently controlling cell elongation, possibly due to the altered charge of the cellular surface (Heptinstall et al. 1970; Yamamoto et al. 2008b). Likewise, the lack of D-alanine modification in WTA from *S. aureus* in fact led to increased lysozyme and vancomycin susceptibility (Peschel et al. 2000). Furthermore, WTA biosynthesis and regulation have been brought in association with cell wall biosynthesis, and loss of WTA results in a spherical cell shape possibly due to the lack of hydrolase activity in *L. monocytogenes* and *B. subtilis* (Bhavsar et al. 2001; Eugster and Loessner 2012). Indeed, the transporter mutant showed an increased negative surface charge, which is similar to a strain completely lacking D-alanylation in a cytochrome C assay. This raises the question if modification and/or WTA content is altered in the ΔesB mutant strain. In line with this is the observation that the ΔesB strain was more resistant towards the antibiotic tunicamycin, which inhibits TarO, the initial enzyme in WTA biosynthesis, implying an increase in WTA content in comparison to the wild type strain. We assumed

that the cellular UDP-GlcNAc pool is increased when the activity of TarO or TarL are inhibited, since UDP-GlcNAc is consumed by TarO and used later on for WTA glycosylation (Brown et al. 2013). Instead, it can then be utilized for the production of peptidoglycan. In addition to the increased resistance towards tunicamycin, supplementation of the antibiotic could restore the growth defect of the $\Delta es/B$ mutant strain during heat stress, indicating that reduction/ inhibition of WTA biosynthesis is beneficial in the $\Delta es/B$ background. In addition, reduction of TarO activity could potentially save glucose-1-phosphate, another substrate of the WTA biosynthesis pathway, which could be redirected into the synthesis of UDP-GlcNAc by GlmMUR. Again, it remains elusive if WTA biosynthesis is altered and if a potentially increased biosynthesis is a result of either an excess UDP-GlcNAc, which cannot be used by MurA due to a dysfunctional PG biosynthesis pathway, or if biosynthesis of PG is reduced since the flux of UDP-GlcNAc into WTA biosynthesis is enhanced because of a so far unknown reason. Interestingly, fosfomycin sensitivity of the $\Delta es/B$ mutant strain is similar to wildtype levels in presence of tunicamycin, suggesting that the inhibition of TarO indeed results in improved MurA activity possibly due to increased availability of UDP-GlcNAc.

The WTA polymer is connected to the PG via a phosphodiester bond at the C6-hydroxyl group of MurNAc (Ward 1981; Brown et al. 2013). The same position is object of *O*-acetylation by the *O*-acetyltransferase OatA, contributing to lysozyme sensitivity. This raises the question if WTA and OatA compete for the same PG side chain and if increased WTA content subsequently decreases *O*-acetylation by blocking the C6-hydroxyl group of MurNAc (Aubry et al. 2011). The question is, if the $\Delta es/B$ strain has indeed more incorporated WTA, and if this is the case, if the decrease in *O*-acetylation is a result from this or if more WTA can be incorporated due to the lack of *O*-acetylation caused by aberrant protein activity of OatA. Decreased *O*-acetylation in combination with an overall more negative surface charge, resulting from enhanced exposure of WTA that facilitates enhanced lysozyme binding and activity, could be an explanation for the lysozyme sensitivity of the $\Delta es/B$ strain. It is tempting to speculate that similar to the regulation of hydrolases by *N*-deacetylation of PgdA, OatA might be involved in the regulation of WTA incorporation and/or synthesis by changing the *O*-acetylation state of the PG. It has to be mentioned that studies in *L. plantarum* showed the WTA content and distribution was not affected by altered *O*-acetylation patterns (Bernard et al. 2012). In general, WTA can contribute to a negative surface charge since they are not completely buried in the peptidoglycan meshwork, but rather expand beyond it. A thinner PG layer could consequently expose more of the negatively charged phosphate backbone, subsequently altering the surface charge and thus the activity of cationic compounds such as lysozyme and hydrolases. So far, a disruption in OatA

activity has not been linked to a heat-associated growth defect, indicating that this effect is OatA-independent (preliminary data not shown). Altogether, the data suggest that the overall surface charge of the $\Delta es/B$ strain is increased, possibly due to increased WTA incorporation and/or enhanced exposure, facilitating enhanced binding and activity of cationic compounds such as lysozyme and hydrolases, and subsequently resulting in the loss of intrinsic lysozyme resistance and overactive hydrolases (Figure 7.1 D).

7.7 Absence of EslB leads to altered localization of cell division proteins

As discussed above, several phenotypes and suppression mechanisms of the $\Delta es/B$ strain hint towards an altered PG biosynthesis. Peptidoglycan precursors are important for both elongation of the lateral cell wall and formation of a division septum that allows the separation of daughter cells after duplication of the bacterial genomic DNA. Both processes involve the coordinated activity of multiple enzymes and require communication and cooperation with the PG biosynthesis pathway. The underlying mechanisms and signals of this crucial communication have yet to be fully elucidated. The $\Delta es/B$ mutant strain has a cell division defect, which could be a symptom of an altered PG biosynthesis pathway, accompanied by altered hydrolase activity (Rismondo et al. 2021). The incorporation of PG, which is necessary to complete division after Z-ring formation might not be possible due to a reduced PG pool. This hypothesis is supported by the observation that the artificial overexpression of Mura can suppress the cell division defect. A link between the production of cell wall precursors, cell elongation and growth rate was, as previously mentioned, shown to be achieved by the serine histidine kinas PrkC in *B. subtilis*, indicating tight intercommunication between the pathways (Sun et al. 2023). In addition, a recent study in *S. aureus* revealed that peptidoglycan synthesis is essential for septum constriction (Puls et al. 2023). In the presence of the cell wall targeting antibiotics vancomycin and telavancin septum constriction was halted independent of FtsZ treadmilling activity. They further demonstrated that recruitment of PBP2 to the septum is required for septum closure and concluded that PG biosynthesis determines proper late-stage cell division. Thus, aberrant PG biosynthesis in the $\Delta es/B$ could be the main reason for the cell division defect. To elucidate the impact of absence of EslB on cell division, we visualized the localization of the early cell division protein ZapA and the late cell division protein DivIVA in the wildtype and the $\Delta es/B$ background. Localization of ZapA was not altered in the $\Delta es/B$ mutant strain, indicating that localization of early cell division proteins is not altered and the initial formation of the septum by FtsZ is not disturbed (Rismondo et al. 2021). Polymerization of

FtsZ filaments into the Z-ring not only marks the position of cell division, but also act as the origin and scaffold for the remaining proteins that are part of the divisome (Bisson-Filho et al. 2017). ZapA was proposed to be involved in the switch from a more dynamic to a more ordered and persistent state of the FtsZ-ring, by transiently binding to FtsZ filaments and straightening them (Caldas et al. 2019). Consequently, it seems to be important for the maturation of the cell division machinery, before the actual modulation of the cell wall takes place (Caldas et al. 2019). Accurate ZapA localization therefore requires proper early-stage assembly of FtsZ filaments in the $\Delta es/B$ strain. This fits to the previously mentioned observation in *S. aureus* that as mentioned above demonstrate that the stop in septum constriction, as a result of altered PG biosynthesis is independent of FtsZ-treadmilling and affects later stages of cell division (Puls et al. 2023). To prevent inappropriate assembly of the divisome, the cell makes use of the Min inhibitory system, which hinders localization of FtsZ and subsequent recruitment of proteins at sites where no chromosomal segregation took place. Specifically, MinCD actively prevents the formation of a Z-ring. In *L. monocytogenes* the proper localization of MinCD is dependent on the late cell division protein DivIVA (Kaval et al. 2014). Consequently, DivIVA localizes at the division site and at the newly formed poles of the daughter cells to prevent Z-ring formation and migrates to the newly formed Z-ring by sensing membrane invaginations. In addition, DivIVA is involved in the recruitment and secretion of the two autolysins P60 and NamA (MurA), which are subsequently secreted by the SecA2 system and essential for daughter cell separation after cell division is completed (Lenz et al. 2003; Lenz and Portnoy 2002; Machata et al. 2005; Halbedel et al. 2012). Interestingly, *B. subtilis* DivIVA has been found to interact with the serine/histidine kinase PrkC^{Bsu} (PrkA in *L. monocytogenes*) in bacterial two-hybrid assays, likely facilitating communication and cooperated execution of the elongation and PG biosynthesis process (Hammond et al. 2019; Pompeo et al. 2018). Localization of DivIVA was altered in the $\Delta es/B$ strain, suggesting that the transporter is involved in processes downstream of ZapA but upstream of DivIVA (Figure S3). This implies that the division defect is not solely due to the lack of peptidoglycan but rather because of mislocalization and altered activity of cell division proteins (Figure 7.1 B). The cell division phenotype could be rescued by enhancing PG levels, decreasing cell wall hydrolysis, or by decreasing the glycosyltransferase activity of PBP A1 and hence decreasing polymerization of newly synthesised peptidoglycan into the growing strand. PBPA1-dependent suppression was achieved *via* mutations in *pbpA1* or *via* supplementation of the antibiotic moenomycin. It is inviting to hypothesise that EsLB plays a role in the communication between proteins involved in cell wall homeostasis, resulting in altered activity of associated proteins. Yet another set of suppressors isolated in presence of glucose

or heat stress carried mutations in either the promoter region or in the gene coding for the ClpX chaperone that can associate with ClpP to form the protease ClpXP (Baker and Sauer 2012) (Table 7.1). The activity of ClpXP was correlated to proper divisome assembly and the cell division machinery in several bacteria, including *E. coli*, *Caulobacter crescentus*, *S. aureus* and *B. subtilis* (Labana et al. 2021; Camberg et al. 2011; Smith et al. 2014; Bæk et al. 2021). Inhibition of ClpXP in *B. subtilis* led to accumulation of FtsZ and DivIVA, as well as the elongasome-associated protein MreB (Labana et al. 2021). In addition, ClpX has been shown to be involved in constriction of the Z-ring likely *via* direct interaction and inhibition of FtsZ assembly (Weart et al. 2005). Interestingly, deletion of ClpX in *S. aureus* results in a growth defect at 30°C that is associated with aberrant, FtsZ-independent septum formation and that can be rescued by specifically inhibiting either peptidoglycan cross-linking or the activity of TarO and consequently WTA biosynthesis (Bæk et al. 2016; Bæk et al. 2021; Jensen et al. 2019). These data suggest that mutations in *clpX* could result in altered activity of cell division proteins, like FtsZ.

Interestingly, several recent studies also suggest a role of the *O*-acetyltransferase OatA in the cell division process. There are several indications in various organisms that underline the tight connection between *O*-acetylation of MurNAc and the cross-linking process. For instance, the extent of *O*-acetylation rapidly increases in association with the incorporation of lipid II and *O*-acetylation was severely reduced after treatment with penicillin, which targets the transpeptidase activity of PBPs (Sychantha et al. 2018). Moreover, PBP2 was suggested to play a direct role in facilitating both transpeptidation and *O*-acetylation of peptidoglycan in *Neisseria gonorrhoea* (Dougherty 1985; Dougherty 1983). As mentioned above, we also isolated an Δ *eslB* suppressor strain that carried a mutation in the gene coding for the penicillin binding protein PBP A1, which could rescue the cell division defect of Δ *eslB*, as well as the growth defect in presence of lysozyme (Schulz et al. 2022). Likewise, the addition of the antibiotic moenomycin, which targets the glycosyltransferase activity of PBPs could suppress the heat sensitivity (Huber and Neesemann 1968).

Aside from its proposed tight collaboration with PBPs and dependency on cross-linked peptidoglycan, OatA was also more recently directly brought in association with the cell division machinery. In *B. anthracis* deletion of the OatA paralogs PatA and PatB resulted in a cell division defect, which was fortified in combinational deletion mutants with *oatA* (Laaberki et al. 2011). Likewise, a strain lacking Adr, an *O*-acetyltransferase in *S. pneumoniae*, had a disturbed cell wall structure, as well as altered septation. Deletion of *adr* not only led to increased susceptibility to the cell wall hydrolase LytA, but also to increased sensitivity towards penicillin, underlining its tight

correlation with peptidoglycan cross-linking (Crisóstomo et al. 2006; Bonnet et al. 2017). Interestingly, further studies revealed that Adr migrates to the future division site before PG biosynthesis and that FtsZ localization is altered in an *adr* deletion strain. Moreover, studies in *Lactococcus plantarum* suggest that OatA plays a role in the spatial-temporal recruitment of the cell division machinery, independent of its *O*-acetyltransferase activity (Bernard et al. 2012). Overexpression of *oatA* in *L. plantarum* led to altered septum formation and to a curved morphology. Interestingly, localization studies of the MinCD system in the *oatA* mutant suggest that OatA is important for proper localization and MinCD-dependent inhibition of aberrant Z-ring formation in this organism (Bernard et al. 2012). While the precise function of OatA in cell division remains elusive, several studies indicate a close relationship between cell division, cross-linking and OatA activities in various organisms, which might be an explanation why OatA homologues are present in lysozyme sensitive and resistant bacterial strains. It is tempting to speculate that OatA has a similar role in cell division in *L. monocytogenes*. So far, no such role of OatA has been described or analysed in this pathogen. However, preliminary bacterial-two hybrid experiments suggest that there is indeed an interaction between MinCD and OatA (Figure S4). It would be interesting to see if an *oatA* deletion strain has similar morphological phenotypes and an increased susceptibility towards cell wall targeting antibiotics, to elucidate its role in cell wall biosynthesis and division. Aberrant localization of cell division proteins in the Δ *esB* deletion strain, as seen for DivIVA, might result in altered localization of OatA and in turn to a dysfunctional protein, which could not only explain the decrease in *O*-acetylation, but could potentially be the missing link between altered cell wall biosynthesis, cell division and cross-linking to increased lysozyme sensitivity in the transporter mutant.

7.8 Conclusion and future remarks

The extensive suppressor screen of the Δ *esB* deletion strain under several different stress conditions revealed a crucial role of the transporter in various separate aspects of the cell wall architecture including cell wall biosynthesis, modification, cross-linking, hydrolysis and WTA biosynthesis. Although, at first glance the phenotypes do not appear to be connected, closer analysis revealed tight interplay between different pathways of cell wall homeostasis. Alterations in one of the pathways could destabilize the balance and control of the others, resulting in an array of different morphological and stress-associated phenotypes. All of these phenotypes and suppression mechanisms suggest a role of EsIB in the production of appropriate peptidoglycan levels, as well as in the proper succession

of the cell division process, and phenotypes are likely a result from several auxiliary factors. For instance, lysozyme sensitivity probably not only results from decreased *O*-acetylation of MurNAc but rather results from a combinational effect of altered cross-linking, alterations in WTA biosynthesis or presentation and an increased overall surface charge. This raises the question if the phenotypes are a consequence from an altered availability and/or distribution of the UDP-GlcNAc pool and if EslB directly or indirectly controls peptidoglycan levels by interacting with proteins that are part of the biosynthesis pathway. It remains elusive if EslABC is involved in translocation of substrates across the membrane that are essential players for cell wall homeostasis, such as import of GlcNAc, MurNAc or recyclable peptidoglycan components. Alternatively, EslB could have a cognate regulatory function, similar to that of the ABC transporter FtsEX, which is solely involved in the regulation of the cell wall hydrolase CwIO. EslB could likewise regulate CwIO, or related hydrolases, or interact with PBPs to regulate their activity upon environmental changes or changes in the cell wall architecture. Even though various aspects and factors involved in the general structure and homeostasis of the cell wall have been studied extensively for decades, the communication, regulation and adaptation of the connected pathways have only recently begun to unravel. Our analysis gives raise to several open questions and opened an array of hypotheses. It would be interesting to analyse if the WTA content is indeed altered in the *eslB* mutant strain or if the increased surface charges solely result from enhanced exposure of WTA in the thinned peptidoglycan layer. This could elucidate if this increased surface charge is the main reason for an enhanced CwIO and lysozyme activity which is detrimental to the cell or just an auxiliary secondary effect contributing to the overall vulnerability of the strain. Furthermore, more in depth studies of the role of the *O*-acetyltransferase OatA in cell division could broaden the knowledge and draw a clearer picture of the general process of cellular growth and communication and harmonization of cell wall maturation. Altogether, EslABC is a prime example for illustrating how the absence of a single factor can have detrimental effects on various vital processes that allow bacterial growth and survival.

7.9 Tolerance towards quaternary ammonium compounds

L. monocytogenes is one of the most successful human pathogens partly due to its great ability to survive and thrive in stressful environments that are particularly found in the food industry as a countermeasure for contaminations in food products. One method to prevent the spread of pathogens is the use of disinfectants that usually contain a mixture of quaternary ammonium compounds as active agents. Here we analysed the ability of the *L. monocytogenes* laboratory strain EGD-e to adapt to benzalkonium chloride (BAC) and cetyltrimethylammonium bromide (CTAB), two quaternary ammonium compounds (QACs) commonly used as active agents in disinfectants. To our knowledge previous studies were solely focused on the acquisition of BAC tolerance in isolated strains from the environment and no studies have addressed the ability of *L. monocytogenes* to adapt to CTAB at all. We found that EGD-e primarily adapts to CTAB stress by overexpressing the multi-drug efflux pumps SugE1 and SugE2, while BAC tolerance results from overexpression of the efflux pump FepA. Interestingly, both suppression mechanisms compensate for each other when the parental strain is lacking either SugE1/2 or FepA and even if both efflux systems are missing, the EGD-e wildtype strain can still acquire tolerance via mutations that potentially alter the synthesis of phospholipids.

7.10 Overexpression of efflux system is the dominant mode of tolerance

The presence or overexpression of efflux systems are often associated with BAC tolerance in *L. monocytogenes* isolates and previous studies focussing on the tolerance mechanism of serial adapted strains revealed that tolerance is primarily achieved by mutations in the gene coding for the TetR-like transcriptional regulator FepR (Guérin et al. 2014; Guérin et al. 2021; Bolten et al. 2022). However, since isolated strains have a high frequency of genomic variations and it is difficult to draw a generalized conclusion, we analysed if the EGD-e wildtype strain acquires similar mutations. Indeed, the adapted laboratory wildtype strain EGD-e likewise readily obtained mutations exclusively in *fepR* upon exposure to BAC. Consistent with previous studies, we also found that *fepR* mutations resulted in the ability to grow at increased BAC concentrations of approximately 6-7 mg L⁻¹ (Aase et al. 2000; Bolten et al. 2022; Guérin et al. 2021). FepR represses itself as well as *fepA*, which codes for the multidrug and toxic compound extrusion (MATE) family efflux pump FepA (Guérin et al. 2014). MATE family efflux pump, which typically facilitate a Na⁺ or H⁺ electrochemical gradient for the efflux of compounds across the membrane, have also been brought in association with BAC tolerance in other organisms, including NorM in *Neisseria meningitidis* and *N. gonorrhoeae*, as well as PmpM in

Pseudomonas aeruginosa (Kuroda and Tsuchiya 2009; Omote et al. 2006; Radchenko et al. 2015; He et al. 2004; Rouquette-Loughlin et al. 2003). Earlier findings showed that the deletion of *fepR* results in 64-fold overexpression of *fepA*, and consequently it was hypothesized that *fepR*-associated mutations result in enhanced FepA levels, which in turn extrudes BAC from the cytoplasm of the cell (Guérin et al. 2021; Bolten et al. 2022). Though, the addition of the efflux pump inhibitor reserpine did not result in reduced BAC tolerance in a *fepR* mutated strain, raising the question whether overexpression of FepA is really the primary reason for the observed tolerance or whether FepR also regulates the expression of other tolerance determinants (Guérin et al. 2014). Here we show that artificial overexpression of *fepA* in the wildtype background phenocopied the growth of that of a *fepR* suppressor mutant and we conclude that the underlying suppression mechanism for BAC tolerance in the *fepR* mutant strains is due to the overexpression of the MATE efflux pump FepA.

While tolerance towards BAC in isolated strains has been extensively described in the literature, the research regarding CTAB tolerance remains limited, apart from the observation that mutations in *fepR* or the presence of genes coding for the efflux pump QacH or SugE1/2 lead to cross-adaptation towards CTAB in addition to BAC or associated disinfectants (Müller et al. 2013; Müller et al. 2014; Jiang et al. 2020). We observed that suppressors readily evolved in presence of CTAB stress and interestingly, isolated suppressors exclusively carried mutations in the gene coding for the TetR-family like regulator SugR. *sugR* is part of the *sugRE1E2* operon, which was proposed to be the chromosomal counterpart of the plasmid-based BAC resistance cassette *bcrABC* operon that is commonly associated with BAC tolerance in *Listeria* isolates (Jiang et al. 2020; Elhanafi et al. 2010). *sugE1* and *sugE2* code similar to *bcrB* and *bcrC* for two SMR efflux pumps and the expression of either SugE1 or SugE2 was found to contribute to QACs' resistance including BAC and CTAB in previous research (Jiang et al. 2020). Furthermore, SugR was shown to bind to the promoter region of the *sug* operon and to negatively regulate the expression of *sugE1/2* (Jiang et al. 2020). Consequently, mutations in either the gene coding for SugR or in the promoter region of the *sug* operon likely diminishes binding of the regulator and results in de-repression of the efflux system. This hypothesis was verified by the observation that the artificial overexpression of SugE1/2 in the wildtype background resulted in CTAB- and BAC-tolerance. Unlike *fepR* associated mutations, no cross-adaptation apart from BAC was observed when SugE1/2 levels were increased, indicating that the efflux system is rather specific for QAC's. These results tie well with previous reports, showing that a strain lacking both *sugE1* and *sugE2* were more sensitive to other QACs' such as benzalkonium bromide, benzethonium chloride and didecyldimethylammoniumchloride but showed similar

tolerance towards antibiotics such as ampicillin, ciprofloxacin or kanamycin (Jiang et al. 2020). In contrast to MATE family transporter, SMR proteins facilitate proton motive force driven efflux (Bay et al. 2008). They were initially classified into two subgroups I) small multidrug proteins (SMP) and II) suppressors of *groEL* mutations (Sug) proteins that were as the name implies previously thought to be involved in the suppression of *groEL* mutations (Paulsen et al. 1996). However, the second class was recently renamed into “riboswitch regulated Gdm* exporter (GDM), since they are typically regulated by riboswitches in gram-negative bacteria (Bay et al. 2008; Bay and Turner 2009). The extensively studied SugE protein from *E. coli* was hence renamed into Gdx. Efflux pumps belonging to the Sug or Gdm subgroup such as Gdx are often only associated with tolerance towards limited range of QAC, including BAC, CTAB or cetylpyridinium (CTP) (Bay and Turner 2009; Bay et al. 2008; Chung and Saier 2002), while SMPs are often associated with tolerance towards QAC, cation based antimicrobials, as well as some antibiotics.

In addition to SugE1/2, several other SMR family efflux pumps have been associated with QAC tolerance, including the previously mentioned BcrABC efflux system (Dutta et al. 2013), as well as QacH, which is commonly localized on the Tn6188 transposon (Müller et al. 2013; Müller et al. 2014) and EmrE which was located as part of the genomic island LGI1 (Kovacevic et al. 2016). In contrast to the other systems, QacH conferred tolerance towards Ethidium bromide (EtBR) in addition to a wide range of QACs.

However, many studies only focus on the presence of these efflux systems in tolerant isolates, but detailed analysis of their function and expression is often missing. In addition, it is difficult to compare their involvement to QAC sensitive strains, due to high genomic variations in isolated strains, where unknown factors could additionally contribute to tolerance. An example for this is the major facilitator superfamily efflux pump MdrL, which is often used as chromosomal marker for BAC tolerance in isolates (Jiang et al. 2019b). However, its actual role in BAC tolerance differed significantly in an allele-substituted mutant of the transporter that was constructed in the *L. monocytogenes* isolate LOTM1 in comparison to a deletion mutant in the EGD-e background (Mata et al. 2000; Jiang et al. 2019b). In the LOTM1 background deletion of *mdrL* resulted in increased sensitivity not only towards BAC, but also to cefotaxime and EtBr in agar-based MIC assays (Mata et al. 2000). This, however, could not be replicated in the EGD-e background, where merely a growth defect was observed at concentrations of 2 µg ml⁻¹ in liquid BHI medium but no decrease in sensitivity using the agar dilution method, nor cross-adaptation (Jiang et al. 2019b). As mentioned above the presence and/or expression levels of MdrL and concomitantly of Lde are often seen as the main chromosomally

based efflux system in *L. monocytogenes* isolates. In contrary, we did not isolate any suppressors containing mutations in either of the two genes, even in the absence of either FepA or SugE1/2, or when both systems are missing. This indicates that they only play a minor, rather insignificant role in the EGD-e wildtype strain for BAC and CTAB tolerance.

Aside from efflux pumps belonging to the MATE or SMR family, several other classes have been described to contribute to QAC tolerance, including ATP-binding cassette (ABC)-transporter, major-facilitator superfamily (MFS)-transporter and resistance-nodulation-division (RND)-transporter (Wand and Sutton 2022). RND-transporter seem to play a particularly important role in QAC tolerance in gram-negative bacteria, likely because they span both, the inner, as well as the outer membrane. Thus, several different RND pumps have been described in various organisms (Wand and Sutton 2022). This includes MdtABC-TolC in *Salmonella enterica* (Horiyama et al. 2010); MexCD-OprJ in *P. aeruginosa*, which confers tolerance towards BAC and chlorhexidindigluconat (CHX) (Morita et al. 2003); OqxAB in *E. coli* and *Enterobacteriaceae*, which was likewise reported to contribute to BAC and CHX tolerance (Hansen et al. 2007) or AcrAB-TolC in *Klebsiella* and *E. coli* (Nordholt et al. 2021).

Similarly, various examples for MFS-transporter have been described in the context of biocide tolerance. In contrast to MATE- or SMR-efflux pumps, MFS-transporter facilitate the alternating excess model to extrude a broad spectrum of substrates (Jardetzky 1966). The MFS efflux systems MdtM was found to be involved in QAC tolerance in *E. coli*, while SmuA and SmfY were identified in *Enterobacteriaceae* and *Serratia marcescens*, respectively.

Many of the mentioned QAC tolerant organisms are human pathogens that pose a threat to the general well-being. However, as mentioned above these efflux systems have mainly been associated with QAC tolerance due to their presence in tolerant isolates and in-depth studies of the underlying mechanisms are rare. The high abundance of different types of biocide-associated efflux systems in pathogenic bacteria and their diverse substrate profile underlines the importance of further research on mechanisms that contribute to QAC tolerance.

As mentioned above, adaptation to QACs is often associated with cross-adaptation. For instance, serial passaging of *Enterococcus faecium* led to increased resistance towards ampicillin, cefotaxime, ciprofloxacin and tetracycline (Gadea et al. 2017). Likewise, a biocide tolerant *Lactobacillus pentosus* strain was additionally resistant to ampicillin, chloramphenicol and ciprofloxacin and the strain showed improved survival at low pH and in the presence of 2%-3% bile acids (Del Casado Muñoz et al. 2016b; Del Casado Muñoz et al. 2016a). Since we did not observe

increased cross-adaptation in CTAB adapted suppressors, it might be recommended to use it more extensively than BAC.

It has to be mentioned that tolerance is often acquired for below-use level concentrations of BAC. Nevertheless, outbreaks and infection was often associated with BAC tolerance for various organisms including *P. aeruginosa* and *S. marcescens* (Kampf 2018) and continuous exposure to lower-levels might facilitate the acquisition of secondary mutations that further enhances tolerance. An example for this is *Klebsiella pneumoniae*, which primarily acquired mutations in the repressor of the MFS efflux pump SmvA that conferred tolerance towards chlorhexidine, as well as the last resort antibiotic colistin (Wand et al. 2017). Prolonged exposure resulted in secondary mutations in the gene coding for proteins associated with the outer membrane or lipopolysaccharide (LPS). Likewise, we were wondering if we could identify efflux-independent tolerance mechanisms in *L. monocytogenes*. Therefore, we further adapt EGD-e strain that lacks one of the transporting system or both FepA and SugE1/2.

7.11 Efflux-independent QAC tolerance

We isolated suppressors from $\Delta fepA$, $\Delta sugE1/2$, and a $\Delta fepA\Delta sugE1/2$ deletion strains in presence of BAC and CTAB. Sanger sequencing revealed that if one of the efflux systems is missing, overexpression of the other could compensate for the loss. Remarkably, in the $\Delta fepA\Delta sugE1/2$ double deletion strain we identified mutations in *lmo1753* in all isolated suppressors. *lmo1753* is a homologue of the diacylglycerol kinase DgkB of *B. subtilis* with 64% sequence identity and 87.2% similarity. DgkB is involved in the recycling of toxic phosphatic acid as part of the biosynthesis of lipoteichoic acids (LTA) (Jerga et al. 2007; Matsuoka et al. 2011). LTA are anchored to the bacterial membrane and make up a significant part of the cell envelope of gram-positive bacteria. They play crucial roles in cellular growth and morphology and contribute to the overall negative charge of the cell surface. The anionic phosphate of the LTA backbone can be masked by positively charged D-alanylation and thus LTA content and decoration play a major role in cation homeostasis of the cellular surface (Percy and Gründling 2014). Taking this into account, it is tempting to speculate that in the suppressor mutants, altered LTA synthesis may modify cation homeostasis of the cellular membrane thereby hindering binding of QACs and subsequent pore formation. Changes in envelope homeostasis and membrane fluidity have been previously proposed to confer tolerance towards BAC. For instance, a tolerant *L. monocytogenes* isolate exhibited a minor shift to longer fatty acids compared to sensitive strains (To et al. 2002). Likewise, overall fatty acid content contributed to QAC resistance in *S. marcescens*

(Chaplin 1952) and adapted *P. aeruginosa* strains showed a global decrease in the percentage of hydroxy fatty acids (Jones et al. 1989; Guerin-Mechin et al. 2000). Furthermore, a comparison of protein expression profiles of sensitive and resistant ciprofloxacin *Edwardsiella tarda* revealed that overexpression of fatty acids biosynthesis not only contributes to ciprofloxacin resistance, but also to increased tolerance towards QACs (Su et al. 2021). So far, no suppressors or isolates of *L. monocytogenes* have been described in the literature that acquired altered LTA biosynthesis to increase tolerance towards BAC or CTAB and our results suggest that other efflux systems, aside from SugE1/2 and FepA, are less effective in the contribution towards QAC tolerance. Apart from LTA synthesis, DgkB is also involved in the production of other glycolipids and phospholipids and mutation might result in an overall altered fatty acid profile (Hashimoto et al. 2013). The importance of the membrane composition for QAC tolerance was also shown in studies that revealed that the downregulation of outer membrane porins such as OprF and OprG likewise contributed to QAC tolerance in *P. aeruginosa*, *E. coli* and *Mycobacterium smegmatis*, likely due to reduced uptake (Frenzel et al. 2011; Machado et al. 2013). Further analysis is required to explore the extend of the mutations in *Imo1753* in *L. monocytogenes* and their role in lipid content, cation homeostasis and QAC tolerance.

Overall, our study showed that the *L. monocytogenes* wildtype strain can readily acquire stable mutations and can make use of different tolerance mechanism to combat QAC stress. While the major mode of resistance is the overexpression of efflux systems that although rather unspecific for BAC or CTAB show different levels of affinity towards the two QACs. While the exposure to subinhibitory concentrations of BAC results in additional resistance towards antibiotics such as gentamycin, which is commonly used in the treatment of serious listeriosis, no cross-resistance could be identified for CTAB-tolerant strains. CTAB might therefore be the QAC of choice especially in food-processing facilities. It has to be mentioned that our approach does not show adaptation towards recommended BAC or CTAB concentrations typically found in commonly used sanitizers. However, subinhibitory levels of BAC and CTAB are often present in niches that are difficult to sanitize or arise due to improper use and comparably tolerant isolates have been found in association with outbreaks in the past (Weber et al. 2007). Aside from the overexpression of efflux systems, we could also show that *L. monocytogenes* can mutate additional routes that seem to be independent from simply extruding the toxic compounds but are rather related to the modification of cell envelope homeostasis.

Chapter 8 | References

- Aase, B., Sundheim, G., Langsrud, S., and Rørvik, L.M. (2000) Occurrence of and a possible mechanism for resistance to a quaternary ammonium compound in *Listeria monocytogenes*. *International journal of food microbiology*, doi: 10.1016/s0168-1605(00)00357-3.
- Adams, D.W., and Errington, J. (2009) Bacterial cell division: assembly, maintenance and disassembly of the Z ring. *Nature reviews. Microbiology*, doi: 10.1038/nrmicro2198.
- Alexander Fleming (1922) On a remarkable bacteriolytic element found in tissues and secretions. *Proc. R. Soc. Lond. B.*, doi: 10.1098/rspb.1922.0023.
- Allerberger, F., and Wagner, M. (2010) Listeriosis: a resurgent foodborne infection. *Clinical microbiology and infection : the official publication of the European Society of Clinical Microbiology and Infectious Diseases*, doi: 10.1111/j.1469-0691.2009.03109.x.
- Alyahya, S.A., Alexander, R., Costa, T., Henriques, A.O., Emonet, T., and Jacobs-Wagner, C. (2009) RodZ, a component of the bacterial core morphogenic apparatus. *Proceedings of the National Academy of Sciences of the United States of America*, doi: 10.1073/pnas.0810794106.
- Araki, Y., and Ito, E. (1989) Linkage units in cell walls of gram-positive bacteria. *Critical reviews in microbiology*, doi: 10.3109/10408418909105745.
- Arends, S.J.R., Kustus, R.J., and Weiss, D.S. (2009) ATP-binding site lesions in FtsE impair cell division. *Journal of bacteriology*, doi: 10.1128/JB.00179-09.
- Aubry, C., Goulard, C., Nahori, M.-A., Cayet, N., Decalf, J., Sachse, M., et al. (2011) OatA, a peptidoglycan O-acetyltransferase involved in *Listeria monocytogenes* immune escape, is critical for virulence. *The Journal of infectious diseases*, doi: 10.1093/infdis/jir396.
- Auger, G., Martin, L., Bertrand, J., Ferrari, P., Fanchon, E., Vaganay, S., et al. (1998) Large-scale preparation, purification, and crystallization of UDP-N-acetylmuramoyl-L-alanine: D-glutamate ligase from *Escherichia coli*. *Protein expression and purification*, doi: 10.1006/prev.1997.0850.
- Badet, B., Vermoote, P., and Le Goffic, F. (1988) Glucosamine synthetase from *Escherichia coli*: kinetic mechanism and inhibition by N3-fumaroyl-L-2,3-diaminopropionic derivatives. *Biochemistry*, doi: 10.1021/bi00407a006.
- Bæk, K.T., Bowman, L., Millership, C., Dupont Søggaard, M., Kaever, V., Siljamäki, P., et al. (2016) The Cell Wall Polymer Lipoteichoic Acid Becomes Nonessential in *Staphylococcus aureus* Cells Lacking the ClpX Chaperone. *mBio*, doi: 10.1128/mBio.01228-16.
- Bæk, K.T., Jensen, C., Farha, M.A., Nielsen, T.K., Paknejadi, E., Mebus, V.H., et al. (2021) A *Staphylococcus aureus* clpX mutant used as a unique screening tool to identify cell wall synthesis inhibitors that reverse β -lactam resistance in MRSA. *Frontiers in molecular biosciences*, doi: 10.3389/fmolb.2021.691569.
- Bakardjiev, A.I., Stacy, B.A., Fisher, S.J., and Portnoy, D.A. (2004) Listeriosis in the pregnant guinea pig: a model of vertical transmission. *Infection and immunity*, doi: 10.1128/IAI.72.1.489-497.2004.

-
- Baker, T.A., and Sauer, R.T. (2012) ClpXP, an ATP-powered unfolding and protein-degradation machine. *Biochimica et biophysica acta*, doi: 10.1016/j.bbamcr.2011.06.007.
- Barreteau, H., Kovac, A., Boniface, A., Sova, M., Gobec, S., and Blanot, D. (2008) Cytoplasmic steps of peptidoglycan biosynthesis. *FEMS microbiology reviews*, doi: 10.1111/j.1574-6976.2008.00104.x.
- Bateman, A. (1999) The SIS domain: a phosphosugar-binding domain. *Trends in biochemical sciences*, doi: 10.1016/s0968-0004(99)01357-2.
- Bay, D.C., Rommens, K.L., and Turner, R.J. (2008) Small multidrug resistance proteins: a multidrug transporter family that continues to grow. *Biochimica et biophysica acta*, doi: 10.1016/j.bbamem.2007.08.015.
- Bay, D.C., and Turner, R.J. (2009) Diversity and evolution of the small multidrug resistance protein family. *BMC evolutionary biology*, doi: 10.1186/1471-2148-9-140.
- Beckerling, C.L., Steil, L., Weber, M.H.W., Völker, U., and Marahiel, M.A. (2002) Genomewide transcriptional analysis of the cold shock response in *Bacillus subtilis*. *Journal of bacteriology*, doi: 10.1128/JB.184.22.6395-6402.2002.
- Benda, M., Schulz, L.M., Stülke, J., and Rismondo, J. (2021) Influence of the ABC Transporter YtrBCDEF of *Bacillus subtilis* on competence, biofilm formation and cell wall thickness. *Frontiers in microbiology*, doi: 10.3389/fmicb.2021.587035.
- Bennett, M.S., Guan, Z., Laurberg, M., and Su, X.D. (2001) *Bacillus subtilis* arsenate reductase is structurally and functionally similar to low molecular weight protein tyrosine phosphatases. *Proceedings of the National Academy of Sciences of the United States of America*, doi: 10.1073/pnas.241397198.
- Bernard, E., Rolain, T., David, B., André, G., Dupres, V., Dufrêne, Y.F., et al. (2012) Dual role for the O-acetyltransferase OatA in peptidoglycan modification and control of cell septation in *Lactobacillus plantarum*. *PloS one*, doi: 10.1371/journal.pone.0047893.
- Beveridge, T.J., and Murray, R.G. (1980) Sites of metal deposition in the cell wall of *Bacillus subtilis*. *Journal of bacteriology*, doi: 10.1128/jb.141.2.876-887.1980.
- Bhavsar, A.P., Beveridge, T.J., and Brown, E.D. (2001) Precise deletion of *tagD* and controlled depletion of its product, glycerol 3-phosphate cytidyltransferase, leads to irregular morphology and lysis of *Bacillus subtilis* grown at physiological temperature. *Journal of bacteriology*, doi: 10.1128/JB.183.22.6688-6693.2001.
- Birk, M.S., Ahmed-Begrich, R., Tran, S., Elsholz, A.K.W., Frese, C.K., and Charpentier, E. (2021) Time-resolved proteome analysis of *Listeria monocytogenes* during infection reveals the role of the AAA+ chaperone ClpC for host cell adaptation. *mSystems*, doi: 10.1128/mSystems.00215-21.
- Bishop, D.K., and Hinrichs, D.J. (1987) Adoptive transfer of immunity to *Listeria monocytogenes*. The influence of in vitro stimulation on lymphocyte subset requirements. *Journal of immunology (Baltimore, Md. : 1950)*, **139**: 2005–2009.
- Bisicchia, P., Noone, D., Lioliou, E., Howell, A., Quigley, S., Jensen, T., Jarmer, H., and Devine, K.M. (2007) The essential YycFG two-component system controls cell wall metabolism in *Bacillus subtilis*. *Molecular microbiology*, doi: 10.1111/j.1365-2958.2007.05782.x.
-

- Bisson-Filho, A.W., Hsu, Y.-P., Squyres, G.R., Kuru, E., Wu, F., Jukes, C., *et al.* (2017) Treadmilling by FtsZ filaments drives peptidoglycan synthesis and bacterial cell division. *Science (New York, N.Y.)*, doi: 10.1126/science.aak9973.
- Biswas, R., Martinez, R.E., Göhring, N., Schlag, M., Josten, M., Xia, G., *et al.* (2012) Proton-binding capacity of *Staphylococcus aureus* wall teichoic acid and its role in controlling autolysin activity. *PloS one*, doi: 10.1371/journal.pone.0041415.
- Blaauwen, T. den, Pedro, M.A. de, Nguyen-Distèche, M., and Ayala, J.A. (2008) Morphogenesis of rod-shaped sacculi. *FEMS Microbiology Reviews*, doi: 10.1111/j.1574-6976.2007.00090.x.
- Bland, R., Waite-Cusic, J., Weisberg, A.J., Riutta, E.R., Chang, J.H., and Kovacevic, J. (2022) Adaptation to a commercial quaternary ammonium compound sanitizer leads to cross-resistance to select antibiotics in *Listeria monocytogenes* isolated from fresh produce environments. *Frontiers in microbiology*, doi: 10.3389/fmicb.2021.782920.
- Blumberg, P.M., and Strominger, J.L. (1974) Interaction of penicillin with the bacterial cell: penicillin-binding proteins and penicillin-sensitive enzymes. *Bacteriological reviews*, doi: 10.1128/br.38.3.291-335.1974.
- Bolten, S., Harrand, A.S., Skeens, J., and Wiedmann, M. (2022) Nonsynonymous mutations in *fepR* are associated with adaptation of *Listeria monocytogenes* and other *Listeria* spp. to low concentrations of benzalkonium chloride but do not increase survival of *L. monocytogenes* and other *Listeria* spp. after exposure to benzalkonium chloride concentrations recommended for use in food processing environments. *Applied and environmental microbiology*, doi: 10.1128/aem.00486-22.
- Boneca, I.G., Dussurget, O., Cabanes, D., Nahori, M.-A., Sousa, S., Lecuit, M., *et al.* (2007) A critical role for peptidoglycan N-deacetylation in *Listeria* evasion from the host innate immune system. *Proceedings of the National Academy of Sciences of the United States of America*, doi: 10.1073/pnas.0609672104.
- Bonnet, J., Durmort, C., Jacq, M., Mortier-Barrière, I., Campo, N., VanNieuwenhze, M.S., *et al.* (2017) Peptidoglycan O-acetylation is functionally related to cell wall biosynthesis and cell division in *Streptococcus pneumoniae*. *Molecular microbiology*, doi: 10.1111/mmi.13849.
- Booth, S., and Lewis, R.J. (2019) Structural basis for the coordination of cell division with the synthesis of the bacterial cell envelope. *Protein science : a publication of the Protein Society*, doi: 10.1002/pro.3722.
- Bore, E., Hébraud, M., Chafsey, I., Chambon, C., Skjæret, C., Moen, B., *et al.* (2007) Adapted tolerance to benzalkonium chloride in *Escherichia coli* K-12 studied by transcriptome and proteome analyses. *Microbiology (Reading, England)*, doi: 10.1099/mic.0.29288-0.
- Borisova, M., Gaupp, R., Duckworth, A., Schneider, A., Dalügge, D., Mühleck, M., *et al.* (2016) Peptidoglycan recycling in gram-positive bacteria is crucial for survival in stationary phase. *mBio*, doi: 10.1128/mBio.00923-16.
- Bouhss, A., Crouvoisier, M., Blanot, D., and Mengin-Lecreulx, D. (2004) Purification and characterization of the bacterial MraY translocase catalyzing the first membrane step of peptidoglycan biosynthesis. *The Journal of biological chemistry*, doi: 10.1074/jbc.M314165200.

- Bouhss, A., Trunkfield, A.E., Bugg, T.D.H., and Mengin-Lecreulx, D. (2008) The biosynthesis of peptidoglycan lipid-linked intermediates. *FEMS microbiology reviews*, doi: 10.1111/j.1574-6976.2007.00089.x.
- Boylan, R.J., Mendelson, N.H., Brooks, D., and Young, F.E. (1972) Regulation of the bacterial cell wall: analysis of a mutant of *Bacillus subtilis* defective in biosynthesis of teichoic acid. *Journal of bacteriology*, doi: 10.1128/jb.110.1.281-290.1972.
- Bradford, M.M. (1976) A rapid and sensitive method for the quantitation of microgram quantities of protein utilizing the principle of protein-dye binding. *Analytical Biochemistry*, doi: 10.1016/0003-2697(76)90527-3.
- Brauge, T., Faille, C., Sadovskaya, I., Charbit, A., Benezech, T., Shen, Y., et al. (2018) The absence of N-acetylglucosamine in wall teichoic acids of *Listeria monocytogenes* modifies biofilm architecture and tolerance to rinsing and cleaning procedures. *PLoS one*, doi: 10.1371/journal.pone.0190879.
- Breukink, E., Wiedemann, I., van Kraaij, C., Kuipers, O.P., Sahl, H.G., and Kruijff, B. de (1999) Use of the cell wall precursor lipid II by a pore-forming peptide antibiotic. *Science (New York, N.Y.)*, doi: 10.1126/science.286.5448.2361.
- Brown, S., Meredith, T., Swoboda, J., and Walker, S. (2010) *Staphylococcus aureus* and *Bacillus subtilis* W23 make polyribitol wall teichoic acids using different enzymatic pathways. *Chemistry & biology*, doi: 10.1016/j.chembiol.2010.07.017.
- Brown, S., Santa Maria, J.P., and Walker, S. (2013) Wall teichoic acids of gram-positive bacteria. *Annual review of microbiology*, doi: 10.1146/annurev-micro-092412-155620.
- Brown, S., Zhang, Y.-H., and Walker, S. (2008) A revised pathway proposed for *Staphylococcus aureus* wall teichoic acid biosynthesis based on in vitro reconstitution of the intracellular steps. *Chemistry & biology*, doi: 10.1016/j.chembiol.2007.11.011.
- Brunet, Y.R., Wang, X., and Rudner, D.Z. (2019) SweC and SweD are essential co-factors of the FtsEX-CwlO cell wall hydrolase complex in *Bacillus subtilis*. *PLoS genetics*, doi: 10.1371/journal.pgen.1008296.
- Burke, T.P., Loukitcheva, A., Zemansky, J., Wheeler, R., Boneca, I.G., and Portnoy, D.A. (2014) *Listeria monocytogenes* is resistant to lysozyme through the regulation, not the acquisition, of cell wall-modifying enzymes. *Journal of bacteriology*, doi: 10.1128/JB.02053-14.
- Burke, T.P., and Portnoy, D.A. (2016) SpoVG is a conserved RNA-binding protein that regulates *Listeria monocytogenes* lysozyme resistance, virulence, and swarming motility. *mBio*, doi: 10.1128/mBio.00240-16.
- Byczynski, B., Mizyed, S., and Berti, P.J. (2003) Nonenzymatic breakdown of the tetrahedral (alpha-carboxyketal phosphate) intermediates of MurA and AroA, two carboxyvinyl transferases. Protonation of different functional groups controls the rate and fate of breakdown. *Journal of the American Chemical Society*, doi: 10.1021/ja0349655.
- Caldas, P., López-Pelegrín, M., Pearce, D.J.G., Budanur, N.B., Brugués, J., and Loose, M. (2019) Cooperative ordering of treadmill filaments in cytoskeletal networks of FtsZ and its crosslinker ZapA. *Nature communications*, doi: 10.1038/s41467-019-13702-4.

- Callewaert, L., and Michiels, C.W. (2010) Lysozymes in the animal kingdom. *Journal of biosciences*, doi: 10.1007/s12038-010-0015-5.
- Camberg, J.L., Hoskins, J.R., and Wickner, S. (2011) The interplay of ClpXP with the cell division machinery in *Escherichia coli*. *Journal of bacteriology*, doi: 10.1128/JB.01317-10.
- Camilli, A., Tilney, L.G., and Portnoy, D.A. (1993) Dual roles of *plcA* in *Listeria monocytogenes* pathogenesis. *Molecular microbiology*, doi: 10.1111/j.1365-2958.1993.tb01211.x.
- Campbell, J., Singh, A.K., Santa Maria, J.P., Kim, Y., Brown, S., Swoboda, J.G., et al. (2011) Synthetic lethal compound combinations reveal a fundamental connection between wall teichoic acid and peptidoglycan biosynthesis in *Staphylococcus aureus*. *ACS chemical biology*, doi: 10.1021/cb100269f.
- Campeotto, I., Percy, M.G., MacDonald, J.T., Förster, A., Freemont, P.S., and Gründling, A. (2014) Structural and mechanistic insight into the *Listeria monocytogenes* two-enzyme lipoteichoic acid synthesis system. *The Journal of biological chemistry*, doi: 10.1074/jbc.M114.590570.
- Carballido-López, R., Formstone, A., Li, Y., Ehrlich, S.D., Noirot, P., and Errington, J. (2006) Actin homolog MreBH governs cell morphogenesis by localization of the cell wall hydrolase LytE. *Developmental cell*, doi: 10.1016/j.devcel.2006.07.017.
- Carlin, C.R., Roof, S., and Wiedmann, M. (2022) Assessment of reference method selective broth and plating media with 19 *Listeria* species highlights the importance of including diverse species in *Listeria* method evaluations. *Journal of food protection*, doi: 10.4315/JFP-21-293.
- Ceragioli, M., Mols, M., Moezelaar, R., Ghelardi, E., Senesi, S., and Abee, T. (2010) Comparative transcriptomic and phenotypic analysis of the responses of *Bacillus cereus* to various disinfectant treatments. *Applied and environmental microbiology*, doi: 10.1128/AEM.03003-09.
- Chaplin, C.E. (1952) Bacterial resistance to quaternary ammonium disinfectants. *Journal of bacteriology*, doi: 10.1128/jb.63.4.453-458.1952.
- Chen, G.Y., Pensinger, D.A., and Sauer, J.-D. (2017) *Listeria monocytogenes* cytosolic metabolism promotes replication, survival, and evasion of innate immunity. *Cellular microbiology*, doi: 10.1111/cmi.12762.
- Cheng, C., Jiang, L., Ma, T., Wang, H., Han, X., Sun, J., et al. (2017) Carboxyl-terminal residues N478 and V479 required for the cytolytic activity of listeriolysin O play a critical role in *Listeria monocytogenes* pathogenicity. *Frontiers in immunology*, doi: 10.3389/fimmu.2017.01439.
- Cho, H., Wivagg, C.N., Kapoor, M., Barry, Z., Rohs, P.D.A., Suh, H., et al. (2016) Bacterial cell wall biogenesis is mediated by SEDS and PBP polymerase families functioning semi-autonomously. *Nature microbiology*, doi: 10.1038/nmicrobiol.2016.172.
- Chung, Y.J., and Saier, M.H. (2002) Overexpression of the *Escherichia coli sugE* gene confers resistance to a narrow range of quaternary ammonium compounds. *Journal of bacteriology*, doi: 10.1128/JB.184.9.2543-2545.2002.

- Claessen, D., Emmins, R., Hamoen, L.W., Daniel, R.A., Errington, J., and Edwards, D.H. (2008) Control of the cell elongation-division cycle by shuttling of PBP1 protein in *Bacillus subtilis*. *Molecular microbiology*, doi: 10.1111/j.1365-2958.2008.06210.x.
- Cleverley, R.M., Rutter, Z.J., Rismondo, J., Corona, F., Tsui, H.-C.T., Alatawi, F.A., et al. (2019) The cell cycle regulator GpsB functions as cytosolic adaptor for multiple cell wall enzymes. *Nature communications*, doi: 10.1038/s41467-018-08056-2.
- Collins, L.V., Kristian, S.A., Weidenmaier, C., Faigle, M., van Kessel, K.P.M., van Strijp, J.A.G., et al. (2002) *Staphylococcus aureus* strains lacking D-alanine modifications of teichoic acids are highly susceptible to human neutrophil killing and are virulence attenuated in mice. *The Journal of infectious diseases*, doi: 10.1086/341454.
- Considine, K.M., Sleator, R.D., Kelly, A.L., Fitzgerald, G.F., and Hill, C. (2011) Identification and characterization of an essential gene in *Listeria monocytogenes* using an inducible gene expression system. *Bioengineered bugs*, doi: 10.4161/bbug.2.3.15476.
- Cortes, B.W., Naditz, A.L., Anast, J.M., and Schmitz-Esser, S. (2019) Transcriptome sequencing of *Listeria monocytogenes* reveals major gene expression changes in response to lactic acid stress exposure but a less pronounced response to oxidative stress. *Frontiers in microbiology*, doi: 10.3389/fmicb.2019.03110.
- Crisóstomo, M.I., Vollmer, W., Kharat, A.S., Inhülsen, S., Gehre, F., Buckenmaier, S., and Tomasz, A. (2006) Attenuation of penicillin resistance in a peptidoglycan O-acetyl transferase mutant of *Streptococcus pneumoniae*. *Molecular microbiology*, doi: 10.1111/j.1365-2958.2006.05340.x.
- Daoud, N.N., Dickinson, N.A., and Gilbert, P. (1983) Antimicrobial activity and physico-chemical properties of some alkyldimethylbenzylammonium chlorides. *Microbios*, **37**: 73–85.
- Davidson, A.L., Dassa, E., Orelle, C., and Chen, J. (2008) Structure, function, and evolution of bacterial ATP-binding cassette systems. *Microbiology and molecular biology reviews : MMBR*, doi: 10.1128/MMBR.00031-07.
- Deaconescu, A.M., Sevostyanova, A., Artsimovitch, I., and Grigorieff, N. (2012) Nucleotide excision repair (NER) machinery recruitment by the transcription-repair coupling factor involves unmasking of a conserved intramolecular interface. *Proceedings of the National Academy of Sciences of the United States of America*, doi: 10.1073/pnas.1115105109.
- Del Casado Muñoz, M.C., Benomar, N., Ennahar, S., Horvatovich, P., Lavilla Lerma, L., Knapp, C.W., Gálvez, A., and Abriouel, H. (2016a) Comparative proteomic analysis of a potentially probiotic *Lactobacillus pentosus* MP-10 for the identification of key proteins involved in antibiotic resistance and biocide tolerance. *International journal of food microbiology*, doi: 10.1016/j.ijfoodmicro.2016.01.012.
- Del Casado Muñoz, M.C., Benomar, N., Lavilla Lerma, L., Knapp, C.W., Gálvez, A., and Abriouel, H. (2016b) Biocide tolerance, phenotypic and molecular response of lactic acid bacteria isolated from naturally-fermented Aloreña table to different physico-chemical stresses. *Food microbiology*, doi: 10.1016/j.fm.2016.06.013.
- D'Elia, M.A., Millar, K.E., Beveridge, T.J., and Brown, E.D. (2006) Wall teichoic acid polymers are dispensable for cell viability in *Bacillus subtilis*. *Journal of bacteriology*, doi: 10.1128/JB.01336-06.

- Dhiman, A., Bhatnagar, S., Kulshreshtha, P., and Bhatnagar, R. (2014) Functional characterization of WalRK: A two-component signal transduction system from *Bacillus anthracis*. *FEBS open bio*, doi: 10.1016/j.fob.2013.12.005.
- Dion, M.F., Kapoor, M., Sun, Y., Wilson, S., Ryan, J., Vigouroux, A., et al. (2019) *Bacillus subtilis* cell diameter is determined by the opposing actions of two distinct cell wall synthetic systems. *Nature microbiology*, doi: 10.1038/s41564-019-0439-0.
- Dobihal, G.S., Brunet, Y.R., Flores-Kim, J., and Rudner, D.Z. (2019) Homeostatic control of cell wall hydrolysis by the WalRK two-component signaling pathway in *Bacillus subtilis*. *eLife*, doi: 10.7554/eLife.52088.
- Dobihal, G.S., Flores-Kim, J., Roney, I.J., Wang, X., and Rudner, D.Z. (2022) The WalR-WalK signaling pathway modulates the activities of both CwIO and LytE through control of the peptidoglycan deacetylase PdaC in *Bacillus subtilis*. *Journal of bacteriology*, doi: 10.1128/JB.00533-21.
- Domínguez-Cuevas, P., Porcelli, I., Daniel, R.A., and Errington, J. (2013) Differentiated roles for MreB-actin isologues and autolytic enzymes in *Bacillus subtilis* morphogenesis. *Molecular microbiology*, doi: 10.1111/mmi.12335.
- Domínguez-Escobar, J., Chastanet, A., Crevenna, A.H., Fromion, V., Wedlich-Söldner, R., and Carballido-López, R. (2011) Processive movement of MreB-associated cell wall biosynthetic complexes in bacteria. *Science (New York, N.Y.)*, doi: 10.1126/science.1203466.
- Douarre, P.-E., Sévellec, Y., Le Grandois, P., Soumet, C., Bridier, A., and Roussel, S. (2022) FepR as a central genetic target in the adaptation to quaternary ammonium compounds and cross-Resistance to ciprofloxacin in *Listeria monocytogenes*. *Frontiers in microbiology*, doi: 10.3389/fmicb.2022.864576.
- Dougherty, T.J. (1983) Peptidoglycan biosynthesis in *Neisseria gonorrhoeae* strains sensitive and intrinsically resistant to beta-lactam antibiotics. *Journal of bacteriology*, doi: 10.1128/jb.153.1.429-435.1983.
- Dougherty, T.J. (1985) Involvement of a change in penicillin target and peptidoglycan structure in low-level resistance to beta-lactam antibiotics in *Neisseria gonorrhoeae*. *Antimicrobial agents and chemotherapy*, doi: 10.1128/AAC.28.1.90.
- Drevets, D.A., and Bronze, M.S. (2008) *Listeria monocytogenes*: epidemiology, human disease, and mechanisms of brain invasion. *FEMS immunology and medical microbiology*, doi: 10.1111/j.1574-695X.2008.00404.x.
- Du, S., Pichoff, S., and Lutkenhaus, J. (2016) FtsEX acts on FtsA to regulate divisome assembly and activity. *Proceedings of the National Academy of Sciences of the United States of America*, doi: 10.1073/pnas.1606656113.
- Dubnau, D. (1991) Genetic competence in *Bacillus subtilis*. *Microbiological reviews*, doi: 10.1128/mr.55.3.395-424.1991.
- Dubrac, S., Bisicchia, P., Devine, K.M., and Msadek, T. (2008) A matter of life and death: cell wall homeostasis and the WalRK (YycGF) essential signal transduction pathway. *Molecular microbiology*, doi: 10.1111/j.1365-2958.2008.06483.x.
- Dubrac, S., Boneca, I.G., Poupel, O., and Msadek, T. (2007) New insights into the WalK/WalR (YycG/YycF) essential signal transduction pathway reveal a major role in controlling cell wall metabolism and biofilm formation in *Staphylococcus aureus*. *Journal of bacteriology*, doi: 10.1128/JB.00645-07.

- Duman, R., Ishikawa, S., Celik, I., Strahl, H., Ogasawara, N., Troc, P., Löwe, J., and Hamoen, L.W. (2013) Structural and genetic analyses reveal the protein SepF as a new membrane anchor for the Z ring. *Proceedings of the National Academy of Sciences of the United States of America*, doi: 10.1073/pnas.1313978110.
- Duncan, K., van Heijenoort, J., and Walsh, C.T. (1990) Purification and characterization of the D-alanyl-D-alanine-adding enzyme from *Escherichia coli*. *Biochemistry*, doi: 10.1021/bi00461a023.
- Durack, J., Burke, T.P., and Portnoy, D.A. (2015) A *prl* mutation in *secY* suppresses secretion and virulence defects of *Listeria monocytogenes secA2* mutants. *Journal of bacteriology*, doi: 10.1128/JB.02284-14.
- Dutta, V., Elhanafi, D., and Kathariou, S. (2013) Conservation and distribution of the benzalkonium chloride resistance cassette *bcrABC* in *Listeria monocytogenes*. *Applied and environmental microbiology*, doi: 10.1128/AEM.01751-13.
- EFSA (2013) Evaluation of monitoring data on residues of didecyldimethylammonium chloride (DDAC) and benzalkonium chloride (BAC). *EFSA Supporting Publications*, doi: 10.2903/sp.efsa.2013.EN-483.
- EFSA (2022) The European Union One Health 2021 Zoonoses Report. *EFSA journal. European Food Safety Authority*, doi: 10.2903/j.efsa.2022.7666.
- Egan, A.J.F., Errington, J., and Vollmer, W. (2020) Regulation of peptidoglycan synthesis and remodelling. *Nature reviews. Microbiology*, doi: 10.1038/s41579-020-0366-3.
- El Ghachi, M., Derbise, A., Bouhss, A., and Mengin-Lecreulx, D. (2005) Identification of multiple genes encoding membrane proteins with undecaprenyl pyrophosphate phosphatase (UppP) activity in *Escherichia coli*. *The Journal of biological chemistry*, doi: 10.1074/jbc.M412277200.
- Elhanafi, D., Dutta, V., and Kathariou, S. (2010) Genetic characterization of plasmid-associated benzalkonium chloride resistance determinants in a *Listeria monocytogenes* strain from the 1998-1999 Outbreak. *Applied and environmental microbiology*, doi: 10.1128/AEM.02056-10.
- Emami, K., Guyet, A., Kawai, Y., Devi, J., Wu, L.J., Allenby, N., Daniel, R.A., and Errington, J. (2017) RodA as the missing glycosyltransferase in *Bacillus subtilis* and antibiotic discovery for the peptidoglycan polymerase pathway. *Nature microbiology*, doi: 10.1038/nmicrobiol.2016.253.
- Erickson, H.P. (1997) FtsZ, a tubulin homologue in prokaryote cell division. *Trends in cell biology*, doi: 10.1016/S0962-8924(97)01108-2.
- Erickson, H.P., and Osawa, M. (2010) Cell division without FtsZ—a variety of redundant mechanisms. *Molecular microbiology*, doi: 10.1111/j.1365-2958.2010.07321.x.
- Errington, J. (2015) Bacterial morphogenesis and the enigmatic MreB helix. *Nature reviews. Microbiology*, doi: 10.1038/nrmicro3398.
- Errington, J., Daniel, R.A., and Scheffers, D.-J. (2003) Cytokinesis in bacteria. *Microbiology and molecular biology reviews : MMBR*, doi: 10.1128/MMBR.67.1.52-65.2003.
- Errington, J., and Wu, L.J. (2017) Cell cycle machinery in *Bacillus subtilis*. *Sub-cellular biochemistry*, doi: 10.1007/978-3-319-53047-5_3.

-
- Eschenburg, D., Priestman, M., and Schönbrunn, E. (2004) Evidence that the fosfomycin target Cys115 in UDP-N-acetylglucosamine enolpyruvyl transferase (MurA) is essential for product release. *Journal of Biological Chemistry*, doi: 10.1074/jbc.M411325200.
- Eschenburg, S., Priestman, M., and Schönbrunn, E. (2005) Evidence that the fosfomycin target Cys115 in UDP-N-acetylglucosamine enolpyruvyl transferase (MurA) is essential for product release. *The Journal of biological chemistry*, doi: 10.1074/jbc.M411325200.
- Eswara, P.J., Brzozowski, R.S., Viola, M.G., Graham, G., Spanoudis, C., Trebino, C., et al. (2018) An essential *Staphylococcus aureus* cell division protein directly regulates FtsZ dynamics. *eLife*, doi: 10.7554/eLife.38856.
- Eswaramoorthy, P., Erb, M.L., Gregory, J.A., Silverman, J., Pogliano, K., Pogliano, J., and Ramamurthi, K.S. (2011) Cellular architecture mediates DivIVA ultrastructure and regulates min activity in *Bacillus subtilis*. *mBio*, doi: 10.1128/mBio.00257-11.
- Eugster, M.R., and Loessner, M.J. (2011) Rapid analysis of *Listeria monocytogenes* cell wall teichoic acid carbohydrates by ESI-MS/MS. *PLoS one*, doi: 10.1371/journal.pone.0021500.
- Eugster, M.R., and Loessner, M.J. (2012) Wall teichoic acids restrict access of bacteriophage endolysin Ply118, Ply511, and PlyP40 cell wall binding domains to the *Listeria monocytogenes* peptidoglycan. *Journal of bacteriology*, doi: 10.1128/JB.00808-12.
- Fischer, M.A., Engelgeh, T., Rothe, P., Fuchs, S., Thürmer, A., and Halbedel, S. (2022) *Listeria monocytogenes* genes supporting growth under standard laboratory cultivation conditions and during macrophage infection. *Genome research*, doi: 10.1101/gr.276747.122.
- Fleming, A. (1929) On the antibacterial action of cultures of a penicillium, with special reference to their use in the isolation of *B. influenzae*. *British journal of experimental pathology*, **10**: 226–236.
- Formstone, A., Carballido-López, R., Noirot, P., Errington, J., and Scheffers, D.-J. (2008) Localization and interactions of teichoic acid synthetic enzymes in *Bacillus subtilis*. *Journal of bacteriology*, doi: 10.1128/JB.01394-07.
- Foulquier, E., Pompeo, F., Byrne, D., Fierobe, H.-P., and Galinier, A. (2020) Uridine diphosphate N-acetylglucosamine orchestrates the interaction of GlmR with either YvcJ or GlmS in *Bacillus subtilis*. *Scientific reports*, doi: 10.1038/s41598-020-72854-2.
- Frenzel, E., Schmidt, S., Niederweis, M., and Steinhauer, K. (2011) Importance of porins for biocide efficacy against *Mycobacterium smegmatis*. *Applied and environmental microbiology*, doi: 10.1128/AEM.02492-10.
- Fukuchi, K., Kasahara, Y., Asai, K., Kobayashi, K., Moriya, S., and Ogasawara, N. (2000) The essential two-component regulatory system encoded by *yycF* and *yycG* modulates expression of the *ftsAZ* operon in *Bacillus subtilis*. *Microbiology (Reading, England)*, doi: 10.1099/00221287-146-7-1573.
- Gadea, R., Fernández Fuentes, M.Á., Pérez Pulido, R., Gálvez, A., and Ortega, E. (2017) Effects of exposure to quaternary-ammonium-based biocides on antimicrobial susceptibility and tolerance to physical stresses in bacteria from organic foods. *Food microbiology*, doi: 10.1016/j.fm.2016.10.037.
-

- Galinier, A., Foulquier, E., and Pompeo, F. (2021) Metabolic control of cell elongation and cell division in *Bacillus subtilis*. *Frontiers in microbiology*, doi: 10.3389/fmicb.2021.697930.
- Gálvez-Iriqui, A.C., Plascencia-Jatomea, M., and Bautista-Baños, S. (2020) Lysozymes: characteristics, mechanism of action and technological applications on the control of pathogenic microorganisms. *Revista Mexicana de Fitopatología, Mexican Journal of Phytopathology*, doi: 10.18781/R.MEX.FIT.2005-6.
- Gamba, P., Veening, J.-W., Saunders, N.J., Hamoen, L.W., and Daniel, R.A. (2009) Two-step assembly dynamics of the *Bacillus subtilis* divisome. *Journal of bacteriology*, doi: 10.1128/JB.01758-08.
- Garner, E.C., Bernard, R., Wang, W., Zhuang, X., Rudner, D.Z., and Mitchison, T. (2011) Coupled, circumferential motions of the cell wall synthesis machinery and MreB filaments in *B. subtilis*. *Science (New York, N.Y.)*, doi: 10.1126/science.1203285.
- Gehring, A.M., Lees, W.J., Mindiola, D.J., Walsh, C.T., and Brown, D.E. (1996) Acetyltransfer precedes uridylyltransfer in the formation of UDP-N-acetylglucosamine in degradable active sites of the bifunctional GlmU Protein of *Escherichia coli*, doi: 10.1021/bi952275a.
- Gerba, C.P. (2015) Quaternary ammonium biocides: efficacy in application. *Applied and environmental microbiology*, doi: 10.1128/AEM.02633-14.
- Ghuysen, J.M. (1968) Use of bacteriolytic enzymes in determination of wall structure and their role in cell metabolism. *Bacteriological reviews*, **32**: 425–464.
- Gilbert, P., and Al-taa, A. (1985) Antimicrobial activity of some alkyltrimethylammonium bromides. *Letters in Applied Microbiology*, doi: 10.1111/j.1472-765X.1985.tb01498.x.
- Glaser, P., Frangeul, L., Buchrieser, C., Rusniok, C., Amend, A., Baquero, F., et al. (2001) Comparative genomics of *Listeria* species. *Science (New York, N.Y.)*, doi: 10.1126/science.1063447.
- Godreuil, S., Galimand, M., Gerbaud, G., Jacquet, C., and Courvalin, P. (2003) Efflux pump Lde is associated with fluoroquinolone resistance in *Listeria monocytogenes*. *Antimicrobial agents and chemotherapy*, doi: 10.1128/AAC.47.2.704-708.2003.
- Goffin, C., and Ghuysen, J.M. (1998) Multimodular penicillin-binding proteins: an enigmatic family of orthologs and paralogs. *Microbiology and molecular biology reviews: MMBR*, doi: 10.1128/MMBR.62.4.1079-1093.1998.
- Golinelli-Pimpaneau, B., Le Goffic, F., and Badet, B. (1989) Glucosamine-6-phosphate synthase from *Escherichia coli*: mechanism of the reaction at the fructose 6-phosphate binding site. *Journal of the American Chemical Society*, doi: 10.1021/ja00190a042.
- Goodell, E.W. (1985) Recycling of murein by *Escherichia coli*. *Journal of bacteriology*, doi: 10.1128/jb.163.1.305-310.1985.
- Gründling, A., Burrack, L.S., Bouwer, H.G.A., and Higgins, D.E. (2004) *Listeria monocytogenes* regulates flagellar motility gene expression through MogR, a transcriptional repressor required for virulence. *Proceedings of the National Academy of Sciences of the United States of America*, doi: 10.1073/pnas.0404924101.

-
- Guérin, A., Bridier, A., Le Grandois, P., Sévellec, Y., Palma, F., Félix, B., *et al.* (2021) Exposure to quaternary ammonium compounds selects resistance to ciprofloxacin in *Listeria monocytogenes*. *Pathogens (Basel, Switzerland)*, doi: 10.3390/pathogens10020220.
- Guérin, F., Galimand, M., Tuambilangana, F., Courvalin, P., and Cattoir, V. (2014) Overexpression of the novel MATE fluoroquinolone efflux pump FepA in *Listeria monocytogenes* is driven by inactivation of its Local repressor FepR. *PloS one*, doi: 10.1371/journal.pone.0106340.
- Guerin-Mechin, L., Dubois-Brissonnet, F., Heyd, B., and Leveau, J.Y. (2000) Quaternary ammonium compound stresses induce specific variations in fatty acid composition of *Pseudomonas aeruginosa*. *International journal of food microbiology*, doi: 10.1016/s0168-1605(00)00189-6.
- Guinane, C.M., Cotter, P.D., Ross, R.P., and Hill, C. (2006) Contribution of penicillin-binding protein homologs to antibiotic resistance, cell morphology, and virulence of *Listeria monocytogenes* EGDe. *Antimicrobial agents and chemotherapy*, doi: 10.1128/AAC.00167-06.
- Hakulinen, J.K., Hering, J., Brändén, G., Chen, H., Snijder, A., Ek, M., and Johansson, P. (2017) MraY-antibiotic complex reveals details of tunicamycin mode of action. *Nature chemical biology*, doi: 10.1038/nchembio.2270.
- Halbedel, S., Hahn, B., Daniel, R.A., and Flieger, A. (2012) DivIVA affects secretion of virulence-related autolysins in *Listeria monocytogenes*. *Molecular microbiology*, doi: 10.1111/j.1365-2958.2012.07969.x.
- Halbedel, S., and Lewis, R.J. (2019) Structural basis for interaction of DivIVA/GpsB proteins with their ligands. *Molecular microbiology*, doi: 10.1111/mmi.14244.
- Hammond, L.R., White, M.L., and Eswara, P.J. (2019) jvIVA la DivIVA! *Journal of bacteriology*, doi: 10.1128/JB.00245-19.
- Hamon, M., Bierne, H., and Cossart, P. (2006) *Listeria monocytogenes*: a multifaceted model. *Nature reviews. Microbiology*, doi: 10.1038/nrmicro1413.
- Hanahan, D. (1983) Studies on transformation of *Escherichia coli* with plasmids. *Journal of molecular biology*, doi: 10.1016/s0022-2836(83)80284-8.
- Hancock, I.C., Wiseman, G., and Baddiley, J. (1976) Biosynthesis of the unit that links teichoic acid to the bacterial wall: inhibition by tunicamycin. *FEBS letters*, doi: 10.1016/0014-5793(76)80657-6.
- Hansen, L.H., Jensen, L.B., Sørensen, H.I., and Sørensen, S.J. (2007) Substrate specificity of the OqxAB multidrug resistance pump in *Escherichia coli* and selected enteric bacteria. *The Journal of antimicrobial chemotherapy*, doi: 10.1093/jac/dkm167.
- Hardt, P., Engels, I., Rausch, M., Gajdiss, M., Ulm, H., Sass, P., *et al.* (2017) The cell wall precursor lipid II acts as a molecular signal for the Ser/Thr kinase PknB of *Staphylococcus aureus*. *International journal of medical microbiology: IJMM*, doi: 10.1016/j.ijmm.2016.12.001.
- Harrington, C.R., and Baddiley, J. (1985) Biosynthesis of wall teichoic acids in *Staphylococcus aureus* H, *Micrococcus varians* and *Bacillus subtilis* W23. Involvement of lipid intermediates containing the disaccharide N-
-

-
- acetylmannosaminyl N-acetylglucosamine. *European journal of biochemistry*, doi: 10.1111/j.1432-1033.1985.tb09348.x.
- Hashimoto, M., Ooiwa, S., and Sekiguchi, J. (2012) Synthetic lethality of the *lytE cw/O* genotype in *Bacillus subtilis* is caused by lack of D,L-endopeptidase activity at the lateral cell wall. *Journal of bacteriology*, doi: 10.1128/JB.05569-11.
- Hashimoto, M., Seki, T., Matsuoka, S., Hara, H., Asai, K., Sadaie, Y., and Matsumoto, K. (2013) Induction of extracytoplasmic function sigma factors in *Bacillus subtilis* cells with defects in lipoteichoic acid synthesis. *Microbiology*, doi: 10.1099/mic.0.063420-0.
- He, G.-X., Kuroda, T., Mima, T., Morita, Y., Mizushima, T., and Tsuchiya, T. (2004) An H(+)-coupled multidrug efflux pump, PmpM, a member of the MATE family of transporters, from *Pseudomonas aeruginosa*. *Journal of bacteriology*, doi: 10.1128/JB.186.1.262-265.2004.
- Henriques, A.O., Glaser, P., Piggot, P.J., and Moran, C.P. (1998) Control of cell shape and elongation by the *rodA* gene in *Bacillus subtilis*. *Molecular microbiology*, doi: 10.1046/j.1365-2958.1998.00766.x.
- Heptinstall, S., Archibald, A.R., and Baddiley, J. (1970) Teichoic acids and membrane function in bacteria. *Nature*, doi: 10.1038/225519a0.
- Höltje, J.V. (1996) A hypothetical holoenzyme involved in the replication of the murein sacculus of *Escherichia coli*. *Microbiology (Reading, England)*, doi: 10.1099/13500872-142-8-1911.
- Höltje, J.V. (1998) Growth of the stress-bearing and shape-maintaining murein sacculus of *Escherichia coli*. *Microbiology and molecular biology reviews: MMBR*, doi: 10.1128/MMBR.62.1.181-203.1998.
- Horiyama, T., Yamaguchi, A., and Nishino, K. (2010) TolC dependency of multidrug efflux systems in *Salmonella enterica* serovar Typhimurium. *The Journal of antimicrobial chemotherapy*, doi: 10.1093/jac/dkq160.
- Howell, A., Dubrac, S., Andersen, K.K., Noone, D., Fert, J., Msadek, T., and Devine, K. (2003) Genes controlled by the essential YycG/YycF two-component system of *Bacillus subtilis* revealed through a novel hybrid regulator approach. *Molecular microbiology*, doi: 10.1046/j.1365-2958.2003.03661.x.
- Hsu, S.-T.D., Breukink, E., Tischenko, E., Lutters, M.A.G., Kruijff, B. de, Kaptein, R., Bonvin, A.M.J.J., and van Nuland, N.A.J. (2004) The nisin-lipid II complex reveals a pyrophosphate cage that provides a blueprint for novel antibiotics. *Nature structural & molecular biology*, doi: 10.1038/nsmb830.
- Huang, W.-Z., Wang, J.-J., Chen, H.-J., Chen, J.-T., and Shaw, G.-C. (2013) The heat-inducible essential response regulator WalR positively regulates transcription of *sigI*, *mreBH* and *lytE* in *Bacillus subtilis* under heat stress. *Research in microbiology*, doi: 10.1016/j.resmic.2013.10.003.
- Huber, G., and Neseemann, G. (1968) Moenomycin, an inhibitor of cell wall synthesis. *Biochemical and biophysical research communications*, doi: 10.1016/0006-291x(68)90704-3.
- Hutter, B., Fischer, C., Jacobi, A., Schaab, C., and Loferer, H. (2004) Panel of *Bacillus subtilis* reporter strains indicative of various modes of action. *Antimicrobial agents and chemotherapy*, doi: 10.1128/AAC.48.7.2588-2594.2004.
-

-
- Ito, E., and Strominger, J.L. (1973) Enzymatic synthesis of the peptide in bacterial uridine nucleotides. *The Journal of biological chemistry*, doi: 10.1016/S0021-9258(19)44017-9.
- Jardetzky, O. (1966) Simple allosteric model for membrane pumps. *Nature*, doi: 10.1038/211969a0.
- Jenni, R., and Berger-Bächi, B. (1998) Teichoic acid content in different lineages of *Staphylococcus aureus* NCTC8325. *Archives of microbiology*, doi: 10.1007/s002030050630.
- Jensen, C., Bæk, K.T., Gally, C., Thalsø-Madsen, I., Xu, L., Jousselin, A., et al. (2019) The ClpX chaperone controls autolytic splitting of *Staphylococcus aureus* daughter cells, but is bypassed by β -lactam antibiotics or inhibitors of WTA biosynthesis. *PLoS pathogens*, doi: 10.1371/journal.ppat.1008044.
- Jerga, A., Lu, Y.-J., Schujman, G.E., Mendoza, D. de, and Rock, C.O. (2007) Identification of a soluble diacylglycerol kinase required for lipoteichoic acid production in *Bacillus subtilis*. *The Journal of biological chemistry*, doi: 10.1074/jbc.M703536200.
- Jiang, M., Su, Y.-B., Ye, J.-Z., Li, H., Kuang, S.-F., Wu, J.-H., et al. (2023) Ampicillin-controlled glucose metabolism manipulates the transition from tolerance to resistance in bacteria. *Science advances*, doi: 10.1126/sciadv.ade8582.
- Jiang, X., Geng, Y., Ren, S., Yu, T., Li, Y., Liu, G., et al. (2019a) The VirAB-VirSR-AnrAB multicomponent system is involved in resistance of *Listeria monocytogenes* EGD-e to cephalosporins, bacitracin, nisin, benzalkonium chloride, and ethidium bromide. *Applied and environmental microbiology*, doi: 10.1128/AEM.01470-19.
- Jiang, X., Ren, S., Geng, Y., Yu, T., Li, Y., Liu, L., et al. (2020) The *sug* operon involves in resistance to quaternary ammonium compounds in *Listeria monocytogenes* EGD-e. *Applied microbiology and biotechnology*, doi: 10.1007/s00253-020-10741-6.
- Jiang, X., Yu, T., Liang, Y., Ji, S., Guo, X., Ma, J., and Zhou, L. (2016) Efflux pump-mediated benzalkonium chloride resistance in *Listeria monocytogenes* isolated from retail food. *International journal of food microbiology*, doi: 10.1016/j.ijfoodmicro.2015.10.022.
- Jiang, X., Yu, T., Xu, Y., Wang, H., Korkeala, H., and Shi, L. (2019b) MdrL, a major facilitator superfamily efflux pump of *Listeria monocytogenes* involved in tolerance to benzalkonium chloride. *Applied microbiology and biotechnology*, doi: 10.1007/s00253-018-9551-y.
- Jiang, X., Zhou, L., Gao, D., Wang, Y., Wang, D., Zhang, Z., et al. (2012) Expression of efflux pump gene *lde* in ciprofloxacin-resistant foodborne isolates of *Listeria monocytogenes*. *Microbiology and immunology*, doi: 10.1111/j.1348-0421.2012.00506.x.
- Johnson, J.W., Fisher, J.F., and Mobashery, S. (2013) Bacterial cell-wall recycling. *Annals of the New York Academy of Sciences*, doi: 10.1111/j.1749-6632.2012.06813.x.
- Jolly, L., Ferrari, P., Blanot, D., van Heijenoort, J., Fassy, F., and Mengin-Lecreulx, D. (1999) Reaction mechanism of phosphoglucosamine mutase from *Escherichia coli*. *European journal of biochemistry*, doi: 10.1046/j.1432-1327.1999.00373.x.
-

-
- Jones, M.V., Herd, T.M., and Christie, H.J. (1989) Resistance of *Pseudomonas aeruginosa* to amphoteric and quaternary ammonium biocides. *Microbios*, **58**: 49–61.
- Jorge, A.M., Hoiczky, E., Gomes, J.P., and Pinho, M.G. (2011) EzrA contributes to the regulation of cell size in *Staphylococcus aureus*. *PLoS one*, doi: 10.1371/journal.pone.0027542.
- Junker, S., Maaß, S., Otto, A., Michalik, S., Morgenroth, F., Gerth, U., Hecker, M., and Becher, D. (2018) Spectral library based analysis of arginine phosphorylations in *Staphylococcus aureus*. *Molecular & cellular proteomics : MCP*, doi: 10.1074/mcp.RA117.000378.
- Kampf, G. (2018) Adaptive microbial response to low-level benzalkonium chloride exposure. *The Journal of hospital infection*, doi: 10.1016/j.jhin.2018.05.019.
- Kapoor, G., Saigal, S., and Elongavan, A. (2017) Action and resistance mechanisms of antibiotics: A guide for clinicians. *Journal of Anaesthesiology, Clinical Pharmacology*, doi: 10.4103/joacp.JOACP_349_15.
- Karamanos, Y. (1997) Endo-N-acetyl-beta-D-glucosaminidases and their potential substrates: structure/function relationships. *Research in microbiology*, doi: 10.1016/S0923-2508(99)80065-5.
- Karimova, G., Dautin, N., and Ladant, D. (2005) Interaction network among *Escherichia coli* membrane proteins involved in cell division as revealed by bacterial two-hybrid analysis. *Journal of bacteriology*, doi: 10.1128/JB.187.7.2233-2243.2005.
- Karimova, G., Pidoux, J., Ullmann, A., and Ladant, D. (1998) A bacterial two-hybrid system based on a reconstituted signal transduction pathway. *Proceedings of the National Academy of Sciences of the United States of America*, doi: 10.1073/pnas.95.10.5752.
- Karimova, G., Ullmann, A., and Ladant, D. (2001) Protein-protein interaction between *Bacillus stearothermophilus* tyrosyl-tRNA synthetase subdomains revealed by a bacterial two-hybrid system. *Journal of molecular microbiology and biotechnology*, **3**: 73–82.
- Karinou, E., Schuster, C.F., Pazos, M., Vollmer, W., and Gründling, A. (2019) Inactivation of the monofunctional peptidoglycan glycosyltransferase SgtB allows *Staphylococcus aureus* to survive in the absence of lipoteichoic acid. *Journal of bacteriology*, doi: 10.1128/JB.00574-18.
- Kaushik, D., Mohan, M., Borade, D.M., and Swami, O.C. (2014) Ampicillin: rise fall and resurgence. *Journal of clinical and diagnostic research : JCDR*, doi: 10.7860/JCDR/2014/8777.4356.
- Kaval, K.G., Hahn, B., Tusamda, N., Albrecht, D., and Halbedel, S. (2015) The PadR-like transcriptional regulator LftR ensures efficient invasion of *Listeria monocytogenes* into human host cells. *Frontiers in microbiology*, doi: 10.3389/fmicb.2015.00772.
- Kaval, K.G., Rismondo, J., and Halbedel, S. (2014) A function of DivIVA in *Listeria monocytogenes* division site selection. *Molecular microbiology*, doi: 10.1111/mmi.12784.
- Kawai, Y., Asai, K., and Errington, J. (2009) Partial functional redundancy of MreB isoforms, MreB, Mbl and MreBH, in cell morphogenesis of *Bacillus subtilis*. *Molecular microbiology*, doi: 10.1111/j.1365-2958.2009.06805.x.
-

-
- Kawai, Y., Marles-Wright, J., Cleverley, R.M., Emmins, R., Ishikawa, S., Kuwano, M., *et al.* (2011) A widespread family of bacterial cell wall assembly proteins. *The EMBO Journal*, doi: 10.1038/emboj.2011.358.
- Kawai, Y., Mercier, R., Mickiewicz, K., Serafini, A., Sório de Carvalho, L.P., and Errington, J. (2019) Crucial role for central carbon metabolism in the bacterial L-form switch and killing by β -lactam antibiotics. *Nature microbiology*, doi: 10.1038/s41564-019-0497-3.
- Kawai, Y., Mercier, R., Wu, L.J., Domínguez-Cuevas, P., Oshima, T., and Errington, J. (2015) Cell growth of wall-free L-form bacteria is limited by oxidative damage. *Current biology: CB*, doi: 10.1016/j.cub.2015.04.031.
- Kelliher, J.L., Grunenwald, C.M., Abrahams, R.R., Daanen, M.E., Lew, C.I., Rose, W.E., and Sauer, J.-D. (2021) PASTA kinase-dependent control of peptidoglycan synthesis via ReoM is required for cell wall stress responses, cytosolic survival, and virulence in *Listeria monocytogenes*. *PLoS pathogens*, doi: 10.1371/journal.ppat.1009881.
- Kern, T., Giffard, M., Hediger, S., Amoroso, A., Giustini, C., Bui, N.K., *et al.* (2010) Dynamics characterization of fully hydrated bacterial cell walls by solid-state NMR: evidence for cooperative binding of metal ions. *Journal of the American Chemical Society*, doi: 10.1021/ja104533w.
- Kim, M., Hatt, J.K., Weigand, M.R., Krishnan, R., Pavlostathis, S.G., and Konstantinidis, K.T. (2018a) Genomic and transcriptomic insights into how bacteria withstand high concentrations of benzalkonium chloride biocides. *Applied and environmental microbiology*, doi: 10.1128/AEM.00197-18.
- Kim, M., Weigand, M.R., Oh, S., Hatt, J.K., Krishnan, R., Tezel, U., Pavlostathis, S.G., and Konstantinidis, K.T. (2018b) Widely used benzalkonium chloride disinfectants can promote antibiotic resistance. *Applied and environmental microbiology*, doi: 10.1128/AEM.01201-18.
- Kock, H., Gerth, U., and Hecker, M. (2004) MurAA, catalysing the first committed step in peptidoglycan biosynthesis, is a target of Clp-dependent proteolysis in *Bacillus subtilis*. *Molecular microbiology*, doi: 10.1046/j.1365-2958.2003.03875.x.
- Kojima, N., Araki, Y., and Ito, E. (1985) Structure of the linkage units between ribitol teichoic acids and peptidoglycan. *Journal of bacteriology*, doi: 10.1128/jb.161.1.299-306.1985.
- Koo, B.-M., Kritikos, G., Farelli, J.D., Todor, H., Tong, K., Kimsey, H., *et al.* (2017) Construction and analysis of two genome-scale deletion libraries for *Bacillus subtilis*. *Cell systems*, doi: 10.1016/j.cels.2016.12.013.
- Kotnik, M., Anderluh, P.S., and Prezelj, A. (2007) Development of novel inhibitors targeting intracellular steps of peptidoglycan biosynthesis. *Current pharmaceutical design*, doi: 10.2174/138161207781368828.
- Kovacevic, J., Ziegler, J., Wałęcka-Zacharska, E., Reimer, A., Kitts, D.D., and Gilmour, M.W. (2016) Tolerance of *Listeria monocytogenes* to quaternary ammonium sanitizers is mediated by a novel efflux pump encoded by *emrE*. *Applied and environmental microbiology*, doi: 10.1128/AEM.03741-15.
- Kovács, M., Halfmann, A., Fedtke, I., Heintz, M., Peschel, A., Vollmer, W., Hakenbeck, R., and Brückner, R. (2006) A functional *dlt* operon, encoding proteins required for incorporation of D-alanine in teichoic acids in gram-positive bacteria, confers resistance to cationic antimicrobial peptides in *Streptococcus pneumoniae*. *Journal of bacteriology*, doi: 10.1128/JB.00336-06.
-

- Kreuzinger, N., Fuerhacker, M., Scharf, S., Uhl, M., Gans, O., and Grillitsch, B. (2007) Methodological approach towards the environmental significance of uncharacterized substances — quaternary ammonium compounds as an example. *Desalination*, doi: 10.1016/j.desal.2006.10.036.
- Kümmerer, K., Eitel, A., Braun, U., Hubner, P., Daschner, F., Mascart, G., et al. (1997) Analysis of benzalkonium chloride in the effluent from European hospitals by solid-phase extraction and high-performance liquid chromatography with post-column ion-pairing and fluorescence detection. *Journal of chromatography. A*, doi: 10.1016/s0021-9673(97)00242-2.
- Kuroda, T., and Tsuchiya, T. (2009) Multidrug efflux transporters in the MATE family. *Biochimica et biophysica acta*, doi: 10.1016/j.bbapap.2008.11.012.
- Laaberki, M.-H., Pfeffer, J., Clarke, A.J., and Dworkin, J. (2011) O-Acetylation of peptidoglycan is required for proper cell separation and S-layer anchoring in *Bacillus anthracis*. *Journal of Biological Chemistry*, doi: 10.1074/jbc.M110.183236.
- Labana, P., Dornan, M.H., Lafrenière, M., Czarny, T.L., Brown, E.D., Pezacki, J.P., and Boddy, C.N. (2021) Armeniaspirols inhibit the AAA+ proteases ClpXP and ClpYQ leading to cell division arrest in gram-positive bacteria. *Cell chemical biology*, doi: 10.1016/j.chembiol.2021.07.001.
- Lai, G.C., Cho, H., and Bernhardt, T.G. (2017) The mecillinam resistome reveals a role for peptidoglycan endopeptidases in stimulating cell wall synthesis in *Escherichia coli*. *PLoS genetics*, doi: 10.1371/journal.pgen.1006934.
- Lambert, M.P., and Neuhaus, F.C. (1972) Mechanism of D-cycloserine action: alanine racemase from *Escherichia coli* W. *Journal of bacteriology*, doi: 10.1128/jb.110.3.978-987.1972.
- Lazarevic, V., and Karamata, D. (1995) The *tagGH* operon of *Bacillus subtilis* 168 encodes a two-component ABC transporter involved in the metabolism of two wall teichoic acids. *Molecular microbiology*, doi: 10.1111/j.1365-2958.1995.tb02306.x.
- Leaver, M., and Errington, J. (2005) Roles for MreC and MreD proteins in helical growth of the cylindrical cell wall in *Bacillus subtilis*. *Molecular microbiology*, doi: 10.1111/j.1365-2958.2005.04736.x.
- Leclercq, S., Derouaux, A., Olatunji, S., Fraipont, C., Egan, A.J.F., Vollmer, W., Breukink, E., and Terrak, M. (2017) Interplay between penicillin-binding proteins and SEDS proteins promotes bacterial cell wall synthesis. *Scientific reports*, doi: 10.1038/srep43306.
- Lecuit, M. (2007) Human listeriosis and animal models. *Microbes and infection*, doi: 10.1016/j.micinf.2007.05.009.
- Lee, T.K., and Huang, K.C. (2013) The role of hydrolases in bacterial cell-wall growth. *Current opinion in microbiology*, doi: 10.1016/j.mib.2013.08.005.
- Lenarcic, R., Halbedel, S., Visser, L., Shaw, M., Wu, L.J., Errington, J., Marenduzzo, D., and Hamoen, L.W. (2009) Localisation of DivIVA by targeting to negatively curved membranes. *The EMBO Journal*, doi: 10.1038/emboj.2009.129.

- Lenz, L.L., Mohammadi, S., Geissler, A., and Portnoy, D.A. (2003) SecA2-dependent secretion of autolytic enzymes promotes *Listeria monocytogenes* pathogenesis. *Proceedings of the National Academy of Sciences of the United States of America*, doi: 10.1073/pnas.2133653100.
- Lenz, L.L., and Portnoy, D.A. (2002) Identification of a second *Listeria* secA gene associated with protein secretion and the rough phenotype. *Molecular microbiology*, doi: 10.1046/j.1365-2958.2002.03072.x.
- Levin, P.A., Kurtser, I.G., and Grossman, A.D. (1999) Identification and characterization of a negative regulator of FtsZ ring formation in *Bacillus subtilis*. *Proceedings of the National Academy of Sciences of the United States of America*, **96**: 9642–9647.
- Li, X., and Brownawell, B.J. (2010) Quaternary ammonium compounds in urban estuarine sediment environments—a class of contaminants in need of increased attention? *Environmental science & technology*, doi: 10.1021/es1011669.
- Libby, E.A., Goss, L.A., and Dworkin, J. (2015) The eukaryotic-like Ser/Thr kinase PrkC regulates the essential WalRK two-component system in *Bacillus subtilis*. *PLoS genetics*, doi: 10.1371/journal.pgen.1005275.
- Liger, D., Masson, A., Blanot, D., van Heijenoort, J., and Parquet, C. (1995) Over-production, purification and properties of the uridine-diphosphate-N-acetylmuramate: L-alanine ligase from *Escherichia coli*. *European journal of biochemistry*, doi: 10.1111/j.1432-1033.1995.0080i.x.
- Locher, K.P. (2016) Mechanistic diversity in ATP-binding cassette (ABC) transporters. *Nature structural & molecular biology*, doi: 10.1038/nsmb.3216.
- Lovering, A.L., Safadi, S.S., and Strynadka, N.C.J. (2012) Structural perspective of peptidoglycan biosynthesis and assembly. *Annual review of biochemistry*, doi: 10.1146/annurev-biochem-061809-112742.
- Löwe, J., and Amos, L.A. (1998) Crystal structure of the bacterial cell-division protein FtsZ. *Nature*, doi: 10.1038/34472.
- Lundén, J., Autio, T., Markkula, A., Hellström, S., and Korkeala, H. (2003) Adaptive and cross-adaptive responses of persistent and non-persistent *Listeria monocytogenes* strains to disinfectants. *International journal of food microbiology*, doi: 10.1016/s0168-1605(02)00312-4.
- Lutkenhaus, J., and Addinall, S.G. (1997) Bacterial cell division and the Z ring. *Annual review of biochemistry*, doi: 10.1146/annurev.biochem.66.1.93.
- Lutkenhaus J. F. Organization of genes in the *ftsA-envA* region of the *Escherichia coli* genetic map and identification of a new *fts* locus (*ftsZ*). *Journal of bacteriology*, doi: 10.1128/jb.142.2.615-620.1980.
- Machado, I., Coquet, L., Jouenne, T., and Pereira, M.O. (2013) Proteomic approach to *Pseudomonas aeruginosa* adaptive resistance to benzalkonium chloride. *Journal of proteomics*, doi: 10.1016/j.jprot.2013.04.030.
- Machata, S., Hain, T., Rohde, M., and Chakraborty, T. (2005) Simultaneous deficiency of both MurA and P60 proteins generates a rough phenotype in *Listeria monocytogenes*. *Journal of bacteriology*, doi: 10.1128/JB.187.24.8385-8394.2005.

- Mächtel, R., Narducci, A., Griffith, D.A., Cordes, T., and Orelle, C. (2019) An integrated transport mechanism of the maltose ABC importer. *Research in microbiology*, doi: 10.1016/j.resmic.2019.09.004.
- Magnúsdóttir, S., Ravcheev, D., Crécy-Lagard, V. de, and Thiele, I. (2015) Systematic genome assessment of B-vitamin biosynthesis suggests co-operation among gut microbes. *Frontiers in genetics*, doi: 10.3389/fgene.2015.00148.
- Marquardt, J.L., Brown, E.D., Lane, W.S., Haley, T.M., Ichikawa, Y., Wong, C.H., and Walsh, C.T. (1994) Kinetics, stoichiometry, and identification of the reactive thiolate in the inactivation of UDP-GlcNAc enolpyruvyl transferase by the antibiotic fosfomycin. *Biochemistry*, doi: 10.1021/bi00201a011.
- Martin, H.A., Porter, K.E., Vallin, C., Ermi, T., Contreras, N., Pedraza-Reyes, M., and Robleto, E.A. (2019) Mfd protects against oxidative stress in *Bacillus subtilis* independently of its canonical function in DNA repair. *BMC Microbiology*, doi: 10.1186/s12866-019-1394-x.
- Martin, H.H., and Gmeiner, J. (1979) Modification of peptidoglycan structure by penicillin action in cell walls of *Proteus mirabilis*. *European journal of biochemistry*, doi: 10.1111/j.1432-1033.1979.tb12988.x.
- Martínez-Carballo, E., González-Barreiro, C., Sitka, A., Kreuzinger, N., Scharf, S., and Gans, O. (2007) Determination of selected quaternary ammonium compounds by liquid chromatography with mass spectrometry. Part II. Application to sediment and sludge samples in Austria. *Environmental pollution (Barking, Essex : 1987)*, doi: 10.1016/j.envpol.2006.07.016.
- Martínez-Suárez, J.V., Ortiz, S., and López-Alonso, V. (2016) Potential impact of the resistance to quaternary ammonium disinfectants on the persistence of *Listeria monocytogenes* in food processing environments. *Frontiers in microbiology*, doi: 10.3389/fmicb.2016.00638.
- Mata, M.T., Baquero, F., and Pérez-Díaz, J.C. (2000) A multidrug efflux transporter in *Listeria monocytogenes*. *FEMS Microbiology Letters*, doi: 10.1111/j.1574-6968.2000.tb09158.x.
- Matias, V.R.F., and Beveridge, T.J. (2006) Native cell wall organization shown by cryo-electron microscopy confirms the existence of a periplasmic space in *Staphylococcus aureus*. *Journal of bacteriology*, doi: 10.1128/JB.188.3.1011-1021.2006.
- Matias, V.R.F., and Beveridge, T.J. (2007) Cryo-electron microscopy of cell division in *Staphylococcus aureus* reveals a mid-zone between nascent cross walls. *Molecular microbiology*, doi: 10.1111/j.1365-2958.2007.05634.x.
- Matsuoka, S., Hashimoto, M., Kamiya, Y., Miyazawa, T., Ishikawa, K., Hara, H., and Matsumoto, K. (2011) The *Bacillus subtilis* essential gene *dgkB* is dispensable in mutants with defective lipoteichoic acid synthesis. *Genes & genetic systems*, doi: 10.1266/ggs.86.365.
- May, J.J., Finking, R., Wiegeshoff, F., Weber, T.T., Bandur, N., Koert, U., and Marahiel, M.A. (2005) Inhibition of the D-alanine: D-alanyl carrier protein ligase from *Bacillus subtilis* increases the bacterium's susceptibility to antibiotics that target the cell wall. *The FEBS journal*, doi: 10.1111/j.1742-4658.2005.04700.x.
- Meeske, A.J., Riley, E.P., Robins, W.P., Uehara, T., Mekalanos, J.J., Kahne, D., et al. (2016) SEDS proteins are a widespread family of bacterial cell wall polymerases. *Nature*, doi: 10.1038/nature19331.

-
- Meeske, A.J., Sham, L.-T., Kimsey, H., Koo, B.-M., Gross, C.A., Bernhardt, T.G., and Rudner, D.Z. (2015) MurJ and a novel lipid II flippase are required for cell wall biogenesis in *Bacillus subtilis*. *Proceedings of the National Academy of Sciences of the United States of America*, doi: 10.1073/pnas.1504967112.
- Meier, A.B., Guldimann, C., Markkula, A., Pöntinen, A., Korkeala, H., and Tasara, T. (2017) Comparative phenotypic and genotypic analysis of swiss and finnish *Listeria monocytogenes* isolates with respect to benzalkonium chloride resistance. *Frontiers in microbiology*, doi: 10.3389/fmicb.2017.00397.
- Meisner, J., Montero Llopis, P., Sham, L.-T., Garner, E., Bernhardt, T.G., and Rudner, D.Z. (2013) FtsEX is required for CwO peptidoglycan hydrolase activity during cell wall elongation in *Bacillus subtilis*. *Molecular microbiology*, doi: 10.1111/mmi.12330.
- Mengaud, J., Ohayon, H., Gounon, P., Mege, R.-M., and Cossart, P. (1996) E-cadherin is the receptor for internalin, a surface protein required for entry of *L. monocytogenes* into epithelial cells. *Cell*, doi: 10.1016/s0092-8674(00)81070-3.
- Mengin-Lecreulx, D., and van Heijenoort, J. (1994) Copurification of glucosamine-1-phosphate acetyltransferase and N-acetylglucosamine-1-phosphate uridyltransferase activities of *Escherichia coli*: characterization of the *glmU* gene product as a bifunctional enzyme catalyzing two subsequent steps in the pathway for UDP-N-acetylglucosamine synthesis. *Journal of bacteriology*, doi: 10.1128/jb.176.18.5788-5795.1994.
- Mengin-Lecreulx, D., and van Heijenoort, J. (1996) Characterization of the essential gene *glmM* encoding phosphoglucosamine mutase in *Escherichia coli*. *The Journal of biological chemistry*, doi: 10.1074/jbc.271.1.32.
- Merchel Piovesan Pereira, B., and Tagkopoulos, I. (2019) Benzalkonium chlorides: uses, regulatory status, and microbial resistance. *Applied and environmental microbiology*, doi: 10.1128/AEM.00377-19.
- Meredith, T.C., Swoboda, J.G., and Walker, S. (2008) Late-stage polyribitol phosphate wall teichoic acid biosynthesis in *Staphylococcus aureus*. *Journal of bacteriology*, doi: 10.1128/JB.01880-07.
- Minarovičová, J., Véghová, A., Mikulášová, M., Chovanová, R., Šoltýs, K., Drahovská, H., and Kačíková, E. (2018) Benzalkonium chloride tolerance of *Listeria monocytogenes* strains isolated from a meat processing facility is related to presence of plasmid-borne *bcrABC* cassette. *Antonie van Leeuwenhoek*, doi: 10.1007/s10482-018-1082-0.
- Mir, M., Asong, J., Li, X., Cardot, J., Boons, G.-J., and Husson, R.N. (2011) The extracytoplasmic domain of the *Mycobacterium tuberculosis* Ser/Thr kinase PknB binds specific muropeptides and is required for PknB localization. *PLoS pathogens*, doi: 10.1371/journal.ppat.1002182.
- Mirouze, N., Ferret, C., Cornilleau, C., and Carballido-López, R. (2018) Antibiotic sensitivity reveals that wall teichoic acids mediate DNA binding during competence in *Bacillus subtilis*. *Nature communications*, doi: 10.1038/s41467-018-07553-8.
- Mohammadi, T., Sijbrandi, R., Lutters, M., Verheul, J., Martin, N.I., den Blaauwen, T., Kruijff, B. de, and Breukink, E. (2014) Specificity of the transport of lipid II by FtsW in *Escherichia coli*. *The Journal of biological chemistry*, doi: 10.1074/jbc.M114.557371.
-

- Mohammadi, T., van Dam, V., Sijbrandi, R., Vernet, T., Zapun, A., Bouhss, A., *et al.* (2011) Identification of FtsW as a transporter of lipid-linked cell wall precursors across the membrane. *The EMBO Journal*, doi: 10.1038/emboj.2011.61.
- Morita, Y., Murata, T., Mima, T., Shiota, S., Kuroda, T., Mizushima, T., *et al.* (2003) Induction of *mexCD-oprJ* operon for a multidrug efflux pump by disinfectants in wild-type *Pseudomonas aeruginosa* PAO1. *The Journal of antimicrobial chemotherapy*, doi: 10.1093/jac/dkg173.
- Müller, A., Rychli, K., Muhterem-Uyar, M., Zaiser, A., Stessl, B., Guinane, C.M., *et al.* (2013) Tn6188 - a novel transposon in *Listeria monocytogenes* responsible for tolerance to benzalkonium chloride. *PLoS one*, doi: 10.1371/journal.pone.0076835.
- Müller, A., Rychli, K., Zaiser, A., Wieser, C., Wagner, M., and Schmitz-Esser, S. (2014) The *Listeria monocytogenes* transposon Tn6188 provides increased tolerance to various quaternary ammonium compounds and ethidium bromide. *FEMS Microbiology Letters*, doi: 10.1111/1574-6968.12626.
- Nagai, K., Murata, T., Ohta, S., Zenda, H., Ohnishi, M., and Hayashi, T. (2003) Two different mechanisms are involved in the extremely high-level benzalkonium chloride resistance of a *Pseudomonas fluorescens* strain. *Microbiology and immunology*, doi: 10.1111/j.1348-0421.2003.tb03440.x.
- Nakano, S., Küster-Schöck, E., Grossman, A.D., and Zuber, P. (2003) Spx-dependent global transcriptional control is induced by thiol-specific oxidative stress in *Bacillus subtilis*. *Proceedings of the National Academy of Sciences of the United States of America*, doi: 10.1073/pnas.2235180100.
- Navarre, W.W., and Schneewind, O. (1999) Surface proteins of gram-positive bacteria and mechanisms of their targeting to the cell wall envelope. *Microbiology and molecular biology reviews: MMBR*, **63**: 174–229.
- Neuhaus, F.C., and Baddiley, J. (2003) A continuum of anionic charge: structures and functions of D-alanyl-teichoic acids in gram-positive bacteria. *Microbiology and molecular biology reviews: MMBR*, doi: 10.1128/MMBR.67.4.686-723.2003.
- Neuhaus, F.C., and Lynch, J.L. (1964) The enzymatic synthesis of D-alanyl-D-alanine. III. On the inhibition of D-Alanyl-D-alanine synthetase by the antibiotic D-cycloserine. *Biochemistry*, doi: 10.1021/bi00892a001.
- Nicoletti, G., Boghossian, V., Gurevitch, F., Borland, R., and Morgenroth, P. (1993) The antimicrobial activity in vitro of chlorhexidine, a mixture of isothiazolinones ('Kathon' CG) and cetyl trimethyl ammonium bromide (CTAB). *The Journal of hospital infection*, doi: 10.1016/0195-6701(93)90014-q.
- Nordholt, N., Kanaris, O., Schmidt, S.B.I., and Schreiber, F. (2021) Persistence against benzalkonium chloride promotes rapid evolution of tolerance during periodic disinfection. *Nature Communications*, doi: 10.1038/s41467-021-27019-8.
- Ogbonna, E.C., Anderson, H.R., and Schmitz, K.R. (2022) Identification of arginine phosphorylation in *Mycobacterium smegmatis*. *Microbiology spectrum*, doi: 10.1128/spectrum.02042-22.

-
- Oliver, H.F., Orsi, R.H., Ponnala, L., Keich, U., Wang, W., Sun, Q., *et al.* (2009) Deep RNA sequencing of *L. monocytogenes* reveals overlapping and extensive stationary phase and *sigma B*-dependent transcriptomes, including multiple highly transcribed noncoding RNAs. *BMC Genomics*, doi: 10.1186/1471-2164-10-641.
- Omote, H., Hiasa, M., Matsumoto, T., Otsuka, M., and Moriyama, Y. (2006) The MATE proteins as fundamental transporters of metabolic and xenobiotic organic cations. *Trends in pharmacological sciences*, doi: 10.1016/j.tips.2006.09.001.
- Osek, J., Lachtara, B., and Wiczorek, K. (2022) *Listeria monocytogenes* - How this pathogen survives in food-production environments? *Frontiers in microbiology*, doi: 10.3389/fmicb.2022.866462.
- Park, W., Seto, H., Hakenbeck, R., and Matsuhashi, M. (1985) Major peptidoglycan transglycosylase activity in *Streptococcus pneumoniae* that is not a penicillin-binding protein. *FEMS Microbiology Letters*, doi: 10.1111/j.1574-6968.1985.tb01635.x.
- Patel, V., Wu, Q., Chandrangsu, P., and Helmann, J.D. (2018) A metabolic checkpoint protein GlmR is important for diverting carbon into peptidoglycan biosynthesis in *Bacillus subtilis*. *PLoS genetics*, doi: 10.1371/journal.pgen.1007689.
- Patel, Y., Soni, V., Rhee, K.Y., and Helmann, J.D. (2023) Mutations in *rpoB* that confer rifampicin resistance can alter levels of peptidoglycan precursors and affect β -lactam susceptibility. *mBio*, doi: 10.1128/mbio.03168-22.
- Paulsen, I.T., Skurray, R.A., Tam, R., Saier, M.H., Turner, R.J., Weiner, J.H., Goldberg, E.B., and Grinius, L.L. (1996) The SMR family: a novel family of multidrug efflux proteins involved with the efflux of lipophilic drugs. *Molecular microbiology*, doi: 10.1111/j.1365-2958.1996.tb02462.x.
- Pazos, M., and Peters, K. (2019) Peptidoglycan. *Sub-cellular biochemistry*, doi: 10.1007/978-3-030-18768-2_5.
- Pederick, J.L., Thompson, A.P., Bell, S.G., and Bruning, J.B. (2020) D-Alanine-D-alanine ligase as a model for the activation of ATP-grasp enzymes by monovalent cations. *Journal of Biological Chemistry*, doi: 10.1074/jbc.RA120.012936.
- Pensinger, D.A., Boldon, K.M., Chen, G.Y., Vincent, W.J.B., Sherman, K., Xiong, M., *et al.* (2016) The *Listeria monocytogenes* PASTA kinase PrkA and its substrate Yvck are required for cell wall homeostasis, metabolism, and virulence. *PLoS pathogens*, doi: 10.1371/journal.ppat.1006001.
- Pensinger, D.A., Gutierrez, K.V., Smith, H.B., Vincent, W.J., Stevenson, D.S., and Black, K.A., *et al.* (2021) *Listeria monocytogenes* GlmR is an accessory uridylyltransferase essential for cytosolic survival and virulence.
- Pensinger, D.A., Gutierrez, K.V., Smith, H.B., Vincent, W.J.B., Stevenson, D.S., Black, K.A., *et al.* (2023) *Listeria monocytogenes* GlmR is an accessory uridylyltransferase essential for cytosolic survival and virulence. *mBio*, doi: 10.1128/mbio.00073-23.
- Percy, M.G., and Gründling, A. (2014) Lipoteichoic acid synthesis and function in gram-positive bacteria. *Annual review of microbiology*, doi: 10.1146/annurev-micro-091213-112949.
-

- Percy, M.G., Karinou, E., Webb, A.J., and Gründling, A. (2016) Identification of a lipoteichoic acid glycosyltransferase enzyme reveals that GW-domain-containing proteins can be retained in the cell wall of *Listeria monocytogenes* in the absence of lipoteichoic acid or its modifications. *Journal of bacteriology*, doi: 10.1128/JB.00116-16.
- Perego, M., Glaser, P., Minutello, A., Strauch, M.A., Leopold, K., and Fischer, W. (1995) Incorporation of D-alanine into lipoteichoic acid and wall teichoic acid in *Bacillus subtilis*. Identification of genes and regulation. *The Journal of biological chemistry*, doi: 10.1074/jbc.270.26.15598.
- Pereira, M.P., D'Elia, M.A., Troczynska, J., and Brown, E.D. (2008) Duplication of teichoic acid biosynthetic genes in *Staphylococcus aureus* leads to functionally redundant poly(ribitol phosphate) polymerases. *Journal of bacteriology*, doi: 10.1128/JB.00526-08.
- Peschel, A., Otto, M., Jack, R.W., Kalbacher, H., Jung, G., and Götz, F. (1999) Inactivation of the *dlt* operon in *Staphylococcus aureus* confers sensitivity to defensins, protegrins, and other antimicrobial peptides. *The Journal of biological chemistry*, doi: 10.1074/jbc.274.13.8405.
- Peschel, A., Vuong, C., Otto, M., and Götz, F. (2000) The D-alanine residues of *Staphylococcus aureus* teichoic acids alter the susceptibility to vancomycin and the activity of autolytic enzymes. *Antimicrobial agents and chemotherapy*, doi: 10.1128/AAC.44.10.2845-2847.2000.
- Pichoff, S., and Lutkenhaus, J. (2005) Tethering the Z ring to the membrane through a conserved membrane targeting sequence in FtsA. *Molecular microbiology*, doi: 10.1111/j.1365-2958.2005.04522.x.
- Pinho, M.G., and Errington, J. (2005) Recruitment of penicillin-binding protein PBP2 to the division site of *Staphylococcus aureus* is dependent on its transpeptidation substrates. *Molecular microbiology*, doi: 10.1111/j.1365-2958.2004.04420.x.
- Plumbridge, J. (2015) Regulation of the utilization of amino sugars by *Escherichia coli* and *Bacillus subtilis*: Same genes, different control. *Journal of molecular microbiology and biotechnology*, doi: 10.1159/000369583.
- Pompeo, F., Byrne, D., Mengin-Lecreux, D., and Galinier, A. (2018) Dual regulation of activity and intracellular localization of the PASTA kinase PrkC during *Bacillus subtilis* growth. *Scientific reports*, doi: 10.1038/s41598-018-20145-2.
- Pompeo, F., Foulquier, E., Serrano, B., Grangeasse, C., and Galinier, A. (2015) Phosphorylation of the cell division protein GpsB regulates PrkC kinase activity through a negative feedback loop in *Bacillus subtilis*. *Molecular microbiology*, doi: 10.1111/mmi.13015.
- Pooley, H.M., and Karamata, D. (2000) Incorporation of 2-3Hglycerol into cell surface components of *Bacillus subtilis* 168 and thermosensitive mutants affected in wall teichoic acid synthesis: effect of tunicamycin. *Microbiology (Reading, England)*, doi: 10.1099/00221287-146-4-797.
- Popowska, M., Kusio, M., Szymanska, P., and Markiewicz, Z. (2009) Inactivation of the wall-associated de-N-acetylase (PgdA) of *Listeria monocytogenes* results in greater susceptibility of the cells to induced autolysis. *Journal of microbiology and biotechnology*, doi: 10.4014/jmb.0810.557.

-
- Price, N.P.J., and Tsvetanova, B. (2007) Biosynthesis of the tunicamycins: a review. *The Journal of antibiotics*, doi: 10.1038/ja.2007.62.
- Prosser, G.A., and Carvalho, L.P.S. de (2013) Kinetic mechanism and inhibition of *Mycobacterium tuberculosis* D-alanine:D-alanine ligase by the antibiotic D-cycloserine. *The FEBS journal*, doi: 10.1111/febs.12108.
- Puls, J.-S., Brajtenbach, D., Schneider, T., Kubitscheck, U., and Grein, F. (2023) Inhibition of peptidoglycan synthesis is sufficient for total arrest of *staphylococcal* cell division. *Science advances*, doi: 10.1126/sciadv.ade9023.
- Quentin, Y., Fichant, G., and Denizot, F. (1999) Inventory, assembly and analysis of *Bacillus subtilis* ABC transport systems. *Journal of molecular biology*, doi: 10.1006/jmbi.1999.2624.
- Radchenko, M., Symersky, J., Nie, R., and Lu, M. (2015) Structural basis for the blockade of MATE multidrug efflux pumps. *Nature Communications*, doi: 10.1038/ncomms8995.
- Rae, C.S., Geissler, A., Adamson, P.C., and Portnoy, D.A. (2011) Mutations of the *Listeria monocytogenes* peptidoglycan N-deacetylase and O-acetylase result in enhanced lysozyme sensitivity, bacteriolysis, and hyperinduction of innate immune pathways. *Infection and immunity*, doi: 10.1128/IAI.00077-11.
- Raengpradub, S., Wiedmann, M., and Boor, K.J. (2008) Comparative analysis of the *sigma B*-dependent stress responses in *Listeria monocytogenes* and *Listeria innocua* strains exposed to selected stress conditions. *Applied and environmental microbiology*, doi: 10.1128/AEM.00951-07.
- Ragland, S.A., and Criss, A.K. (2017) From bacterial killing to immune modulation: Recent insights into the functions of lysozyme. *PLoS pathogens*, doi: 10.1371/journal.ppat.1006512.
- Rakic-Martinez, M., Drevets, D.A., Dutta, V., Katic, V., and Kathariou, S. (2011) *Listeria monocytogenes* strains selected on ciprofloxacin or the disinfectant benzalkonium chloride exhibit reduced susceptibility to ciprofloxacin, gentamicin, benzalkonium chloride, and other toxic compounds. *Applied and environmental microbiology*, doi: 10.1128/AEM.05941-11.
- Ravikumar, V., Shi, L., Krug, K., Derouiche, A., Jers, C., Cousin, C., et al. (2014) Quantitative phosphoproteome analysis of *Bacillus subtilis* reveals novel substrates of the kinase PrkC and phosphatase PrpC. *Molecular & cellular proteomics : MCP*, doi: 10.1074/mcp.M113.035949.
- Reichmann, N.T., and Gründling, A. (2011) Location, synthesis and function of glycolipids and polyglycerolphosphate lipoteichoic acid in gram-positive bacteria of the phylum Firmicutes. *FEMS Microbiology Letters*, doi: 10.1111/j.1574-6968.2011.02260.x.
- Rietberg, K., Lloyd, J., Melius, B., Wyman, P., Treadwell, R., Olson, G., Kang, M.-G., and Duchin, J.S. (2016) Outbreak of *Listeria monocytogenes* infections linked to a pasteurized ice cream product served to hospitalized patients. *Epidemiology and infection*, doi: 10.1017/S0950268815003039.
- Rismondo, J., Cleverley, R.M., Lane, H.V., Großhennig, S., Steglich, A., Möller, L., et al. (2016) Structure of the bacterial cell division determinant GpsB and its interaction with penicillin-binding proteins. *Molecular microbiology*, doi: 10.1111/mmi.13279.
-

- Rismondo, J., Halbedel, S., and Gründling, A. (2019) Cell shape and antibiotic resistance are maintained by the activity of multiple FtsW and RodA enzymes in *Listeria monocytogenes*. *mBio*, doi: 10.1128/mBio.01448-19.
- Rismondo, J., Möller, L., Aldridge, C., Gray, J., Vollmer, W., and Halbedel, S. (2015) Discrete and overlapping functions of peptidoglycan synthases in growth, cell division and virulence of *Listeria monocytogenes*. *Molecular microbiology*, doi: 10.1111/mmi.12873.
- Rismondo, J., and Schulz, L.M. (2021) Not just transporters: Alternative functions of ABC transporters in *Bacillus subtilis* and *Listeria monocytogenes*. *Microorganisms*, doi: 10.3390/microorganisms9010163.
- Rismondo, J., Schulz, L.M., Yacoub, M., Wadhawan, A., Hoppert, M., Dionne, M.S., and Gründling, A. (2021) EsLB is required for cell wall biosynthesis and modification in *Listeria monocytogenes*. *Journal of bacteriology*, doi: 10.1128/JB.00553-20.
- Rismondo, J., Wamp, S., Aldridge, C., Vollmer, W., and Halbedel, S. (2018) Stimulation of PgdA-dependent peptidoglycan N-deacetylation by GpsB-PBP A1 in *Listeria monocytogenes*. *Molecular microbiology*, doi: 10.1111/mmi.13893.
- Rohde, M. (2019) The gram-positive bacterial cell wall. *Microbiology spectrum*, doi: 10.1128/microbiolspec.GPP3-0044-2018.
- Rohs, P.D.A., Buss, J., Sim, S.I., Squyres, G.R., Srisuknimit, V., Smith, M., et al. (2018) A central role for PBP2 in the activation of peptidoglycan polymerization by the bacterial cell elongation machinery. *PLoS genetics*, doi: 10.1371/journal.pgen.1007726.
- Romanova, N., Favrin, S., and Griffiths, M.W. (2002) Sensitivity of *Listeria monocytogenes* to sanitizers used in the meat processing industry. *Applied and environmental microbiology*, doi: 10.1128/AEM.68.12.6405-6409.2002.
- Romanova, N.A., Wolffs, P.F.G., Brovko, L.Y., and Griffiths, M.W. (2006) Role of efflux pumps in adaptation and resistance of *Listeria monocytogenes* to benzalkonium chloride. *Applied and environmental microbiology*, doi: 10.1128/AEM.72.5.3498-3503.2006.
- Rosenberg, J., Dickmanns, A., Neumann, P., Gunka, K., Arens, J., Kaefer, V., et al. (2015) Structural and biochemical analysis of the essential diadenylate cyclase CdaA from *Listeria monocytogenes*. *Journal of Biological Chemistry*, doi: 10.1074/jbc.M114.630418.
- Rouquette-Loughlin, C., Dunham, S.A., Kuhn, M., Balthazar, J.T., and Shafer, W.M. (2003) The NorM efflux pump of *Neisseria gonorrhoeae* and *Neisseria meningitidis* recognizes antimicrobial cationic compounds. *Journal of bacteriology*, doi: 10.1128/JB.185.3.1101-1106.2003.
- Rowlett, V.W., and Margolin, W. (2013) The bacterial Min system. *Current biology : CB*, doi: 10.1016/j.cub.2013.05.024.
- Rubino, F.A., Kumar, S., Ruiz, N., Walker, S., and Kahne, D.E. (2018) Membrane potential is required for MurJ function. *Journal of the American Chemical Society*, doi: 10.1021/jacs.8b00942.
- Ruiz, N. (2008) Bioinformatics identification of MurJ (MviN) as the peptidoglycan lipid II flippase in *Escherichia coli*. *Proceedings of the National Academy of Sciences of the United States of America*, doi: 10.1073/pnas.0808352105.

-
- Ruiz, N. (2016) Filling holes in peptidoglycan biogenesis of *Escherichia coli*. *Current opinion in microbiology*, doi: 10.1016/j.mib.2016.07.010.
- Sakagami, Y., Yokoyama, H., Nishimura, H., Ose, Y., and Tashima, T. (1989) Mechanism of resistance to benzalkonium chloride by *Pseudomonas aeruginosa*. *Applied and environmental microbiology*, doi: 10.1128/aem.55.8.2036-2040.1989.
- Salamaga, B., Kong, L., Pasquina-Lemonche, L., Lafage, L., zur Und Muhlen, M. von, Gibson, J.F., et al. (2021) Demonstration of the role of cell wall homeostasis in *Staphylococcus aureus* growth and the action of bactericidal antibiotics. *Proceedings of the National Academy of Sciences of the United States of America*, doi: 10.1073/pnas.2106022118.
- Sauvage, E., Kerff, F., Terrak, M., Ayala, J.A., and Charlier, P. (2008) The penicillin-binding proteins: structure and role in peptidoglycan biosynthesis. *FEMS microbiology reviews*, doi: 10.1111/j.1574-6976.2008.00105.x.
- Scheffers, D.-J., and Pinho, M.G. (2005) Bacterial cell wall synthesis: new insights from localization studies. *Microbiology and molecular biology reviews: MMBR*, doi: 10.1128/MMBR.69.4.585-607.2005.
- Scheurwater, E., Reid, C.W., and Clarke, A.J. (2008) Lytic transglycosylases: bacterial space-making autolysins. *The international journal of biochemistry & cell biology*, doi: 10.1016/j.biocel.2007.03.018.
- Schirmer, F., Ehrt, S., and Hillen, W. (1997) Expression, inducer spectrum, domain structure, and function of MopR, the regulator of phenol degradation in *Acinetobacter calcoaceticus* NCIB8250. *Journal of bacteriology*, doi: 10.1128/jb.179.4.1329-1336.1997.
- Schlag, M., Biswas, R., Krismer, B., Kohler, T., Zoll, S., Yu, W., et al. (2010) Role of staphylococcal wall teichoic acid in targeting the major autolysin Atl. *Molecular microbiology*, doi: 10.1111/j.1365-2958.2009.07007.x.
- Schmidt, A., Trentini, D.B., Spiess, S., Fuhrmann, J., Ammerer, G., Mechtler, K., and Clausen, T. (2014) Quantitative phosphoproteomics reveals the role of protein arginine phosphorylation in the bacterial stress response. *Molecular & cellular proteomics: MCP*, doi: 10.1074/mcp.M113.032292.
- Schmidt, K.L., Peterson, N.D., Kustus, R.J., Wissel, M.C., Graham, B., Phillips, G.J., and Weiss, D.S. (2004) A predicted ABC transporter, FtsEX, is needed for cell division in *Escherichia coli*. *Journal of bacteriology*, doi: 10.1128/JB.186.3.785-793.2004.
- Schneider, E. (2001) ABC transporters catalyzing carbohydrate uptake. *Research in microbiology*, doi: 10.1016/s0923-2508(01)01201-3.
- Schubert, W.D., Urbanke, C., Ziehm, T., Beier, V., Machner, M.P., Domann, E., et al. (2002) Structure of internalin, a major invasion protein of *Listeria monocytogenes*, in complex with its human receptor E-cadherin. *Cell*, doi: 10.1016/s0092-8674(02)01136-4.
- Schulz, L.M., Dreier, F., Sousa Miranda, L.M. de, and Rismondo, J. (2023) Adaptation mechanisms of *Listeria monocytogenes* to quaternary ammonium compounds. *bioRxiv*, doi: 10.1101/2023.03.30.534860.
- Schulz, L.M., Rothe, P., Halbedel, S., Gründling, A., and Rismondo, J. (2022) Imbalance of peptidoglycan biosynthesis alters the cell surface charge of *Listeria monocytogenes*. *Cell surface*, doi: 10.1016/j.tcs.2022.100085.
-

-
- Schuster, C.F., Wiedemann, D.M., Kirsebom, F.C.M., Santiago, M., Walker, S., and Gründling, A. (2020) High-throughput transposon sequencing highlights the cell wall as an important barrier for osmotic stress in methicillin resistant *Staphylococcus aureus* and underlines a tailored response to different osmotic stressors. *Molecular microbiology*, doi: 10.1111/mmi.14433.
- Shah, I.M., Laaberki, M.-H., Popham, D.L., and Dworkin, J. (2008) A eukaryotic-like Ser/Thr kinase signals bacteria to exit dormancy in response to peptidoglycan fragments. *Cell*, doi: 10.1016/j.cell.2008.08.039.
- Sham, L.-T., Butler, E.K., Lebar, M.D., Kahne, D., Bernhardt, T.G., and Ruiz, N. (2014) Bacterial cell wall. MurJ is the flippase of lipid-linked precursors for peptidoglycan biogenesis. *Science (New York, N.Y.)*, doi: 10.1126/science.1254522.
- Shen, Y., Boulos, S., Sumrall, E., Gerber, B., Julian-Rodero, A., Eugster, M.R., et al. (2017) Structural and functional diversity in *Listeria* cell wall teichoic acids. *Journal of Biological Chemistry*, doi: 10.1074/jbc.M117.813964.
- Shen, Y., Naujokas, M., Park, M., and Ireton, K. (2000) InlB-dependent internalization of *Listeria* is mediated by the Met receptor tyrosine kinase. *Cell*, doi: 10.1016/s0092-8674(00)00141-0.
- Sidow, T., Johannsen, L., and Labischinski, H. (1990) Penicillin-induced changes in the cell wall composition of *Staphylococcus aureus* before the onset of bacteriolysis. *Archives of microbiology*, doi: 10.1007/BF00249181.
- Slotboom, D.J. (2014) Structural and mechanistic insights into prokaryotic energy-coupling factor transporters. *Nature reviews. Microbiology*, doi: 10.1038/nrmicro3175.
- Smith, A.J., Pernstich, C., and Savery, N.J. (2012) Multipartite control of the DNA translocase, Mfd. *Nucleic acids research*, doi: 10.1093/nar/gks775.
- Smith, A.J., Szczelkun, M.D., and Savery, N.J. (2007) Controlling the motor activity of a transcription-repair coupling factor: autoinhibition and the role of RNA polymerase. *Nucleic acids research*, doi: 10.1093/nar/gkm019.
- Smith, K., and Youngman, P. (1992) Use of a new integrational vector to investigate compartment-specific expression of the *Bacillus subtilis* *spoII*M gene. *Biochimie*, doi: 10.1016/0300-9084(92)90143-3.
- Smith, M.A., Takeuchi, K., Anderson, G., Ware, G.O., McClure, H.M., Raybourne, R.B., Mytle, N., and Doyle, M.P. (2008) Dose-response model for *Listeria monocytogenes* induced stillbirths in nonhuman primates. *Infection and immunity*, doi: 10.1128/IAI.01366-06.
- Smith, S.C., Joshi, K.K., Zik, J.J., Trinh, K., Kamajaya, A., Chien, P., and Ryan, K.R. (2014) Cell cycle-dependent adaptor complex for ClpXP-mediated proteolysis directly integrates phosphorylation and second messenger signals. *Proceedings of the National Academy of Sciences of the United States of America*, doi: 10.1073/pnas.1407862111.
- Smith, T.J., Blackman, S.A., and Foster, S.J. (2000) Autolysins of *Bacillus subtilis*: multiple enzymes with multiple functions. *Microbiology*, doi: 10.1099/00221287-146-2-249.
- Snowden, M.A., Perkins, H.R., Wyke, A.W., Hayes, M.V., and Ward, J.B. (1989) Cross-linking and O-acetylation of newly synthesized peptidoglycan in *Staphylococcus aureus*. *Journal of general microbiology*, doi: 10.1099/00221287-135-11-3015.
-

-
- Soldo, B., Lazarevic, V., and Karamata, D. (2002) *tagO* is involved in the synthesis of all anionic cell-wall polymers in *Bacillus subtilis* 168. *Microbiology (Reading, England)*, doi: 10.1099/00221287-148-7-2079.
- Soumet, C., Ragimbeau, C., and Maris, P. (2005) Screening of benzalkonium chloride resistance in *Listeria monocytogenes* strains isolated during cold smoked fish production. *Letters in applied microbiology*, doi: 10.1111/j.1472-765X.2005.01763.x.
- Stone, K.J., and Strominger, J.L. (1971) Mechanism of action of bacitracin: complexation with metal ion and C 55 - isoprenyl pyrophosphate. *Proceedings of the National Academy of Sciences of the United States of America*, doi: 10.1073/pnas.68.12.3223.
- Su, Y.-B., Kuang, S.-F., Ye, J.-Z., Tao, J.-J., Li, H., Peng, X.-X., and Peng, B. (2021) Enhanced biosynthesis of fatty acids is associated with the acquisition of ciprofloxacin resistance in *Edwardsiella tarda*. *mSystems*, doi: 10.1128/mSystems.00694-21.
- Sugai, M., Yamada, S., Nakashima, S., Komatsuzawa, H., Matsumoto, A., Oshida, T., and Suginaka, H. (1997) Localized perforation of the cell wall by a major autolysin: atl gene products and the onset of penicillin-induced lysis of *Staphylococcus aureus*. *Journal of bacteriology*, doi: 10.1128/jb.179.9.2958-2962.1997.
- Sumrall, E.T., Keller, A.P., Shen, Y., and Loessner, M.J. (2020) Structure and function of *Listeria* teichoic acids and their implications. *Molecular microbiology*, doi: 10.1111/mmi.14472.
- Sun, L., Rogiers, G., Courtin, P., Chapot-Chartier, M.-P., Bierne, H., and Michiels, C.W. (2021a) AsnB mediates amidation of meso-diaminopimelic acid residues in the peptidoglycan of *Listeria monocytogenes* and affects bacterial surface properties and host cell invasion. *Frontiers in microbiology*, doi: 10.3389/fmicb.2021.760253.
- Sun, L., Rogiers, G., and Michiels, C.W. (2021b) The natural antimicrobial trans-Cinnamaldehyde interferes with UDP-N-Acetylglucosamine biosynthesis and cell wall homeostasis in *Listeria monocytogenes*. *Foods (Basel, Switzerland)*, doi: 10.3390/foods10071666.
- Sun, Y., Hürlimann, S., and Garner, E. (2023) Growth rate is modulated by monitoring cell wall precursors in *Bacillus subtilis*. *Nature microbiology*, doi: 10.1038/s41564-023-01329-7.
- Sychantha, D., Brott, A.S., Jones, C.S., and Clarke, A.J. (2018) Mechanistic pathways for peptidoglycan O-Acetylation and de-O-Acetylation. *Frontiers in microbiology*, doi: 10.3389/fmicb.2018.02332.
- Taguchi, A., Welsh, M.A., Marmont, L.S., Lee, W., Sjodt, M., Kruse, A.C., et al. (2019) FtsW is a peptidoglycan polymerase that is functional only in complex with its cognate penicillin-binding protein. *Nature microbiology*, doi: 10.1038/s41564-018-0345-x.
- Takada, H., Shiwa, Y., Takino, Y., Osaka, N., Ueda, S., Watanabe, S., et al. (2018) Essentiality of WalRK for growth in *Bacillus subtilis* and its role during heat stress. *Microbiology (Reading, England)*, doi: 10.1099/mic.0.000625.
- Tandukar, M., Oh, S., Tezel, U., Konstantinidis, K.T., and Pavlostathis, S.G. (2013) Long-term exposure to benzalkonium chloride disinfectants results in change of microbial community structure and increased antimicrobial resistance. *Environmental science & technology*, doi: 10.1021/es401507k.
-

- Tavares, J.R., Souza, R.F. de, Meira, G.L.S., and Gueiros-Filho, F.J. (2008) Cytological characterization of YpsB, a novel component of the *Bacillus subtilis* divisome. *Journal of bacteriology*, doi: 10.1128/JB.00064-08.
- Temple, M.E., and Nahata, M.C. (2000) Treatment of listeriosis. *The Annals of pharmacotherapy*, doi: 10.1345/aph.19315.
- Tesson, B., Dajkovic, A., Keary, R., Marlière, C., Dupont-Gillain, C.C., and Carballido-López, R. (2022) Magnesium rescues the morphology of *Bacillus subtilis mreB* mutants through its inhibitory effect on peptidoglycan hydrolases. *Scientific reports*, doi: 10.1038/s41598-021-04294-5.
- Tezel, U., and Pavlostathis, S.G. (2015) Quaternary ammonium disinfectants: microbial adaptation, degradation and ecology. *Current Opinion in Biotechnology*, doi: 10.1016/j.copbio.2015.03.018.
- Thomas, J., Govender, N., McCarthy, K.M., Erasmus, L.K., Doyle, T.J., Allam, M., et al. (2020) Outbreak of listeriosis in South Africa associated with processed meat. *The New England journal of medicine*, doi: 10.1056/NEJMoa1907462.
- Tilney, L.G., and Portnoy, D.A. (1989) Actin filaments and the growth, movement, and spread of the intracellular bacterial parasite, *Listeria monocytogenes*. *The Journal of cell biology*, doi: 10.1083/jcb.109.4.1597.
- To, M.S., Favrin, S., Romanova, N., and Griffiths, M.W. (2002) Postadaptational resistance to benzalkonium chloride and subsequent physicochemical modifications of *Listeria monocytogenes*. *Applied and environmental microbiology*, doi: 10.1128/AEM.68.11.5258-5264.2002.
- Toledo-Arana, A., Dussurget, O., Nikitas, G., Sesto, N., Guet-Revillet, H., Balestrino, D., et al. (2009) The *Listeria* transcriptional landscape from saprophytism to virulence. *Nature*, doi: 10.1038/nature08080.
- Trentini, D.B., Suskiewicz, M.J., Heuck, A., Kurzbauer, R., Deszcz, L., Mechtler, K., and Clausen, T. (2016) Arginine phosphorylation marks proteins for degradation by a Clp protease. *Nature*, doi: 10.1038/nature20122.
- Turner, R.D., Mesnage, S., Hobbs, J.K., and Foster, S.J. (2018) Molecular imaging of glycan chains couples cell-wall polysaccharide architecture to bacterial cell morphology. *Nature communications*, doi: 10.1038/s41467-018-03551-y.
- Uchikawa, K., Sekikawa, I., and Azuma, I. (1986) Structural studies on lipoteichoic acids from four *Listeria* strains. *Journal of bacteriology*, doi: 10.1128/jb.168.1.115-122.1986.
- Vadyvaloo, V., Arous, S., Gravesen, A., Héchar, Y., Chauhan-Haubrock, R., Hastings, J.W., and Rautenbach, M. (2004) Cell-surface alterations in class II bacteriocin-resistant *Listeria monocytogenes* strains. *Microbiology (Reading, England)*, doi: 10.1099/mic.0.27059-0.
- van Heijenoort, J. (2001) Formation of the glycan chains in the synthesis of bacterial peptidoglycan. *Glycobiology*, doi: 10.1093/glycob/11.3.25r.
- van Heijenoort, J. (2007) Lipid intermediates in the biosynthesis of bacterial peptidoglycan. *Microbiology and molecular biology reviews : MMBR*, doi: 10.1128/MMBR.00016-07.

-
- Vermassen, A., Leroy, S., Talon, R., Provot, C., Popowska, M., and Desvaux, M. (2019) Cell wall hydrolases in bacteria: insight on the diversity of cell wall amidases, glycosidases and peptidases toward peptidoglycan. *Frontiers in microbiology*, doi: 10.3389/fmicb.2019.00331.
- Vinogradov, E., Sadovskaya, I., Li, J., and Jabbouri, S. (2006) Structural elucidation of the extracellular and cell-wall teichoic acids of *Staphylococcus aureus* MN8m, a biofilm forming strain. *Carbohydrate research*, doi: 10.1016/j.carres.2006.01.012.
- Vollmer, W., Blanot, D., and Pedro, M.A. de (2008) Peptidoglycan structure and architecture. *FEMS microbiology reviews*, doi: 10.1111/j.1574-6976.2007.00094.x.
- Walsh, C.T. (1989) Enzymes in the D-alanine branch of bacterial cell wall peptidoglycan assembly. *The Journal of biological chemistry*, doi: 10.1016/s0021-9258(19)81624-1.
- Walsh, C.T., Benson, T.E., Kim, D.H., and Lees, W.J. (1996) The versatility of phosphoenolpyruvate and its vinyl ether products in biosynthesis. *Chemistry & biology*, doi: 10.1016/s1074-5521(96)90282-3.
- Wamp, S., Rothe, P., Stern, D., Holland, G., Döhling, J., and Halbedel, S. (2022) MurA escape mutations uncouple peptidoglycan biosynthesis from PrkA signaling. *PLoS pathogens*, doi: 10.1371/journal.ppat.1010406.
- Wamp, S., Rutter, Z.J., Rismondo, J., Jennings, C.E., Möller, L., Lewis, R.J., and Halbedel, S. (2020) PrkA controls peptidoglycan biosynthesis through the essential phosphorylation of ReoM. *eLife*, doi: 10.7554/eLife.56048.
- Wand, M.E., Bock, L.J., Bonney, L.C., and Sutton, J.M. (2017) Mechanisms of increased resistance to chlorhexidine and cross-resistance to colistin following exposure of *Klebsiella pneumoniae* clinical isolates to chlorhexidine. *Antimicrobial agents and chemotherapy*, doi: 10.1128/AAC.01162-16.
- Wand, M.E., and Sutton, J.M. (2022) Efflux-mediated tolerance to cationic biocides, a cause for concern? *Microbiology*, doi: 10.1099/mic.0.001263.
- Wang, Q.M., Peery, R.B., Johnson, R.B., Alborn, W.E., Yeh, W.K., and Skatrud, P.L. (2001) Identification and characterization of a monofunctional glycosyltransferase from *Staphylococcus aureus*. *Journal of bacteriology*, doi: 10.1128/JB.183.16.4779-4785.2001.
- Ward, J.B. (1981) Teichoic and teichuronic acids: biosynthesis, assembly, and location. *Microbiological reviews*, doi: 10.1128/mr.45.2.211-243.1981.
- Warren, M.A., Kucharski, L.M., Veenstra, A., Shi, L., Grulich, P.F., and Maguire, M.E. (2004) The CorA Mg²⁺ transporter is a homotetramer. *Journal of bacteriology*, doi: 10.1128/JB.186.14.4605-4612.2004.
- Watanakunakorn, C. (1984) Mode of action and in-vitro activity of vancomycin. *The Journal of antimicrobial chemotherapy*, doi: 10.1093/jac/14.suppl_d.7.
- Weart, R.B., Nakano, S., Lane, B.E., Zuber, P., and Levin, P.A. (2005) The ClpX chaperone modulates assembly of the tubulin-like protein FtsZ. *Molecular microbiology*, doi: 10.1111/j.1365-2958.2005.04673.x.
- Weber, D.J., Rutala, W.A., and Sickbert-Bennett, E.E. (2007) Outbreaks associated with contaminated antiseptics and disinfectants. *Antimicrobial agents and chemotherapy*, doi: 10.1128/AAC.00138-07.
-

- Wenzel, M., Kohl, B., Münch, D., Raatschen, N., Albada, H.B., Hamoen, L., *et al.* (2012) Proteomic response of *Bacillus subtilis* to lantibiotics reflects differences in interaction with the cytoplasmic membrane. *Antimicrobial agents and chemotherapy*, doi: 10.1128/AAC.01380-12.
- Wessels, S., and Ingmer, H. (2013) Modes of action of three disinfectant active substances: a review. *Regulatory toxicology and pharmacology : RTP*, doi: 10.1016/j.yrtph.2013.09.006.
- Yamaguchi, H., Furuhashi, K., Fukushima, T., Yamamoto, H., and Sekiguchi, J. (2004) Characterization of a new *Bacillus subtilis* peptidoglycan hydrolase gene, *yvcE* (named *cw/O*), and the enzymatic properties of its encoded protein. *Journal of bioscience and bioengineering*, doi: 10.1016/S1389-1723(04)00262-2.
- Yamamoto, H., Hashimoto, M., Higashitsuji, Y., Harada, H., Hariyama, N., Takahashi, L., *et al.* (2008a) Post-translational control of vegetative cell separation enzymes through a direct interaction with specific inhibitor IseA in *Bacillus subtilis*. *Molecular microbiology*, doi: 10.1111/j.1365-2958.2008.06398.x.
- Yamamoto, H., Miyake, Y., Hisaoka, M., Kurosawa, S.-I., and Sekiguchi, J. (2008b) The major and minor wall teichoic acids prevent the sidewall localization of vegetative DL-endopeptidase LytF in *Bacillus subtilis*. *Molecular microbiology*, doi: 10.1111/j.1365-2958.2008.06397.x.
- Yang, D.C., Peters, N.T., Parzych, K.R., Uehara, T., Markovski, M., and Bernhardt, T.G. (2011) An ATP-binding cassette transporter-like complex governs cell-wall hydrolysis at the bacterial cytokinetic ring. *Proceedings of the National Academy of Sciences of the United States of America*, doi: 10.1073/pnas.1107780108.
- Yocum, R.R., Rasmussen, J.R., and Strominger, J.L. (1980) The mechanism of action of penicillin. Penicillin acylates the active site of *Bacillus stearothermophilus* D-alanine carboxypeptidase. *The Journal of biological chemistry*, **255**: 3977–3986.
- Yoshida, K.I., Fujita, Y., and Ehrlich, S.D. (2000) An operon for a putative ATP-binding cassette transport system involved in acetoin utilization of *Bacillus subtilis*. *Journal of bacteriology*, doi: 10.1128/JB.182.19.5454-5461.2000.
- Yu, T., Jiang, X., Zhang, Y., Ji, S., Gao, W., and Shi, L. (2018) Effect of benzalkonium chloride adaptation on sensitivity to antimicrobial agents and tolerance to environmental stresses in *Listeria monocytogenes*. *Frontiers in microbiology*, doi: 10.3389/fmicb.2018.02906.
- Zapun, A., Vernet, T., and Pinho, M.G. (2008) The different shapes of cocci. *FEMS Microbiology Reviews*, doi: 10.1111/j.1574-6976.2007.00098.x.
- Zhang, C., Tezel, U., Li, K., Liu, D., Ren, R., Du, J., and Pavlostathis, S.G. (2011) Evaluation and modeling of benzalkonium chloride inhibition and biodegradation in activated sludge. *Water research*, doi: 10.1016/j.watres.2010.09.037.
- Zhao, H., Sun, Y., Peters, J.M., Gross, C.A., Garner, E.C., and Helmann, J.D. (2016) Depletion of undecaprenyl pyrophosphate phosphatases disrupts cell envelope biogenesis in *Bacillus subtilis*. *Journal of bacteriology*, doi: 10.1128/JB.00507-16.

- Zhu, X., Liu, W., Lametsch, R., Aarestrup, F., Shi, C., She, Q., Shi, X., and Knøchel, S. (2011) Phenotypic, proteomic, and genomic characterization of a putative ABC-transporter permease involved in *Listeria monocytogenes* biofilm formation. *Foodborne pathogens and disease*, doi: 10.1089/fpd.2010.0697.
- Zinchenko, A.A., Sergeyev, V.G., Yamabe, K., Murata, S., and Yoshikawa, K. (2004) DNA compaction by divalent cations: structural specificity revealed by the potentiality of designed quaternary diammonium salts. *ChemBiochem: a European journal of chemical biology*, doi: 10.1002/cbic.200300797.

Chapter 9 | Supplementary material

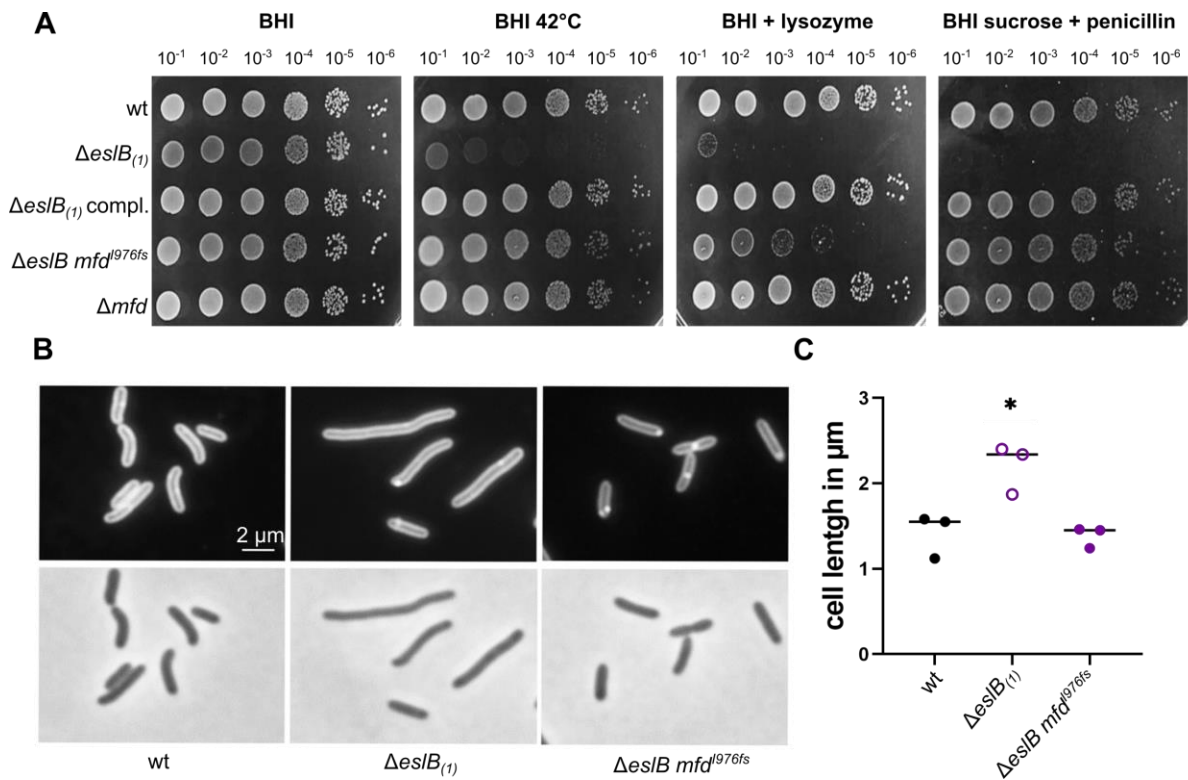
9.1 Mutation F976fs in *mfd* suppresses *eslB* phenotypes

Figure S1 | Mutation F976fs in *mfd* suppresses *eslB* phenotypes. **A** Drop dilution assay. Dilutions of *L. monocytogenes* strains 10403S (wt), $\Delta eslB_{(1)}$, $\Delta eslB_{(1)}$ compl. And $\Delta eslB_{(1)} mfd^{F976fs}$ were spotted on BHI plates, BHI plates containing 100 $\mu\text{g ml}^{-1}$ lysozyme or containing 0.5 M sucrose and 0.025 $\mu\text{g ml}^{-1}$ penicillin G and were incubated at 37°C or at 42°C. **B** Microscopy images of the 10403S (wt), $\Delta eslB_{(1)}$ and the $\Delta eslB_{(1)} mfd^{F976fs}$. Nile red was used to stain the bacterial membranes. **C** Cell length of 50 cells per strain was measured using the ImageJ software and the median cell length was calculated. The average value and standard deviations of three independent experiments were plotted. For statistical analysis, a one-way ANOVA coupled with Turkey's multiple comparison test was used (* $p \leq 0.1$).

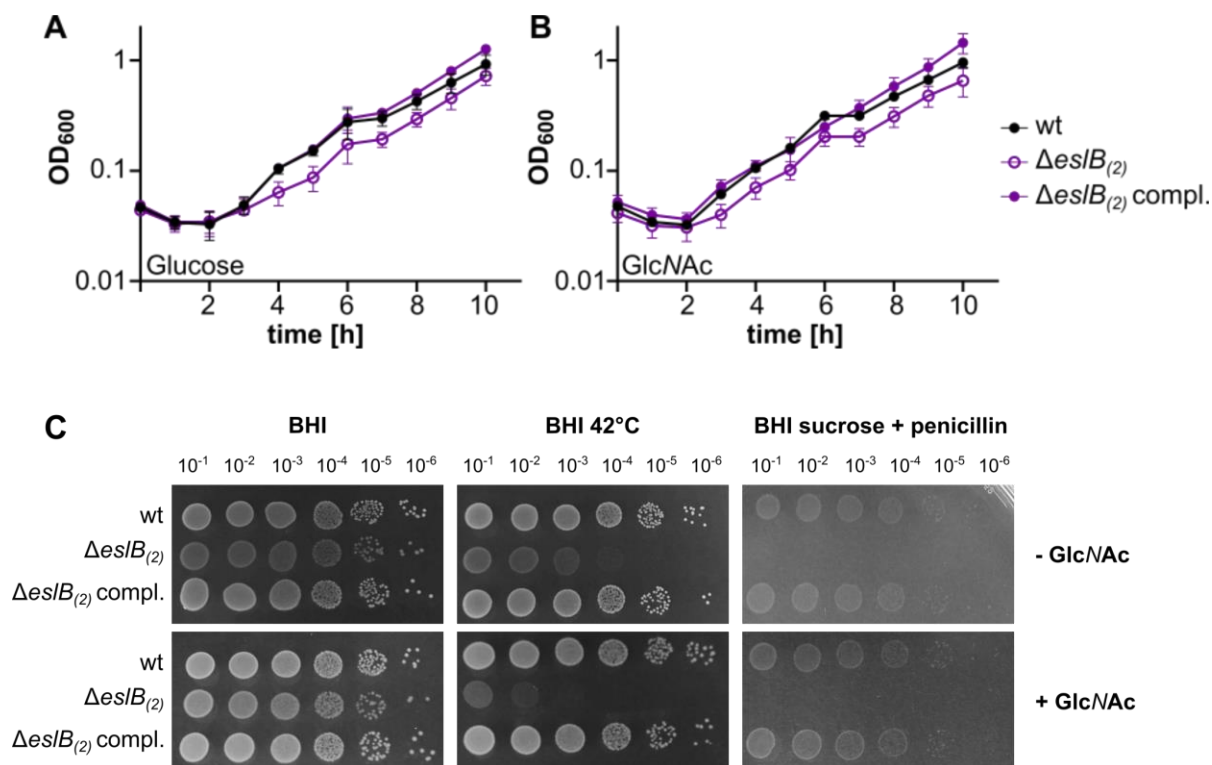
9.2 GlcNAc utilization of the $\Delta esIB$ strain

Figure S2 | GlcNAc utilization of the $\Delta esIB$ strain. **A** and **B** Bacterial growth curves are shown for *L. monocytogenes* 10403S (wt), $\Delta esIB_{(2)}$ and the $\Delta esIB_{(2)}$ compl.. Strains were grown in LSM defined minimal medium containing Glucose (A) or GlcNAc (B) as the sole carbon source. The OD₆₀₀ was measured at hourly intervals and the average value and standard deviations from three independent experiments are depicted. **C** Drop dilution assay. Dilutions of *L. monocytogenes* strains 10403S (wt), $\Delta esIB_{(1)}$, and $\Delta esIB_{(1)}$ compl. Were spotted on BHI plates, BHI plates containing 100 $\mu\text{g ml}^{-1}$ lysozyme or containing 0.5 M sucrose and 0.025 $\mu\text{g ml}^{-1}$ penicillin G and were incubated at 37°C or at 42°C with and without the addition of 0.5 M GlcNAc. All plates were supplemented with 1 mM IPTG.

9.3 Aberrant localization of mNeonGreen-DivIVA in $\Delta es/B$

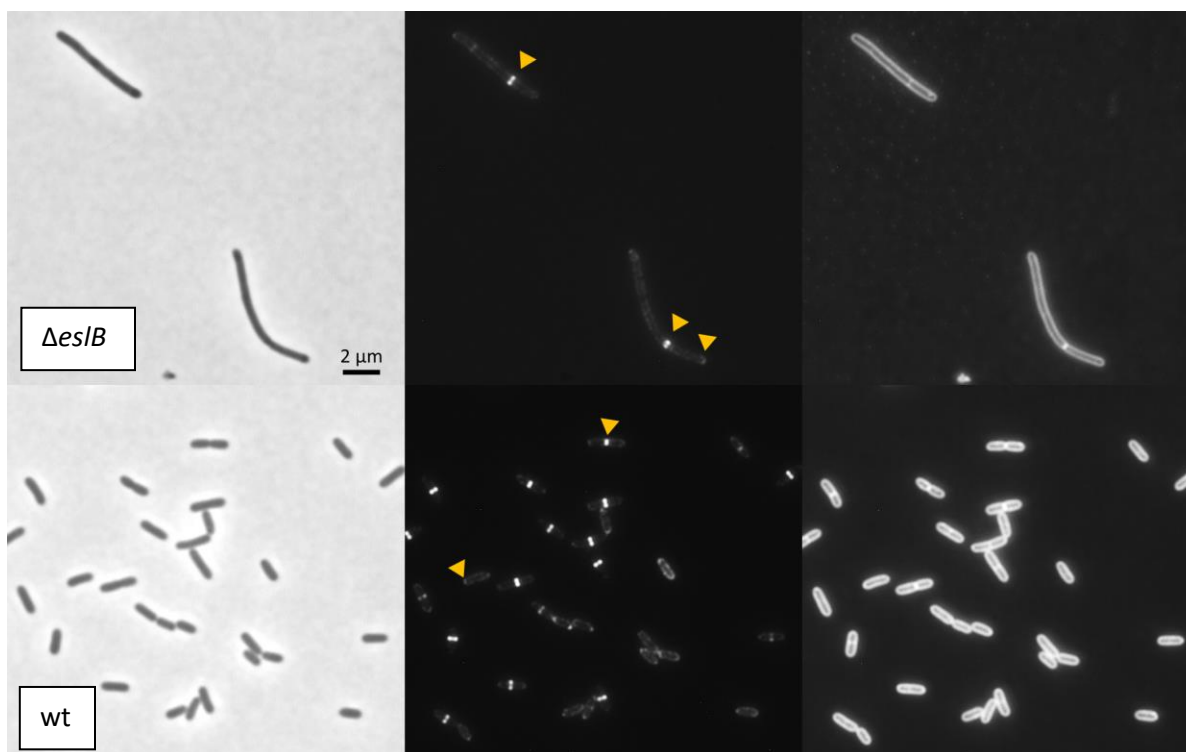


Figure S3 | Aberrant localization of mNeonGreen-DivIVA in $\Delta es/B$. Localization of mNeonGreen-DivIVA in *L. monocytogenes* 10403S (wt) and $\Delta es/B_{(2)}$. Bacterial membranes were stained with Nile red, and cells were examined by phase-contrast microscopy (left) and by fluorescence microscopy to analyse mNeonGreen (middle) and Nile red (right) fluorescence signals. Representative images from three independent experiments are shown.

9.4 Interaction of OatA with the Min system

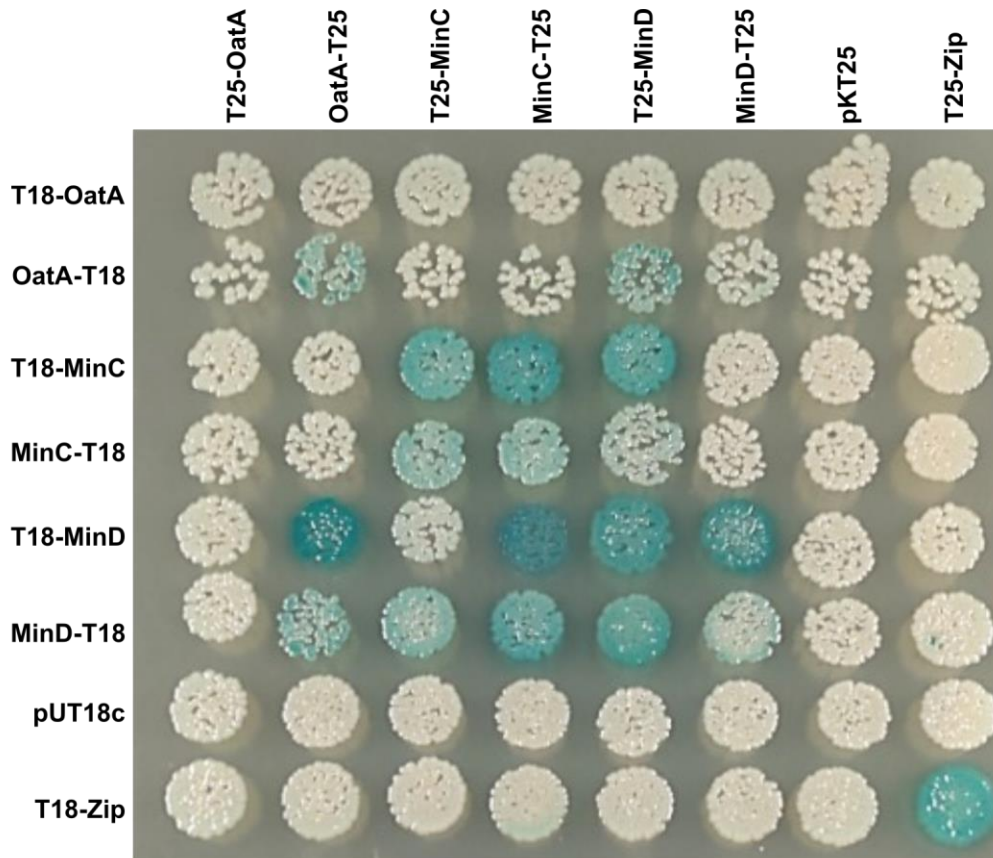


Figure S4 | Interaction of OatA with the Min system. Bacterial two-hybrid analysis of interactions with OatA, MinC and MinD. Plasmids encoding OatA, MinC and MinD each fused to the T18 and T25 fragments were co-transformed into *E. coli* BTH101. pKT25-Zip and pUT18c-Zip were used as a positive control, while the empty vectors pKT25 and pUT18c were used as negative controls. A representative image of three independent experiments is shown.

9.5 *E. coli* strains used in this study

Strain	Genotype	Reference/Construction
ANG1264	DH5 α pKSV7; AmpR	(Smith and Youngman 1992)
ANG1265	XL1-Blue pKT25; KanR	(Karimova et al. 2001)
ANG1266	XL1-Blue pKNT25; KanR	(Karimova et al. 2005)
ANG1267	XL1-Blue pUT18; AmpR	(Karimova et al. 2001)
ANG1268	XL1-Blue pUT18C; AmpR	(Karimova et al. 2001)
ANG1269	XL1-Blue pKT25- <i>zip</i> ; KanR	(Karimova et al. 1998)
ANG1270	XL1-Blue pUT18C- <i>zip</i> ; AmpR	(Karimova et al. 1998)
ANG4242	XL1-Blue pIMK2; KanR	(Monk et al., 2008)
ANG4243	XL1-Blue pIMK3; KanR	(Monk et al., 2008)
ANG4236	XL1-Blue pKSV7- Δ <i>esB</i> ; AmpR	(Rismondo et al. 2021)
ANG4647	XL1-Blue pIMK3- <i>esB</i> ; KanR	(Rismondo et al. 2021)
ANG5181	XL1-Blue pPL3e- <i>lacZ</i> ; CamR	(Rismondo et al. 2019)
ANG5660	XL1-Blue pPL3e- <i>P_{esIA}-es/ABC</i> ; CamR	(Rismondo et al. 2021)
ANG5661	SM10 pPL3e- <i>P_{esIA}-es/ABC</i> ; KanR CamR	(Rismondo et al. 2021)
EJR4	XL1-Blue pKNT25- <i>esA</i> ; KanR	(Rismondo et al. 2021)
EJR5	XL1-Blue pKT25- <i>esA</i> ; KanR	(Rismondo et al. 2021)
EJR6	XL1-Blue pUT18- <i>esA</i> ; AmpR	(Rismondo et al. 2021)
EJR7	XL1-Blue pUT18C- <i>esA</i> ; AmpR	(Rismondo et al. 2021)
EJR8	XL1-Blue pKNT25- <i>esB</i> ; KanR	(Rismondo et al. 2021)
EJR9	XL1-Blue pKT25- <i>esB</i> ; KanR	(Rismondo et al. 2021)
EJR10	XL1-Blue pUT18- <i>esB</i> ; AmpR	(Rismondo et al. 2021)
EJR11	XL1-Blue pUT18C- <i>esB</i> ; AmpR	(Rismondo et al. 2021)
EJR12	XL1-Blue pKNT25- <i>esC</i> ; KanR	(Rismondo et al. 2021)
EJR13	XL1-Blue pKT25- <i>esC</i> ; KanR	(Rismondo et al. 2021)
EJR14	CLG190 pUT18- <i>esC</i> ; AmpR	(Rismondo et al. 2021)
EJR15	XL1-Blue pUT18C- <i>esC</i> ; AmpR	(Rismondo et al. 2021)
EJR50	XL1-Blue pAC7- <i>P_{dlt}</i> ; AmpR	(Rismondo et al. 2021)
EJR51	XL1-Blue pAC7- <i>P_{dlt}*</i> ; AmpR	(Rismondo et al. 2021)
EJR52	XL1-Blue pIMK3- <i>murA</i> ; KanR	(Rismondo et al. 2021)
EJR56	S17-1	(Hanahan 1983)
EJR58	S17-1 pIMK3; KanR	(Rismondo et al. 2021)
EJR59	S17-1 pIMK3- <i>murA</i> ; KanR	(Rismondo et al. 2021)
EJR116	XL1-Blue pKSV7- <i>mfd</i>	Primer: LMS328/LMS329 and LMS330/LMS331 Template: gDNA 10403S; LFH: LMS328/LMS331; <i>Bam</i> HI and <i>Kpn</i> I, ligated into pKSV7
EJR149	XL10-Gold pWH844; AmpR	(Schirmer et al. 1997)
EJR227	XL10-Gold pIMK3- <i>fepA</i> ; KanR	(Schulz et al. 2023)
EJR229	XL1-Blue pKSV7- Δ <i>sugE1/2</i> ; AmpR	(Schulz et al. 2023)
EJR230	XL1-Blue pKSV7- Δ <i>fepA</i> ; AmpR	(Schulz et al. 2023)
EJR242	XL10-Gold pWH844- <i>fepR</i> ; AmpR	(Schulz et al. 2023)

EJR248	XL10-Gold pWH844- <i>fepR</i> ^{L24F} ; AmpR	(Schulz et al. 2023)
EJR257	DH5α pPL3e- <i>P_{fepR}-lacZ</i> ; CamR	(Schulz et al. 2023)
EJR258	DH5α pPL3e- <i>P_{fepR}^{A-33G}-lacZ</i> ; CamR	(Schulz et al. 2023)
EJR259	XL10-Gold pIMK3- <i>sugE1/2</i> ; KanR	(Schulz et al. 2023)
EJR260	DH5α pPL3e- <i>P_{fepR}^{G-27T}-lacZ</i> ; CamR	(Schulz et al. 2023)

9.6 *E. coli* strains constructed in this study

Strain	Genotype	Reference/Construction
EJR39	XL1-Blue pIMK2- <i>mNeonGreen-zapA</i> ; KanR	(Rismondo et al. 2021)
EJR43	XL1-Blue pKSV7- <i>ΔeslC</i> ; AmpR	(Rismondo et al. 2021)
EJR44	XL1-Blue pKSV7- <i>ΔeslA-R</i> ; AmpR;	Primer: JR13/TA10 and JR14/TA6 Template: gDNA 10403S; LFH: TA6/TA10; <i>BamHI KpnI</i> , ligated into pKSV7
EJR45	XL1-Blue pKSV7- <i>Δwalk</i> ; AmpR	Primer: LMS95/96 and LMS97/98 Template: gDNA 10403S; LFH: LMS96/97; <i>BamHI KpnI</i> , ligated into pKSV7
EJR46	XL1-Blue pKSV7- <i>ΔeslA-C</i> ; AmpR	Primer: JR16/17 and JR15/TA10 Template: gDNA 10403S; LFH: TA10/JR17; <i>BamHI KpnI</i> , ligated into pKSV7
EJR47	SM10 pHPL3	Empty vector pHPL3 → SM10
EJR48	SM10 pSLIV2	Empty vector pSLIV2 → SM10
EJR49	SM10 pHLIV2	Empty vector pHLIV2 → SM10
EJR54	XL1-Blue pKSV7- <i>ΔeslA</i> ; AmpR	(Rismondo et al. 2021)
EJR60	S17-1 pIMK2- <i>mNeonGreen-zapA</i> ; KanR	(Rismondo et al. 2021)
EJR62	XL1-Blue pKSV7- <i>ΔftsEX</i> ; AmpR;	Primer: LMS100/101 and LMS102/103 Template: gDNA 10403S; LFH: LMS101/102; <i>BamHI KpnI</i> , ligated into pKSV7
EJR63	XL1-Blue pKSV7- <i>ΔcwI/O</i> ; AmpR	Primer: LMS100/101 and LMS102/103 Template: gDNA Lmo 10403S; LFH: LMS101/102; <i>BamHI KpnI</i> , ligated into pKSV7
EJR64	XL1-Blue pKSV7- <i>ΔwalH</i> ; AmpR	Primer: LMS104/LMS105 and LMS106/LMS107 Template: gDNA Lmo 10403S; LFH: LMS105/LMS106; <i>BamHI KpnI</i> , ligated into pKSV7
EJR65	XL1-Blue pUT18c- <i>oatA</i> ; AmpR	Primer: JR118/119 Template: gDNA 10403S; <i>XbaI KpnI</i> , ligated into pUT18c

EJR66	XL1-Blue pUT18- <i>oatA</i> ; AmpR	Primer: JR118/119 Template: gDNA 10403S; <i>XbaI KpnI</i> , ligated into pUT18
EJR67	XL1-Blue pKNT25- <i>oatA</i> ; KanR	Primer: JR118/119 Template: gDNA 10403S; <i>XbaI KpnI</i> , ligated into pKT25
EJR68	XL1-Blue pKNT25- <i>oatA</i> ; KanR	Primer: JR118/119 Template: gDNA 10403S; <i>XbaI KpnI</i> , ligated into pKNT25
EJR69	XL1-Blue pUT18c- <i>oatA</i> ; AmpR	Primer: JR120/121 Template: gDNA 10403S; <i>XbaI KpnI</i> , ligated into pUT18c
EJR70	XL1-Blue pUT18- <i>oatA</i> ; AmpR	Primer: JR120/121 Template: gDNA 10403S; <i>XbaI KpnI</i> , ligated into pUT18
EJR71	pKT25- <i>oatA</i> ; KanR	Primer: JR120/121 Template: gDNA 10403S; <i>XbaI KpnI</i> , ligated into pKT25
EJR72	pKNT25- <i>oatA</i> ; kanR	Primer: JR120/121 Template: gDNA 10403S; <i>XbaI KpnI</i> , ligated into pKNT25
EJR73	XL1-Blue pKSV7- Δ <i>corA</i> ; AmpR	Primer: LMS211/LMS212 and LMS213/LMS214 Template: gDNA 10403S; LFH: LMS211/LMS214; <i>BamHI KpnI</i> , ligated into pKSV7
EJR74	XL1-Blue pKSV7- Δ <i>anrA</i> ; AmpR	Primer: LMS218/LMS219 and LMS220/LMS221 Template: gDNA 10403S; LFH: LMS218/LMS221; <i>BamHI KpnI</i> , ligated into pKSV7
EJR75	XL1-Blue pKSV7- Δ <i>kat</i> ; AmpR	Primer: LMS197/LMS198 and LMS199/LMS200 Template: gDNA 10403S; LFH: LMS197/LMS200; <i>BamHI KpnI</i> , ligated into pKSV7
EJR76	XL1-Blue pKSV7- Δ <i>sod</i> ; AmpR	Primer: LMS204/LMS205 and LMS206/LMS207 Template: gDNA 10403S; LFH: LMS204/LMS207; <i>BamHI KpnI</i> , ligated into pKSV7
EJR77	XL1-Blue pUT18c- <i>pbpA1</i> ; AmpR	Primer: JR122/123 Template: gDNA 10403S; <i>XbaI KpnI</i> , ligated into pUT18c
EJR78	XL1-Blue pUT18- <i>pbpA1</i> ; AmpR	Primer: JR122/123 Template: gDNA 10403S; <i>XbaI KpnI</i> , ligated into pUT18

EJR79	XL1-Blue pKT25- <i>pbpA1</i> , KanR	Primer: JR122/123 Template: gDNA 10403S; <i>XbaI KpnI</i> , ligated into pKT25
EJR80	XL1-Blue pKNT25- <i>pbpA1</i> ; KanR	Primer: JR122/123 Template: gDNA 10403S; <i>XbaI KpnI</i> , ligated into pKNT25
LJR83	XL10-Gold pGP570- <i>walR</i>	DNA: Lmo 10403s, primer: LMS444/445, enzymes: <i>HindIII/XhoI</i> , ligated with pGP570
EJR90	S17-1 pIMK2- <i>divIVA-mNeonGreen</i> ; KanR	EJR92 → S17-1
EJR91	XL1-Blue pDR244	pDR244 → XL1-blue
EJR92	XL1-Blue pIMK2- <i>DivIVA-mNeonGreen</i> ; KanR	Primer: LMS93/94 and LMS95/96 Template: gDNA 10403S; LFH: LMS93/96; <i>Sall KpnI</i> , ligated into pIMK2
EJR93	XL1-Blue pIMK2- <i>eslA-mNeonGreen-eslB</i>	DNA: Lmo LJR16, primer: JR97/98, enzymes: <i>NcoI/Sall</i> , ligated with pIMK2
EJR94	S17-1-pIMK2- <i>eslA-mNeonGreen-eslB</i>	EJR93 → S17-1
EJR95	XL1-Blue pIMK3- <i>lmo0041</i> ^{EGD-e}	DNA: Lmo EGD-e, primer: LMS258/259, enzymes: <i>NcoI/BamHI</i> , ligated with pIMK3
EJR96	XL1-Blue pIMK3- <i>lmo0552</i> ^{EGD-e}	DNA: Lmo EGD-e, primer: LMS252/253, enzymes: <i>NcoI/BamHI</i> , ligated with pIMK3
EJR97	XL1-Blue pIMK3- <i>lmo2698</i> ^{EGD-e}	DNA: Lmo EGD-e, primer: LMS232/233, enzymes: <i>NcoI/PstI</i> , ligated with pIMK3
JR98	XL1-Blue pIMK3- <i>lmo2732</i> ^{EGD-e}	DNA: Lmo EGD-e, primer: LMS238/239, enzymes: <i>NcoI/PstI</i> , ligated with pIMK3
EJR99	XL1-Blue pIMK3- <i>lmo2795</i> ^{EGD-e}	DNA: Lmo EGD-e, primer: LMS246/247, enzymes: <i>NcoI/PstI</i> , ligated with pIMK3
EJR100	Dh5α pIMK2- <i>eslAB-mNeonGreen</i> ; KanR,	Primer: JR99/97 gDNA LJR16; LFH: LMS96/97; enzymes <i>NcoI/Sall</i> , ligated into pIMK2
EJR101	Dh5α-blue pIMK3- <i>gshf</i> ; KanR	Primer: LMS224/LMS225 gDNA 10403S; enzymes: <i>NcoI/PstI</i>
EJR102	S17-1 pIMK2- <i>eslAB-mNeonGreen</i> ; KanR	EJR100 → in S17-1
EJR103	S17-1 pIMK3- <i>gshf</i> ; KanR	EJR101 → in S17-1
EJR106	XL1-Blue pIMK3- <i>glmR</i> ; KanR	(Schulz et al. 2022)
EJR107	XL1-Blue pIMK3- <i>glmU</i> ; KanR	(Schulz et al. 2022)
EJR108	XL1-Blue pIMK3- <i>glmM</i> ; KanR	(Schulz et al. 2022)

EJR110	S17-1 pIMK3- <i>lmo1315</i> ; KanR	EJR109 → S17-1
EJR112	XL1-Blue pIMK3- <i>glmS</i> ; KanR	(Schulz et al. 2022)
EJR114	XL1-Blue pIMK3- <i>cw/O</i> ; KanR	(Schulz et al. 2022)
EJR115	S17-1 pIMK3- <i>cw/O</i> ; KanR	(Schulz et al. 2022)
EJR129	XL 10-Gold pUT18c- <i>murZ</i> ; AmpR	DNA: Lmo 10403s, primer: JR116/117, enzymes: <i>XbaI/KpnI</i> , ligated into pUT18c
EJR130	XL 10-Gold pUT18- <i>murZ</i> ; AmpR	DNA: Lmo 10403s, primer: JR116/117, enzymes: <i>XbaI/KpnI</i> , ligated into pUT18
EJR132	S17-1 pIMK3- <i>glmR</i> ; KanR	(Schulz et al. 2022)
EJR133	S17-1 pIMK3- <i>glmU</i> ; KanR	(Schulz et al. 2022)
EJR134	S17-1 pIMK3- <i>glmM</i> ; KanR	(Schulz et al. 2022)
EJR135	S17-1 pIMK3- <i>glmS</i> ; KanR	(Schulz et al. 2022)
EJR150	XL 10-Gold pIMK2- <i>eslAB-His</i> ; KanR	DNA: Lmo 10403s, primer: JR162/197, enzymes: <i>NcoI/SalI</i> , ligated into pIMK2
EJR162	XL1-Blue pIMK2- <i>mNeonGreen-His</i> ; KanR	DNA: Lmo 10403s, primer: JR188/73, enzymes: <i>NcoI/SalI</i> , ligated into pIMK2
EJR163	XL1-Blue pWH844- <i>prfA</i>	DNA: Lmo EGD-e, primer: JR189/190, enzymes: <i>PstI/SalI</i> , ligated into pWH844
EJR166	XL1-Blue pMC38; CatR	ANG2668 → XL1-Blue
EJR167	XL1-Blue pMC39; CatR	ANG2669 → XL1-Blue
EJR168	XL1-Blue pIMK3- <i>lmo1071</i> ; KanR	ANG4261 → XL1-Blue
EJR169	XL1-Blue pIMK3- <i>lmo2427</i> ; KanR	ANG4892 → XL1-Blue
EJR170	XL1-Blue pIMK3- <i>lmo2687</i> ; KanR	ANG4893 → XL1-Blue
EJR171	XL1-Blue pIMK2- <i>GFP-linker-lmo1071</i> ; KanR	ANG4913 → XL1-Blue
EJR172	XL1-Blue pIMK2- <i>GFP-linker-lmo2427</i> ; KanR	ANG4914 → XL1-Blue
EJR173	XL1-Blue pIMK2- <i>GFP-linker-lmo2428</i> ; KanR	ANG4915 → XL1-Blue
EJR174	XL1-Blue pIMK2- <i>GFP-linker-lmo2687</i> ; KanR	ANG4916 → XL1-Blue
EJR175	XL1-Blue pIMK2- <i>GFP-linker-lmo2688</i> ; KanR	ANG4917 → XL1-Blue
EJR176	XL1-Blue pIMK3- <i>lmo2428</i> ; KanR	ANG4976 → XL1-Blue
EJR177	XL1-Blue pIMK3- <i>lmo2688</i> ; KanR	ANG4977 → XL1-Blue
EJR178	XL1-Blue pIMK3- <i>lmo1071-linker-mNeonGreen</i> ; KanR	ANG5041 → XL1-Blue
EJR179	XL1-Blue pIMK3- <i>lmo2427-linker-mNeonGreen</i> ; KanR	ANG5042 → XL1-Blue
EJR180	XL1-Blue pIMK3- <i>lmo2428-linker-mNeonGreen</i> ; KanR	ANG5043 → XL1-Blue
EJR181	XL1-Blue pIMK3- <i>lmo2687-linker-mNeonGreen</i> ; KanR	ANG5044 → XL1-Blue

EJR182	XL1-Blue pIMK3- <i>lmo2688-linker-mNeonGreen</i> ; KanR	ANG5045 → XL1-Blue
EJR183	S17-1 pIMK3- <i>lmo1071</i> ; KanR	ANG4261 → S17-1
EJR184	S17-1 pIMK3- <i>lmo2427</i> ; KanR	ANG4892 → S17-1
EJR185	S17-1 pIMK3- <i>lmo2687</i> ; KanR	ANG4893 → S17-1
EJR186	S17-1 pIMK2- <i>GFP-linker-lmo1071</i> ; KanR	ANG4913 → S17-1
EJR187	S17-1 pIMK2- <i>GFP-linker-lmo2427</i> ; KanR	ANG4914 → S17-1
EJR188	S17-1 pIMK2- <i>GFP-linker-lmo2428</i> ; KanR	ANG4915 → S17-1
EJR189	S17-1 pIMK2- <i>GFP-linker-lmo2687</i> ; KanR	ANG4916 → S17-1
EJR190	S17-1 pIMK2- <i>GFP-linker-lmo2688</i> ; KanR	ANG4917 → S17-1
EJR191	S17-1 pIMK3- <i>lmo2428</i> ; KanR	ANG4976 → S17-1
EJR192	S17-1 pIMK3- <i>lmo2688</i> ; KanR	ANG4977 → S17-1
EJR193	S17-1 pIMK3- <i>lmo1071-linker-mNeonGreen</i> ; KanR	ANG5041 → S17-1
EJR194	S17-1 pIMK3- <i>lmo2427-linker-mNeonGreen</i> ; KanR	ANG5042 → S17-1
EJR195	S17-1 pIMK3- <i>lmo2428-linker-mNeonGreen</i> ; KanR	ANG5043 → S17-1
EJR196	S17-1 pIMK3- <i>lmo2687-linker-mNeonGreen</i> ; KanR	ANG5044 → S17-1
EJR197	S17-1 pIMK3- <i>lmo2688-linker-mNeonGreen</i> ; KanR	ANG5045 → S17-1
EJR263	XL10-Gold pUT18c- <i>minC</i>	DNA: 10403S, primer: JR291/292, enzymes: <i>XbaI/KpnI</i> , ligiert in pUT18C
EJR264	XL10-Gold pUT18- <i>minC</i>	DNA: 10403S, primer: JR291/292, enzymes: <i>XbaI/KpnI</i> , ligiert in pUT18
EJR265	XL10-Gold pKT25- <i>minC</i>	DNA: 10403S, primer: JR291/292, enzymes: <i>XbaI/KpnI</i> , ligiert in pKT25
EJR266	XL10-Gold pKT25N- <i>minC</i>	DNA: 10403S, primer: JR291/292, enzymes: <i>XbaI/KpnI</i> , ligiert in pKNT25
EJR267	XL10-Gold pUT18c- <i>minC</i>	DNA: 10403S, primer: JR293/294, enzymes: <i>XbaI/KpnI</i> , ligiert in pUT18C
EJR268	XL10-Gold pUT18- <i>minC</i>	DNA: 10403S, primer: JR293/294, enzymes: <i>XbaI/KpnI</i> , ligiert in pUT18
EJR269	XL10-Gold pKT25- <i>minC</i>	DNA: 10403S, primer: JR293/294, enzymes: <i>XbaI/KpnI</i> , ligiert in pKT25
EJR270	XL10-Gold pKT25N- <i>minC</i>	DNA: 10403S, primer: JR293/294, enzymes: <i>XbaI/KpnI</i> , ligiert in pKNT25

9.7 *L. monocytogenes* strains used in this study

Strain	Genotype	Reference/Construction
ANG873	EGD-e	(Glaser et al. 2001)
ANG1263	10403S; StrepR	(Bishop and Hinrichs 1987)
ANG4275	10403SΔ <i>esB</i> ₍₁₎ ; StrepR	(Rismondo et al. 2021)
ANG4678	10403S pIMK3- <i>esB</i> ; StrepR KanR	(Rismondo et al. 2021)
ANG4688	10403SΔ <i>esB</i> ₍₁₎ pIMK3- <i>esB</i> (or short: 10403SΔ <i>esB</i> ₍₁₎ compl.); StrepR KanR	(Rismondo et al. 2021)
ANG1263	10403S; StrepR	(Bishop and Hinrichs 1987)
ANG4275	10403SΔ <i>esB</i> ₍₁₎ ; StrepR	(Rismondo et al. 2021)
ANG4678	10403S pIMK3- <i>esB</i> ; StrepR KanR	(Rismondo et al. 2021)
ANG4688	10403SΔ <i>esB</i> ₍₁₎ pIMK3- <i>esB</i> (or short: 10403SΔ <i>esB</i> ₍₁₎ compl.); StrepR KanR	(Rismondo et al. 2021)
ANG5386	10403SΔ <i>esB</i> ₍₁₎ <i>murZ</i> ^{M240fs} ; StrepR	(Schulz et al. 2022)
ANG5479	10403SΔ <i>esB</i> ₍₁₎ <i>walk</i> ^{R553H} ; StrepR	(Schulz et al. 2022)
ANG5480	10403SΔ <i>esB</i> ₍₁₎ <i>walk</i> ^{N283E} ; StrepR	(Schulz et al. 2022)
ANG5488	10403SΔ <i>esB</i> ₍₁₎ <i>ftsX</i> ^{G253R} ; StrepR	(Schulz et al. 2022)
ANG5489	10403SΔ <i>esB</i> ₍₁₎ <i>walk</i> ^{A570V} ; StrepR	(Schulz et al. 2022)
ANG5499	10403SΔ <i>esB</i> ₍₁₎ <i>reoM</i> ^{K23fs} ; StrepR	(Schulz et al. 2022)
ANG5662	10403SΔ <i>esB</i> ₍₂₎ ; StrepR	(Rismondo et al. 2021)
ANG5663	10403SΔ <i>esB</i> ₍₂₎ pPL3e-P _{esIA} - <i>esABC</i> (or short: 10403SΔ <i>esB</i> ₍₂₎ compl.); ErmR StrepR	(Rismondo et al. 2021)
ANG5685	10403SΔ <i>esB</i> ₍₃₎ ; StrepR	(Schulz et al. 2022)
ANG5698	10403SΔ <i>esB</i> ₍₁₎ <i>murZ</i> ^{O307fs} ; StrepR	(Schulz et al. 2022)
ANG5699	10403SΔ <i>esB</i> ₍₂₎ <i>walk</i> ^{I583T} ; StrepR	(Schulz et al. 2022)
ANG5708	10403SΔ <i>esB</i> ₍₂₎ <i>prpC</i> ^{P159L} ; StrepR	(Schulz et al. 2022)
ANG5710	10403SΔ <i>esB</i> ₍₂₎ <i>cwlO</i> ^{R106H} ; StrepR	(Schulz et al. 2022)
ANG5714	10403SΔ <i>esB</i> ₍₂₎ <i>ftsE</i> ^{Q220} ; StrepR	(Schulz et al. 2022)
ANG5717	10403SΔ <i>esB</i> ₍₂₎ <i>pbpA1</i> ^{G125D} ; StrepR	(Schulz et al. 2022)
ANG5729	10403SΔ <i>esB</i> ₍₃₎ <i>tarL</i> ^{P282L} ; StrepR	(Schulz et al. 2022)
ANG5730	10403SΔ <i>esB</i> ₍₃₎ <i>cwlO</i> ^{R135P} ; StrepR	(Schulz et al. 2022)
ANG5733	10403SΔ <i>esB</i> ₍₂₎ <i>walR</i> ^{S216G} ; StrepR	(Schulz et al. 2022)
ANG5734	10403SΔ <i>esB</i> ₍₂₎ <i>walk</i> ^{H463D} ; StrepR	(Schulz et al. 2022)
ANG5737	10403SΔ <i>esB</i> ₍₂₎ <i>walk</i> ^{V234L} ; StrepR	(Schulz et al. 2022)
ANG5741	10403SΔ <i>esB</i> ₍₂₎ <i>walk</i> ^{R480H} ; StrepR	(Schulz et al. 2022)
ANG5746	10403SΔ <i>esB</i> ₍₃₎ <i>P_{dlt}*</i> ; StrepR	(Schulz et al. 2022)
ANG5749	10403SΔ <i>esB</i> ₍₃₎ <i>walk</i> ^{H368Y} ; StrepR	(Schulz et al. 2022)
ANG5750	10403SΔ <i>esB</i> ₍₃₎ <i>walR</i> ^{E12G} ; StrepR	(Schulz et al. 2022)
ANG5754	10403SΔ <i>esB</i> ₍₃₎ <i>walk</i> ^{P600S} ; StrepR	(Schulz et al. 2022)
LJR24	10403S pIMK3; StrepR KanR	(Schulz et al. 2022)
LJR25	10403SΔ <i>esB</i> ₍₂₎ pIMK3; StrepR KanR	(Schulz et al. 2022)
LJR26	10403S pIMK3- <i>murA</i> ; StrepR KanR	(Schulz et al. 2022)

LJR27	10403S <i>DesB</i> ₍₂₎ pIMK3- <i>murA</i> ; StrepR KanR	(Schulz et al. 2022)
LMJR138	EGD-e Δ <i>clpC</i>	(Rismondo et al., 2016)
LJR187	EGD-e <i>fepR</i> ^{N170fs}	(Schulz et al. 2023)
LJR188	EGD-e <i>P</i> _{<i>fepR</i>} ^{G-27T}	(Schulz et al. 2023)
LJR190	EGD-e <i>fepR</i> ^{G157*}	(Schulz et al. 2023)
LJR194	EGD-e <i>fepR</i> ^{Δ45-46}	(Schulz et al. 2023)
LJR196	EGD-e <i>fepR</i> ^{Δ99}	(Schulz et al. 2023)
LJR208	EGD-e <i>fepR</i> ^{Q140*}	(Schulz et al. 2023)
LJR209	EGD-e <i>fepR</i> ^{Y155*}	(Schulz et al. 2023)
LJR210	EGD-e <i>fepR</i> ^{Q140*}	(Schulz et al. 2023)
LJR211	EGD-e <i>fepR</i> ^{V115D}	(Schulz et al. 2023)
LJR212	EGD-e <i>fepR</i> ^{Δ45-46}	(Schulz et al. 2023)
LJR213	EGD-e <i>fepR</i> ^{S23L}	(Schulz et al. 2023)
LJR214	EGD-e <i>fepR</i> ^{Q140*}	(Schulz et al. 2023)
LJR215	EGD-e <i>P</i> _{<i>fepR</i>} ^{A-33G}	(Schulz et al. 2023)
LJR216	EGD-e <i>fepR</i> ^{M126fs}	(Schulz et al. 2023)
LJR217	EGD-e <i>fepR</i> ^{Δ45-46}	(Schulz et al. 2023)
LJR218	EGD-e <i>fepR</i> ^{L24F}	(Schulz et al. 2023)
LJR219	EGD-e <i>fepR</i> ^{INS29DIA}	(Schulz et al. 2023)
LJR220	EGD-e <i>fepR</i> ^{Δ45-46}	(Schulz et al. 2023)
LJR221	EGD-e <i>fepR</i> ^{W137fs}	(Schulz et al. 2023)
LJR222	EGD-e <i>fepR</i> ^{M126fs}	(Schulz et al. 2023)
LJR231	EGD-e pIMK3- <i>fepA</i> ; KanR	(Schulz et al. 2023)
LJR234	EGD-e <i>P</i> _{<i>sugR</i>} ^{G-11T}	(Schulz et al. 2023)
LJR235	EGD-e <i>sugR</i> ^{F49fs}	(Schulz et al. 2023)
LJR248	EGD-e <i>sugR</i> ^{D122*}	(Schulz et al. 2023)
LJR249	EGD-e <i>sugR</i> ^{D122*}	(Schulz et al. 2023)
LJR250	EGD-e <i>sugR</i> ^{D122*}	(Schulz et al. 2023)
LJR261	EGD-e Δ <i>fepA</i>	(Schulz et al. 2023)
LJR262	EGD-e Δ <i>sugE1/2</i>	(Schulz et al. 2023)
LJR265	EGD-e Δ <i>fepA</i> pIMK3- <i>fepA</i> ; KanR	(Schulz et al. 2023)
LJR266	EGD-e Δ <i>fepA sugR</i> ^{D71*}	(Schulz et al. 2023)
LJR267	EGD-e Δ <i>fepA sugR</i> ^{F49fs}	(Schulz et al. 2023)
LJR268	EGD-e Δ <i>fepA sugR</i> ^{S44*}	(Schulz et al. 2023)
LJR269	EGD-e Δ <i>fepA sugR</i> ^{A23D}	(Schulz et al. 2023)
LJR270	EGD-e Δ <i>sugE1/2 fepR</i> ^{G157*}	(Schulz et al. 2023)
LJR271	EGD-e Δ <i>sugE1/2 fepR</i> ^{I185fs}	(Schulz et al. 2023)
LJR272	EGD-e Δ <i>sugE1/2 fepR</i> ^{D171fs}	(Schulz et al. 2023)
LJR273	EGD-e Δ <i>sugE1/2 fepR</i> ^{P107L}	(Schulz et al. 2023)
LJR274	EGD-e Δ <i>sugE1/2 fepR</i> ^{E89fs}	(Schulz et al. 2023)
LJR275	EGD-e Δ <i>sugE1/2 fepR</i> ^{A154E}	(Schulz et al. 2023)
LJR276	EGD-e Δ <i>sugE1/2 fepR</i> ^{V115fs}	(Schulz et al. 2023)
LJR277	EGD-e Δ <i>sugE1/2 fepR</i> ^{V115fs}	(Schulz et al. 2023)

LJR280	EGD-e $\Delta fepA sugR^{L57*}$	(Schulz et al. 2023)
LJR281	EGD-e $\Delta fepA sugR^{Y19fs}$	(Schulz et al. 2023)
LJR282	EGD-e $\Delta fepA sugR^{S81*}$	(Schulz et al. 2023)
LJR283	EGD-e $\Delta fepA sugR^{S81*}$	(Schulz et al. 2023)
LJR301	EGD-e pIMK3- <i>sugE1/2</i> ; KanR	(Schulz et al. 2023)
LJR302	EGD-e pPL3e- P_{fepR}^{A-33G} - <i>lacZ</i> ; ErmR	(Schulz et al. 2023)
LJR303	EGD-e pPL3e- P_{fepR}^{G-27T} - <i>lacZ</i> ; ErmR	(Schulz et al. 2023)
LJR326	EGD-e $\Delta fepA \Delta sugE1/2 Imo1753^{K19fs}$, short: $\Delta fepA \Delta sugE1/2$ BAC1	(Schulz et al. 2023)
LJR327	EGD-e $\Delta fepA \Delta sugE1/2 Imo1753^{K19fs}$, short: $\Delta fepA \Delta sugE1/2$ CTAB1	(Schulz et al. 2023)
LJR328	EGD-e $\Delta fepA \Delta sugE1/2 Imo1753^{K19fs}$, short: $\Delta fepA \Delta sugE1/2$ CTAB2	(Schulz et al. 2023)
LJR329	EGD-e $\Delta fepA \Delta sugE1/2$	(Schulz et al. 2023)
LJR330	EGD-e $\Delta fepA \Delta sugE1/2 Imo1753^{V225fs}$ $P_{Imo1682}^{G-37A}$, short: $\Delta fepA \Delta sugE1/2$ BAC2	(Schulz et al. 2023)
LJR336	EGD-e pPL3e- P_{fepR} - <i>lacZ</i> ; ErmR	(Schulz et al. 2023)

9.8 *L. monocytogenes* strains constructed in this study

Strain	Genotype	Reference/Construction
LJR6	10403S pKSV7- ΔesC ; StrepR; CamR	EJR43 \rightarrow 10403S (ANG1263), deletion protocol performed
LJR7	10403S ΔesC ; StrepR	(Rismondo et al. 2021)
LJR14	10403S <i>attB::P_{eslA}-lacZ</i> ; StrepR, ErmR	pPL3e- P_{eslA} (EJR2) \rightarrow 10403S (ANG1263)
LJR15	10403S ΔesR <i>attB::P_{eslA}-lacZ</i> ; StrepR, ErmR	pPL3e- P_{eslA} (EJR2) \rightarrow 10403S ΔesR (ANG5588)
LJR18	10403S $\Delta esIA-R$; StrepR	EJR44 \rightarrow 10403S (ANG1263), deletion protocol performed
LJR19	10403S $\Delta esIA-R$; StrepR	EJR44 \rightarrow 10403S (ANG1263), deletion protocol performed
LJR21	10403S $\Delta esIC$ pPL3e- P_{eslA} - <i>esIABC</i> (or short: 10403S $\Delta esIC$ compl.); ErmR, StrepR	(Rismondo et al. 2021)
LJR27	10403S $\Delta esIB_{(2)}$ pIMK3- <i>murA</i> ; StrepR, KanR	(Schulz et al. 2022)
LJR28	10403S pIMK2- <i>mNeonGreen-zapA</i> ; StrepR, KanR	(Rismondo et al. 2021)
LJR29	10403S $\Delta esIB_{(2)}$ pIMK2- <i>mNeonGreen-</i> <i>zapA</i> ; StrepR, KanR	(Rismondo et al. 2021)
LJR33	10403S $\Delta esIA$; StrepR	(Rismondo et al. 2021)

LJR34	10403S Δ <i>es</i> /A pPL3e- <i>P_{esIA}-es/ABC</i> (or short: 10403S Δ <i>es</i> /C compl.); ErmR, StrepR	(Rismondo et al. 2021)
LJR35	10403S pKSV7- <i>cwI</i> O; StrepR, AmpR	pKSV7- <i>cwI</i> O (EJR63) → 10403S
LJR37	10403S Δ <i>cwI</i> O; StrepR	(Schulz et al. 2022)
LJR38	10403S pIMK2- <i>divIVA-mNeonGreen</i> , StrepR, KanR	pIMK2- <i>divIVA-mNeonGreen</i> (EJR92) → 10403S using S17-1 as donor (EJR90)
LJR39	10403S Δ <i>es</i> /B pIMK2- <i>divIVA-mNeonGreen</i> ; StrepR, KanR	pIMK2- <i>divIVA-mNeonGreen</i> (EJR92) → 10403S Δ <i>es</i> /B (ANG5662) using S17 as donor (EJR90)
LJR42	10403S pIMK2- <i>esIAB-mNeonGreen</i> ; StrepR, KanR	pIMK2- <i>esIAB-mNeonGreen</i> (EJR101) → 10403S using S17-1 as donor (EJR102)
LJR43	10403S Δ <i>es</i> /B pIMK2- <i>esIAB-mNeonGreen</i> ; StrepR, KanR	pIMK2- <i>esIAB-mNeonGreen</i> (EJR101) → 10403S Δ <i>es</i> /B (ANG5662) using S17-1 as donor (EJR102)
LJR53	10403S pKSV7- <i>sod</i> ; StrepR, AmpR	pKSV7- <i>sod</i> (EJR76) → 10403S
LJR54	10403S pKSV7- <i>corA</i> ; StrepR, AmpR	pKSV7- <i>corA</i> (EJR73) → 10403S
LJR55	10403S pKSV7- <i>kat</i> ; StrepR, AmpR	pKSV7- <i>kat</i> (EJR75) → 10403S
LJR56	10403S Δ <i>es</i> /B ₍₃₎ pPL3e- <i>P_{esIA}-es/ABC</i> (or short: 10403S Δ <i>es</i> /B ₍₃₎ compl.); ErmR, StrepR	(Schulz et al. 2022)
LJR61	10403S <i>P_{cwI}O-lacZ</i> ; ErmR, StrepR	pPL3e- <i>P_{cwI}O-lacZ</i> (EJR41) → 10403S using S17-1 as donor
LJR62	10403S Δ <i>es</i> /B ₍₂₎ - <i>P_{cwI}O-lacZ</i> ; ErmR, StrepR	pPL3e- <i>P_{cwI}O-lacZ</i> (EJR41) → 10403S Δ <i>es</i> /B (ANG5662) using S17-1 as donor
LJR63	10403S Δ <i>es</i> /B ₍₂₎ pIMK3- <i>glmR</i> ; StrepR, KanR	(Schulz et al. 2022)
LJR64	10403S Δ <i>es</i> /B ₍₂₎ pIMK3- <i>glmU</i> ; StrepR; KanR	(Schulz et al. 2022)
LJR65	10403S Δ <i>es</i> /B ₍₂₎ pIMK3- <i>glmM</i> ; StrepR; KanR	(Schulz et al. 2022)
LJR66	10403S Δ <i>es</i> /B ₍₂₎ pIMK3- <i>glmS</i> ; StrepR; KanR	(Schulz et al. 2022)
LJR67	10403S pIMK3- <i>glmR</i> ; StrepR, KanR	EJR106 → 10403S using S17-1 as donor (EJR132)
LJR68	10403S pIMK3- <i>glmU</i> ; StrepR, KanR	EJR107 → 10403S using S17-1 as donor (EJR133)
LJR69	10403S pIMK3- <i>glmM</i> ; StrepR, KanR	EJR108 → 10403S using S17-1 as donor (EJR133)
LJR70	10403S pIMK3- <i>glmS</i> ; StrepR, KanR	EJR112 → 10403S using S17-1 as donor (EJR133)

LJR71	10403S pKSV7- <i>anrA</i> ; StrepR, AmpR	pKSV7- <i>anrA</i> (EJR74) → 10403S,
LJR76	10403SΔ <i>corA</i> ; StrepR	pKSV7- <i>corA</i> (EJR73) → 10403S, deletion protocol performed
LJR77	10403SΔ <i>kat</i> ; StrepR,	pKSV7- <i>kat</i> (EJR75) → 10403S, deletion protocol performed
LJR78	10403SΔ <i>anrA</i> ; StrepR	pKSV7- <i>anrA</i> (EJR74) → 10403S, deletion protocol performed
LJR79	10403S pPL3e- <i>lacZ</i> ; StrepR, EryR	pPL3e- <i>lacZ</i> (ANG5181) → 10403S using S17-1 as donor
LJR80	10403SΔ <i>eslB</i> ₍₂₎ pPL3e- <i>lacZ</i> ; StrepR, EryR	pPL3e- <i>lacZ</i> (ANG5181) → 10403S Δ <i>eslB</i> (ANG5662) using S17-1 as donor
LJR81	10403S pIMK2- <i>mNeonGreen</i> -His; StrepR, KanR	pIMK2- <i>mNeonGreen</i> -His (EJR162) → 10403S using S17-1 as donor
LJR82	10403S pIMK2- <i>eslAB</i> -His; StrepR, KanR	pIMK2- <i>eslAB</i> -His (EJR150) → 10403S Δ <i>eslB</i> (ANG5662) using S17-1 as donor
LJR84	10403SΔ <i>eslB</i> , StrepR, <i>Imrg_0267</i> deletion_first 1333 bp deletion of <i>Imrg_02674</i> ; StrepR	ANG5662 suppressos evolved in presence of Glucose stress
LJR85	10403S Δ <i>eslB Imo1268</i> ^{A81D} ; StrepR	ANG5662 suppressos evolved in presence of glucose stress
LJR86	10403S Δ <i>eslB cwIO</i> ^{R106H} <i>walR</i> ^{N117S} ; StrepR	ANG5710 suppressos evolved in presence of lysozyme stress
LJR87	10403SΔ <i>eslB cwIO</i> ^{R106H} <i>Imo1821</i> ^{D8N} ; StrepR	ANG5710 suppressos evolved in presence of lysozyme stress
LJR88	10403SΔ <i>eslB P</i> _{<i>Imo1268</i>} [*] ; StrepR	ANG5662 suppressos evolved in presence of heat stress
LJR89	10403SΔ <i>eslB Imo1079</i> ^{Del, K59fs} ; StrepR	ANG5662 suppressos evolved in presence of heat stress
LJR90	10403SΔ <i>eslB Imo2240</i> ^{T40K} ; StrepR	ANG5662 suppressos evolved in presence of heat stress
LJR91	10403 Δ <i>eslB Imo1268</i> ^{G215D} ; StrepR	ANG5662 suppressos evolved in presence of heat stress
LJR98	10403S pKSV7- <i>eslABC</i> ; StrepR, AmpR	EJR105 (pKSV7- <i>eslABC</i>) → 10403S (ANG1263),
LJR101	10403SΔ <i>eslABC</i> ; StrepR,	EJR105 (pKSV7- <i>eslABC</i>) → 10403S (ANG1263), deletion protocol performed
LJR103	10403SΔ <i>cwIO</i> pIMK3- <i>cwIO</i> ; StrepR, KanR	(Schulz et al. 2022)

LJR112	10403S pIMK3- <i>lmo1315</i> ; StrepR, KanR	pIMK3- <i>lmo1315</i> (EJR109) → 10403S (ANG1263), using S17 (EJR110) as donour
LJR113	10403SΔ <i>eslB</i> pIMK3- <i>lmo1315</i> ; StrepR, KanR	pIMK3- <i>lmo1315</i> (EJR109) → 10403S Δ <i>eslB</i> (ANG5662), using S17 (EJR110) as donour
LJR114	10403SΔ <i>cw/O</i> pIMK3- <i>cw/O</i> pKSV7-Δ <i>eslB</i> ; StrepR, KanR, CamR	(Schulz et al. 2022)
LJR119	10403SΔ <i>cw/O</i> pIMK3- <i>cw/O</i> Δ <i>eslB</i> ; StrepR, KanR	(Schulz et al. 2022)
LJR120	10403S pIMK3- <i>cw/O</i> ; StrepR, KanR	pIMK3- <i>cw/O</i> (LJR114) → 10403S (ANG1263, using S17 (EJR115) as donour strain
LJR121	10403S <i>eslB</i> pIMK3- <i>cw/O</i> ; StrepR, KanR	pIMK3- <i>cw/O</i> (LJR114) → 10403S Δ <i>eslB</i> (ANG5662), using S17 (EJR115) as donour strain
LJR257	EGD-e <i>sugR</i> ^{L64*}	(Schulz et al. 2023)
LJR258	EGD-e <i>sugR</i> ^{F49fs}	(Schulz et al. 2023)
LJR259	EGD-e <i>sugR</i> ^{F49fs}	(Schulz et al. 2023)
LJR260	EGD-e <i>sugR</i> ^{F49fs}	(Schulz et al. 2023)

9.9 *B. subtilis* strains used in this study

Strain	Genotype	Reference/Construction
168	<i>trpC2</i>	AG-stuelke
PG389	<i>amyE::P_{comG}-lacZ-gfp-cat</i>	(Gamba et al., 2015)
GP2630	<i>trpC amyE::P_{comG}-lacZ-gfp-cat</i>	(Benda et al. 2021)
GP2646	<i>trpC2 ΔytrGABCDEF::ermC</i>	(Benda et al. 2021)
GP2647	<i>trpC2 ΔytrA::ermC</i>	(Benda et al. 2021)
GP2664	<i>trpC2 amyE::P_{comG}-lacZ-gfp ΔftsH::aphA3</i>	(Benda et al. 2021)
GP2665	<i>trpC2 amyE::P_{comG}-lacZ-gfp ΔnrnA::aphA3</i>	(Benda et al. 2021)
GP2666	<i>trpC2 amyE::P_{comG}-lacZ-gfp ΔgreA::aphA3</i>	(Benda et al. 2021)
GP2667	<i>trpC2 amyE::P_{comG}-lacZ-gfp ΔytrA::spc</i>	(Benda et al. 2021)
GP2671	<i>trpC2 amyE::P_{comG}-lacZ-gfp ΔcomEC::spc</i>	(Benda et al. 2021)
GP2672	<i>trpC2 amyE::P_{comG}-lacZ-gfp ΔdegU::aphA3</i>	(Benda et al. 2021)
GP2700	<i>trpC2 ΔytrF::cat</i>	(Benda et al. 2021)
GP3186	<i>trpC2 ΔytrGABCDE::ermC</i>	(Benda et al. 2021)
GP3187	<i>trpC2 ΔytrF::cat ΔytrA::ermC</i>	(Benda et al. 2021)
GP3193	<i>trpC2 ΔytrA::ermC ΔytrB</i>	(Benda et al. 2021)
GP3194	<i>trpC2 ΔytrA::ermC ΔytrC</i>	(Benda et al. 2021)
GP3195	<i>trpC2 ΔytrA::ermC ΔytrD</i>	(Benda et al. 2021)
GP3205	<i>trpC2 ΔytrCD::cat</i>	(Benda et al. 2021)
GP3206	<i>trpC2 ΔytrA::ermC ΔytrB ΔytrE</i>	(Benda et al. 2021)

GP3212	<i>comI</i> ^{Q121} Δ <i>trA::spc</i>	(Benda et al. 2021)
--------	--	---------------------

9.10 *B. subtilis* strains constructed in this study

Strain	Genotype	Reference/Construction
BLMS2	<i>trpC2</i> Δ <i>trCD</i>	(Benda et al. 2021)
BLMS3	<i>trpC2</i> Δ <i>trA::erm</i> Δ <i>trCD</i>	(Benda et al. 2021)
BLMS4	168 + pAC7-P _{<i>dlt</i>} ; AmpR	(Schulz et al. 2022)
BLMS5	168 + pAC7-P _{<i>dlt</i>} [*] ; AmpR	(Schulz et al. 2022)

Curriculum vitae

Name: Lisa Maria Schulz
Date of birth: 29.08.1992
Place of birth: Coesfeld, Germany
Nationality: German

Education

01/2020 – 04/2023 **PhD student in the GGNB Program Microbiology and Biochemistry**
Department of General Microbiology
Institute of Microbiology and Genetics
Georg-August-Universität Göttingen, 37073 Göttingen, Germany

Doctoral Thesis Project: Identification of factors involved in cell wall homeostasis and tolerance towards quaternary ammonium compounds in *Listeria monocytogenes* by genomic adaptation

10/2017-10/2019 **MSc in Molecular Life Science: Microbiology, Biotechnology and Biochemistry**
Georg-August-Universität Göttingen
Department of General Microbiology
Institute of Microbiology and Genetics
Georg-August-Universität Göttingen, 37073 Göttingen, Germany

Project: Identification of novel c-di-AMP targets in *Listeria monocytogenes* by genomic adaptation

09/2014-08/2017 **Bachelor of Applied Biology**
Hochschule Bonn-Rhein-Sieg

Project: Influence of CO₂ on growth and production of bioactive compounds in cyanobacteria

09/2016-07/2017 **BSc Hons Bioscience with Biomedical Sciences**
Robert Gordon University

Project: Determination on the influence of CO₂ on toxin production